ANALYSIS OF NITROGEN DYNAMICS IN SOIL COLUMNS TO EVALUATE NITRATE POLLUTION DUE TO RECLAIMED WASTEWATER IRRIGATION(Dissertation_全文)

AUTHOR(S):

DAYANTHI, WANNIARACHCHI KANKANAMGE CHANDRANI NEETHA

ANALYSIS OF NITROGEN DYNAMICS IN SOIL COLUMNS TO EVALUATE NITRATE POLLUTION DUE TO RECLAIMED WASTEWATER IRRIGATION

下水再生水の灌漑利用による硝酸汚染評価のための土壌カラム中の窒素動態の解析

BY

W.K.C.N. DAYANTHI

B.Sc. (Eng.), University of Peradeniya, Sri Lanka, 1999
M.Eng., University of Moratuwa, Sri Lanka, 2001
M.Eng., Asian Institute of Technology, Thailand, 2003

DISSERTATION

Submitted in partial fulfillment of the requirements for the degree of
Doctor of Engineering in the Department of Urban and Environmental Engineering,
Graduate School of Engineering of
Kyoto University

Kyoto, Japan
September 2007

ACKNOWLEDGEMENT

First of all, I would like to extend my enormous gratitude to my supervisor, Professor Hiroaki Tanaka for his superb guidance, excellent supervision, generous time and praiseworthy commitment that made me complete my doctoral work successfully. Indeed, I owe him special gratitude for stimulating my analytical thinking and encouraging me to develop independent thinking throughout my doctoral work. Next, I am very much grateful for the assistance, encouragement and praiseworthy support I received from Dr. Naoyuki Yamashita. His assistance in solving numerous problems encountered in the experimental series is one factor behind the success of my doctoral work. It is with great appreciation I hereby mention Professor Shigeo Fujii whose remarkable commitments were a great helping hand in the success of my doctoral work. I owe a special note of gratitude to him for introducing me to my supervisor that made me granted by this opportunity to pursue a doctoral degree course at Kyoto University. Next my heartfelt appreciation goes to Dr. Joseph E. Odencrantz whose infectious enthusiasm, vast knowledge in the field of groundwater modeling, valuable suggestions and the remarkable commitment were one of the major driving forces through the latter part of my doctoral research. My sincere thanks also go out to Professor Shimizu Yoshihisa for supporting me in many ways. I would also be very much grateful to the enormous support I received from Dr. Ikeda Kazuhiro and Dr. Shuhei Tanaka on numerous occasions. I hereby appreciate very much the help I received from Associate professor Minoru Yoneda for the analysis of cations.

Next, my heartiest admiration goes to the Government of Japan for providing me with a full scholarship to pursue my doctoral degree course without any financial shortage.

Further, my enormous admiration goes to Mr.Takayuki Shigematsu, my research group member, for the help he has given with the nitrogen stable isotope analysis presented in this dissertation and with other aspects of my research and life at the *RCEQM*. Especially, I need to express my gratitude and deep appreciation to Ms.Hattori Kozumi, Ms.Yuki Hayabara, Ms. Fukunaga Kinuyo and Ms.Ikuko Moro for their contribution and good-natured support. I must acknowledge as well all my friends and colleagues past and present at the *RCEQM*, who assisted me over the last three years.

I make a very special note to offer my heartiest gratitude to my dear husband, whose giant support came as a shower of blessings throughout the thick and thin of my doctoral work and life in Japan. I dedicate this dissertation to him. At last, but by no means the least, I hereby mention my dear ones, my parents, brother, sister & brother-in- law, two nieces

and in-laws, whose blessings, emotional support and patience were the hidden driving forces of the success of my doctoral work and life in Japan.

ABSTRACT

Reclaimed wastewater will be used for the agricultural irrigation on large-scale in Okinawa, Japan in the near future. However, the high NH_4^+ concentration in reclaimed wastewater (RWW) is likely to contribute to NO_3^- pollution. Therefore, the primary objective of this dissertation was to analyze the belowground nitrogen dynamics, caused by RWW irrigation, on the two most abundant soil types on Okinawa Island, in order to evaluate NO_3^- pollution.

The belowground dynamics of nitrogenous compounds were studied using two series of laboratory scale unsaturated soil column experiments on two soil types, which are low and high porous, respectively. First, the experiment on low porous soil was conducted on two soil columns. The study was first conducted by continuous and intermittent irrigation of the soil columns for 120 days with simulated reclaimed wastewater (*SRW*). Next, the effects of the concurrent applications of simulated rainwater and *SRW* intermittently were studied. Approximately 90% of NH_3-*N* in the *SRW* diminished at the upper soil layers in both the columns, due to nitrification and adsorption. In the intermittent application, $NO_3^- - N$ concentration of the pore water obtained from various depths and the effluent were characterized by a gradual increase, which eventually approached a plateau where the concentration remained approximately constant. In the continuous application, $NO_3^- - N$ concentration of all pore water & effluent samples increased to a maximum, and then decreased preceding the steady state. The maximum $NO_3^- - N$ concentrations of the pore water samples collected from above 55 cm depth were considerably higher than those collected from below 55 cm depth and the effluent. The nitrogen mass balance indicated that the mass of *T-N* that was lost by off-gassing to the soil air of the continuous and intermittent applications were 41.5% and 13.0%, respectively. The acceleration of denitrification in the continuous application was verified further by the high enrichment of ^{15}N of NO_3^- in the effluent. Besides, the results indicated that the analysis of nitrogen stable isotopes is an effective tool to understand nitrogen dynamics in the soil. The rainfall experiment suggested that the rainfall would accelerate the leaching of accumulated NO_3^- from soil.

After that, two similar-type soil columns, loaded with the high porous soil, were given the same treatment as that of the low porous soil. The simultaneous occurrence of

nitrification, denitrification and adsorption of NH_4^+ on to soil was proved by the results. In the intermittent application, $NO_3^- - N$ concentration of the water samples obtained from various depths were characterized by a gradual increase in $NO_3^- - N$ concentrations to a peak followed by a slight decrease toward the end of the experiment. In the continuous application, $NO_3^- - N$ concentration of all water samples increased to a maximum before attaining the steady state successively. The nitrogen mass balance indicated that the mass of *T-N* that was lost by off-gassing to the soil air of the continuous and intermittent applications were 30.0 % and 2.1 %, respectively. The carbon mass balance evidenced that the dissolved organic carbon in the soil solution may have been used for denitrification and the consumption of that in the continuous application may have been greater than that of the intermittent application. Therefore, it is concluded that denitrification accelerated in the continuous application in comparison with the intermittent application.

The coupled material balance equations for both NH_3-*N* and $NO_3^- - N$ on the entire soil volume were solved analytically to simulate the distribution of $NO_3^- - N$ concentrations with time along the soil depth for the continuous applications. The optimized apparent first-order rate constants for nitrification (k_1) and denitrification (k_2) for the high porous soil were 0.09 d^{-1} and 0.003 d^{-1}, respectively. The model on the low porous soil was calibrated in terms of k_1 both on soil and soil solution, and k_2. The apparent k_1 on soil and soil solution, and k_2 were 1.0 d^{-1}, 0.4 d^{-1} and 0.03 d^{-1}, respectively. These models can make reasonable predictions of NO_3^- movements, and with certain limitations they can be used as a means of testing strategies and assessing risks.

Based on the results of the research, it is concluded that the irrigation of RWW, either continuously or at shorter intervals with low rates, using the surface drip irrigation method, under a green house, would mitigate the NO_3^- contamination. The developed models could give reasonable predictions to the steady state $NO_3^- - N$ that may exist in the groundwater of the fields containing high and low porous soils in Okinawa, due to the continuous drip irrigation under a green house. The fields with high porous soil are at high risk of groundwater contamination with NO_3^-, whereas the fields with low porous soil may be affected if the groundwater table is shallower than 60 cm. The appropriate reduction of the proposed irrigation rate or blending *RWW* with other types of water along with the drip irrigation under a green house would be a solution for the NO_3^- contamination in Okinawa.

TABLE OF CONTENTS

LIST OF SYMBOLS

Fundamental dimensions

L	Length
M	Mass
T	Time

English Symbols

a, b	Dimensionless constants
A, B	Dimensionless constants
A_1, A_2	Dimensionless constants
A_1^0, A_2^0	Dimensionless constants
A_3, A_4	Dimensionless constants
A_c	Cross sectional area of the control volume (L^2)
B_1^0, B_2^0	Dimensionless constants
C_i^0	Initial solute 'i' concentration in soil solution (ML^{-3})
C_1^0	Initial solute NH_3-N concentration in soil solution (ML^{-3})
C_2^0	Initial solute NO_3^--N concentration in soil solution (ML^{-3})
$\overline{C}_1$	Laplace transformation of C_1
$\overline{C}_2$	Laplace transformation of C_2
C_1^p	Concentration of NH_3-N in soil solution during $0 < t < T_1$ in low porous-soil model (ML^{-3})
C_2^p	Concentration of NO_3^--N in soil solution during $0 < t < T_1$ in low porous-soil model (ML^{-3})
C_1	Concentration of NH_3-N in soil solution (ML^{-3})
C_2	Concentration of NO_3^--N in soil solution (ML^{-3})
C_i	Solute 'i' concentration in soil solution (ML^{-3})
D_1	Apparent molecular diffusion coefficient for NH_3 (L^2T^{-1})
D_2	Apparent molecular diffusion coefficient for NO_3^- (L^2T^{-1})
erfc	Complementary error function

ET_c	Crop evapotranspiration (LT^{-1})
J_x	Solute flux in the direction of x ($ML^{-2}T^{-1}$)
k_2	First order rate constant of denitrification in soil solution (T^{-1})
k_1	First order rate constant of nitrification in soil solution (T^{-1})
k_1'	First order rate constant of nitrification on solid phase (T^{-1})
K_d	Sorption partition coefficient (L^3 -soil solution/ M- soil)
L_w	Annual hydraulic loading rate (LT^{-1})
m	Total mass of adsorbent (soil) (M)
M, N	Constants
m_s	Total weight of soil in the column (M)
m_w	Total weight of water in the column (M)
M', N'	Constants
n	Constant in non-linear Freundlich isotherm
NR	Designed net irrigation rate (M/T)
q_i	Solute 'i' concentration on adsorbent phase (M- solute/ M- soil)
R	Retardation factor
R^2	Correlation coefficient
r	Constant (L^{-1})
r_1	Net effect of transformation of solute NH_3-N (sink-source term) ($ML^{-3}T^{-1}$)
r_2	Net effect of transformation of solute NO_3^--N (sink-source term) ($ML^{-3}T^{-1}$)
r_i	Net effect of transformation of solute 'i' (sink-source term)($ML^{-3}T^{-1}$)
s	Variable that denotes t in the Laplace transformed function
t	Time (T)
T	Total time of irrigation (T)
T_1	Duration for which microorganism grows in case of low porous soil (T)
$\overline{T}$	Variable of integration to denote t
U	Darcy velocity (LT^{-1})
u	Variable of integration to denote t
v	Interstitial pore water velocity (LT^{-1})
V_s	Total volume of soil in the column (L^3)
V_t	Total volume of the column (L^3)
V_v	Total volume of voids in the column (L^3)
V_w	Total volume of water in the column (L^3)

x	Length along the soil column (L)
x'	Total mass of adsorbate (solute) on the adsorbent (M)
z_1, z_2, z_3	Constants

Greek Symbols

ρ_b	Average bulk density of soil (M/L^3)
ε_h	Dispersion coefficient (L^2/T)
φ	Porosity
τ	Variable of integration to denote t
φ_w	Volumetric moisture content
$\delta\ ^{15}N$ ‰.	Amount of ^{15}N relative to a standard, given in parts per thousand
α, β, γ	Dimensionless constants
δ, η, μ	Dimensionless constants
ξ, λ, σ	Dimensionless constants
α', λ'	Dimensionless constants

Chemical Formulae

Al^{3+}	Aluminum ion
Ba^{2+}	Barium
C	Carbon
^{13}C	Carbon stable isotope
Ca^{2+}	Calcium ion
Cd	Cadmium
$C_5H_7O_2N$	Synthesized bacterial cells
Cl^-	Chloride ion
CO_2	Carbon dioxide
Cr	Chromium
Cu	Copper
$CuSO_4$	Copper sulfate
Fe^{2+} & Fe^{3+}	Iron
HCO_3^-	Hydrogen carbonate ion

H_2CO_3	Carbonic acid
H_2O	Water
K^+	Potassium ion
KCl	Potassium chloride
Mg^{2+}	Magnesium ion
Mo	Molybdenum
N	Nitrogen
^{14}N	Stable isotope of nitrogen
^{15}N	Stable isotope of nitrogen
N_2	Nitrogen gas
Na^+	Sodium ion
NaCl	Sodium chloride
NH_3	Ammonia
NH_4^+	Ammonium ion
NH_4Cl	Ammonium chloride
$NH_3 - N$	Ammonia nitrogen
$NH_4^+ - N$	Ammonium nitrogen
NH_4OAc	Ammonium acetate
Ni	Nickel
NO_2^-	Nitrite ion
NO_3^-	Nitrate ion
N_2O	Nitrous oxide
$NO_3^- - N$	Nitrate nitrogen
$NO_2^- - N$	Nitrite nitrogen
O_2	Oxygen
P	Phosphorous
Pb	Lead
PO_4^{3-}	Phosphate ion
$PO_4^{3-} - P$	Phosphate- phosphorous
Sr^{2+}	Strontium
SO_4^{2-}	Sulfate ion
Zn^{2+}	Zinc

LIST OF ABBREVIATIONS

BOD_5	5- Day Biochemical Oxygen Demand
CA	Continuous Application
CT	Contact Time
DO	Dissolved Oxygen
DW	Deionized Water
E	Effluent
EAEC	Exchangeable Anion Exchange Capacity
EC	Electrical Conductivity
ECEC	Exchangeable Cation Exchange Capacity
EDCs	Endocrine Disrupters
GW	Groundwater
IA	Intermittent Application
NDMA	N-nitrosodimethylamine
NWTP	Naha Wastewater Treatment Plant
PAC	Poly Aluminum Chloride
PCBs	Polychlorinated Biphenyls
PPCPs	Pharmaceuticals and Personal Care Products
PW	Pore water
PW1	Pore water sample collected at 15 cm depth of column
PW2	Pore water sample collected at 35 cm depth of column
PW3	Pore water sample collected at 45 cm depth of column
PW4	Pore water sample collected at 55 cm depth of column
PW5	Pore water sample collected at 70 cm depth of column
PW6	Pore water sample collected at 80 cm depth of column
RWW	Reclaimed wastewater
RWW1	Chlorinated reclaimed wastewater
RWW2	UV disinfected reclaimed wastewater
SR	Simulated Rainwater
SRW	Simulated Reclaimed Wastewater
T-C	Total Carbon
TKN	Total Kjeldahl Nitrogen
T-N	Total Nitrogen

TOC	Total Organic Carbon
T-P	Total Phosphorous
UV	Ultra Violet

LIST OF FIGURES

Page No.

LIST OF TABLES

Page No

CHAPTER 1

INTRODUCTION

1.1 RESEARCH BACKGROUND

Water scarcity is one of the highly focused issues in the present world. Water recycling and reuse sounds well as an alternative to ever increasing water demand in the world. Water reuse is equally important in both developing and developed countries. *RWW* irrigation has become a must in the present world to address the irrigation water scarcity. Okinawa in Japan has been suffering from water scarcity and recently, the *RWW* has been introduced as an alternative irrigation water source. A large-scale project on the *RWW* irrigation has already been planned, and will be implemented during the next few years. However, the environmental issues and health risks always follow the *RWW* irrigation. The risks caused by the *RWW* irrigation depends largely on the degree of treatment that the secondary treated wastewater receives in the reclamation process. According to the above-mentioned project, there will be no advanced treatment-unit process for the removal of excess nitrogen in the treatment train of *RWW*. However, the targeted secondary treated wastewater to produce *RWW* contains NH_4^+ in high concentrations, which is likely to contribute to NO_3^- contamination in the subsurface water. Hence, NO_3^- tops the list of likely pollutants due to the irrigation of *RWW* production on the island. It is extremely possible that high NH_4^+ would convert to NO_3^- in the belowground, and NO_3^- would transfer into the subsurface water bodies.

NO_3^- is also in the list of most likely pollutants due to the irrigation of *RWW* elsewhere. As stated by El-Sadek et al. (2003), the fate of nitrogen in the soils is of major concern because of the potential hazard for nitrogen, applied in excess of the natural decomposing capacity of the soil, to contaminate shallow and deep aquifers. Excess NO_3^- may causes adverse effects on humans, animals and plants. Being considered to be the most stable nitrogen component in the soil, NO_3^- is of highly concern in terms of its sorption capacity, distribution and evaporation in the soil. The absence of the advanced unit process of nitrification and denitrification in the reclamation unit in Okinawa is a direct result of the cost-prohibitive treatment cost of RWW. Therefore, alternative, low-cost measures are currently being investigated to reduce the NO_3^- pollution. Well-managed

irrigation practices of altering the existing conservative irrigation scenarios may be an economically feasible option to minimize the NO_3^- pollution. Jiao et.al. (2004) stated that leaching of nitrogen from agricultural lands to groundwater poses a threat to the water quality, but it may be possible to control the leaching of dissolved nutrients by choosing appropriate management practices. An investigation on the belowground dynamics of nitrogenous compounds with respect to hydraulic loading rates, climatic conditions, soil conditions, degradation, transport modes toward the groundwater and etc. seems a way to disaugment the surface and groundwater pollution likely to be caused by the *RWW* irrigation. In accordance with Meisinger et al. (2002), the potential for the NO_3^- loss through leaching can be predicted from the soil $NO_3^- - N$ concentrations and water movement through the soil profile. Misra et.al. (1974) indicated the importance of investigating NO_3^- dynamics by stating that the application of large quantities of nitrogenous fertilizers in the form of urea, NH_4^+ and NO_3^- salts to the surface of agricultural fields along with irrigation water triggers a number of physical, chemical and microbiological reactions, which need to be analyzed simultaneously, to determine the ultimate fate and location of these solutes and their reaction products. Therefore, it is expected that a laboratory scale soil column break through data are able to predict the NO_3^- loss through the soil.

Simulation of nitrogen dynamics using mathematical models is crucial in investigating nitrogen dynamics of soil because a model can estimate $NO_3^- - N$ concentration that may exist in the groundwater as a result of the *RWW* itself. Much research has focused on modeling nitrogen dynamics in soil, and many of these models incorporate the nitrogen dynamics due to the fertilizer. Most of such attempts have been taken by the agriculture-based researches. It is very rare that there is an attempt of modeling nitrogen dynamics in soil due to *RWW* irrigation. In order to understand the interrelation of the mechanisms properly, a model which incorporates the synchronization of these mechanisms would be essential. Hence, a model simulating the belowground nitrogen dynamics based on a laboratory scale soil column would be a more meaningful way to understand the ultimate fate of nitrogen contained in *RWW*, upon the irrigation.

1.2 LITERATURE REVIEW

1.2.1 Overview on wastewater reclamation and reuse focusing Japan

Further treatment of secondary treated wastewater so that it can be reused is called wastewater reclamation. *RWW* is directly utilized in both agricultural and landscape irrigation, industrial applications, urban applications and dual water systems. Water scarcity has led many water preservative activities. Wastewater reclamation and reuse sound imperative not only in the viewpoint of water preservation but also as a solution to the burning issue of wastewater disposal. The land application of *RWW* has been experienced since a couple of decades ago in various forms such as agricultural and landscape irrigation, groundwater recharge and recreational activities. It controls water pollution, augment water supplies through replenishment of groundwater or surface water resources, and acts as an alternative water source for some applications preserving higher quality water resources.

As adapted from U.S. Environmental Agency (1992), when current volumes of the utilization of *RWW* worldwide are arranged in the descending order, the categories of municipal wastewater reuse are urban use including landscape irrigation, agricultural irrigation, recreational use, environmental enhancement, groundwater recharge, industrial reuse, and potential reuse (Asano, 1998). Unplanned indirect wastewater reuse that is wastewater reuse through effluent disposal to streams and groundwater has been accepted practice in many developed countries including Japan (Asano, 1998). Irrigation is called the major beneficial use of *RWW* in the arid and semi-arid regions of the world whereas wastewater reuse activities in Japan are dominated by non- potable urban use such as toilet flushing, industrial use, stream restoration and flow augmentation. In most cases, secondary treated domestic wastewater followed by sand filtration and disinfection is used for toilet flushing in business or commercial premises, car washing, garden watering, park or other open space planting, and fire fighting (Japan Sewage Works Association, 2005).Other non-potable usages such as industrial use, stream restoration and flow augmentation are also in practice. Tokyo is one of the leading cities that are successfully implementing wastewater reuse, such as dual distribution systems and stream augmentation (UNEP & GEC, 2005).In addition, Japan implements a unique approach by utilizing the nature of water as a heat medium(UNEP& GEC, 2005). As a comparison, California's total volume of *RWW* usage comprises 54% on agricultural irrigation whereas it is 14% in Japan (Asano, 1998). *RWW* is not utilized as a direct groundwater recharge

option in Japan while 20% of *RWW* in California is applied for groundwater recharge (Asano, 1998). Dillon (2000) argued that agricultural irrigation would play a major role in the reuse of urban wastewater as recycling percentage increases from 10% to 20% over this decade. However, Okinawa is the only place in Japan where *RWW* is utilized in agricultural irrigation on dry-state.

However, *RWW* has already been utilized for the irrigation in rice fields (wet-state) in several places in Japan. For instance, in Kumamoto City, it is reported that the treated wastewater, which receives no advanced treatment, mixed with the general irrigation water in an equiponderance, is used for the irrigation in rice fields; and it has caused a reduction in the demand of chemical fertilizer. These experiments demonstrated that successful rice cultivation could be achieved with treated wastewater applications, thereby reducing river water volume as well as fertilizer applications (Kumamoto Municipal Government, 1983).

1.2.2 Risks likely to be caused by RWW irrigation

Dillon (2000) has stated that biophysical, hydrological, economic and social factors, salinity, sodicity, nutrients, and health issues should be taken into account in assessing the risks associated with the *RWW* irrigation. Though the correct levels of nutrients in *RWW* provide a fertilizer value to crops or landscape productions, the elevated nutrient levels are beyond the plant requirement and cause problems related to the excessive vegetative growth, delayed or uneven maturity or reduced quality. Wastewater containing pathogens can contaminate crops directly by contacting during the irrigation or indirectly as a result of the soil contact (Asano, 1998). Traditionally, the concerns have been based on pathogens, but over the last few years, this has been expanded to endocrine disrupters and other xenobiotic chemicals (Gardner et al., 2004).Furthermore, the environmental pollution posed by the land application of *RWW* is unavoidable. Though, a sort of soil aquifer treatment is expected for wastewater pollutants, it is highly possible that these contaminants can reach groundwater aquifers. Moreover, some contaminants such as nitrogen species can run off to surface water bodies leading to the euthrophication. As described in many studies, there are high possibilities for groundwater to get contaminated with infiltrated NO_3^- through soil. According to Murphy et al. (2000), dissolved organic nitrogen compounds may possibly be transformed into NO_3^- as they travel through the soil profile. NO_3^- causes adverse effects on humans, animals and plants. Excess NO_3^- in the drinking water (more than 45 mg/L) may cause a disease called methemoglobinemia (blue

baby syndrome) in human infants. It has recently been found out that NO_3^- might be a thyroid hormone disrupter. The following studies have noted that the soil being subject to the *RWW* over an extended time period is in excess of nitrogenous compounds, which can lead to the ground and surface water pollution. NO_3^- from both natural and anthropogenic sources is possibly the most widespread contaminant in the groundwater because NO_3^- is both soluble and mobile (Hallberg et al., 1993). NO_3^- is the most stable nitrogen in the soil, and the excess NO_3^- may cause adverse effects on humans, animals and plants. NO_3^- can persist in the shallow groundwater for years (Pucket, 1994). As stated by Nolan et al. (2002), the shallow groundwater is more susceptible to NO_3^- contamination than the deep groundwater. However, the same author asserted that contaminants may migrate to deeper groundwater supplies too.

Trace elements in *RWW* normally occur in low concentrations that are not hazardous, but some are toxic at elevated concentrations; *Cu*, *Cd*, *Mo*, *Ni* and *Zn* are of greatest concern at elevated levels (Asano, 1998). In addition, *EDCs* and *PPCPs* are considered as potential groundwater pollutants due to the *RWW* irrigation (Shinohara et al., 2004).

1.2.3 Nitrogen stable isotopes

Nitrogen has two stable isotopes (^{14}N and ^{15}N). Natural variation of these isotopes is useful for tracing nitrogen cycling in ecosystems and for tracing the source of nitrogen to surface and groundwater. The isotopic composition and the mass of isotopes of an element can be measured by the mass spectrometer. All compounds contain both isotopes, but because of isotopic fractionation they are incorporated into compounds in differing ratios depending on the nature of the reactions that produce the compounds. The heavier isotope can cause it to react a little more slowly than its lighter counterpart resulting in a ratio of heavy isotope to light isotope in the product of a reaction that is different from the ration found in the reactant. Stable isotopes as ^{15}N have been used in the following areas of agricultural and soil researches: studying the turn over of nitrogen in soil, following nitrogen movements in soils, measuring nitrogen loss and studying denitrification. The ^{15}N values tend to be higher suggesting that microbes discriminate against the light isotope during decomposition. Results from environmental and agricultural studies using isotopically enriched traces are usually reported in units of atom (*At %*). This value gives the absolute number of atoms of a given isotope in 100 atoms of total element as:

$$At\ \%\ ^{15}N = \left[{}^{15}N/\left({}^{14}N+{}^{15}N\right)\right](100\,At\ \%) \qquad (1.1)$$

Studies examining the isotopes at or near natural abundance levels are usually reported as δ, a value given in parts per thousand or per million (‰). δ values are not absolute isotope abundances but differences between sample readings and one or another of the widely used natural abundance standards, in which δ is considered to be equal to zero.(eg: air for *N*, *At %*^{15} *N*= 0.3663033). Absolute isotope ratios are measured for the sample and the standard, and then the relative δ is calculated using the following equation.

$$\delta^{15}N‰\ \ vs.\ \ [std] = \left[\left(R'_{sample} - R'_{std}\right)/R'_{std}\right](1000\delta‰) \qquad (1.2)$$

where

$$R' = \left[At\%^{15}N/At\%^{14}N\right] \qquad (1.3)$$

For instance, if a leaf of sample is found to have R' ($^{15}N/^{14}N$) greater than the standard's by 5 parts per thousand, this value is reported as $\delta\ ^{15}N$=+5‰. The transformation of absolute *At%* values into relative (to a certain standard) δ values is used because the absolute differences between samples and standard are quite small at natural abundance levels and might appear only in the third or fourth decimal place if *At%* were reported.

The δ^{15} of total soil *N* is affected by many factors including soil depth, vegetation, climate, particle size, cultural history etc. It has been found that there is an inverse correlation of NO_3^- -$\delta^{15}N$ and NO_3^- concentration beneath agricultural fields when denitrification increases with depth. Commercial fertilizers, animal or human waste, precipitation and organic nitrogen within the soil are common sources of NO_3^- in groundwater. Each of the NO_3^- source categories has a distinguishable isotopic signature, ($^{15}N/^{14}N$). Stable isotope abundances of *N* ($\delta^{15}N$) have been used extensively to provide information on the origin and transformation of inorganic *N* in surface and groundwater (Heaton, 1986). Numerous studies have shown that the $\delta^{15}N$ values of NO_3^- in ground water can be used to indicate the dominant sources of the NO_3^-. Biologically mediated reactions (e.g. assimilation, nitrification, and denitrification) strongly control nitrogen and nitrogen isotopes compositions in both soil and water. Fractionation during denitrification causes the $\delta^{15}N$ of residual NO_3^- to increase exponentially as NO_3^- concentrations decrease due to the fractionation. These reactions almost always result in ^{15}N enrichment of the

substrate and depletion of the product. The combined use of ^{13}C and ^{15}N will provide a better assessment of below ground contribution to *N* and soil organic matter dynamics and ultimately to the contribution of these inputs to soil fertility. Cadisch et al. (2002) stated that in order to better understand belowground nitrogen dynamics, it is necessary to evaluate both ^{13}C and ^{15}N.

1.2.4 Analytical modeling of nitrogenous compounds

Since soil nitrogen dynamics directly affect the soil quality and productivity, it has been focused in many studies over several decades. Modeling nitrogen dynamics have been attempted in number of fields focusing different outcomes. Specially, this issue has been constantly in the limelight of agriculture based studies. Much research on nitrogen dynamics can be found on plant-soil system. Nitrogen dynamics in soil is of concern to the researchers representing different disciplines such as Agricultural Sciences, Soil Sciences, Civil and Environmental Engineering and Ecological Engineering. Therefore, studies and modeling of soil nitrogen dynamics have so far been considered in wider perspective. At present, the popularity of *RWW* irrigation has made this issue be focused on in different angle, i.e. in terms of subsurface water pollution. It has recently become an interest to the researchers in Environmental Engineering. However, so far, minimal attempts have been taken to simulate nitrogen dynamics caused by the reclaimed wastewater.

The attempts of analytical modeling of soil nitrogen dynamics spans several decades back. In the initial stage, analytical models describing the simultaneous occurrence of nitrification, denitrification and nitrogen movement in soil water have been presented by McLaren (1969a, 1969b, 1970, 1971), Cho (1971) and Misra et al. (1974).The convective transport of nitrogen compounds has been the basis for these analytical models. As explained by Cho (1971), any analysis of the convective transport of NH_4^+ in soil should take into account the decrease in NH_4^+ concentration as nitrification takes place, as well as its participation in ion-exchange reactions. The same author detailed the convective transport of surface-applied NH_4^+ due to the percolating water is such a way that during the course of travel, the ion participates in exchange reactions, which cause the ion to travel more slowly than the percolating water. It is also subject to nitrification, which tends to decrease its concentration. When NO_2^- or NO_3^- is produced, the convective movement of these ions takes place without much retardation. McLaren (1969, 1970) derived mathematical solutions of the steady – state concentrations for NH_4^+, NO_2^- and NO_3^- in the

absence of the ion-exchange reactions and ionic dispersion. It can be applied only to a convective system. Cho (1971) derived mathematical equations that describe nitrogen movement in a soil-like system with simple nitrification and adsorption relations. He described the convective transport of NH_3^+ in soil, with nitrification and dentrification, by applying dispersion equations with first-order reaction rates for nitrogen transformations. He could obtain the equations describing the concentrations of NH_3^+, NO_2^- and NO_3^- as functions of position, time, rate constants, average solution velocity and the distribution coefficient of NH_4^+ between soil and soil solution. In his study, several values of parameters were chosen to obtain the concentration profiles of NH_3^+, NO_2^- and NO_3^- along the soil column at several times. Several steady –state concentration profiles and the time required to attain the steady-state were also discussed. However, it is not clear whether the equations have been derived for saturated or unsaturated flow conditions. Those equations were derived for a constant flow system. These solutions have the possibilities to be applied to a non-convective system if the dispersion coefficient is interpreted as a diffusion coefficient in a porous material.

Misra et al. (1974) modified the equations demonstrated by Cho (1971), by presenting equations for a pulse application of a solute. Transport equations to describe the dynamics of nitrogenous compounds were set up in that study, and solved for a continuous application of NH_3^+ (C_1^0) and/or NO_3^- (C_2^0) salt at the soil surface. Both ionic adsorption owing to the cation exchange and microbial transformations have been considered. The reversible type of sorption-desorption reaction for an ion has been described in such a way that the solute adsorbed on the solid phase is linearly proportional to the solute concentration in the soil solution. The proportionality constant is called the distribution coefficient of the solute between the free and the sorbed phases in the solution, and it is independent of the solute concentration in the solution. In addition, the solutions for a continuous application of a solute, C_i^0, duration of which is '$0 \le t < T$', can be extended by the principle of superposition for $t > T$. Therefore, solution to a pulse application of C_i^0 for a duration of T, is given by replacing C_i^0 by ($-C_i^0$), and t by ($t-T$) in the solution for $0 \le t < T$ and adding them to those for times less than T. Equations were derived to incorporate the process that the NH_4^+ adsorbed on the solid phase, too, would undergo nitrification. However, the solutions were not given. Lindstrom and Boersma (1973) have already treated irreversible sorption-desorption models.

However, the models had not been assessed by quantifying these processes in an open soil system except for the oxidation of NO_2^- to NO_3^- in a mixed sand-soil column (Ardakani et al., 1973) until Starr et al. (1974) studied the simultaneous occurrence of nitrification, denitriifcation, and nitrogen movement in a soil column during a continuous unsaturated leaching. During a continuous application of NH_4Cl solution, analyses were made of the soil solution with soil depth and time for N as NH_4^+, NO_2^- and NO_3^-; and of the soil atmosphere for O_2, CO_2, N_2O and N_2. Solutions to the appropriate equations using measured reaction rate coefficients, pore-water velocities, and diffusion coefficients adequately described the steady state $NH_4^+ - N$ and $NO_3^- - N$ concentration distribution in the soil profile. Kirda et al. (1974) analyzed the nitrification and denitriifcation during the leaching of a pulse of NH_4NO_3 applied to the surface of unsaturated soil columns experimentally and theoretically. He used the equations derived by Misra et al. (1974) by using the principle of superposition. In many researches of this nature, the rate constants for the biodegradation of nitrogenous compounds have been derived using the curve fitting method. Kumar et al. (1984) stated that analytical solutions of miscible displacement equations have been used in several leaching studies of nitrogen transformation and these approaches allow estimation of nitrogen degradation rate coefficients from the nitrogen concentrations measured in leaching experiments as soil column effluents. In recent researches, numerical-analytical approaches have been used to simulate nitrogen dynamics in soil.

1.3 AIMS AND OBJECTIVES

The aim of this dissertation was to investigate qualitatively and quantitatively, the belowground behavior of nitrogen contained in *RWW*, using laboratory scale soil columns on two soil types, in order to evaluate the nitrate contamination due to the reclaimed wastewater irrigation. The research contained the following objectives:

1. Qualitative analyses of the dynamics of nitrogenous compounds together with several other water quality parameters using their transient and steady state profiles of the soil column experiments. The interrelation among the contaminants in this context were discussed, and the comparison of the intermittent and continuous irrigation of *RWW* was done using nitrogen & carbon mass balance calculations and the analyses of the stable isotopes of nitrogen;

2. Developing research-oriented analytical models to simulate nitrogen dynamics as a function of time and the spatial arrangement to estimate the apparent rate constants for the nitrification and denitrification, and to predict the quantity of NO_3^- -*N* leaching to the groundwater;
3. Conducting batch sorption experiments using vials to quantify the characteristics of adsorption and desorption of NH_4^+ and leaching of NO_3^-, of two soil types used for the column experiments;
4. Demonstration of the effects of concurrent applications of the simulated rainwater and simulated reclaimed wastewater intermittently, on the belowground behavior of nitrogenous compounds; and
5. Evaluation of simple precautionary measures to prevent nitrate pollution, using above-mentioned studies.

1.4 SCOPE OF STUDY

Two series of soil column experiments were conducted on two major soil types, found in the agricultural lands of Okinawa, namely mudstone (low porous) and limestone (high porous). One column from each soil type was loaded continuously and the other two columns were intermittently with *SRW*. The characteristic, in terms of nitrogenous compounds, of *SRW* was made approximately same as that of the *RWW* produced under the proposed project in Okinawa. The soil columns, which were unsaturated during the experiments, modelled the unsaturated zone of soil. The concurrent applications of *SR* and *IA* of *SRW* were meant to investigate the effects only due to the quantity of water. The effect of the composition of *SR* was beyond the scope.

The developed models only incorporate the processes of nitrification, denitrification and sorption of NH_4^+ onto soil. The sorption of NH_4^+ onto the negatively charged zones of soil was addressed using the linear form of Freundlich isotherm. First – order rate constants were assumed for both nitrification and denitrification. Two models were developed using the results of two soil columns irrigated continuously. The apparent rate constants of nitrification and denitrification for each column experiment were optimized.

1.5 RESEARCH METHODOLOGY

Figure 1.1 depicts the structure of the dissertation. First, a case study was conducted to study the activities of wastewater reclamation and reuse in Okinawa. The results of the experiments on several field lysimeters, which had been conducted by the Okinawa General Bureau, were analyzed to investigate the nitrogen dynamics.

Then, the laboratory scale soil column experiments were conducted. Before, the application of *SRW*, soil inside each column was leached with deionized water to remove all readily flushable compounds. The characteristics of initial and final soil, pore water and effluent collected periodically during the entire experimental runs were used to qualitatively analyze the dynamics of nitrogenous compounds due to *RWW* irrigation. An analysis on variation of the characteristics of nitrogen stable isotopes was conducted on the effluent and soil samples collected from the soil column experiments on low porous soil. In addition, the column, filled with low porous soil and having been subject to *IA* of *SRW*, was used to conduct an additional experiment to demonstrate the effects of concurrent applications of *SR* and *IA* of *SRW*, on the belowground behavior of nitrogenous compounds. Batch sorption experiments were conducted on both soil types to characterize the sorption of NH_4^+ and leaching of NO_3^-.

After that, analytical models were developed to simulate the dynamics of *NH_3-N* and $NO_3^- - N$ due to *CA* on two soil types. The models were calibrated in terms of the apparent rate constants of nitrification and denitrification.

Finally, the obtained results of the above-mentioned qualitative and quantitative analyses were used to discuss low-cost precautionary measures to prevent NO_3^- pollution due to *RWW* irrigation in Okinawa.

1.6 MAIN FINDINGS

It was found from the case study of the experiments on lysimeters in Okinawa, that the leaching of accumulated NO_3^- (originally present in the soil) into the percolating water had led to an inaccurate assessment of the actual dynamics of NO_3^- originating from the *RWW* itself. According to the soil column experiments, *CA* of *SRW* promotes denitrification in comparison with that of *IA*. In addition, the experiments demonstrated that the analysis of nitrogen stable isotope is an effective tool to determine nitrogen

dynamics in the soil. The nitrogen dynamics of low porous soil is more complicated than that of the high porous soil. The batch sorption experiments on both soil types, indicated that the adsorption of NH_4^+ onto soil is very quick, and leaching of soil NO_3^- into the solution of *SRW* is negligible. The adsorption capacity of NH_4^+ is higher in low porous soil than that of the high porous soil. The rainfall experiment suggested that the rainfall would accelerate the leaching of accumulated NO_3^- from soil.

Apparent rate constants for nitrification and denitrification of high and low porous soils subject to *CA*, could be optimized. These constants indicated that the nitrification and denitrification both had a significant effect on the NO_3^- dynamics. Therefore, with these rate constants, the developed models can be used to make reasonable predictions of NO_3^- leaching to the groundwater. These models could also be good enough to predict NO_3^- concentrations due to *CA* of *RWW* in low and high porous soils. In addition, if the rate constants and other input parameters are known, these models could be applied to any other place with some limitations.

The major finding of the study is that continuous or low-rate & short-interval drip irrigation under a green house would reduce the NO_3^- pollution in Okinawa. In accordance with the developed models, the steady state $NO_3^- - N$ concentration, due to the drip irrigation under a green house, that may exist in the groundwater in the fields containing high porous soil may exceed 10 mg/L, whereas the fields containing low porous soil are likely to be posed by the NO_3^- pollution if the groundwater table is shallower than 60 cm. Therefore, the appropriate reduction of the proposed irrigation rate of Okinawa-project or blending *RWW* with other type of water along with the drip irrigation under a green house would be a solution for the NO_3^- contamination on the island.

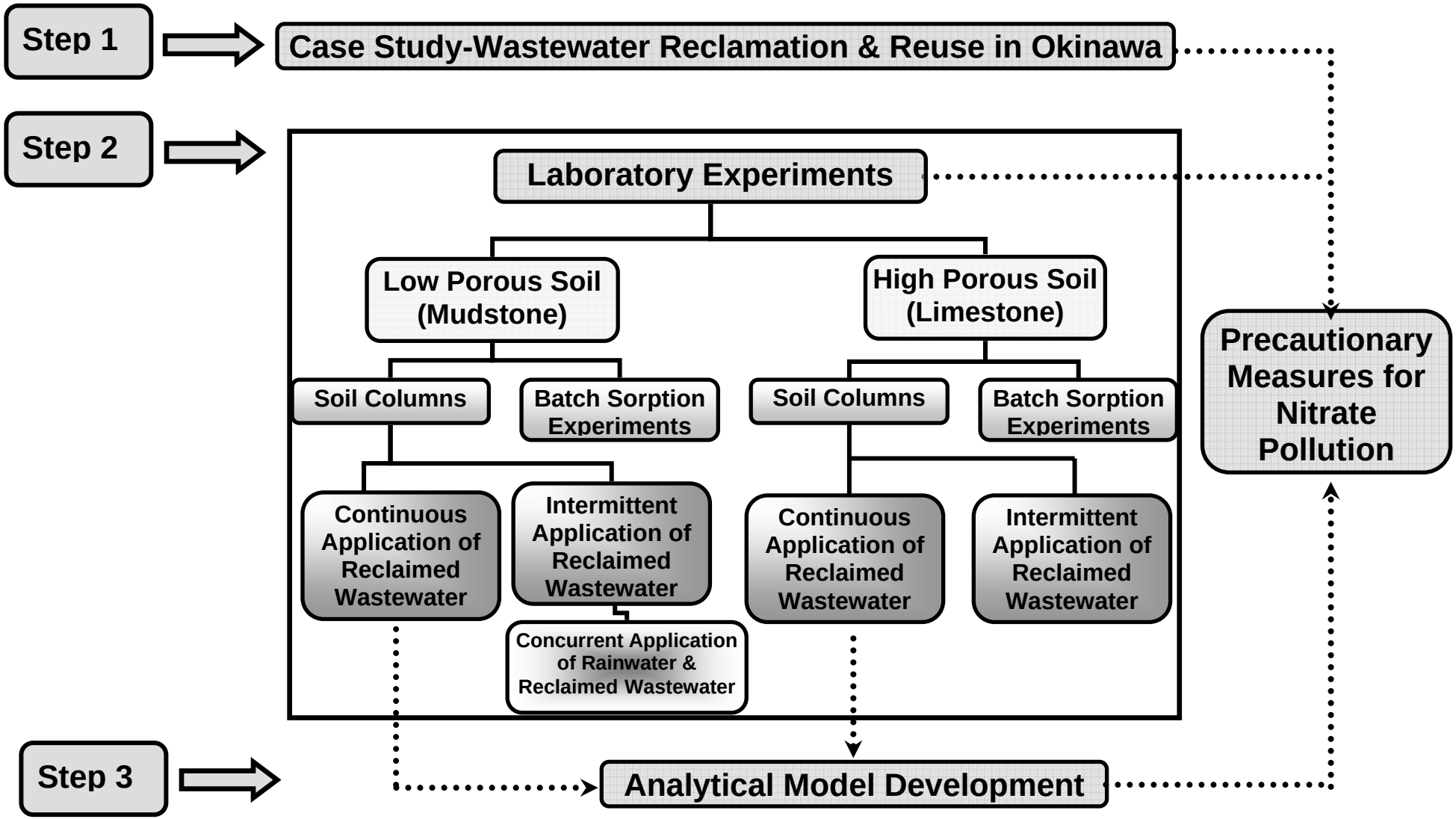

Fig. 1.1 Structure of the dissertation

1.7 PRESENTATION OF CHAPTERS

The dissertation consists of 7 chapters. Chapter 2 describes a case study carried out on the use of *RWW* for irrigation and urban activities in Okinawa, Japan. In this chapter, ongoing and planned activities of wastewater reclamation and reuse are discussed in detail. These include a proposed project on *RWW* irrigation, the experimental reclamation facility for irrigation, reclamation plant for urban use and experiments on field lysimeters.

Both chapter 3 and chapter 4 are on the two laboratory scale soil column experiments and two batch sorption experiments conducted on the low porous soil and high porous soil, respectively. In these chapters, belowground dynamics of nitrogenous compounds, together with several other compounds, due to *RWW* irrigation are discussed. In addition, the sorption kinetics of NO_3^- and NH_4^+ are discussed based on batch experiments.

Chapter 5 is on the analytical modeling based on the soil column experiments. It describes the derivation of governing equations, solution of the equations and optimization of the model-calibration parameters.

Chapter 6 is a discussion of the low-cost precautionary measures, based on the laboratory experiments and analytical models, that can be applied in Okinawa to mitigate the NO_3^- pollution.

Chapter 7 is the conclusions of the dissertation and further recommendations.

Appendix A shows more graphs related to the soil column experiments described in chapter 3 & 4.

Appendix B shows the data on soil physical characteristics, calculations of several model input parameters and several correlation graphs related to the developed models.

Appendix C shows the complete procedure of the solution of model equations.

Appendix D depicts several figures & photos related to the laboratory column experiments.

RFERENCES

Ardakani, M.S., J.T. Rehbock, and A.D. McLaren (1973), Oxidation of nitrite to nitrate in a soil column, *Soil Sci. Soc. Amer. Proc*., **37,** 53-56.

Asano, T. (1998), *Wastewater Reclamation and Reuse,* Vol. 10, Technomic Publishing Company, USA.

Cadisch, G., J.K. Ndufa, K. Yasmin, P. Mutuo, E.M. Baggs, G. Keerthisinghe, and A. Albrecht (2002), Use of stable isotopes in assessing belowground contributions to N and soil organic matter dynamics, 17th WCSS, Thailand, 14-21 August.

Cho, C.M. (1971), Convective transport of ammonium with nitrification in soil, *Can. J. of Soil Sci.*, *51***,** 339-350.

Dillon, P. (2000), Water Reuse in Australia: Current Status, Projections and Research. *In: Water Recycling Australia*, P. Dillon (ed.), CSIRO and AWA, 99-104.

El-Sadek, A., K. Oorts, L. Sammels, A. Timmerman, M. Radwan, and J. Feyen (2003), Comparative Study of Two Nitrogen Models, *Journal of Irrigation and Drainage Engineering*, *129*(1), 44-52.

Gardner, T., A.Vieritz (2004), Assessment of the Risks Associated with Irrigation Using Reclaimed Water; Sewage Management: Risk Assessment and Triple Bottom line, EPA Conference: Cairns.

Hallberg, G. R., D. R. Keeney (1993), *Nitrate in Regional Ground-Water Quality*; W.M. Alley (ed), Van Nostrand Reinhold: New York, USA.

Heaton, T.H.E. (1986), Isotope studies of nitrogen pollution in the hydrosphere and atmosphere: a review, *Chem. Geol.*, *59*, 87-102.

Jiao, Y., W.H. Hendershot, J. K. Whalen (2004), Agricultural Practices Influence Dissolved Nutrients Leaching through Intact Soil Cores, *Soil Sci. Soc. Am. J., 68***,** 2058.

Kirda, C., J.L. Starr, C. Misra, J.W. Biggar, and D.R. Nielsen (1974), Nitrification and denitrification during miscible displacement in unsaturated soil, *Soil Sci. Soc. Amer. Proc*., *38***,** 772-776.

Kumar, V., R.J. Wagenet (1984), Salt effects on urea hydrolysis and nitrification during leaching through laboratory soil columns, *Plant and Soil 85*, pp. 219-227, Martinus Nihoff/Dr. W. Junk publishers, The Nethrlands.

Lindstrom, F.T., and L. Boersma (1973), A theory on the mass transport of previously distributed chemicals in a water saturated sorbing porous medium: III. Exact solution for first order kinetic sorption, *Soil Sci.*, *115*, 5-10.

McLaren, A. D. (1969a), Steady State Studies of Nitrification in Soil: Theoretical Considerations, *Soil Sci. Soc. Amer. Proc*., *33***,** 273-275.

McLaren, A. D. (1969b), Nitrification in soil: Systems approaching a steady state, *Soil Sci. Soc. Amer. Proc*., *33***,** 551-556.

McLaren, A. D. (1970), Temporal and vectorial reactions of nitrogen in soil: A review, *Can. J. of Soil Sci.*, *50***,** 97-109.

McLaren, A. D. (1971), Kinetics of nitrification in soil growth of nitrifiers, *Soil Sci. Soc. Amer. Proc*., *35***,** 91-95.

Meisinger, J.J. and J.A. Delgado (2002), Principles for managing nitrogen leaching, *J. Soil Water Conserv.*, **57**, 485-498.

Misra, C., D. R. Nielsen, and J. W. Biggar (1974), Nitrogen Transformations in Soil during Leaching; I. Theoretical Considerations, *Soil Sci. Soc. Amer. Proc*., *38***,** 289.

Murphy, D.V., A.J. Macdonald, E.A. Stockdale, K.W.T.Goulding, S. Fortune, J.L. Gaunt, P.R. Poulton, J.A. Wakefield, C.P. Webster, and W.S. Wilmer (2000), Soluble organic nitrogen in agricultural soils, *Boil. Fertil. Soils.*, *30*, 374-387.

Nolan, B. T., K. J. Hitt, and B. C. Ruddy (2002), Probability of Nitrate Contamination of Recently Recharged Groundwaters in the Conterminous United States, *Environmental Science and Technology*, *36***,** 10.

Pucket, L. J. (1994), Nonpoint and Point Sources of Nitrogen in Major Watersheds of the United States, *Report Geological Survey Water- Resources Investigations*, 94-4001, USA.

Report on Public Sewage Treated Water for Agriculture Use (1983), Kumamoto Municipal Government, Japanese Version.

Sewage Works in Japan (2005), Japan Sewage Works Association, Tokyo, Japan.

Shinohara, H., T. Tanishima, S. Kojima, S. Managaki, H.Takeda, N. Nakada, H. Tanaka, and H. Furumai (2004), Water-soluble organic micro-pollutants in municipal wastewater and their removal during advanced treatment, Proceedings of 2nd International Symposium on Southeast Asian Water Environment, Department of Urban Engineering and Research Center for Water, 356-363.

Starr, J. L., F. E Broadbent, and D. R. Nielsen (1974), Nitrogen transformations during continuous leaching, *Soil Sci. Soc. Amer. Proc*., *38***,** 283.

Water and wastewater reuse, an environmentally sound approach for sustainable urban water management (2005), United Nations Environment Program (UNEP) and Global Environment Center (GEC) Foundation, Division of Technology, Industry and Economics (DTIE), Nairobi, Kenya.

CHAPTER 2

CASE STUDY: UTILIZATION OF RECLAIMED WASTEWATER FOR IRRIGATION AND URBAN ACTIVITIES IN OKINAWA, JAPAN

2.1 INTRODUCTION TO OKINAWA

Okinawa Island is located southwards of the Japan main island. It has very few surface water bodies for rainfall retention and therefore, fresh water resource is a limited commodity. It suffers terribly from a scarcity of water resources due to the island being lack of natural water bodies to retain the plentiful annual precipitation (about 2000 mm/year) and being deficient in appropriate lands for the construction of dams. Being a threat to an endangered fish species and a bird habitat has prevented the construction of dams as a solution. In addition, nowadays, securing water resources using dams is difficult owing to the opposition from the public for constructing new dams as a result they are well aware of the importance of conserving the global and local environments. Hence, *RWW* irrigation has been introduced as an alternative to the ever increasing irrigation water demand on the island. Currently, *RWW* is utilized for various urban activities on large-scale. At present, *RWW* plays a vital role in toilet flushing, road washing, and sprinkling on trees and plants in some urban areas in Naha City, the Capital of the Okinawa Prefecture. Okinawa General Bureau, the Cabinet Office and Okinawa Prefecture promote using *RWW* for these activities. The largest project centres on the *NWTP* where the secondary treated wastewater is further given advanced treatments to produce *RWW*, which is sent to buildings in Naha City. Recently, cultivations of vegetables, tropical fruits and floriculture in Simajiri District, located in the southern part of the main island of Okinawa, have been making healthy profits. This is because the district is located in close proximity to Naha City, the largest commercial area in Okinawa, with a major harbour and an airport for shipping goods to the other commercial areas in Japan. The outskirt of the district is covered by a cultivation of sugarcane. However, the condition is often obstructed by the prevailing deficiency of the irrigation water for which this region relies on the water resources such as ponds and the underground water. The insufficiency and the unstable nature associated with such means of irrigation have drawn the attention immensely over

the profitable usage of *RWW* as an agricultural water resource in this region. It has targeted the discharged secondary treated wastewater of the *NWTP*, located in the neighbourhood of the district, the capacity of which is about 130,000 m^3 /day as the discharging rate. The discharging rate of the *NWTP* is sufficient to supply the total agricultural water demand in Simajiri District (about 2300ha). In relation to this, a project on *RWW* irrigation has been planned and will be implemented in the real practice on large-scale within the next few years. Upon the implementation of this project, Okinawa will pioneer utilizing *RWW* as an alternative water source for the agricultural irrigation in Japan. This project will benefit an area of 2051 ha of sugarcanes, vegetables, fruits and flowers by supplying *RWW* for the irrigation. People in Okinawa show strong enthusiasm in the water reuse and reclamation. As stated by Dillon (2000), the acceptance of *RWW* irrigation schemes is invariably high in market research surveys. It shows that the public reaction regarding the *RWW* irrigation is positive not only in Okinawa but also in the other parts of the world.

Currently, the secondary treated wastewater at abundant levels in the *NWTP* is reclaimed in conjunction with the above-mentioned project targeting a discharging rate of 60,000 m^3/day in the future. Various investigations have been executed to date, following the establishment of a committee in 1998 to examine the possibility and the validity of the scheme of *RWW* irrigation. Issues related to the safety in using *RWW*, the influence on the crop quality and the environmental effects in terms of soil and groundwater pollution have been of concern since then. Health issues are usually near the top of the list when surveys are undertaken on community and scientific concerns about reuse (Asano, 1998 and Dillon, 2000). Likewise, the past and ongoing investigations in Okinawa have been paying the greatest attention on adverse effects on the human health caused by pathogenic organisms, in relation to the consumption of the crops irrigated with *RWW*. The issues related to the adverse effects on the environment are comparatively paid less attention. Among the few investigations on adverse environmental effects, the experiments on field lysimeters play a major role. Field lysimeters are located in several experimental fields. In these lysimeters, the percolating water through soil, after being irrigated with *RWW*, is collected to conduct water quality analyses. However, the leaching of accumulated NO_3^- (originally present in the soil) into the percolating water has led to an inaccurate assessment of the actual dynamics of NO_3^- originating from the *RWW* itself.

The irrigation water criteria on *RWW* have not yet been decided in Japan because there exists only a few number of irrigation projects using *RWW*, and there are various

types of crops, and the standards should be established separately for each type of crop. However, the guidelines for the quality of *RWW* for the planned project have already been established based on the 'Title22' ordinance (CDHS, 1978) of the California State of United States that is the most stringent standard of recycling the wastewater in the world to ensure the personal safety in a scientific manner. The 'Title 22' system has been preferred owing to the fact that the treatment train described in 'Title 22' seems guaranteeing the sufficient safety for pathogenic infectious risks represented by enteric viruses, which may occur due to uncooked vegetables irrigated with *RWW* (Tanaka et al., 1998).

2.1.2 Wastewater Treatment Plant in Naha City, Okinawa (NWTP)

2.1.2.1 Preliminary, primary and secondary treatments

Raw wastewater in combined sewers, in which the sewage consists of wastewater from industries, households and rainwater pipes are pumped to the *NWTP* (**Fig. 2.1**), which belongs to the Water Service Management Office, Okinawa Prefecture. The secondary treatment includes the coarse screening, grit removal, primary sedimentation and the activated sludge process. Nitrification is depressed in the process due to the limitation of the capability. Following the activated sludge process, a part of the secondary treated wastewater is directed to a wastewater reclamation unit.

Fig. 2.1 Aerial view of NWTP.

2.1.2.2 Experimental reclamation facility for irrigation

Figure 2.2 depicts the schematic diagram of the experimental reclamation facility adopted in the *NWTP*. This will be the source of *RWW* for the agricultural irrigation in

Simajiri district under the planned project. A portion of the secondary treated wastewater will be transported to this unit, which will have a capacity of 7×10^4 m^3/d although the present bench scale experimental facility has 40 m^3/d. *RWW* applied to experimental fields at present is delivered by vehicles. However, *RWW* will be pumped with the force mains stored in farm ponds and distributed to the farming areas, once the aforesaid project is in practice. The effluent from this plant will be supplied to an agricultural area of 2050 ha.

As stated by Asano (1998), upon the specific application of *RWW*, the degree of treatment required and the extent of necessary monitoring are determined. Irrigation on crops consumed as foods and the application of *RWW* on lands having frequent human contacts demand a higher degree of treatments. It is compulsory that every *RWW* application should at least be preceded by an effective secondary treatment (Asano, 1998). The process of disinfection for the control of pathogenic organisms is often the final treatment step prior to distribution for reuse. The quality of *RWW* discharged by this plant is in accordance with the "Title22" ordinance. Initially, the necessity for confirming the possibility of applying the "Title22" ordinance was important because of the difference of the meteorological and sewage disposal conditions, etc. between the Simajiri District and the California State. In order to achieve this, a demonstrating plant {cohesion precipitation → sand filtration → disinfection} in accordance with the reclamation facility adopted in the United States was first established, and the suitability was confirmed following an event of reclaiming the secondary treated wastewater from the *NWTP*.

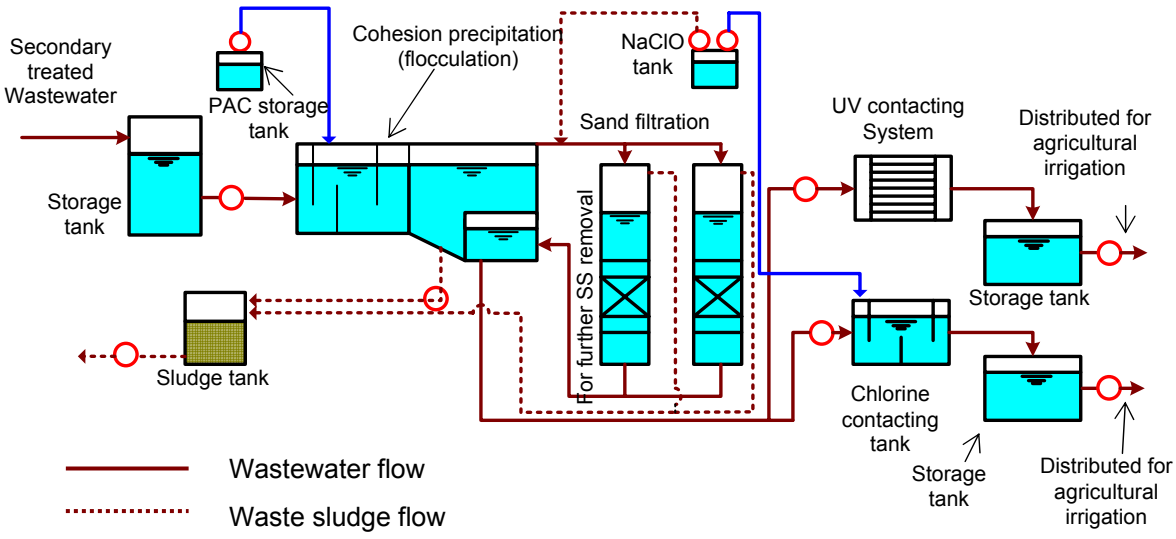

Fig. 2.2 Schematic diagram of the experimental reclamation facility for agricultural irrigation at NWTP.

In this plant, the secondary treated wastewater is first directed to a process of cohesion precipitation using *PAC* in order to remove suspended solids and pathogens further. Then, the effluent is directed to a downward multimedia filtration unit, in which the further removal of solids and pathogens takes place following the sedimentation. Then, a portion of the filtered wastewater is carried to a *UV* chamber where a low-pressure *UV* light is passed through the wastewater to remove pathogenic micro organisms. The other portion is directed to chlorine contact chambers. The rate of chorine application is either 3.18 mg/L or 7.6 mg/L with *CT* values being 382 and 912, respectively. The objective of applying two disinfection processes is to compare the efficiency of both the processes in removing different pathogenic organisms. According to the previous experiments, chlorination has responded better in the viewpoint of removing coliforms. Other than that, there has been no significant difference in the treated effluent quality with regard to being chlorinated or *UV* disinfected. However, there is no unit process for the removal of excess nitrogen.

Monitoring of coliforms and colipharges indicated that at least 6-log removal of viruses can be expected in the total reclamation system, which applies both *UV* and chlorine disinfections. It guarantees the enough ability of removing enteric viruses as high as the treatment system described in 'Title 22'. The infectious risk caused by the enteric viruses if the vegetables irrigated with *RWW* are eaten raw, is expected to be lower than 10^{-4} per year. It is considered to be acceptable according to the drinking water standards of *USEPA* (Tanaka et al., 1998). *RWW* from the above plant can meet with the standards of the regulated toxic contaminants in the drinking water accepted by the Ministry of Heath and Labour in Japan. However, unregulated contaminants including estrogens and suspected *EDCs* really exist at trace levels. Emerging *PPCPs* are suspected to remain in *RWW* (Shinohara et al., 2004). The effect of *EDCs* and *PPCPs* on the human health via the irrigation is still unknown. Some trace organics such as estrogens seem easily biodegradable during the soil aquifer treatment system (Tanaka et al., 2005), but others may be persistent.

2.1.2.3 Secondary treated wastewater reclamation for miscellaneous uses

There exists another reclamation facility (**Fig. 2.3**) in the *NWTP* for supplying *RWW* for miscellaneous purposes except the agricultural irrigation. At present, this plant runs at a capacity of 2300 m^3/d. The secondary treated wastewater is first directed to a biological contact filter, in which the influent is sprayed from the top of the tank for the aeration.

100 % of NH_4^+ is nitrified and the residual organics are further removed before proceeding to an ozonation tank. BOD_5 drops from 15 mg/L to 1.5 mg/L. The final process is chlorine disinfection, which takes place inside the distribution mains. The quality of the produced *RWW* is automatically assessed in terms of *pH*, temperature, conductivity, residual chlorine, color and turbidity by means of respective meters kept in a control panel. The initial residual chlorine concentration at the wastewater reclamation plant is kept at 10 mg/L in order to achieve a minimum concentration of 0.4 mg/L at any point in the distributing mains. Currently, *RWW* from this plant is distributed in an area measuring maximum 1 km distance from the reclamation plant in order to be used for various activities in buildings such as high schools, condominiums and government offices; road washing and sprinkling on trees.

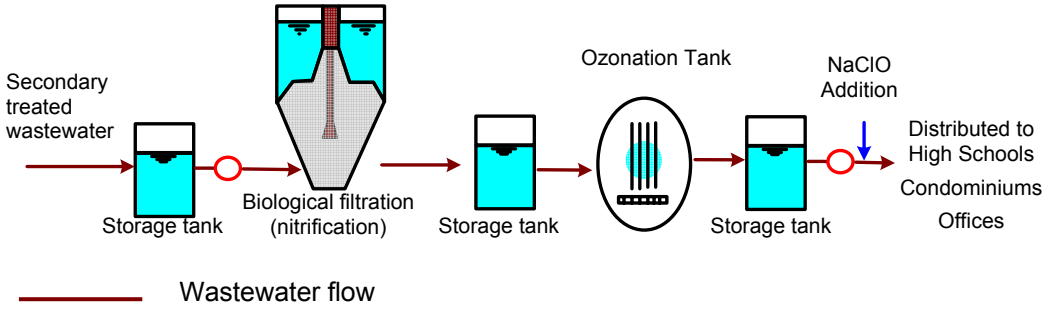

Fig 2.3 Schematic diagram of the reclamation facility for miscellaneous usage at NWTP.

2.1.3 Ongoing Environmental Based Researches in Okinawa

2.1.3.1 Field lysimeters at Tomigusuku city

There is an experimental field at Tomigusuku city in Okinawa, which houses three field lysimeters. The major soil type of this field is mudstone (called 'Jargal'in Japanese). It is a less porous, calcareous and gray plateau soil, which is the dominant soil type in Okinawa. The Okinawa General Bureau conducted two field experiments during the periods from 14th November 2003 to 19th March 2004 (Experiment 1) and from 29th September 2005 to 22nd March 2006 (Experiment 2). The possibility of using *RWW* produced by the *NWTP* for the agricultural irrigation was the primary objective of these experiments. These investigations comprised both crop quality and environmental quality surveys.

Lysimeter experiments belonged to the environmental quality survey, objective of which was to understand the influence exerted on the underground water and soil by the

constituents contained in *RWW* used for the cultivation. *T-N* of *RWW* from the *NWTP* was 20-30 mg/L, of which 70-80% was $NH_4^+ - N$. Since the possibility of the occurrence of NO_3^- is extremely high, the web of adverse effects resulting from the excess NO_3^- are likely to arise. Therefore, the below ground dynamics of $NO_3^- - N$ were the main subject of these experiments. Na^+ and Cl^- concentrations of *RWW* were within 300 – 500 mg/L and more than 500 mg/L, respectively because of the influence of the inflow of seawater into sewers. Therefore, the influence of Na^+ and Cl^- on the crop quality and the salt accumulation in the soil were also focused on, as they seem to be prominent threats.

2.1.3.2 Field lysimeters at the Faculty of Agriculture, Ryukyu University

There is an earthen lysimeters at the Faculty of Agriculture of Ryukyu University, Okinawa. This lysimeters contains the high porous limestone soil (called 'Simajiri-mahji' in Japanese) extracted from a field that was used for the cultivation previously. Limestone, which is comparatively high in porosity, is the second most available soil in Okinawa. There is a series of researches carried out using this experimental field. An experiment (Experiment 3) carried out during the period from October 2004 to February 2005 is described in detail in this chapter. The objectives were to conduct a survey of nitrogen dynamics and to understand the adverse environmental effects. Investigating how *RWW* would affect the crop quality and cultivation was also among the objectives.

Fig. 2.4 Green housed experimental field.

2.1.3.3 Green housed experimental field

Figure 2.4 illustrates another experimental field, which is in a greenhouse, managed by the Okinawa Prefectural Agricultural Experimental Centre. The primary objective of the past experiments conducted in this field was to investigate how much fertilizer could be reduced by applying *RWW* because it contains nitrogenous compounds, Na^+ and Cl^-. Examinations on the tolerance limit of salt in pumpkin and lettuce etc. have been conducted, and the accumulation of Na^+ and Cl^- in soil have been investigated too. In this

chapter, an experiment (Experiment 4), which was conducted in this field from 18th November 2004 to 25th January 2005 to assess the effect of *RWW* on the crop quality and the fertilizer value of *RWW*, is described in detail.

2.2 METHODOLOGY

2.2.1 Field lysimeters at Tomigusuku city

Figure 2.5 schematizes the Tomigusuku city- experimental field. The field is divided into three blocks each having a field lysimeters adjacent to it. Each block has three 12 m x 3m sized rows. Each lysimeter (**Fig. 2.6 and Fig. 2.7**) is 1 m deep. There were $1m^2$ - blocks on either side of each lysimeter, as shown by the plan view of Fig. 2.7, which was applied with *RWW* so that the percolating water could be collected at different levels of the underneath soil. Two $1m^2$- blocks on either side of each lysimeters were given the same treatment as the respective adjacent field. When the field was cultivated, these two blocks were cultivated with the same crop too. The large area was used for the experiments related to the agricultural purposes. There were three ports at 30 cm, 60 cm and 90 cm depths below the ground level, on both sides of the lysimeters so that each two ports at the same level faces each other. These ports are extended to 0.5 m inside the soil so that samples can be collected along a vertical line that goes through the centre of each 1 m^2-block. A porous cup-soil water sampler attached to a vacuum pump was used to extract the percolating water through these ports (*S1*, *S2* and *S3*). There were two containers kept at the bottom at 100 cm level in order to collect the percolating water at that level (*S4*). During the experiments 1 & 2, each block was irrigated with *RWW1*, *RWW 2* and *GW*, respectively, as shown by Fig. 2.5. The block irrigated with *GW* containing negligible contaminants, was considered as the control field. *RWW* was obtained from the experimental reclamation facility and stored in the storage tanks at the experimental site. Irrigation was done using a traditional watering can on each $1m^2$-block (**Fig. 2.8**) while the rest of the field was irrigated using a sprinkler system.

2.2.1.1 Experiment 1

Pumpkins were transplanted on 14th November 2003 and were harvested on 19th March 2004. Chemical fertilizers were applied on all the blocks during the cultivation. The entire experiment 1 was carried out during the cultivation period. On the previous day of each sampling, $1m^2$ - block was given *RWW* up to 30 mm height above the surface. At *S1*,

S2, *S3* and *S4*, percolating water was sampled once every two- week (from 25th December 2003 to 4th February 2004), and the percolating water and the influent were analyzed in terms of $NH_4^+ - N$, $NO_3^- - N$, *T-N*, Cl^-, SO_4^{2-} and several cations.

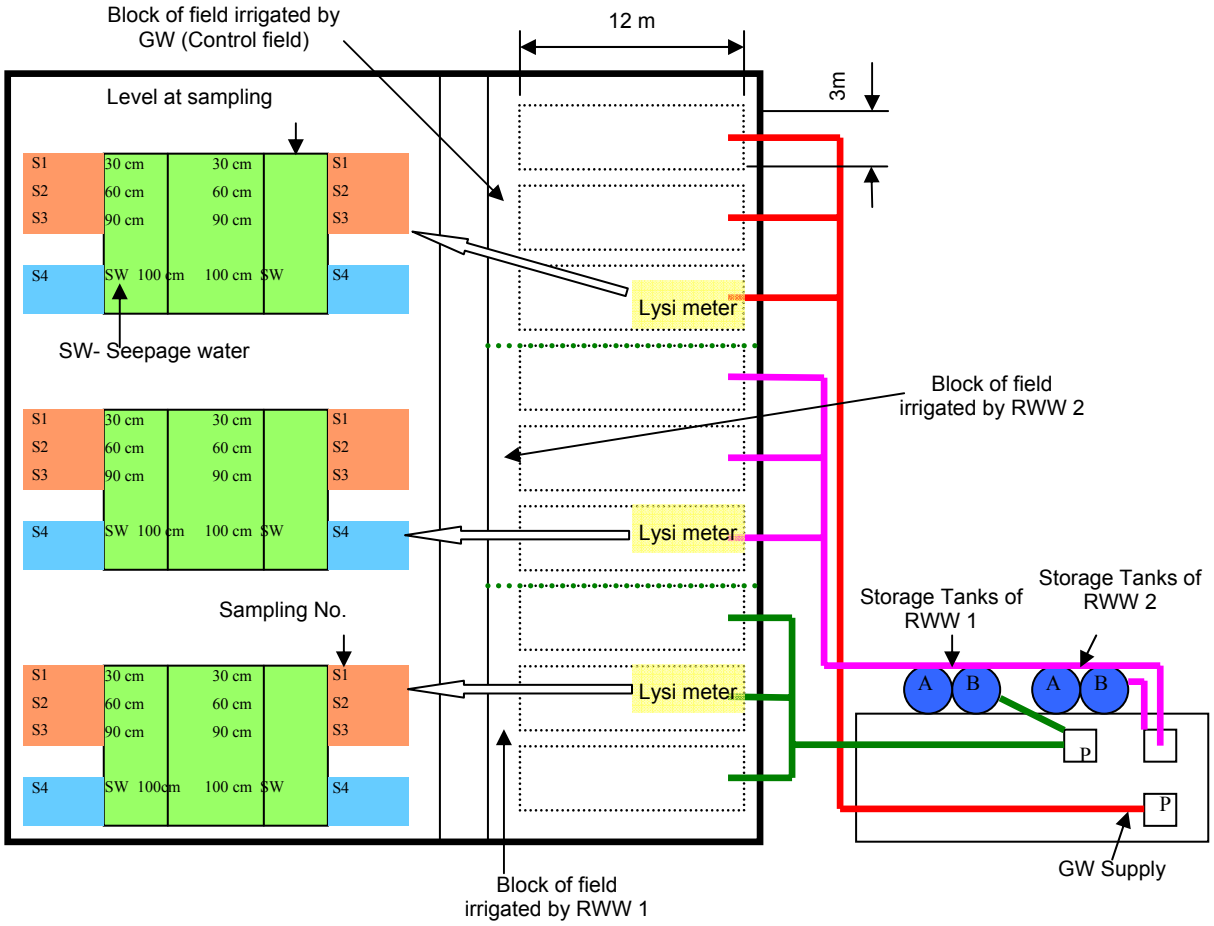

Fig. 2.5 Schematic diagram of Tomigusuku city experimental field.

Fig. 2.6 Lysimeter at Tomigusuku city.

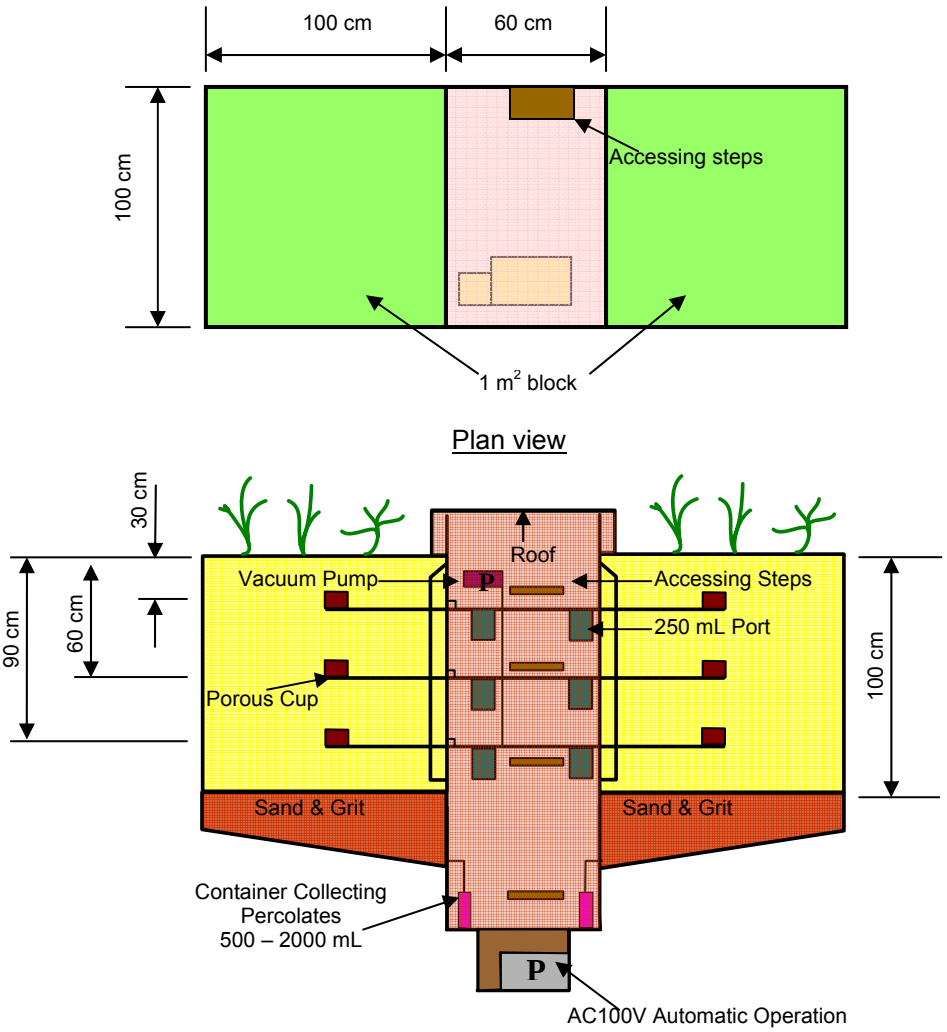

Fig. 2.7 Plan view and sectional elevation of the lysimeters at Tomigusuku city.

Fig 2.8 Lysimeter at Tomigusuku city when being irrigated.

2.2.1.2 Experiment 2

The influence of fertilizer on the characteristics of the percolating water was remarkably confirmed in the experiment 1. Therefore, the usage of fertilizer was much

avoided in the experiment 2 in order to investigate the sole effect due to *RWW*. Comparing both the experiments 1 & 2, the experiment 2 can be considered to be in favor of assessing the environmental impacts the most. Pumpkins were transplanted on 19th November 2005 and were harvested on 22nd March 2006. *RWW* was applied three times every week during the experimental period so that the ground was covered by total of 30 mm depth of water per every week. The frequency of sampling was once every 1-2 week. From 29th September 2005 to 9th November 2005, samples were collected 6 times prior to the cultivation. From 16th November 2005 to 7th December 2005, samples were collected 3 times during the cultivation. Nitrogenous compounds in terms of *T-N* and $NO_3^- - N$, Na^+, Cl^- and *EC* were analyzed in the collected percolating water samples and the influent.

2.2.2 Field lysimeters at the Faculty of Agriculture, Ryukyu University (Experiment 3)

Figure 2.9 depicts the lysimeters at Ryukyu University premises, which consists of four blocks (1, 2, 3 and 4) each is 364 cm x 210 cm. The experimental field is not affected by the rainfall since it is covered. There are four sample-collecting tanks in the underground of the lysimeters at approximately 1m depth from the surface (**Fig. 2.10**). During the experimental period, bitter gourd was grown on two blocks (1 & 2), and there was no cultivation on the other two blocks (3 & 4). The blocks 1 & 3 were irrigated with *RWW2* while the blocks 2 & 4 were with the tap water. Water samples collected from each block was allowed to accumulate in the respective sample-collecting tank in the underground. The collected samples were analyzed in terms of *pH*, *EC*, $NH_4^+ - N$, $NO_3^- - N$, PO_4^{3-}, Cl^-, Na^+, K^+, Ca^{2+} and Mg^{2+}. Samplings and analyses were executed three times for each block keeping the duration between two consecutive samplings to be 2 weeks. The irrigation rate was 30 mm/week. The influent characteristics were in the similar nature as that of the experiments in Tomigusuku city- field. The significant feature of the influent is that it possessed a high average *T-N* content of 22 mg/L, which mainly existed as $NH_4^+ - N$.

2.2.3 Green housed experimental field (Experiment 4)

Lettuce was grown under the influence of the fertilizer. Fertilizer was applied on the field on 18th November 2004 preceding the transplant on 24th November 2004, and the

harvesting was done on 25th January 2005. *RWW* was sprinkled at a frequency of 20 mm /week. The width and length of leaves, number of leaves, chlorophyll meter value (*GM* value) and the weight were obtained in order to investigate the effect of *RWW* irrigation on the crop quality. An inorganic element analysis of crops was carried out in terms of *N*, Ca^{2+}, Mg^{2+}, Na^{+}, *Fe*, *Mn*, *Zn* and *Mo*. In addition, the soil chemistry before and after the cultivation was examined in terms of exchangeable cations such as Na^{+},K^{+},Ca^{2+},Mg^{2+} and anions such as Cl^{-}, SO_4^{2-}, PO_4^{3-} and NO_3^{-}, pH, *T-N* and *EC*.

Fig. 2.9 Earthen lysimeters.

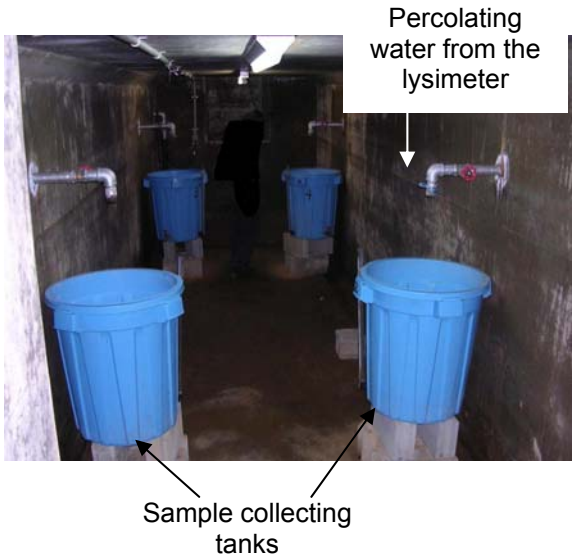

Fig. 2.10 Earthen lysimeters-underground.

2.3 RESULTS AND DISCUSSION

2.3.1 Field lysimeters at Tomigusuku city

2.3.1.1 Experiment 1

Figure 2.11 (a), (b), (c) & (d) indicates the variation of $NH_4^{+}-N$, $NO_3^{-}-N$ and *T-N* with depth for the percolating water collected from the lysimeters irrigated with *RWW1* and *RWW2* at 1st, 2nd, 3rd and 4th samplings, respectively. The diminution of $NH_4^{+}-N$ contained in the influent occurred within a depth of 30 cm from the ground level. Figure 2.11 (d) indicates that both $NO_3^{-}-N$ and *T-N* rapidly increased at 30 cm-level at the 4th sampling, and there was a trend for both the concentrations to commence decreasing in the layers below 30 cm depth. $NO_3^{-}-N$ concentration of the water samples collected at all the levels exceeded *T-N* concentration of the influent at 1st sampling onward.

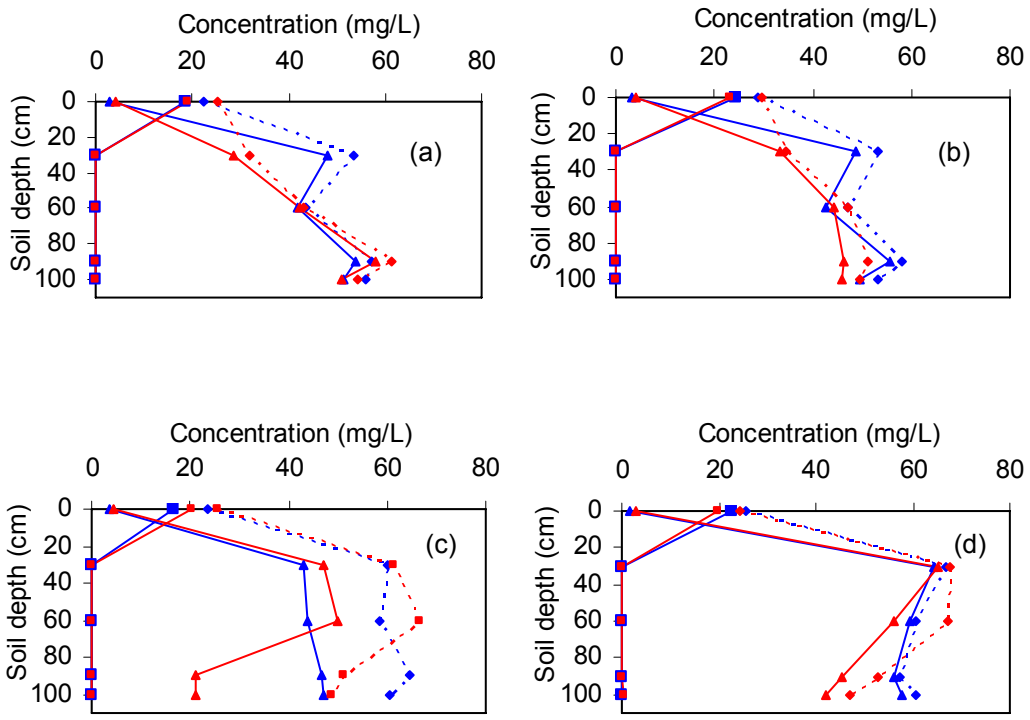

Fig. 2.11 Variation of NH_4^+-N (solid line with boxes) , NO_3^--N (solid line with triangles) and T-N (dashed line with diamonds) with depth at (a) 1st sampling; (b) 2nd sampling; (c) 3rd sampling; and (d) 4th sampling (experiment 1) due to RWW 1(blue) and RWW 2 (red).

The diminution of $NH_4^+ - N$ may possibly be due to the nitrification and adsorption onto the negatively charged soil colloidal particles. Some adsorbed NH_4^+ may have been used by the crops as a nutrient. The elevated levels of $NO_3^- - N$ & $T\text{-}N$, which exceeded the respective concentration in the influent, may be the result of the leaching of accumulated nitrogenous compounds of the soil and soil water into the percolating water. It can be guessed that NO_3^- may have originated from the applied manure too and $NO_3^- - N$ of the manure may have leached as NO_3^-. The decreasing trend of $NO_3^- - N$ and $T\text{-}N$ concentrations beyond the 30 cm level can be attributed to the effect of denitrification in the underlying layers. The extent of the contribution of RWW to $NO_3^- - N$ of the percolating water is uncertain in this experiment. There were several occasions that the volume of percolating water was insufficient and some additional water (approximately 20 L on each $1m^2$-block at each sampling) was applied in order to collect enough samples. Therefore, the results obtained from this experiment do not seem very much realistic.

2.3.1.2 Experiment 2

Figure 2.12 (a) & (b) depicts the variations of $NO_3^- - N$ and *T-N* with time of all the water samples collected from the lysimeters irrigated with *RWW1*, respectively, while the same for the samples collected from the lysimeters irrigated with *RWW2* is depicted by **Fig. 2.13 (a) & (b)**, respectively. There was a gradual increment of $NO_3^- - N$ with time in the water samples at every level of the fields irrigated with *RWW1* & *RWW2* {Fig. 2.12 (a) & 2.13 (a)}. *T-N* of the influent totally became $NO_3^- - N$ within 30 cm depth in both the cases {Fig. 2.12 (b) & 2.13 (b)}. Further, as shown by Fig. 2.12 & 2.13, there was a trend that both $NO_3^- - N$ and *T-N* concentrations gradually decreased with depth. There was a rapid increment of $NO_3^- - N$ and *T-N* concentrations between the last two consecutive samplings, which were under the influence of manure. In addition, *T-N* concentration of all the water samples exceeded the respective influent concentration except one case at the 8th sampling, in which the influent (*RWW1* & *RWW2*) contained a very high *T-N*.

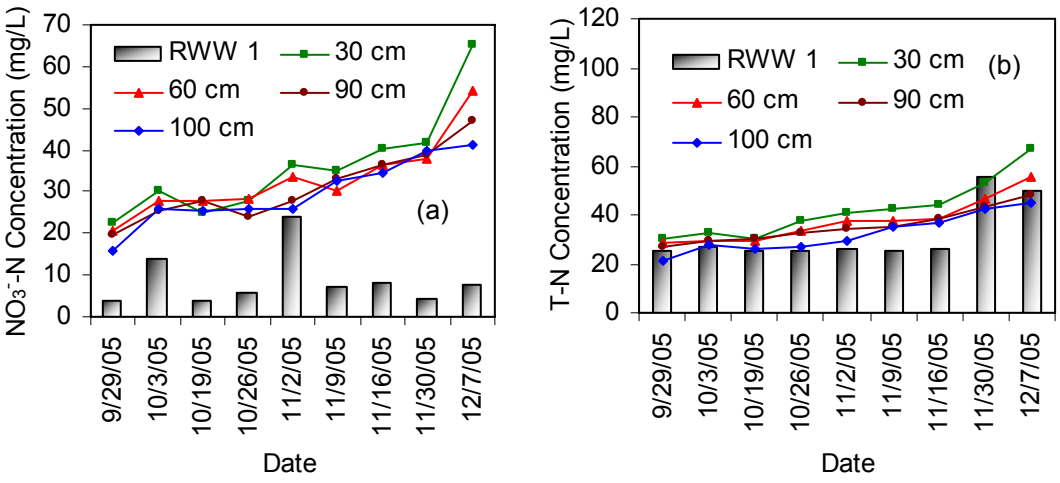

Fig. 2.12 Variation of (a) NO_3^--N and (b) T-N with time for the percolating water collected from the lysimeters irrigated with RWW 1 in experiment 2.

Figure 2.14 (a) and (b) denotes the variation of $NO_3^- - N$ and *T-N* with time in the water samples collected from the lysimeters irrigated with *GW*. $NO_3^- - N$ concentration of *GW* was always less than 0.5 mg/L. However, $NO_3^- - N$ in all the samples rose to about 30-40 mg/L. Therefore, it is assumed that it may have occurred due to the leaching of accumulated nitrogenous compounds from the soil and soil solution. It can be assumed that the source of NO_3^- from the soil and soil solution has started to attenuate because

$NO_3^- - N$ and *T-N* gradually increased and then started to decrease at 6th sampling in the sample collected at 30 cm depth preceding that the percolating water collected at 60 cm depth underwent the same behavior at 7th sampling. The percolating water collected at both 90 cm and 100 cm depths would have undergone the same trend if the duration of the experiment had been extended. In the case of *RWW*, there were two sources of NO_3^-, which were the influent and soil, the former of which caused the concentration to be still in the increasing phase though the latter had commenced the attenuation.

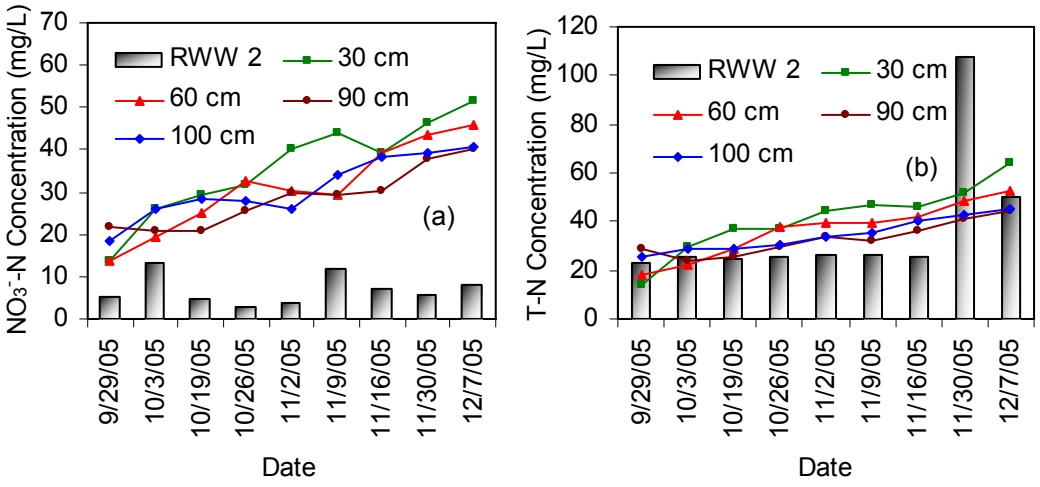

Fig. 2.13 Variation of (a) NO_3^--N and (b) T-N with time for the percolating water collected from the lysimeters irrigated with RWW 2 in experiment 2.

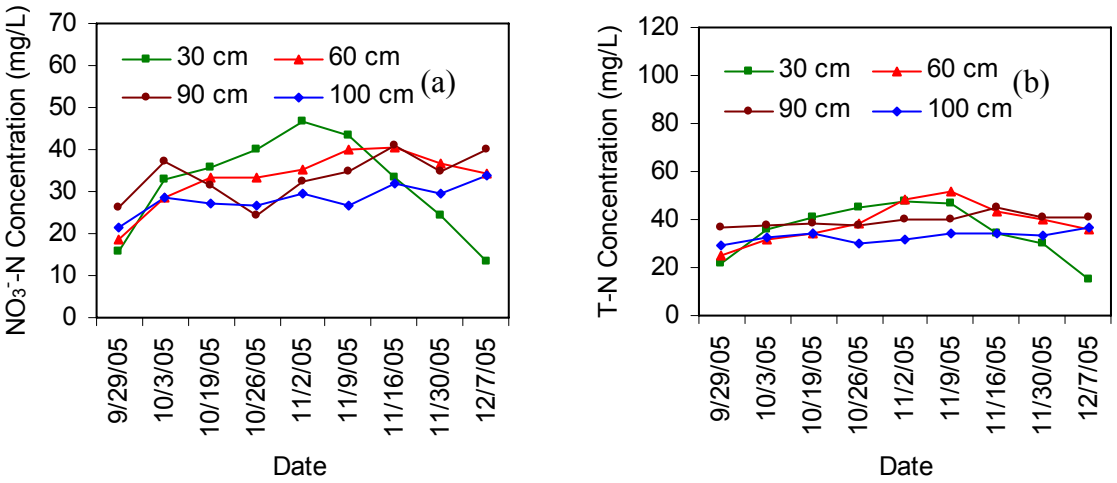

Fig. 2.14 Variation of (a) NO_3^--N and (b) T-N with time for the percolating water collected from the lysimeters irrigated with GW in experiment 2.

Figure 2.15 (a), (b) & (c) show the variation of $NO_3^- - N$ and *T-N* with depth for the percolating water collected from the lysimeters irrigated with *GW*, *RWW1* & *RWW2* at the first sampling, last sampling & for the average of all the samplings, respectively. It is visible that *T-N* almost occupied $NO_3^- - N$ by the conclusion of the experiment (Fig.2.15 b). It can be assumed that the nitrification of the influent $NH_4^+ - N$ may have completely undergone within the zone above the 30 cm level because there was a larger gap between *T-N* and $NO_3^- - N$ above the 30 cm-level, and the gap narrowed below the 30 cm-level.

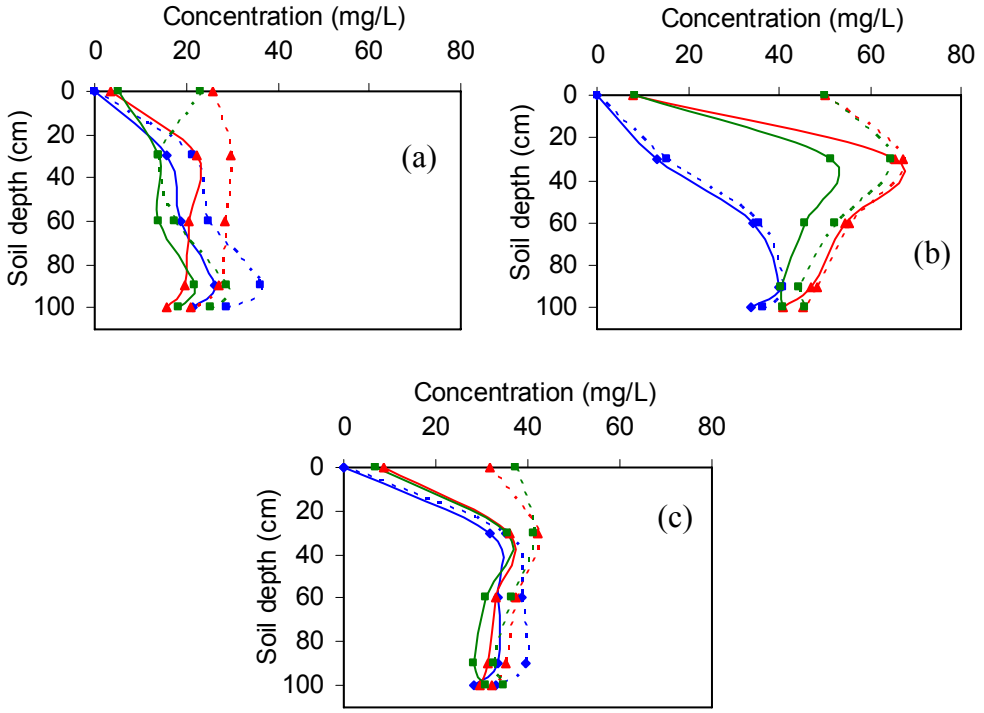

Fig. 2.15 Variation of NO_3^--N (solid line) and T-N (dashed line) with depth for the percolating water collected from the lysimeters irrigated with RWW 1(green) , RWW 2 (red) and GW (blue) in experiment 2 (a) at 1st sampling (b) at last sampling (c) average of all the samplings.

Figure 2.16 depicts the variation of the average $NO_3^- - N$ of all the depths vs. time. Trend lines have been plotted for $NO_3^- - N$ of the water samples collected from the lysimeters irrigated with *GW*, *RWW1* and *RWW2*. Data representing the first sampling and the samplings following the cultivation were excluded in the graph because it was expected that the condition of soil was not steady after the first irrigation and after it had been manured. Therefore, the time has been calculated considering that the 2nd sampling was

conducted on 1st day after the 1st irrigation. The approximate rising of $NO_3^- - N$ of the water samples collected from the field irrigated with *GW*, *RWW1* and *RWW2* are 0.13 mg/L, 0.21 mg/L and 0.3 mg/L per day, respectively. It is a significant observation that there is a considerable rising in the $NO_3^- - N$ profile that belongs to the lysimeters irrigated with *GW* despite the fact that there was no load of nitrogen in *GW*. On the other hand, the inclination of $NO_3^- - N$ in the lysimeters irrigated with *RWW1* and *RWW2* are more than that of *GW*, with *RWW2* possessing the largest inclination of 0.3 mg/L per day. In contrast to *GW*, the effect of *RWW2* in increasing $NO_3^- - N$ in a percolating water sample is 0.17 mg/L per day.

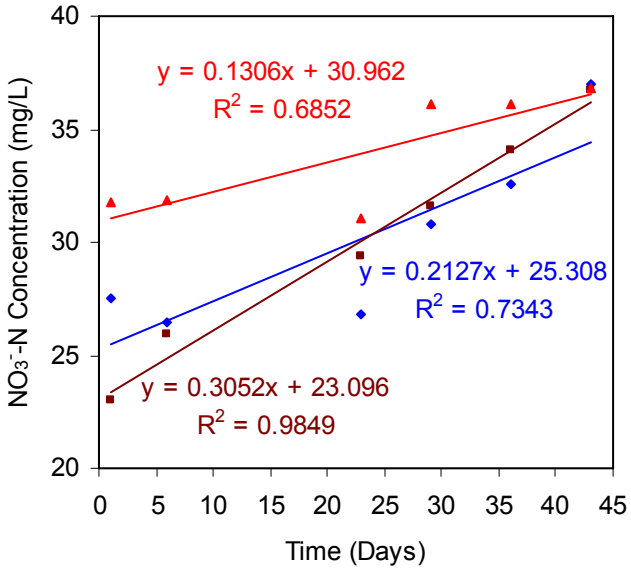

Fig. 2.16 Variation of average NO_3^--N concentration with the number of samplings (experiment 2).

Figure 2.17 (a), (b) & (c) denotes the variation of Na^+ concentration with time for the percolating water samples collected from the lysimeters irrigated with *RWW1*, *RWW2* and *GW*, respectively. Na^+ concentrations (100~300 mg/L) of the profiles of *RWW1* and *RWW2* were half the respective influent concentration (300~500 mg/L). The concentration of Na^+ that represented all the levels gradually increased with time (Fig. 2.17 a & b). Na^+ concentration of all the collected water samples of *GW* remained approximately constant at 100 mg/L (Fig. 2.17 c). The rising of Na^+ with time in the profiles of *RWW* has been caused by Na^+ of the influent because the rise was very straight and the increasing rate was comparatively constant. Therefore, the results show that Na^+ contained in *RWW* tends to accumulate in soil while percolating downward.

Figure 2.18 (a), (b) & (c) denotes the variation of Cl^- concentration with time for the percolating water samples collected from the lysimeters irrigated with *RWW1*, *RWW2* and *GW*, respectively. Though the Cl^- concentration of *GW* was about 30 mg/L, the percolating water increased to values close to100~200 mg/L (Fig. 2.18 c) due to the effect of leaching of Cl^- from soil. In the case of *RWW*1 and *RWW*2, Cl^- concentration in the percolating water at all the depths rose gradually before it started to decrease with the commencement of cultivation along with the addition of fertilizer (Fig. 2.18 a & b). With the addition of fertilizer, the ionic strength of the percolating water alters. This may have caused the above variation.

2.3.2 Field lysimeters at the Faculty of Agriculture, Ryukyu University (Experiment 3)

Table 2.1 presents the results of the water quality analysis conducted for the percolating water collected from the above lysimeters. *T-N* concentration of the irrigated *RWW* was around 22 mg/L, of which more than 75 % was occupied by $NH_4^+ - N$. Despite the variation of the conditions set on each block of the lysimeters, almost all $NH_4^+ - N$ in the influent diminished while percolating through soil. $NO_3^- - N$ had a rapid increment in all the blocks following the 2nd sampling. It exceeded the *T-N* concentration of the influent at 1st sampling onward. There was no significant difference in the parameters such as Na^+, K^+, Ca^{2+} and Mg^{2+} among different conditions set on the lysimeters. There was an unusual increment in the desorption of PO_4^{3+} into the percolating water from the blocks irrigated with the tap water. This may be because no block may have had the same characteristic as each other. Soil has been extracted from an agricultural land and there may have been plentiful adsorbed *P* due to the usage of chemical fertilizers. The distribution of *P*-sorption sites may have been different among the different blocks too. Otherwise, it is likely that the tap water may have been contaminated during the storage time at the site. The variation of nitrogenous compounds agreed with the experiments described above. Nitrification of influent $NH_4^+ - N$ and the leaching of accumulated nitrogenous compounds of soil and soil water into the percolating water are again the most appropriate factors that describe the variation meaningfully. The difficulty in determining the real effect of *RWW* in the soil due to the obstruction from the compounds originating from the soil and soil solution was visible in this experiment too.

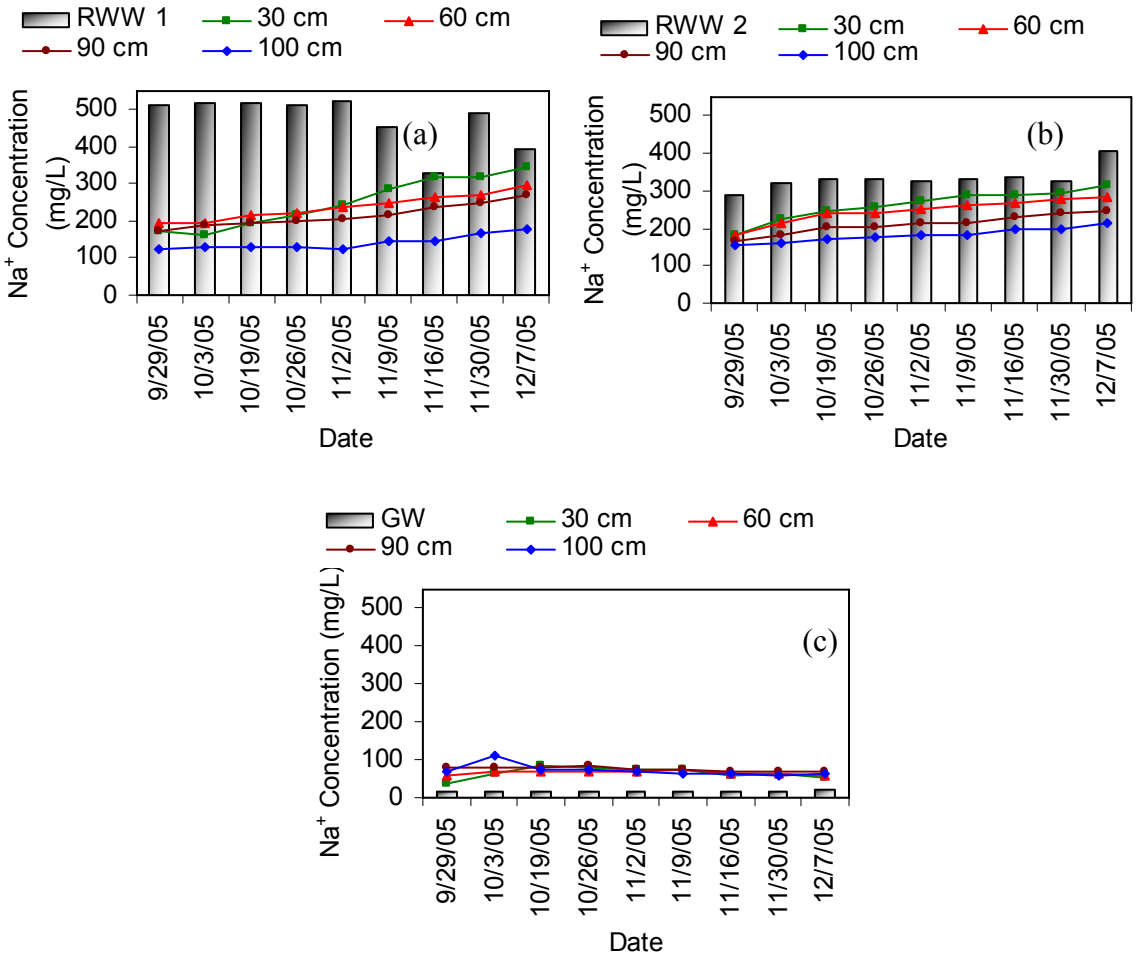

Fig. 2.17 Variation of Na^+ with time for the percolating water collected from the lysimeters irrigated with (a) RWW1 and (b) RWW2 (c) GW (Experiment 2).

Table 2.1 Data on water quality analysis of the percolating water from the earthen lysimeters at Ryukyu University (Experiment 3).

Type of irrigation	Crop Type	Sampling No.	pH	EC mS/m	NH_4^+-N(mg/L)	NO_3^--N (mg/L)	PO_4^{3-} (mg/L)	Na^+ (mg/L)	K^+ (mg/L)	Ca^{2+} (mg/L)	Mg^{2+} (mg/L)
RWW 2	Bitter	1	7.7	178.8	0.06	18.26	5.6	49.93	10.0	16.5	4.33
	gourd	2	8.1	238.0	0.41	27.64	3.7	50.10	10.1	16.6	4.32
		3	7.9	336.0	0.88	135.07	3.7	50.12	8.1	16.7	4.34
Tap	Bitter	1	7.7	153.3	0.25	25.54	25.6	50.10	19.4	16.2	4.33
water	gourd	2	8.0	169.8	0.15	33.17	25.6	50.14	17.6	16.4	4.33
		3	8.1	218.0	0.56	88.87	26.6	50.15	13.6	16.4	4.33
RWW 2	No	1	7.8	255.0	0.03	28.48	5.6	50.14	11.5	16.9	4.34
	crop	2	7.9	289.0	0.42	22.74	3.7	50.08	11.0	16.9	4.31
		3	8.1	287.0	0.16	83.44	1.8	50.10	7.9	17.0	4.33
Tap	No	1	8.0	168.3	0.28	31.98	4.7	50.14	9.5	16.5	4.31
water	crop	2	7.9	184.9	0.32	34.29	2.8	50.11	10.2	16.6	4.33
		3	8.1	162.1	0.19	87.47	25.6	50.10	7.3	16.7	4.32

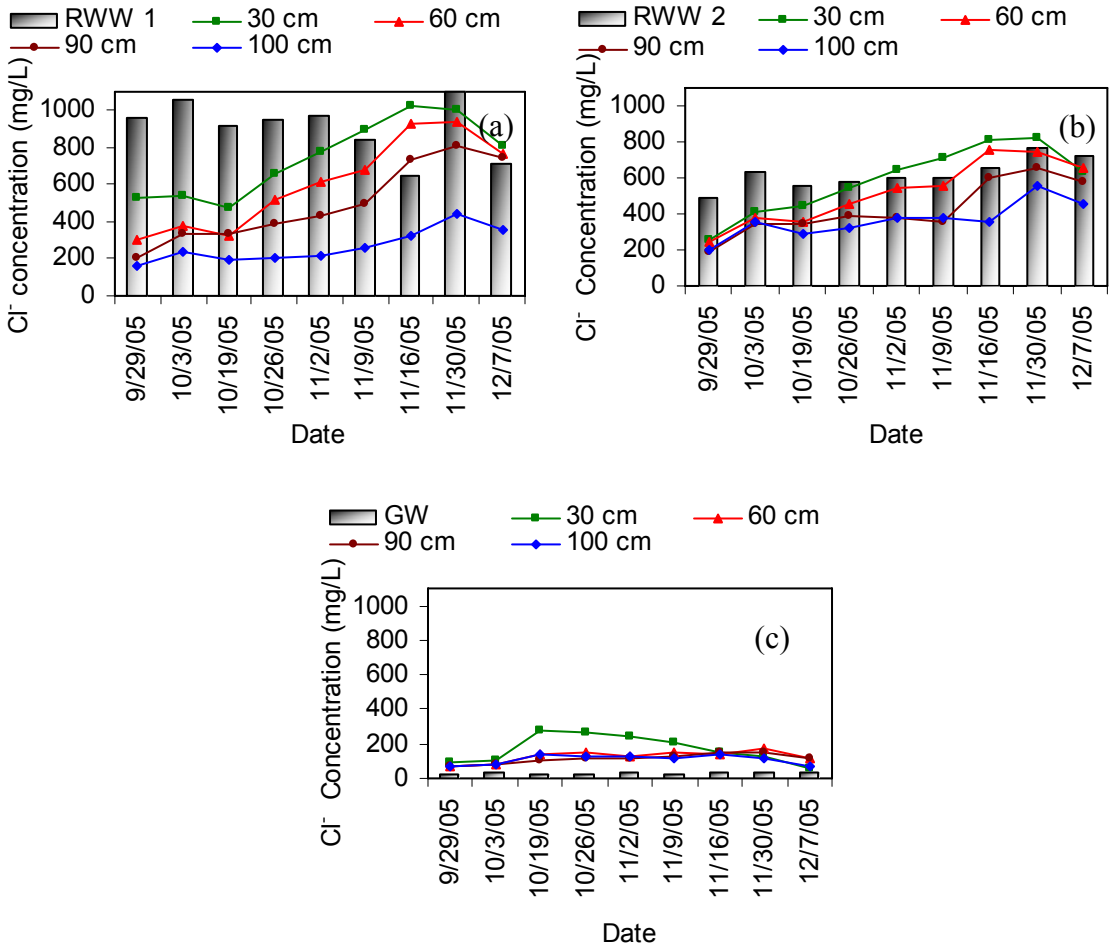

Fig. 2.18 Variation of Cl^- with time for the percolating water collected from the lysimeters Irrigated with (a) RWW1 (b) RWW2 and (c) GW (Experiment 2).

2.3.3 Green housed experimental field (Experiment 4)

There was a great reduction of soil NO_3^- (more than 50 %) and increase of soil Ca^{2+} at the end of the experimental period. There was an overall slight reduction of soil Mg^{2+} and Na^+ whereas it was a slight increase for soil K^+. The positive effect that *RWW* exerted on the preservation of the vegetables was confirmed. Most of the people who had tasted the crops from this field had the opinion that the crops irrigated by the tap water were better in quality than those by *RWW*. There was no significant difference observed in the crop quality between the application of *RWW1* and *RWW2*. The high level of salinity in *RWW* is a serious issue associated with the *RWW* activities in Okinawa. The pipelines transporting *RWW* have got corroded due to the saline environment, and as a result, the pipelines possess some leakages, through which the saline water intrudes into them. *NaCl* is visible in the block irrigated with *RWW* in this experimental field. It is assumed that the low

quality of the crops irrigated with *RWW* may have been attributed to the high salinity content. As stated by Hillel (2000), salinity is a major treat to the sustainability of all irrigation areas-not just *RWW* irrigation.

2.3.4 Overall discussion on the lysimeters experiments

Following is understood from the obtained dynamics of nitrogenous compounds. $NH_4^+ - N$ of *RWW* rapidly undergoes nitrification as well as adsorption on to the negatively charged soil particles. Cation exchange capacity of a clayey soil is high, and the anion exchange capacity is low. It can be assumed that NH_4^+ may have been adsorbed on to the negatively charged soil colloidal particles because NH_4^+ has a positive charge, and is held by the negative sites on the clay in the soil. It is possible that the adsorbed NH_4^+ may nitrify too.

The inclination of the rise of $NO_3^- - N$ with time in the percolating water of the lysimeters irrigated with *RWW* and *GW* were positive while that of the latter was more gradual. The leaching of NO_3^- from soil is highly responsible for the rise of $NO_3^- - N$ in the percolating water. $NO_3^- - N$ of the water samples collected from the lysimeters irrigated with *GW* in experiment 2 (Fig. 2.14a), commenced decreasing at the cessation of the NO_3^- leaching. Therefore, $NO_3^- - N$ leaching from the soil seems time dependent and can slightly attenuate. However, $NO_3^- - N$ concentration of the percolating water for the case of *RWW*, kept on increasing with time due to the effect of *RWW*. In addition, denitrification may have occurred in the low-lying layers of all the lysimeters described in the experiment 1 & 2 because the maximum $NO_3^- - N$ of each percolating water was seen at 30 cm level and it decreased after that. The authenticity of above fact is uncertain because the profiles were in the transient state. It is possible that NH_3 may have been produced because of the breakdown of organic *N* compounds such as urea, and the produced NH_3 may have dissolved in water and readily nitrified. This may also have contributed to the elevated $NO_3^- - N$ concentrations found in the percolating water of all the experiments. A detailed discussion on the role of the above-mentioned biochemical reactions on nitrogen dynamics is provided in the section 3.1.3.1 under the sub topics nitrification, ion exchange reactions, denitriifcation and ammonification.

According to the obtained results from these lysimeter experiments, a clear understating of the fate of the contaminants originating from the *RWW* has not been grasped. The importance of cleansing the lysimeters until the readily flushable contaminants originated from the soil and soil water escape, has been confirmed. The soil and soil water contaminants have played a great role in determining the characteristics of the percolating water. Therefore, the determination of the degree of involvement of *RWW* in the characteristics of the percolating water has become very difficult in this context. There was a control field applied with *GW* for the comparison. However, the involvement of soil and soil water was so dominating and irregular that *GW*-field has become less representative agent for the comparison. No lysimeters has reached the steady state during the course of experiment. Even in this kind of situation, it would take some time for the soil and soil water barrier to attenuate. The durations of these experiments were not enough for it to fade so that the effect of *RWW* would become visible. In experiment 2, it seemed that it commenced attenuation at 6^{th} sampling onward (Fig. 2. 14). However, if the duration of the experiment had been longer, there would have been a possibility of bringing the effect of *RWW* into the focus.

These facts suggest that a laboratory scale soil column would solve this problem to great extent as it can be cleansed because of the size and not being the real field. It is beyond the argument that there are certain limitations in a laboratory scale soil column that makes it far beyond the reality. The conditions under cultivation is difficult to be attained in such a column. Therefore, it is clear that both field lysimeters and laboratory scale soil columns have their own merits and demerits. Therefore, a well-planned study that combines both these investigations would be a successful way of investigating the ultimate fate of the contaminants contained in *RWW*.

2.4 CONCLUSIONS

RWW has been identified as potential alternative water recourse for the prevailing water scarcity in Okinawa, Japan. At present, *RWW* is largely utilized for many activities enumerated as various activities in public buildings, road washing and sprinkling on trees. However, severely threatened agricultural irrigation has not yet been receiving the service of *RWW* on large-scale. *RWW* irrigation will be introduced within a few years later on large-scale by implementing an already planned large-scale project into the real practice. The large-scale application of *RWW* for the irrigation is still delayed because the

authorities concern very much on the adverse effects likely to arise in relation to this. Therefore, a number of investigations have been conducted to seek the feasibility in utilizing *RWW* for the crop irrigation since several years ago. Since the major issues coupled with the wastewater reclamation and reuse are often related to health considerations, protection of the public health due to pathogens has immensely been of concern to the past and ongoing investigations. In addition, the issues related to the crop quality and the possible adverse effects on the environment are addressed by these investigations.

Among the investigations related to the environmental issues are experimenting the production of better quality *RWW* and conducting field lysimeter experiments. Several lysimeter experiments have been conducted in the experimental fields to date. Attempts have been taken to investigate the ultimate fate of the contaminants found in *RWW* in the soil. Investigating the NO_3^- pollution and the salt accumulation in soil were among the major objectives of these lysimeter experiments. The obtained results from the lysimeter experiments proved that high NH_4^+ content of *RWW* would diminish in the soil due to the readily nitrification and adsorption. It is possible that the ions such as Na^+ and Cl^- heavily contained in *RWW* would accumulate in the soil under a long-term application. In addition, it proves to some extent that there is a possibility for NO_3^- to travel toward the groundwater. However, the obtained results do not seem too reliable owing to the fact that they are lacking important features to address the issue properly. It may be because these experiments were carried out to address the crop quality and the environmental issues simultaneously. It indicates the importance of conducting an exclusive investigation on adverse environmental effects. The leaching of NO_3^- accumulated in soil into the percolating water has made barriers in providing the better understanding of the real fate of *RWW*.

REFERENCES

Asano, T. (1998), *Wastewater Reclamation and Reuse*, Vol.10, Technomic Publishing Companync, USA.

CDHS (1978), California code of regulations. In wastewater reclamation criteria, *Title 22*, California Department of Health Services, Sanitary Engineering Section, Berkeley.

Dillon, P (2000), Water reuse in Australia: current status, projections and research, *In: Water Recycling Australia*, 99-104 pp, CSIRO and AWA.

Hillel, D. (2000), Salinity management for sustainable irrigation: integrating science, environment and economics, *World Bank 2000*, Washington DC, USA.

Shinohara, H., T. Tanishima, S. Kojima, S. Managaki, H.Takeda, N. Nakada, H.Tanaka, and H. Furumai (2004), Water-soluble organic micro-pollutants in municipal wastewater and their removal during advanced treatment, Proceedings of 2nd International Symposium on Southeast Asian Water Environment, Department of Urban Engineering and Research Center for Water, 356-363.

Tanaka, H., T. Asano, E. Schroeder, and G.Tchobanoglus (1998), Estimating the safety of wastewater reclamation and reuse using enteric virus monitoring data, *Water Environmental Research*, *70*, 39.

Tanaka, H., N. Nakada, N.Yamashita, A. Harada, K. Miyajima, Y. Suzuki, H. Shinohara, H. Takada, N. Sato, M.Suzuki, M. Ito, F. Nakajima, and H. Furumai (2005), Reduction of trace pollutants in reclaimed wastewater through solid aquifer treatment, Proceedings of the 78th Annual Technical Exhibition and Conference of Water Environment Federation (CD-ROM), Session 66.

CHAPTER 3

DYNAMICS OF NITROGEN AND OTHER CONTAMINANTS IN LOW POROUS SOIL DUE TO RECLAIMED WASTEWATER IRRIGATION

3.1 LABORATORY SCALE SOIL COLUMN EXPERIMENT

3.1.1 Introduction

This section explains a study of belowground dynamics of nitrogenous compounds using two laboratory scale unsaturated soil columns, which were loaded with the low porous mudstone **(Fig. D-5 & D-6)**. This is a calcareous soil (gray in color), which was obtained from a land to be cultivated under the proposed *RWW* irrigation project in Okinawa. It is described as a strong mucilaginous semi- consolidated sedimentary rock. It has a strong physical characteristics such as stickiness and high plasticity that make the farming difficult in that soil. It is the most abundant soil type there. In the Okinawa grounds containing mudstone, the bed rock level is found at 90 cm depth. The water infiltration rate is low. The study was first conducted by continuous and intermittent irrigation of the soil columns for 120 days with *SRW*. Then, the effects of the concurrent applications of *SR* and *SRW* were also studied. The aim of this study was to investigate the underground behavior of nitrogenous compounds contained in *RWW* with time. The objectives included the comparison of *CA* and *IA* in terms of NO_3^- pollution, the use of the $\delta\ ^{15}N$ of NO_3^- in influent, effluent and soil for the verification of the presence of nitrification and denitrification in the soil columns, and demonstration of the effects of concurrent applications of *SR* and *IA* of *SRW* on the belowground behavior of nitrogenous compounds.

3.1.2 Methodology

3.1.2.1 Soil columns

Two laboratory scale acrylic plastic columns (**Fig. 3.1, Fig. D-1, D-2, D-3 & D-4**) of cylindrical shape (20 cm i.d. by 90 cm height) were filled up to 85 cm height, with the soil. Soil was collected from the surface to about 1 m depth. Very large clumps (15 cm-20 cm)

of original soil were first air – dried, and then crushed into a particle size less than the size of a square sieve of 0.2 cm×0.2 cm. Crushed soil was mixed well and 10 samples, each having 100g soil, were grabbed from the soil mixture, for the analysis of the average moisture content. Soil was filled in the columns as layers, each of 10 cm in thickness, so that the average density of each layer on wet weight basis was 1.25 g/cm^3. Therefore, the average bulk density of the soil inside the entire column was 1.25 g/cm^3. This average density is similar to the average bulk density of the source of soil at shallow depths. The base of the soil column was perforated with a finely woven plastic mesh segregating the soil and the base of the column. The soil surface was exposed to the atmosphere. Soil column was surrounded by a water jacket to maintain the temperature at 20 ºC. In order to collect the *PW* at different depths (15, 35, 45, 55, 70 and 80 cm below the soil surface), 6 ports (*PW* 1-6), each being 12.5 mm in internal diameter, were located around the column such that the centre line of each port was at an angle of 60˚ from the centerlines of adjacent ports, as visualized by the plan view (Fig D-1).

3.1.2.2 Experimental procedure and sampling

Reclaimed wastewater application

Initially, both the columns were leached with deionized water continuously at 450 mL/h (14 mm/h) for 18 days until both *PW* and *E*, from the bottom, did not receive any readily flushable contaminants from soil. Then, *SRW* was irrigated on one column at a rate of 900 mL/h (28.65 mm/h) for 2 hours every week, while the other column was continuously irrigated at a rate of 11 mL/h (0.35 mm/h) so that both the columns received the same content of water every week. The application of reclaimed wastewater was continued for 120 days. No significant difference was observed in the total soil depth before and after leaching.

The influent was pumped on to the top of the column by means of a peristaltic pump and discharged through a shower that was to ensure a homogeneous distribution of the influent throughout the soil surface. The irrigation rate was calculated based on the proposed irrigation rate of the Okinawa - project. The proposed irrigation rate and frequency are 30 mm depth for 2 h every week. The irrigation rate of this column experiment was calculated with a safety factor equal to 2. The proposed irrigation rate (Okinawa) was multiplied by the cross sectional area of the column and then divided by 2 h and 7 d in order to obtain the irrigation rate of *IA* and *CA*, respectively. The characteristic of *SRW* was similar to that of the *RWW* to be used in the same project.

Secondary treated wastewater prior to chlorination obtained from the Municipal Wastewater Treatment Plant, Otsu, Japan was used to prepare *SRW*. It was filtered and mixed with anhydrous NH_4Cl so that the final NH_3-*N* concentration approximately became 18 mg/L in *SRW*. **Table 3.1** depicts the characteristics of both *SRW*, and the raw soil before it was filled in the column.

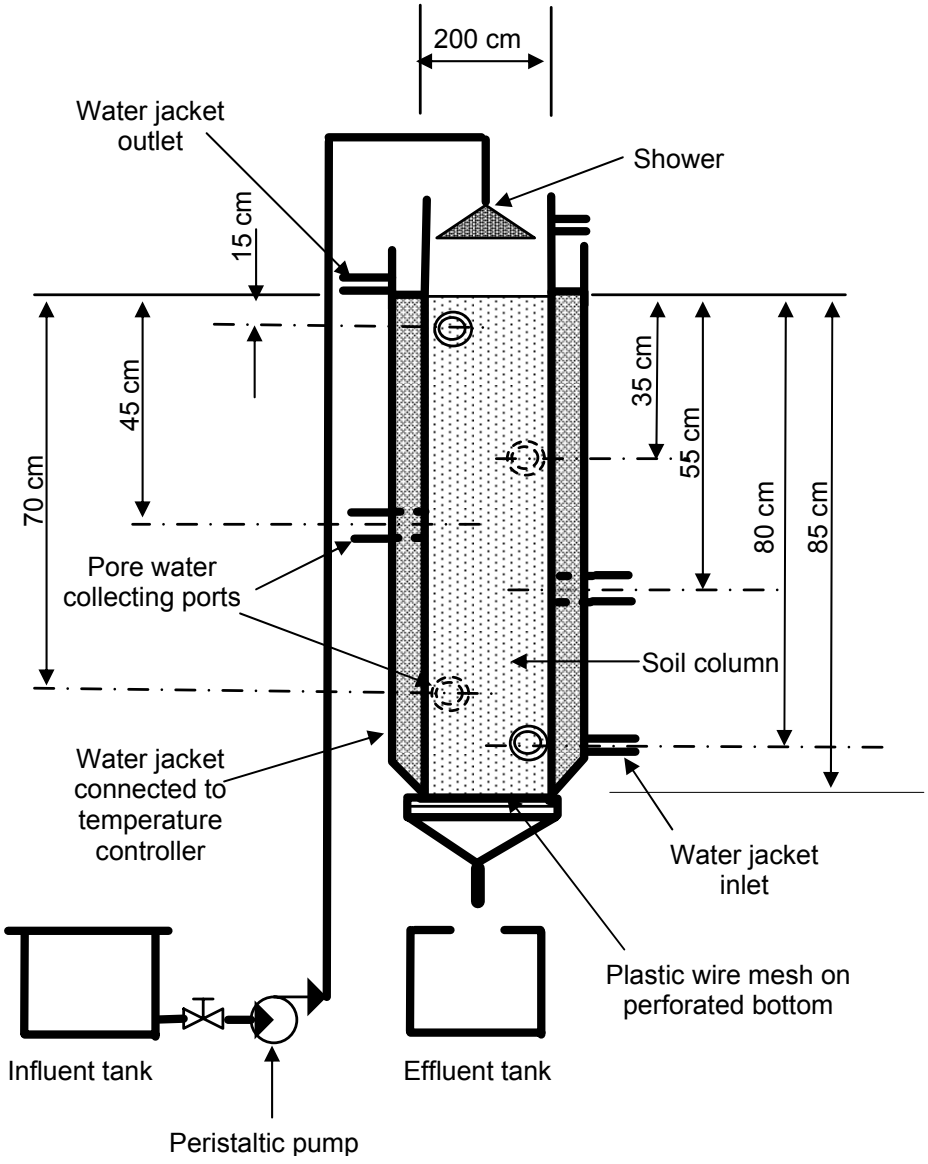

Fig. 3.1 Schematic diagram of the laboratory scale soil column.

The effluents from both the applications were collected once every day during the entire experimental run. *PW* was collected by means of a porous cup soil water sampler (a product of Soilmoisture Equipment Corp., Santa Barbara, CA, USA; purchased from Namoto Trading Company, Chiba, Japan). *PW* was collected from *CA* twice a week, and that for *IA* was on three days between two consecutive irrigations. The accumulated volume of water in the effluent tank by each sampling was recorded for the entire

experimental period. Each effluent sample was filtered through a 0.45 -μm filter paper. All the wastewater samples were frozen before analysis and periodically (within 7 days after collection) analyzed for nitrogenous $\{NO_3^- - N, NO_2^- - N$, *NH₃-N* and *T-N*$\}$ and *P* $\{$*T-P*, $PO_4^{3-} - P\}$ compounds, SO_4^{2-} and Cl^-. Selected number of effluent samples were also analyzed for cations such as Ca^{2+}, Mg^{2+}, Na^+ and K^+. Both conductivity and pH were analyzed as soon as the samples were collected. In addition, several influent and effluent samples were analyzed in terms of $\delta^{15}N$ of NH_4^+ and NO_3^-. Raw soil and the soil sample collected from each port at the conclusion of the experimental run were characterized in terms of the gravimetric moisture content, $NO_3^- - N$, *NH₃-N*, $\delta^{15}N$ and the above-mentioned cations. The concentrations of exchangeable cations and anions were summed up to obtain the *ECEC* and *EAEC*, respectively.

Table 3.1 Characteristics of SRW and raw mudstone (low porous soil).

Description	SRW	Raw Soil (per kg of oven-dry soil)
NO_3^--N+NO_2^--N	2.5-3.5 mg/L	0.11 cmole
NH_3-N	18.0 mg/L	0.02 cmole
T-N	23 mg/L	9.4 cmole
T-C	17.2 mg/L	150.6 cmole
δ^{15}N	-	+ 6.0 ‰
δ^{15}N of NO_3^-	10.2 ‰	-
δ^{15}N of NH_4^+	-6.5 ‰	-
TOC	4.3 mg/L	-
PO_4^{3-}-P	0.0 mg/L	0.01 cmole
SO_4^{2-}	30-40 mg/L	0.01 cmole
Cl^-	90-110 mg/L	1.05 cmole
TP	0.06 mg/L	-
Ca^{2+}	0.66 mmole/L	23.5 cmole
Mg^{2+}	0.17 mmole/L	1.74 cmole
K^+	0.21 mmole/L	1.12 cmole
Na^+	1.79 mmole/L	1.18 cmole
Ionic strength	3.2 mmole/L	-
ECEC	-	27.5 cmole
EAEC	-	1.55 cmole
pH	7.1-7.7	8.47
Conductivity	53-60 ms/m	-

At the end of the experiment, the calculations of both water balance and *T-N* mass balance were performed. In calculating the cumulative mass of *T-N* discharged from each column as the effluent throughout the experimental period, *T-N* concentration of each effluent sample was multiplied by the respective total volume of accumulated water in the effluent tank. To obtain the initial *T-N* content of soil, the total mass of *T-N* having flushed

out with the effluent during the cleansing period was subtracted from the *T-N* of the raw soil. In calculating *T-N* of soil at the end of the experiment, it was assumed that the soil sample collected from each port had represented the portion of soil lying between the same port and the adjacent upper port. *T-N* of soil after leaching did not show any significant difference with that of raw soil. Therefore, the change of organic-*N* content in soil is negligible. The quantity of $NO_3^- - N$ and NH_3-*N* is only 5.3% of *T-N* in raw soil. Therefore, it was very difficult to quantify the change of $NO_3^- - N$ and NH_3-*N* content in soil at the end of the experiment, using the final *T-N* value of soil. Hence, *T-N* of soil at the end was considered equal to the *T-N* of raw soil plus the content of accumulated $NO_3^- - N$ and NH_3-*N* in soil at the end.

3.1.2.3 Concurrent applications of SR and IA of SRW

On completion of the aforementioned experimental run, the column used for *IA*, was applied concurrently with *SR* and *SRW* for a period of 1 month. Deionized water was used as *SR* because the effect of composition of *SR* was beyond the scope. *SR* was applied on random 10 days within a month so that the column received *SR* for 1.7 h every day, at an intensity of 12.8 mm/h. In the mean time, the application of *SRW* was continued at the same rate as the previous *IA* of *SRW*. The application rate of *SR* was obtained using the recorded maximum of the average monthly rainfall values during the last 25 years on the Okinawa Island, i.e. 217 mm/month. Both *PW* and *E* were collected appropriately during the experiment, and the samples were analyzed in terms of $NO_3^- - N$, $NO_2^- - N$, NH_3-*N*, *T-N*, *pH* and conductivity.

3.1.2.4 Analyses

Wastewater

$NO_3^- - N$ and $NO_2^- - N$ of the collected water samples were analyzed by means of an automated analyzer (purchased from BRAN-LUEBBE Corporation, Tokyo, Japan) utilizing the *Cd* reduction method and an ion chromatograph (purchased from Nihon DIONEX Corporation, Osaka, Japan). In the *Cd* reduction method, NO_3^- is quantitatively converted to NO_2^- in the presence of *Cd* granuals treated with $CuSO_4$ and packed in a glass column. NO_2^- produced thus is diazotized with sulfanilamide coupling with *N*-(1-naphthyl)–ethylenediamine dihydrochloride to form a highly colored azo dye that is

measured colorimetrically. SO_4^{2-}, $PO_4^{3-} - P$ and Cl^- were analyzed by using an ion chromatograph. NH_3-N was analyzed by using an automated analyzer (purchased from BRAN-LUEBBE Corporation, Tokyo, Japan) utilizing the phenate method, in which alkaline phenol and hypochlorite react with NH_3 to form the indophenol blue that is proportional to the NH_3 concentration, and the blue color formed is intensified with sodium nitroprusside to make it be measured colorimetrically. *T-N* and *T-P* were analyzed manually following the standard methods in the reference mentioned below. *T-N* and *T-P* were digested into NO_3^- and orthophosphate, respectively, and were measured by the automated analyzer and a spectrophotometer (purchased from Shimadzu Corporation, Japan), respectively. Cations were analyzed by means of an inductively coupled plasma spectrometer (Hewlett Packard purchased from Yokogawa Analytical Systems, Japan). All the analyses of the wastewater samples were in accordance with Clesceri et al. (1998).

Analyses of $\delta^{15}N$ in water samples and soil

A simple and rapid method for the $\delta^{15}N$ determination of NH_4^+ and NO_3^- in samples developed by Sakata (2001) was used for the analysis. This method is based on an on-line isotope analysis using an elemental analyzer {'Flash EA' (Thermo Electron) - EA1108}according to the conditions recommended by Carlo Erba, coupled to a mass spectrometer {'Delta Plus XL' (Thermo Electron) - Finnigan MAT} through a ConFlo II interface. In this method, NH_4^+ and NO_3^- in sample solutions are separated from each other as NH_4^+ into diluted H_2SO_4 by sequential distillation techniques. Then, the NH_4^+ in the distillate is precipitated directly as an insoluble salt of $(C_6H_5)_4BNH_4$, which is subsequently combusted in an elemental analyzer for $\delta^{15}N$ determination (Sakata, 2001).Soil was prepared for the on-line isotope analysis by grinding into small particles after drying at about 20℃. L-Histidine ($\delta^{15}N$: - *8.62 ‰*) was used as the standard.

Soil

NO_3^-, NO_2^- and NH_4^+ of soil were extracted in 100 mL of *1M KCl* from 10 g of soil. Cations and the anions such as Cl^- and SO_4^{2-} of the soil were extracted from 10 g of soil using 100 mL of *1M* NH_4OAc extractant (at *pH*=7). *pH* was measured in a solution of 15 g soil thoroughly mixed with 30 mL deionized water. *ECEC* was calculated in terms of Ca^{2+},

Na^+, K^+, Mg^{2+} and Al^{3+} while *EAEC* was determined in terms of NO_3^-, NO_2^-, SO_4^{2-}, Cl^- and PO_4^{3-}. *T-N* of soil was measured on a C-H-N analyzer, in which *T-N* is combusted into N_2. All the analyses of the soil were in accordance with Robertson et al. (1999).

3.1.3 Results & Discussion

3.1.3.1 Reclaimed wastewater application

Nitrogenous compounds dynamics due to CA

Figure 3.2 depicts the $NO_3^- - N$ & *T-N* profiles denoting all *PW* and *E* samples due to *CA*. Upon receiving *SRW*, both $NO_3^- - N$ & *T-N* concentrations of *PW1*, *PW2*, *PW3*, *PW4*, *PW5*, *PW6* and *E* increased to a maximum in succession. The successive attainment of the steady state by these water samples occurred within approximately 80 days of the experimental run. The peak $NO_3^- - N$ & *T-N* concentrations reached by the profiles of *PW1*, *PW2*, *PW3* and *PW4* were considerably higher than those reached by *PW5*, *PW6* and *E*.

Figure 3.3 depicts the average NH_3-*N*, $NO_3^- - N$ & *T-N* distributions in the soil column of *CA*, during the steady state. The steady state is considered to have existed 80 days onward. Both *T-N* and $NO_3^- - N$ concentrations below 45 cm depth have gradually decreased with depth. Transient and steady state NH_3-*N* concentrations of all *PW*s & *E* were almost invariant at values less than 3.0 mg/L. **Figure A-1** shows the variation of NH_3-*N* concentration in *PW*s and *E* due to *CA*. $NO_2^- - N$ concentration was never found significant in either *PW* or *E* during the transient or steady state. **Figure 3.4** indicates that $\delta^{15}N$ profile rose to a peak, during which $NO_3^- - N$ profile fell from the peak, and $\delta^{15}N$ of NO_3^- in the effluent has increased more than threefold as that of the influent. An enrichment of $\delta^{15}N$ can also be seen in NH_4^+ of the effluent (**Fig. 3.5**).

Transient and steady state variations of the other contaminants due to CA

Figure 3.6 & **Fig. 3.7** denote the profiles of Cl^- and SO_4^{2-} in the effluent due to *CA*. The breakthrough of both Cl^- and SO_4^{2-} occurred within 25 days of the experimental run, and both the ions attained the steady state within 80 days of experimental run. Both Cl^- and SO_4^{2-} of *SRW* varied within 90 – 105 mg/L and 28 - 45 mg/L, respectively.

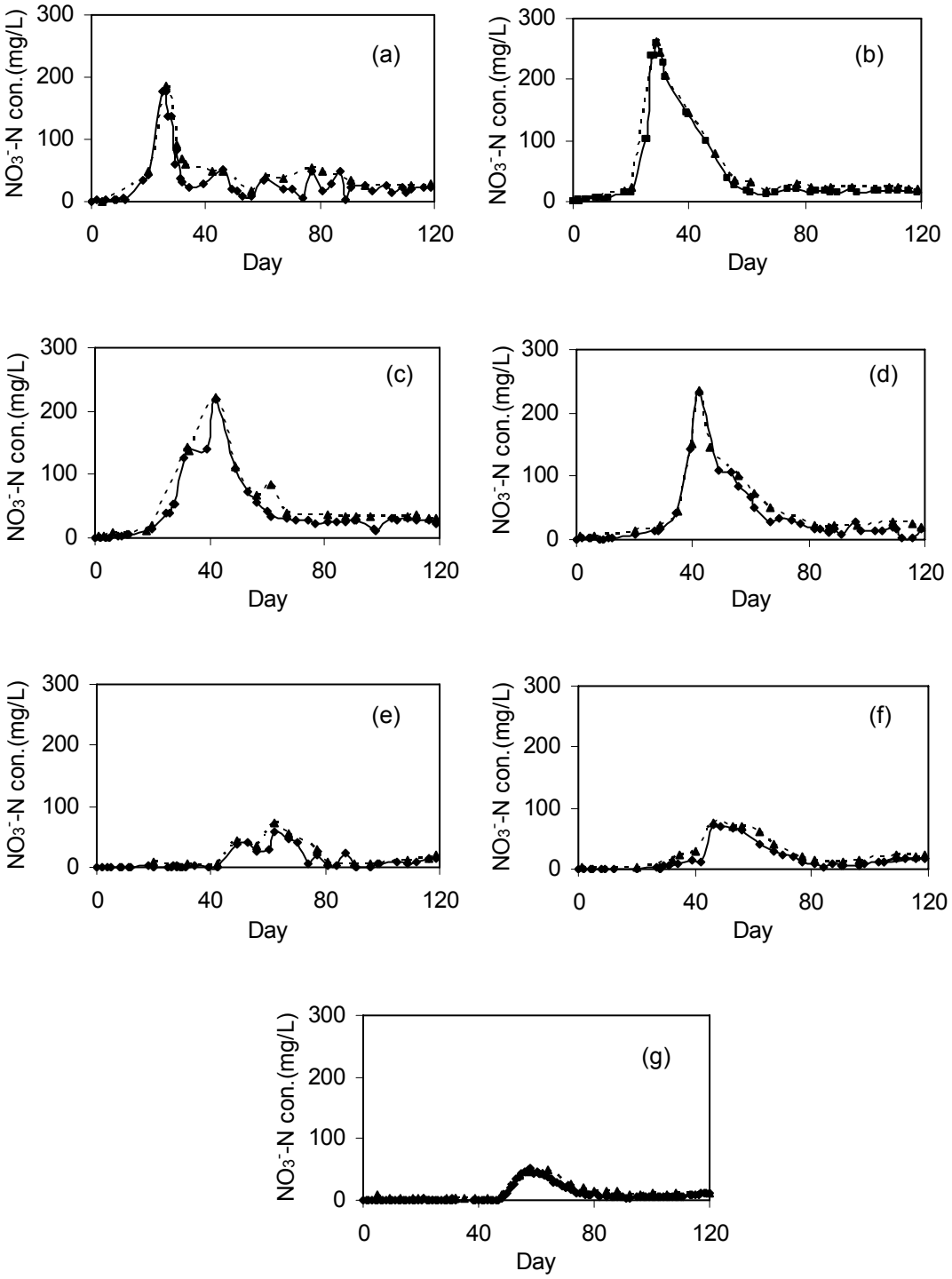

Fig. 3.2 Variation of NO_3^--N (diamonds with solid line) & T-N (triangles with dashed line) concentration of the water samples due to CA (a) PW1 (b) PW2 (c) PW3 (d) PW4 (e) PW5 (f) PW6 and (g) E (low porous soil).

Eventually, Cl^- concentration reached the steady-state with the concentration (110 mg/L) approximately equal to the maximum concentration of Cl^- in *SRW*. SO_4^{2-} exceeded its maximum concentration in the influent and attained the steady state. It may be due to the anion repulsion and ionic diffusion. Since, Cl^- has not undergone significant ion exchange

reactions, its profile can be used as an indication of the flow path of the percolating water. Therefore, the percolating water seems not to have been influenced greatly by any preferential flow.

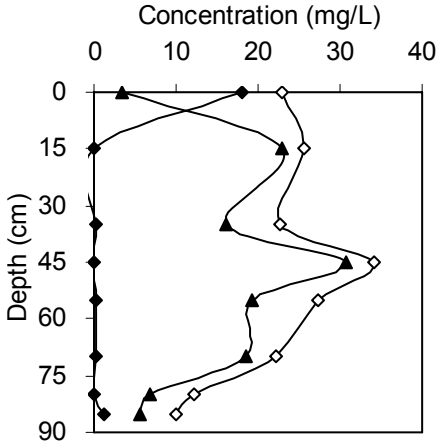

Fig. 3.3 Steady state T-N (hollow diamonds), NO_3^--N (triangles) & NH_3-N (solid diamonds) concentration distributions with soil depth in CA (low porous soil).

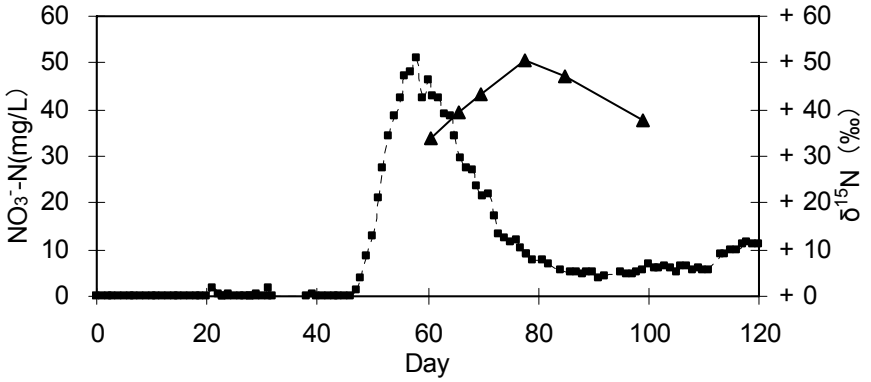

Fig. 3.4 Variation of NO_3^--N concentration (boxes with dashed line) of the effluent, NO_3^--$\delta^{15}N$ of the effluent (triangles with solid line), with time, for CA (low porous soil)

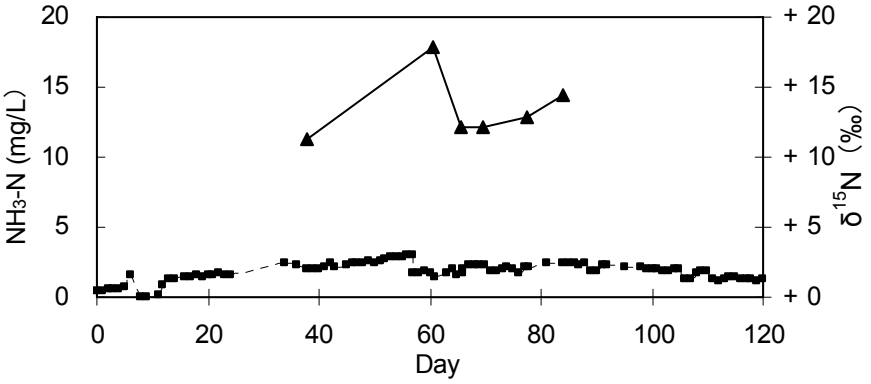

Fig. 3.5 Variation of NH_3-N concentration (boxes with dashed line) of the effluent, & NH_4^+-$\delta^{15}N$ of the effluent (triangle with solid line) with time, for CA (low porous soil)

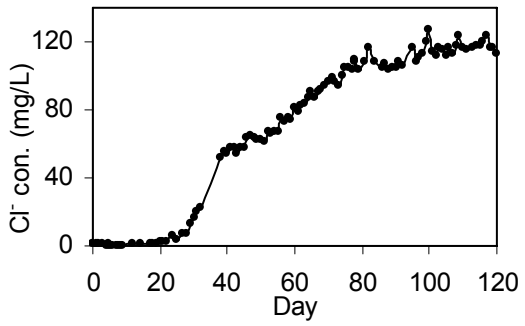

Fig. 3.6 Variation of Cl^- concentration in E of CA (low porous soil).

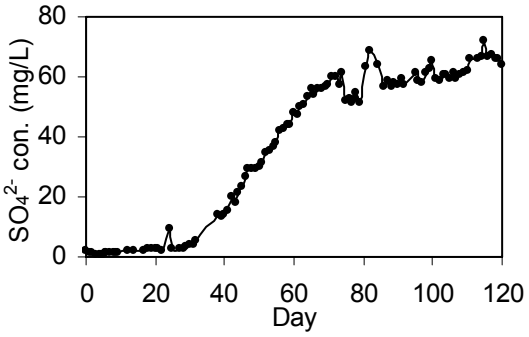

Fig. 3.7 Variation of SO_4^{2-} concentration in E of CA (low porous soil).

Figure 3.8 & 3.9 depict the distributions of Ca^{2+}, Mg^{2+}, K^+ and Na^+ in *E* due to *CA*. Ca^{2+} reached elevated levels rapidly once received *SRW*. Mg^{2+}, K^+ and Na^+ too increased to a maximum and then remained constant at the steady state. Steady state concentrations of Ca^{2+}, Mg^{2+} and K^+ were in excess of those present in *SRW*, while Na^+ concentration was contrary to that observation. The result indicates that all these cations have involved ion exchange reactions.

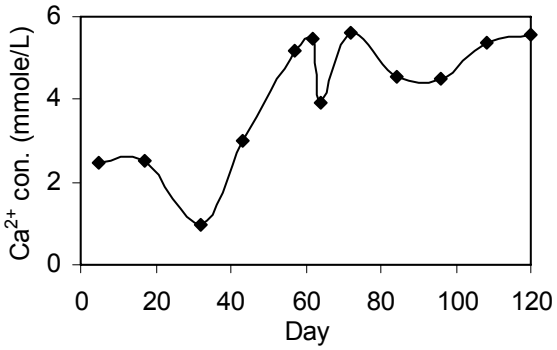

Fig. 3.8 Variation of Ca^{2+} concentration in E of CA (low porous soil).

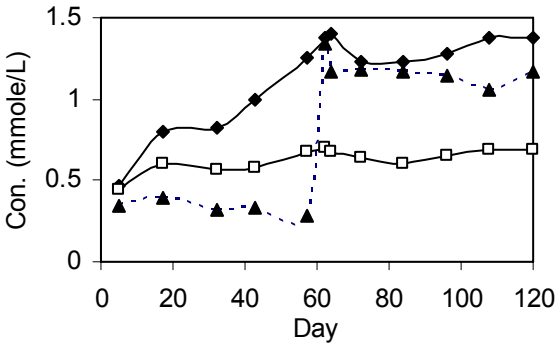

Fig. 3.9 Variation of Mg^{2+} (diamonds), Na^+ (triangles) and K^+ (hollow boxes) concentration in E of CA (low porous soil).

Conductivity of the effluent due to *CA* ranged from 60-120 ms/m during the steady state (**Fig. A-2**). **Figure A-3** depicts that *pH* in the effluent has slightly decreased from about 8.8 to 8.4 during the steady state. The ionic strength of the effluent due to *CA* at the steady state was about 5 times higher than that of *SRW*. The existence of *P* compounds in the effluent due to *CA* was insignificant. This is on account of the concentrations of *P* compounds in *SRW* being negligible and the sorption sites of PO_4^{3-} not yet being saturated to leach any.

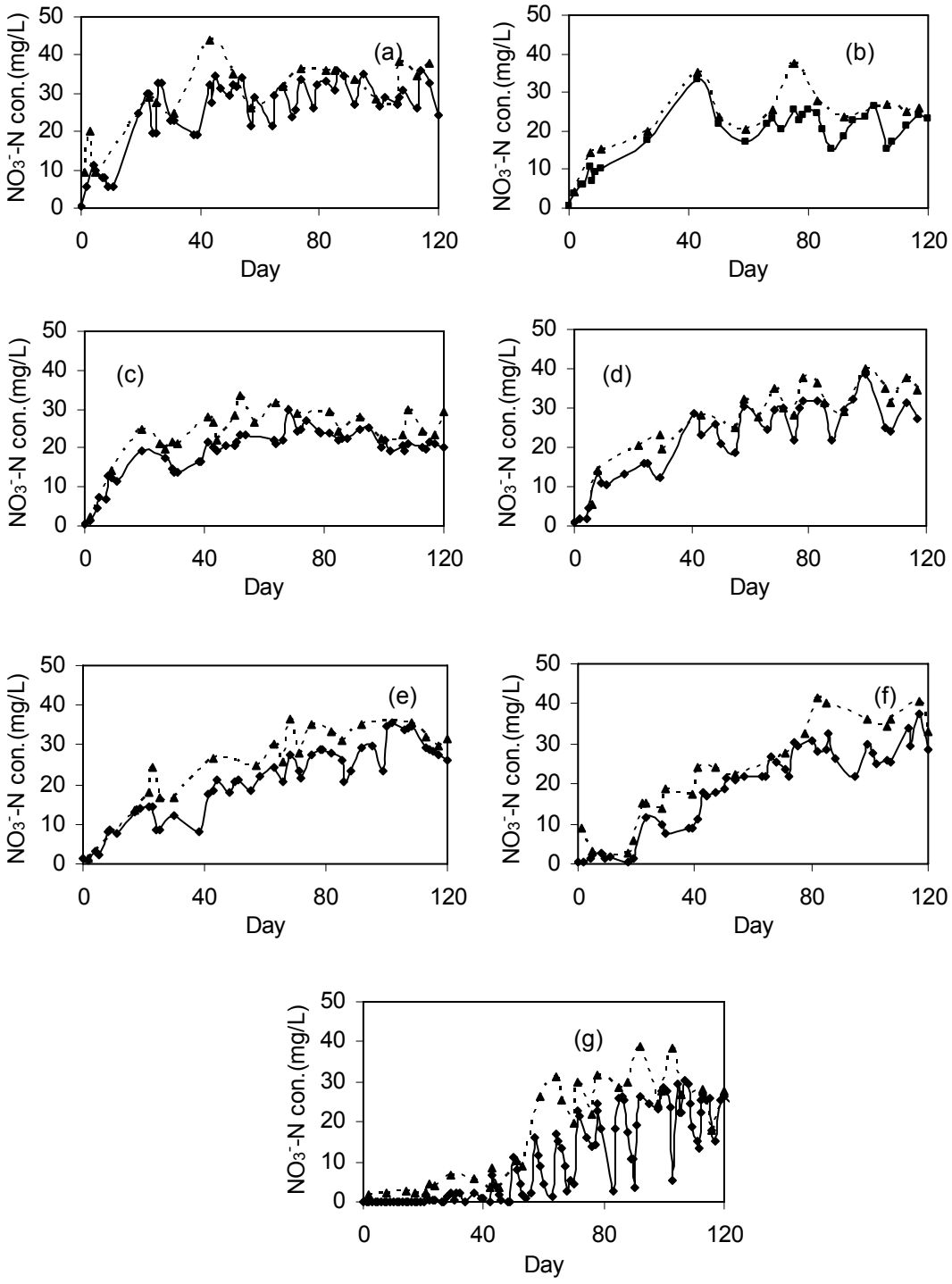

Fig. 3.10 Variation of NO_3^--N (diamonds with solid line) & T-N (triangles with dashed line) concentration of the water samples due to IA (a) PW1 (b) PW2 (c) PW3 (d) PW4 (e) PW5 (f) PW6 and (g) E (low porous soil).

Nitrogenous compounds dynamics due to IA

Figure 3.10 shows the profiles of $NO_3^- - N$ and *T-N* in *PW*s and *E* due to *IA*. $NO_3^- - N$ of all the collected water samples, which became negligible at the end of the cleansing period, commenced increasing upon receiving *SRW*. Once received *SRW*, both

$NO_3^- - N$ & *T-N* concentrations in *PW1*, *PW2*, *PW3*, *PW4*, *PW5*, *PW6* and *E* gradually increased to a maximum value in succession. Thereafter, the concentration remained approximately constant. At various depths, it exhibited similar profiles. As shown by Fig. 3.9g, the effluent samples collected on the following day of each *SRW* application denoted a higher concentration than that of all the samples collected until the next application. It indicates that at every application, the concentration increased to a higher level, and then decreased as the percolation rate gradually became low. However, every subsequent application of *SRW* made the peak concentration at each application increase.

Figure 3.11 depicts the distribution of NH_3-*N*, $NO_3^- - N$ and *T-N* with depth of the soil column due to *IA*, at the end of the experimental run. Unlike that of *CA*, the soil depth seems not to have caused great variations in both *T-N* and $NO_3^- - N$ concentrations of the *PW* and effluent. Profiles of NH_3-*N* of *IA* were always less than 3.0 mg/L. **Figure A-4** shows the variation of NH_3-*N* concentration in *PWs* and *E* due to *IA*. $NO_2^- - N$ never existed in significant concentrations in either the *PW* or effluent. **Figure 3.12** indicates that $\delta^{15}N$ values of NO_3^- in the several effluent samples have been enriched by more than two fold of that in the influent. The degree of the enrichment of $\delta^{15}N$ of NH_4^+ in several effluents due to *IA* is the same as that of *CA*.

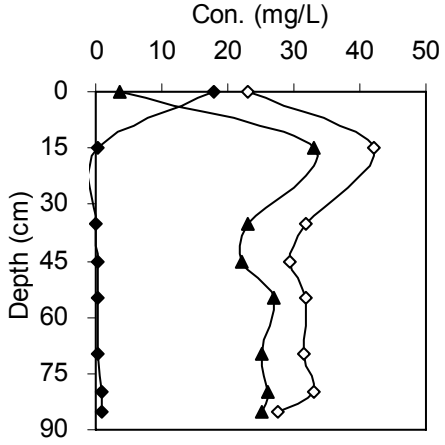

Fig. 3.11 T-N (hollow diamonds), NO_3^--N (triangles) & NH_3-N (solid diamonds) concentration distributions with soil depth in IA at the end of the experimental run (low porous soil).

Transient and steady state variations of the other contaminants due to IA

As shown by **Fig. 3.14** & **Fig. 3.15**, the profiles of Cl^- and SO_4^{2-} of IA were similar to those of *CA* except that there were fluctuations within the period between every two

consecutive irrigations, which may have been caused by immobile conditions likely to have existed due to the variation of the percolation rate in *IA*. Both concentrations decreased with the gradual reduction of the percolation rate having experienced in the period between every two consecutive irrigations. Eventually, the peak Cl^- during such periods reached the steady-state at a value approximately equal to the maximum Cl^- concentration of *SRW*. The Cl^- profile, which has undergone negligible ion exchanging, is an indication of the flow path of the soil column. Therefore, the flow apparently has not been influenced by any preferential flow.

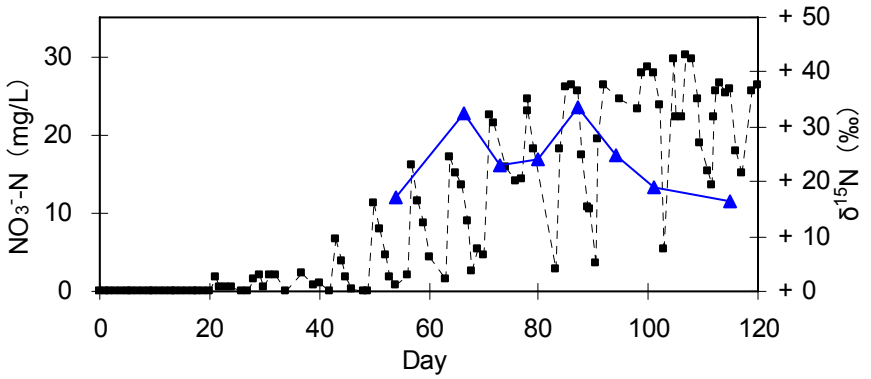

Fig. 3.12 Variation of NO_3^--N concentration (boxes with dashed line) of the effluent, & NO_3^--$\delta^{15}N$ of the effluent (blue), with time, for IA (low porous soil).

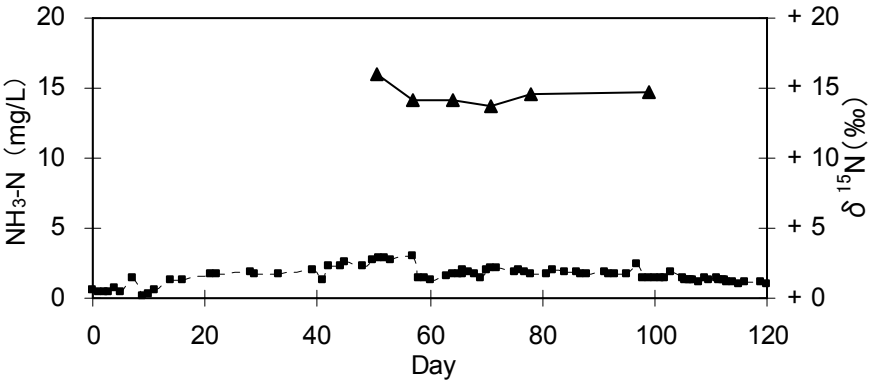

Fig. 3.13 Variation of NH_3-N concentration (boxes with dashed line) of the effluent, & NH_4^+-$\delta^{15}N$ of the effluent (triangles with solid line) with time, for IA (low porous soil).

Figure 3.16 & 3.17 indicate that Ca^{2+} concentration of effluent due to *IA*, reached elevated levels rapidly once received *SRW*. Mg^{2+}, K^+ and Na^+ concentrations in the influent increased as well. The difference of the respective profiles between *CA* and *IA* is the fluctuation of the concentration of IA. As explained in an above section, it may be due to the variation of the water percolating rate. The ultimate Ca^{2+}, Mg^{2+} and K^+

concentrations in the effluent were in excess of those present in *SRW*, while Na^+ concentration is opposite to that observation.

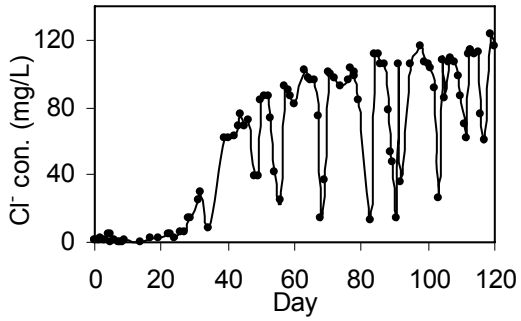

Fig. 3.14 Variation of Cl^- concentration in E of IA (low porous soil).

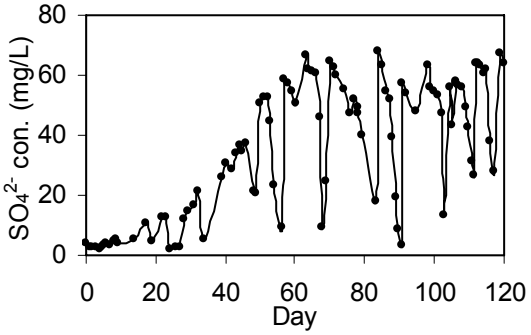

Fig. 3.15 Variation of SO_4^{2-} concentration in E in IA (low porous soil).

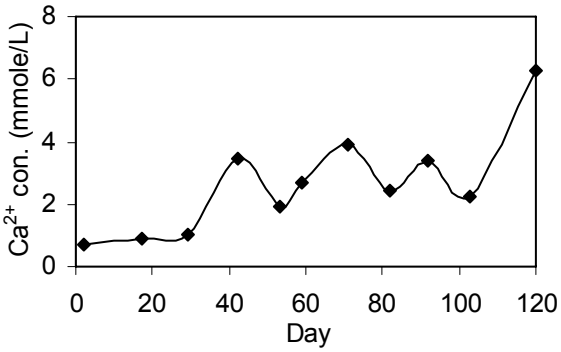

Fig. 3.16 Variation of Ca^{2+} concentration in E of IA (low porous soil).

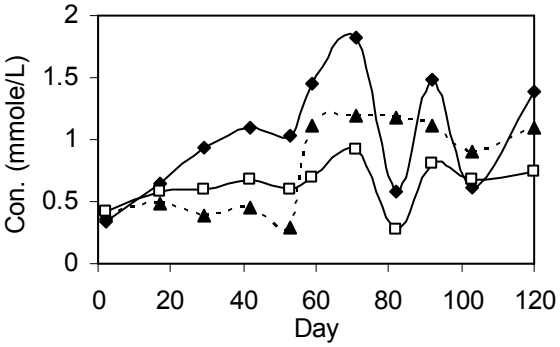

Fig. 3.17 Variation of Mg^{2+} (diamonds), Na^+ (triangles) and K^+ (hollow boxes) concentration in E of IA (low porous soil).

Conductivity of *E* due to *IA* ranged from 60-120 ms/m toward the end of experimental run (Fig. A-2). *pH* in *E* due to *IA* has slightly decreased from about 8.8 to 8.4 during the steady state (Fig. A-3). The steady state-*pH* of the effluent was also higher than that of *SRW*. The ionic strength of the effluent due to *IA* at the end of the experiment was 6 times higher than that of the *SRW*. The existence of *P* compounds in the water samples of *IA* was insignificant.

Final soil characteristics and nitrogen mass balance

Table 3.2 & 3.3 show the soil characteristics before and after cleansing; and final soil characteristics, respectively. **Figure 3.18 (a & b)** depicts the variation of cumulative mass of *T-N*, applied on the column via influent, and the cumulative mass of *T-N* and $NO_3^- - N$ discharged from the column as the effluent. The gap between the cumulative

mass of *T-N* in the influent and effluent indicates that the balance amount of *T-N* may have either accumulated on soil or off-gassed to the soil air, probably as N_2O and N_2; or both. Though there is a sharp increase on the profiles of both *T-N* and $NO_3^- - N$ of *CA*, from the 50th day to about 60th day, the gradients of the profiles have started to decrease after 60th day, and the gap between $NO_3^- - N$ and *T-N* seems to have increased toward the end (Fig. 3.18a). However, in Fig. 3.18b, the gradients of the profiles of *T-N* and $NO_3^- - N$ were on a rapid rise after 60th day. **Figure 3.19(a & b)** shows the variation of the cumulative volume of water applied on a column as the influent and the cumulative volume of water discharged as the effluent. Water lost in *IA* is lower than that of *CA*. This discrepancy may be attributed to the fact that the evaporation may have been higher in *CA* owing to the relatively high retention time.

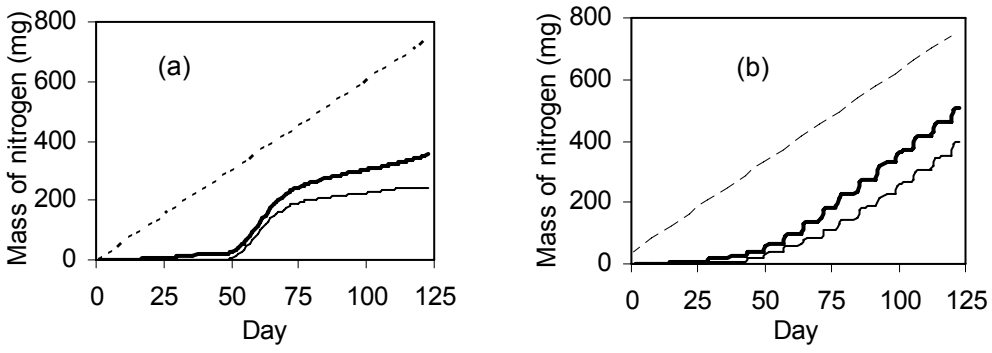

Fig. 3.18 Variation of the cumulative mass of T-N applied on the column via influent (dashed line), and the cumulative mass of T-N (thick solid line) and NO_3^- -N (thin solid line) discharged as effluent, in (a) CA and (b) IA (low porous soil).

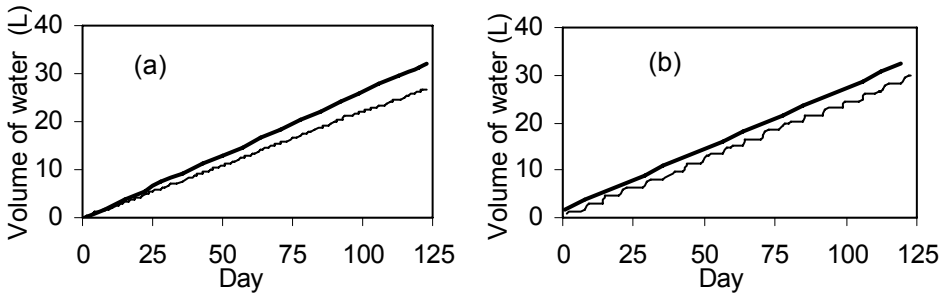

Fig. 3.19 Variation of the cumulative volume of water applied on the column via influent (thick line) and discharged as effluent (thin line), in (a) CA and (b) IA (low porous soil).

Table 3.4 shows the components of the input and output of each system, in terms of cumulative mass of *T-N*. In Table 3.4, the ultimate cumulative mass of *T-N* lost by off-gassing is the ultimate cumulative mass of *T-N* in the influent minus ultimate cumulative mass of *T-N* in the effluent plus the total accumulated *T-N* in soil. The mass of *T-N* (mainly N_2O and N_2) that has been lost by off-gassing to the soil air, for *CA* and *IA* are 41.5% and 13%, respectively, relative to the ultimate cumulative mass of *T-N* applied via the influent. Above values do not represent the dissolved gas in the soil solution. In accordance with Starr et al. (1974), N_2O is highly soluble in water, and there is a possibility that dissolved N_2O may have remained in the soil solution sufficiently long to be further reduced to N_2. However, no measurement was made for dissolved N_2O. The partial pressure of any gaseous compound in the soil atmosphere was not considered.

$\delta^{15}N$ of soil below 25 cm depth in *CA* has been enriched at the end of the run, where as in *IA*, except at 15 cm and 80 cm depths, $\delta^{15}N$ has depleted (**Fig. 3.20**).

Table 3.2 Soil characteristics before and after cleansing on low porous soil.

Description	CA			IA		
	NO_3^--N	NH_3-N	T-N	NO_3^--N	NH_3-N	T-N
Content in the column before cleansing (mg)	469.83	88.09	40756	469.83	88.09	40756
Content removed during cleansing (mg)	385.45	5.28	-	378.32	6.42	-
Content in the column before loading SRW (mg)	84.38	82.81	-	91.51	81.67	-

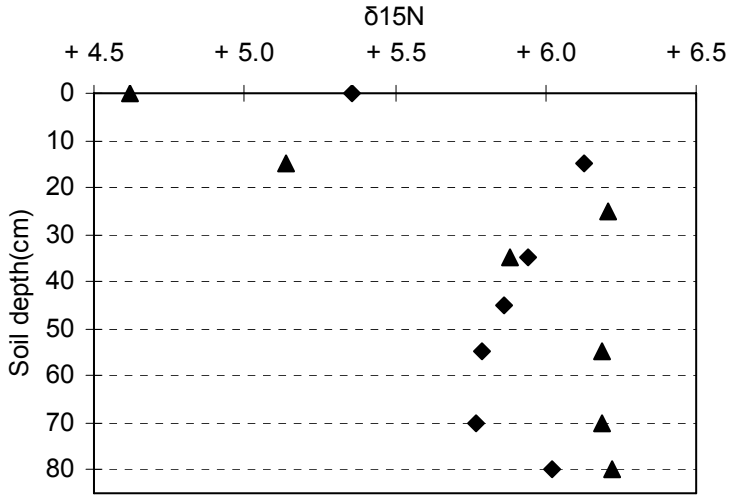

Fig. 3.20 Variation of $\delta^{15}N$ ‰ along the soil depth of CA (triangles) and IA (diamonds) at the conclusion of the experiment (low porous soil).

Table 3.3 Final soil characteristics on low porous soil.

Depth (cm)	CA			IA		
	Oven-dry wt. of soil (kg)	NO_3^--N (mg)	NH_3-N (mg)	Oven-dry wt. of soil (kg)	NO_3^--N (mg)	NH_3-N (mg)
0-15	5.45	28.37	16.55	5.45	41.78	17.65
15-35	7.38	31.71	14.45	7.38	38.06	25.04
35-45	3.64	9.46	8.49	3.64	20.23	13.02
45-55	3.64	34.10	12.49	3.64	16.72	12.51
55-70	5.45	25.60	10.61	5.45	43.04	18.76
70-85	5.45	29.79	25.07	5.45	40.10	22.90
Total	31.01	159.03	87.66	31.01	199.93	109.87

Table 3.4 Nitrogen mass balance of the experiment on low porous soil.

Description	CA	IA
Cumulative T-N supplied as influent (mg)	743.0	743.0
Accumulated T-N in soil after leaching (mg)	79.5	136.6
Cumulative T-N discharged as effluent (mg)	355.2	510.0
Cumulative T-N lost by off-gassing to the soil air (mg)	308.5	97.0

Nitrification

Nitrification has commenced above 15 cm depth in both the columns, because the profiles of NH_3-N have reduced to less than 3.5 mg/L at 15 cm depth (Fig.3.3, 3.11, A-1 & A-4), while it was 18 mg/L in *SRW*. In addition, $NO_3^- - N$ concentration of the *PW* and effluent exceeded the *SRW*- $NO_3^- - N$ within a very short time (Fig. 3.2 & Fig. 3.10). For instance, *PW1* and *PW2* of *CA* did so within less than 5 days. Nitrogen transformation could have occurred as the sum of both zero and first order reactions. According to a study of the nitrogen transformation of a continuous leaching, the nitrification rate coefficients were not constant at various depths (Starr et al., 1974).This may have been due to the different values of soil *pH* and/or biomass as a function of soil depth. The rate of nitrification may be enhanced in this system compared with that in a system where the ions do not get sorbed, due to the fact that the charged soil particle surfaces increase the local concentration of NH_4^+ near the nitrifiers in the vicinity of the surfaces. Hence, NH_4^+ may diffuse faster into and through the cell walls of the microbes resulting in increased nitrification rates (Misra et al., 1974a).

The fluctuations of $NO_3^- - N$ concentrations in all the profiles (Fig.3.10) of IA may be due to the desiccation effect of soil. Soil remains relatively dry after first two days following each application of *SRW*. It may have retarded nitrification because extreme dry conditions and lack of water inhibit the nitrification process. NH_4^+ may have failed to

nitrify due to the desiccation that soil had sustained during the period between two consecutive irrigations. The depressive effect of microbial activity caused by the soil desiccation during the dry season has been confirmed by Jewitt (1950).

As stated by Ostrom et al. (1998), N isotope data can provide considerable insight into microbial processes in soils and the dynamics of the mineralization process. Fig. 3.5 & 3.13 show that NH_4^+- $\delta^{15}N$ variability in the effluent of *CA* and *IA* ranged from +11.3 to +17.9 ‰ and from +13.7 to +16.0 ‰, respectively during day 38-day 84 and day 50 to day 99, respectively; whereas the average NH_4^+- $\delta^{15}N$ in the *SRW* was -6.5 ‰ because the source of *SRW*- NH_4^+ is NH_4Cl. This observation indicates that $\delta^{15}N$ of *SRW*- NH_4^+ increased during percolating through the soil as a result of the isotopic fractionation caused by the nitrification. During nitrification, the light isotope is preferentially incorporated into NO_3^- and a decrease in $\delta^{15}N$ during this process is frequently observed (Mariotti et al., 1981). Hence, ^{15}N should accumulate in the residual NH_4^+ post nitriifcation. Fractionation during nitrification is most marked when NH_4^+ is abundant in soils, as occurs following the applications of NH_4^+ based fertilizers, and may be small or negligible when NH_4^+ is not readily available (Heaton, 1986). The dominant processes affecting the NO_3^--$\delta^{15}N$ in most soils are nitrification and mineralization, in which depletion in the ^{15}N content of NO_3^- are expected, and denitrifcation, which causes an enrichment in ^{15}N in NO_3^- (Ostrom et al., 1998). This implies that the above mentioned isotopic variation is, to great extent, a result of the microbial transformation of nitrogen. Since there is no significant difference of the isotopic variability between *CA* and *IA*, the degree of nitrification can be considered the same in both cases.

Ion exchange reactions

The great reduction of NH_3-*N* contained in *SRW* in high concentrations, at very top soil layers (Fig. 3.3 & Fig. 3.11) is attributed not only to nitrification but also to adsorption. This is highly possible because NH_4^+ has a positive charge, and is held by the negative sites on the clay in the soil. According to the obtained results, it can be deduced that NH_4^+ of both *CA* and *IA* has been adsorbed largely on to the negatively charged soil colloidal particles, preceding the nitrification. There was an overall increase of soil NH_3-*N* content in the soil at the end of the experiment too.

$NO_3^- - N$ concentration of the water samples collected from the upper four ports of the continuous column, indicates very high peak concentrations which remained only for very short time {Fig. 3.2 (a, b, c & d)}. The NH_4^+, which was adsorbed onto soil, may not have rapidly nitrified in the beginning. The population of nitrifiers on soil may not have been sufficient for nitrification to take place. However, about 30 days after the commencement of *SRW* loading, $NO_3^- - N$ concentration of *PW1* increased rapidly. It was successively followed by the $NO_3^- - N$ concentrations of the other *PW*s and the effluent. It means that NH_4^+, which had been adsorbed previously, may have nitrified rapidly, once enough population of nitrifiers was established for nitrification to take place very rapidly. Then, it leaches into the soil solution as NO_3^-.The soil apparently possesses high capacity for the adsorption of ions owing to the high specific surface area of soil grains as a result of being low porous. The batch sorption experiments described in the section 3.2 are evidenced that the soil has high sorption capacity for NH_4^+ adsorption. The leaching potential of NH_4^+ in soils is very low as it, being a positive charge, is held by the negative sites on clay in soils. The cation concentration adjusts to a condition of exchange equilibrium upon receiving NH_4^+. Soil clays can retain significant amounts of NH_4^+ in excess of the cation exchange capacity and out of competition for exchange sites. Freeze et al. (1979) stated that the equilibrium-cation concentration depends on the cation concentration of the water entering the pore space, in which the exchange occurs and the mole fractions of adsorbed cations on the pore surfaces immediately prior to the entry of new pore water; and a new equilibrium state is built according to the new set of conditions caused by each new volume of water that moves through the pore space.

According to Fig. 3.8, 3.9, 3.16 & 3.17, overall, Ca^{2+} Mg^{2+} and K^+ have released from soil into the percolating water, while Na^+ supplied by the *SRW* retained in soil. It shows that Na^+ and NH_4^+ contained in the *SRW* exchanged with Ca^{2+} Mg^{2+} and K^+ retained in the water film on the colloid surfaces due to their predominantly negative charge. Especially, NH_4^+ tends to be exchanged with Ca^{2+} in accordance with Bohn et al. (1985) who stated, on the basis of past studies, that passing an ammonium sulfate solution through soil columns resulted in a column leachate that was primarily calcium sulfate. Even though, Na^+ possessed the highest relative ion replaceability among the above-mentioned cations, Na^+ has retained in the soil. This may be due to the Na^+ concentration

in *SRW* being relatively high. On the other hand, Ca^{2+}, which has the highest relative affinity for specific colloids, has desorbed into the soil solution. This can be rationalized by the fact that raising soil pH can also change cation selectivity by increasing soil CEC and thus increasing the preference for polyvalent versus monovalent ions (Bohn et al., 1985). This agrees with mudstone, which has high *pH* and *CEC*. As mentioned by Bohn et al. (1985), the generalized opinion about the cation exchange in soil is that the reactions are reversible, stoichiometric and rapid. Further, the same author stated that even strongly adsorbed cations can normally be replaced through proper manipulation of solution conditions. If an ion represents a cation (such as NH_4^+) that enters into ion exchange reactions and is sorbed onto a negatively charged soil particle surface, it is considered to be held up temporarily but is capable of being replaced eventually by similar or other ions; such a temporarily loss and gain of ions is termed reversible (Misra et al., 1974a). Hence, the temporary occurrences of both adsorption and desorption are inherent in the cations that involve inter-ion exchange reactions. Desorption of adsorbed NH_4^+ is possible when sorption sites with high affinity to NH_4^+ become saturated. More NH_3 is sorbed on dry clays than on wet ones (Dontsova et al., 2005). Therefore, due to the soil being dry for a long time, there is a possibility that *IA*-soil possessed a high sorption capacity to NH_4^+.

Denitrification

The profiles of $NO_3^- - N$ due to *CA* (Fig. 3.2 and Fig. 3.3) lead to the hypothesis that denitrification has been accelerated in the lower soil layers of the continuous column during the transient and steady states. The nitrogen mass balance is one proof to the acceleration of denitrification in *CA*, because the mass of *T-N* lost by off-gassing to the soil air of the continuous column is considerably high in comparison with that of *IA*. In addition, Fig. 3.4 and 3.12 verify the presence of denitriifcation in both the columns as $NO_3^- \text{-} \delta\,^{15}N$ in the effluent is higher than that of the influent. Further, they verify that denitrification happened more in *CA* than *IA* since enrichment of $NO_3^- \text{-} \delta\,^{15}N$ was always higher by threefold than that in the influent. During denitriifcation, the light isotope is preferentially incorporated into the gaseous products of this reaction and the remaining NO_3^- is enriched in ^{15}N (Mariotti et al., 1981). When the above expression coupled with Fig. 3.4, it can be deduced that denitrification caused the fall of $NO_3^- - N$ from the peak.

Losses of NO_3^- due to denitrification as low as 20% can result in increase in $\delta^{15}N$ by 8 ‰ (Heaton, 1984). NO_3^--$\delta^{15}N$ and NH_4^+-$\delta^{15}N$ of the influent are 10.2 ‰ and -6.5 ‰, respectively. Given that NO_3^-, which has denitrified, was mostly derived from the *SRW*-NH_4^+, NO_3^--$\delta^{15}N$ prior to denitriifcation is not exactly 10.2 ‰**.** However, according to a discussion in an above-section, NO_3^--$\delta^{15}N$ prior to denitrification would be less than -6.5 ‰**.** It means, in *CA*, the maximum increase of NO_3^--δ ^{15}N in the effluent relative to NO_3^--$\delta^{15}N$ prior to denitrification is well above 40 ‰.

In the absence of denitrification, $NO_3^- - N$ concentration may have remained a constant maximum value equal to the influent $NH_4^+ - N$ concentration at greater soil depths (Erh et al., 1967; McLaren, 1969). This statement is valid if the nitrogen compounds, such as NO_2^- and N_2O, are not considered. However, the following results ascertain that the above statement is valid for this experiment. $NO_2^- - N$ concentration in all the percolated water samples are negligible. *T-N* concentrations of the *PW*s above 55 cm are higher than that of the *PW*s below 55 cm and the effluent, during both the transient and steady states. Figure 3.3 that depicts the average *T-N* concentration distribution along the soil depth during the steady state, agrees with the above statement. It has been observed that the heterotrophic flora easily outgrow the autotrophes, which are known to be poor competitors with the former group of organisms (Misra et al., 1974b). Very compacted soil retards nitrification. The underlying layers carry the water load and the soil load. Hence, the soil may have been more compacted in the underlying layers than the top layers, thus denitrification has been promoted. In addition, there may have been water logged conditions that have created an anoxic environment. Soil, which is rich in organic matter owing to the clayey nature, may have been the main supplier of the carbon source for denitrifiers.

It is visible that denitrification had not been significant in the underlying layers of *IA*, when the steady state $NO_3^- - N$ distribution of *CA* and *IA* are contrasted (Fig.3.3 and Fig.3.11). A favorable microenvironment for the denitrifiers could not have developed in *IA*. The acceleration of denitrification in *CA* may have been attributed to the high retention time owing to the less percolation rate.

Ammonification

Dissolved NH_3 reacts with water to form NH_4^+, resulting in a sharp increase of pH, which leads to the solubilization of the organic matter (Stehouwer et al., 1993). Dissolved organic *C* is considered to be a readily available substrate for soil microorganisms (Brye et al., 2001) and could stimulate dissolved organic *N* mineralization and nitrification in the soil profile, leading to an increase in the dissolved $NO_3^- - N$ concentration with depth (Jiao et al., 2004). Mineralization of soil organic matter is generally considered to favor incorporation of the light isotope in NH_4^+ (Nadelhoffer and Fry, 1994). Therefore, if mineralization of soil organic nitrogen had happened, NH_4^+- $\delta^{15}N$ would have been less than δ^{15}N of soil, which is approximately +6 ‰. However, Fig.3.5 & 3.13 evinces that the NH_4^+ present in the effluent is not a result of soil organic nitrogen mineralization.

3.1.3.2 Effect of concurrent applications of SR and IA of SRW

Figure 3.21 shows the variation of both $NO_3^- - N$ & *T-N* during the concurrent applications of *SR* and *IA* of *SRW*. Both $NO_3^- - N$ & *T-N* concentrations seem to have been in the decreasing phase at the end of the experiment. **Figure 3.22** is the variation of the cumulative mass of *T-N* applied via the influent and discharged as the effluent. **Figure 3.23** indicates the variation of cumulative water applied on the column via the influent and discharged as the effluent. According to Fig. 3.22, approximately 5 days after the commencement of the SR application, the cumulative mass of *T-N* discharged as the effluent has overtaken that applied via the influent; whereas, before the application of SR, the effluent profile never exceeded the influent profile. The ultimate cumulative mass of *T-N* discharged as the effluent was approximately 1.9 times greater than that applied via the influent. It ascertains that there may have been a source that desorbed nitrogenous compounds into the percolating water, during the concurrent applications of *SR* and *SRW*.

In order to estimate the contribution of the high dissolved oxygen found in *SR*, upon the nitrification process, the following calculation was carried out. The overall oxidation and synthesis reaction for NH_4^+ can be given by Eq. (3.1):

$$NH_4^+ + 1.83O_2 + 1.98HCO_3^- \rightarrow 0.021C_5H_7O_2N + 0.98NO_3^- + 1.041H_2O + 1.88H_2CO_3 \quad (3.1)$$

(Metcalf & Eddy, 1991)

Therefore, the oxygen required to oxidize NH_4^+ to NO_3^- is expressed as 4.3 mgO_2 /mg $NH_4^+ - N$. The saturated *DO* concentration in fresh water at 20°C and at normal pressure is 9.1 mg/L. So, it is assumed that *DO* concentration of the de-ionized water as 7.0 mg/L. Then, the ultimate cumulative *DO* applied via *SR* is 47.72 mg. If it is assumed that the total cumulative *DO* applied via *SR* is utilized for the oxidation of NH_3 applied via *SRW*, 23.3 % mass of $NH_4^+ - N$ oxidized relative to the total applied mass. Therefore, it can be said that the nitrification has been accelerated by the application of SR.

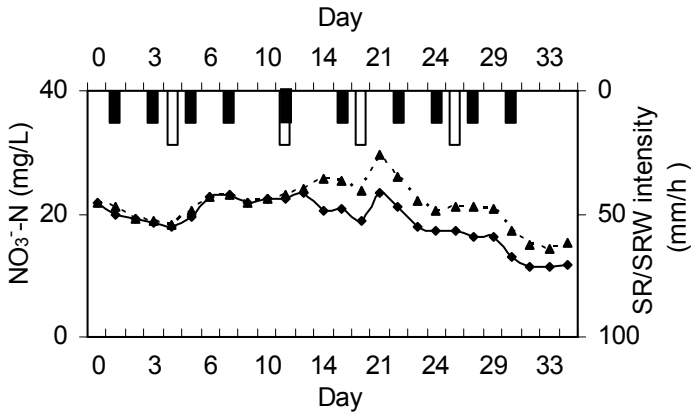

Fig. 3.21 Variation of NO_3^--N (diamonds with solid line) & T-N (triangles with dashed line) concentration in the effluent during the concurrent applications of SRW (white bar) and SR (black bar).

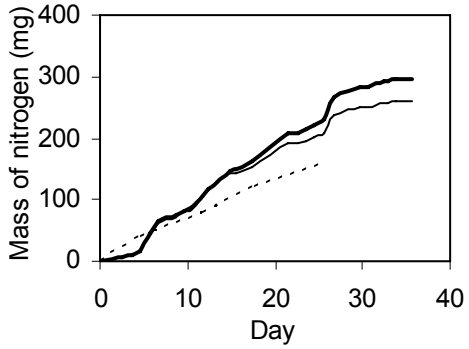

Fig. 3.22 Variation of the cumulative mass of T-N applied via influent (dashed line) and cumulative mass of T-N (thick solid line) & NO_3^--N (thin solid line) during concurrent application of IA of SRW & SR.

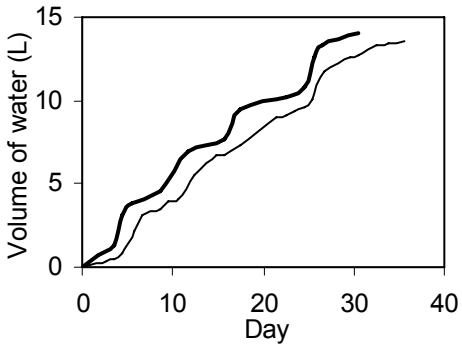

Fig. 3.23 Variation of the cumulative volume of water applied via influent (thick line) and discharged as effluent (thin line) during concurrent application of IA of SRW and SR.

However, the most possible source of $NO_3^- - N$ is the soil that may have leached the accumulated NO_3^- in soil, into the percolating water. Jiao et al. (2004) stated, on discussing a soil column experiment, that the $NO_3^- - N$ load in leachates had been positively related

to the $NO_3^- - N$ concentration in soil columns. NO_3^- is repelled from soils due to the high negative charge of the cation exchange capacity. Negatively charged NO_3^- generally tends to be repelled by the negatively charged soil particles, resulting it to remain in the soil solution. Because NO_3^- is extremely soluble in water, water carries it along with moving through the soil. As stated by Donn and Menzies (2005), changes to the *pH* and ionic strength of the soil solution would result in changes to the charge chemistry of soil. As a result of the variation of *pH* or the ionic strength of the soil solution, the equilibrium-relationship between the adsorbed NO_3^- and the positive charge density is likely to be altered. Therefore, during the application of *SR*, the equilibration of the soil solution with the rainwater solution (*DW*) possessing low ionic strength has resulted in a lessening of both the positive and negative charge, and therefore NO_3^- has leached into the soil solution.

This phenomenon can be applied in a real field, which is irrigated with the *RWW* for a long time, where the cumulative nitrogen content in both soil and soil solution is relatively high. Normally, the ionic strength of the rainwater is low relative to that of the reclaimed wastewater. Hence, upon receiving rainfall, the possibility of leaching accumulated nitrogenous compounds in soil, into the percolating water, is high in such a field.

3.2 BATCH SORPTION EXPERIMENTS

3.2.1 Introduction

Sorptive uptake and withdrawal of compounds by soils and sediments from aqueous solution is usually measured by sorption experiments at constant temperature that yield sorption isotherms. Batch tests are commonly used to measure K_d values. The test is conducted by spiking a solution with the element of concern, mixing the spiked solution with a solid for a specified period of time, separating the solution from the solid, and measuring the concentration of the spiked element remaining in the solution. The concentration of contaminant associated with the solid is determined by the difference between initial and final contaminant concentration.

Two series of batch sorption experiments were conducted using the low porous mudstone soil. The particle size of soil was less than 2 mm square screen. *DW* & *SRW* were used as aqueous solutions. The 1st batch experiment was conducted to optimize the time required for NH_4^+ to attain the equilibrium state in a batch reactor that undergoes a

sorption experiment of NH_4^+ contained in *SRW* (100 mL) with 10 g soil, and to quantify the sorptive uptake or withdrawal of NO_3^-. The 2nd experiment was conducted to derive the sorptive uptake or withdrawal of NH_4^+ by cleansed soil, and to obtain the K_d for NH_4^+.

3.2.2 Theory

For non-linear sorption, K_d changes with concentration and the Freundlich isotherm is most commonly used to describe the sorption isotherm:

$$q = \frac{x'}{m} = K_d C^{1/n} \text{ (Bohn et al., 1985)} \qquad (3.2)$$

In Eq. (3.2), sorption is quantified by K_d. If the sorption is linear, K_d is constant with varying concentrations. Then Eq. (3.2) becomes:

$$q = \frac{x'}{m} = K_d C \qquad (3.3)$$

3.2.3 Experiment 1

3.2.3.1 Methodology

Each of 30 vials was filled with 10 g soil. 100 mL *DW* was filled in each of 10 vials, while 100 mL of *SRW* was filled in each of the rest. Five sets of 6 vials, containing *DW* in duplicate and *SRW* in 4 replicates, were kept in a mechanical shaker at 120 rpm for 6h, 12h, 24h, 48h and 72h, respectively. The mechanical shaker was kept inside an incubator at 20 ^{0}C. The characteristics of the *SRW* and the supernatant at the equilibrium state, were obtained in terms of $NO_3^- - N$, NH_3-*N*, cations such as Ca^{2+}, Mg^{2+}, Na^+ and K^+, *pH* and conductivity.

3.2.3.2 Result & Discussion

Figure 3.24 shows the equilibrium concentrations of NH_3-*N* vs. total time of shaking. It clearly shows that nearly half the NH_3-*N* present in *SRW* (NH_3-*N* of *SRW* is 18 mg/L) was withdrawn from the solution. Results indicate that the equilibrium state reached less than 12h. **Figure 3.25** is the variation of increase of $NO_3^- - N$ concentration in the solution. It seems that $NO_3^- - N$ concentration has slightly increased in both *SRW* and *DW*. It is most probably due to the NO_3^- leaching from soil. The increase is higher in *DW* than in

SRW. It is because the ionic strength of *DW* is lower than that of *SRW*. The reader is directed to the discussion in the section 3.1.3.2. This indicates that both NH_4^+ and NO_3^- have not undergone any microbial transformations significantly. Therefore, it can be verified that the withdrawal of NH_4^+ from the solution is mainly due to the adsorption. Also, leaching of NO_3^- from soil is not so significant when the solvent is *SRW*.

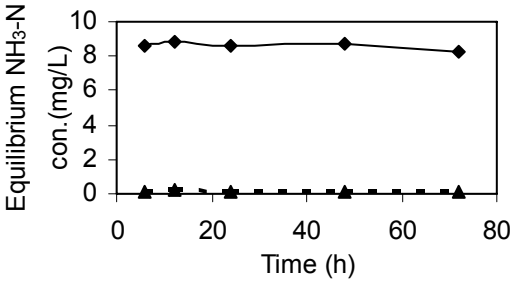

Fig. 3.24 Variation of equilibrium NH_3-N concentration in the supernatant of DW (triangles with dashed line) & SRW (diamonds with solid line) (low porous soil).

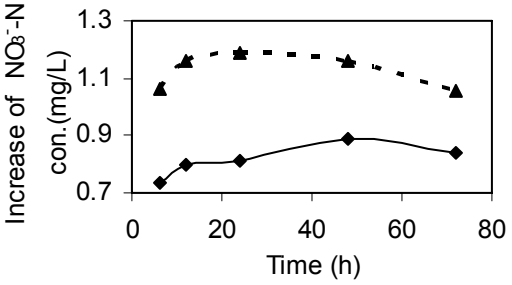

Fig. 3.25 Variation of increase of NO_3^--N concentration in the supernatant of DW (triangles with dashed line) & SRW (diamonds with solid line) (low porous soil).

3.2.4 Experiment 2

3.2.4.1 Methodology

First, the soil was cleansed in the following way. 3 no. of containers were filled each with 100 g of soil and 1L of *DW*. Then, the containers were kept in a shaker at 120 rpm for 24 h. After 24h, 300 mL supernatant was replaced with fresh 300 mL of *DW*, and kept again in the shaker for another 44 h. After total of 68 h, 340 mL of supernatant was replaced with 340 mL fresh *DW* and kept until total of 89 h passed. Then, the supernatant was removed from soil as much as possible, and then soil was dried at 35 ^{0}C for 48 h in order to reduce the moisture content. The moisture content of soil after drying was 1.64 %. Each 4 of 12 vials was filled with 5g, 10g, 20g and 25g of cleansed soil, respectively. 100 mL of *SRW* was filled in each vial. Then, all the vials were kept in a shaker at 120 rpm for 72h, as the experiment 1 shows that it is adequate for NH_4^+ to become the equilibrium state. The characteristics of the *SRW* and the equilibrium supernatant were obtained in terms of $NO_3^- - N$, NH_3-N, Ca^{2+}, Mg^{2+}, K^+, Na^+, pH and conductivity.

3.2.4.2 Result & Discussion

Figure 3.26 is the solute (NH_3-N) concentration on soil (q) vs. the equilibrium concentration of the solute in the solvent. The curve is non –linear. It can be excellently fit

into a Freundlich isotherm with K_d = 7E-06 (L/mg)$^{1.9075}$ and n = 1.9075. If it is approximated to the linear form of Freundlich isotherm, R^2 reduces very much as shown by the figure. Then, K_d is equal to 4E-05 (L/mg) (40 cm^3/g). The primary disadvantage of the batch sorption experiments for measuring K_d is that it does not necessarily reproduce the chemical reaction conditions that take place in the real environment. For instance, in a soil column, water passes through at a finite rate and both reaction time and degree of mixing between water and soil can be much less than those occurring in a laboratory batch test. Consequently, K_d values from batch experiments can be high relative to the extent of sorption occurring in a real system, and thus result in an estimate of contaminant retardation that is too large.

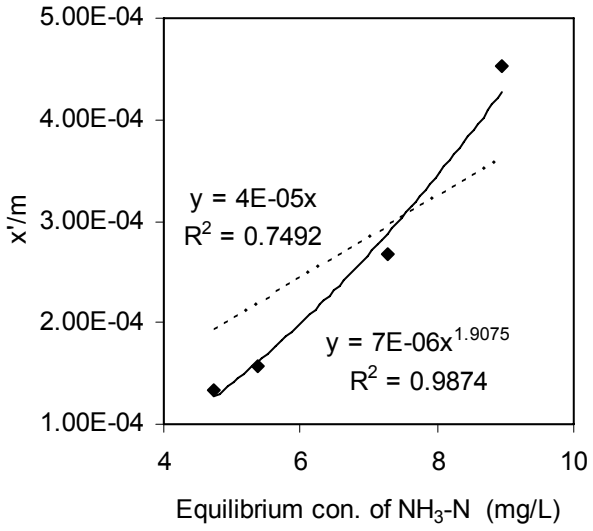

Fig. 3.26 Variation of NH_3-N concentration on the solid phase vs. equilibrium NH_3-N concentration in the supernatant (low porous soil)

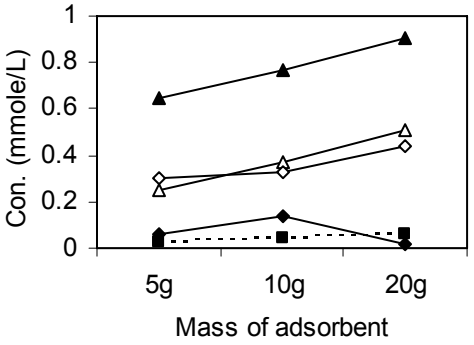

Fig. 3.27 Increase of Ca^{2+} (hollow diamonds), Na^+ (solid diamond), K^+ (boxes) and Mg^{2+} (hollow triangles), and decrease of NH_4^+ (triangles), in supernatant vs. mass of low porous soil).

Figure 3.27 shows that there was an increase of Ca^{2+}, Mg^{2+}, Na^+ and K^+ concentrations in the supernatant after shaking. All the above cations from soil have exchanged with NH_4^+ contained in the adsorbate. This observation verifies that in the aforementioned soil column experiment, NH_4^+ contained in the *SRW* exchanged with the cations such as Ca^{2+}, $Mg^{2+}$and K^+ from soil liquid interphase, however Na^+ contained in *SRW* retained in soil in that case. Bohn et al. (1985) stated that the exchange step itself is virtually instantaneous, and the rate-limiting step often is ion diffusion to or from the colloid surface. The same author further clarified the above fact by stating that it is

particularly true under field conditions, where ions may have to move through tortuous pores or through relatively thick, stagnant water films on soil colloid surfaces to reach an exchange site. The same author further added that under laboratory conditions, samples normally are shaken during exchange reactions, to speed ion movement and to minimize the thickness of stagnant water layers on soil particle surfaces. These facts indicate that the ion-exchange in the soil column, being closer to that of the field conditions, may be considerably affected by the diffusion and hence may result in different products from those of batch experiments, which is the least likely to be affected by diffusion.

3.3 CONCLUSIONS

This study was conducted to investigate the dynamics of nitrogen in the low porous mudstone soil, as a result of continuous and intermittent irrigation of *RWW*. Two laboratory scale unsaturated soil columns, loaded with the soil, were applied with *SRW* continuously and intermittently for a period of 120 days. The simultaneous occurrence of nitrification, denitrification and adsorption of NH_4^+ on to soil was proved by the profiles of nitrogenous compounds, analysis of the nitrogen stable isotopes and the nitrogen mass balance performed at the end of the experiment. Approximately 90% of *NH_3-N* in *SRW* diminished at the upper soil layers in both the columns, due to nitrification and adsorption. In *IA*, $NO_3^- - N$ concentration of the *PW*s and effluent obtained from various depths exhibited similar profiles. These profiles were characterized by a gradual increase in $NO_3^- - N$ concentrations, which eventually approached a plateau where the concentration remained approximately constant. In *CA*, $NO_3^- - N$ concentration of all the *PW*s & effluent increased to a maximum, and then decreased preceding the steady state. The maximum $NO_3^- - N$ concentrations of *PW*s collected from above 55 cm depth were considerably higher than those collected from below 55 cm depth and the effluent. In addition, NO_3^--$\delta^{15}N$ ‰ in 6 effluent samples of CA increased from 30 to 50, while $NO_3^- - N$ concentration dropped from the peak at the same time. The nitrogen mass balance indicated that the ultimate cumulative mass of *T-N* that was lost by off-gassing to the soil air due to *CA* and *IA* are 41.5% and 13.0%, respectively. Therefore, the results concluded that the lower soil layers of the continuous column have promoted denitrification in comparison to that of *IA*. In addition, the experiment of the concurrent applications of *SR*

and *IA* of *SRW* proved that the leaching of accumulated NO_3^- in soil, into the percolating water would be enhanced with the dilution effect of rainfall. Further, the batch sorption experiments showed that the adsorption of NH_3^+ onto mudstone soil is very quick and the leaching of soil-NO_3^- into the solution of *SRW* is negligible. Moreover, the results of the variation of $\delta^{15}N$ also postulates that the analysis of nitrogen stable isotopes is an effective tool to understand nitrogen dynamics in the soil.

REFERENCES

Bohn, H. L., B. L. McNeal, G. A. O'Connor (1985), *Soil Chemistry*, John Wiley & Sons, Inc., New York.

Brye, K. R., J. M. Norman, L. G. Bundy, and S. T. Gower (2001), Nitrogen and carbon leaching in agro ecosystems and their role in denitrification potential, *J. Environ. Qual*., *30*, 58-70.

Clesceri, L. S., A. E. Greenberg, and A. D. Eaton (1998), *Standard Methods for the Examination of Water and Wastewater*, American Public Health Association, 1015 Fifteenth Street, NW, Washington, DC 20005-2605.

Donn, M. J., and N. W. Menzies (2005), Simulated rainwater effects on anion exchange capacity and nitrate retention in ferrosols, *Australian Journal of Soil Research, 43*, 33-42.

Dontsova, K. M., L. D. Norton, and C. T. Johnston (2005), Calcium and magnesium effects on ammonia adsorption by soil clays, *Soil Sci. Soc. Am. J., 69*, 1225-1232.

Erh, K. T., D. E. Elrick, R. L. Thomas, and C. T. Corke (1967), Dynamics of nitrification in soils using a miscible displacement technique, *Soil Sci. Soc. Amer. Proc*., *31*, 585-591.

Freeze, R. A., J. A. Cherry (1979), *Groundwater,* Prentice-Hall, Inc., Englewood Cliffs, N. J. 07632.

Heaton, T.H.E. (1984), Source of nitrate in phreatic groundwater in the Western Kalihari, *J. Hydrol*., *67*, 249-259.

Heaton, T.H.E. (1986), Isotope studies of nitrogen pollution in the hydrosphere and atmosphere: a review, *Chem. Geol.*, *59*, 87-102.

Jewitt, T. N. (1950), Field nitrates in Gezira soil, *J. Agr. Sci.*, *40*, 160- 165.

Jiao, Y., W. H. Hendershot, and J. K.Whalen (2004), Agricultural practices influence dissolved nutrients leaching through intact soil cores, *Soil Sci. Soc. Am. J., 68*, 2058-2068.

Mariotti, A., J.C. Germon, P.Hubert, P. Kaiser, R. Letolle, A. Tardieux, and P. Tardieux (1981), Experimental determination of nitrogen kinetic isotope fractionation: some principles: illustration for the denitrification and nitrification processes, *Plant Science*, *62*, 423-430.

McLaren, A. D. (1969), Steady state studies of nitrification in soil: theoretical considerations, *Soil Sci. Soc. Amer. Proc*., *33*, 273-275.

Metcalf & Eddy, Inc. (1991), *Wastewater Engineering: Treatment, Disposal, and Reuse,* 3rd ed., McGraw-Hill International Editions.

Misra, C., D. R. Nielsen, and J. W.Biggar (1974a), Nitrogen transformations in soil during leaching; i. Theoretical considerations, *Soil Sci. Soc. Amer. Proc*., *38*, 289-293.

Misra, C., D. R. Nielsen, and J. W.Biggar (1974b), Nitrogen transformations in soil during leaching: iii. Nitrate reduction in soil columns, *Soil Sci. Soc. Amer. Proc*., *38*, 300-304.

Nadelhoffer, K.J., and B. Fry (1994), Nitrogen isotope studies in forest ecosystems, in *Stable Isotopes in Ecology and Environmental Science*, edited by K. Lajtha, and R. Michner, pp. 22-45, Blackwell, London.

Ostrom, N. E., K.E. Knoke, L.O.Hedin, G.P. Robertson, and A.J.M. Smucker (1998), Temporal trends in nitrogen isotope values of nitrate leaching from an agricultural soil, Chem. *Geol.*, 146, 219-227.

Robertson, G. P., D. C. Colema, C. S. Bledsoe, and P. Sollins (1999), *Standard Soil Methods for long-Term Ecological Research*, Oxford University Press, Inc., 198 Madison Avenue, New York 10016.

Sakata, M. (2001), A simple and rapid method for $\delta^{15}N$ determination of ammonium and nitrate in water samples, *Geochemical Journal*, *35*, 271-275.

Starr, J. L., F. E Broadbent, and D. R. Nielsen (1974), Nitrogen transformations during continuous leaching, *Soil Sci. Soc. Amer. Proc*., *38*, 283-289.

Stehouwer, R. C., S.J. Traina, and J. W. Johnson (1993), Potassium adsorption and exchange selectivity within an anhydrous ammonia fertilizer band, *Soil Sci. Soc. Am. J., 57*, 346-350.

CHAPTER 4

DYNAMICS OF NITROGEN AND OTHER CONTAMINANTS IN HIGH POROUS SOIL DUE TO RECLAIMED WASTEWATER IRRIGATION

4.1 LABORATORY SCALE SOIL COLUMN EXPERIMENT

4.1.1 Introduction

This section presents a soil column experiment, which was conducted in two other similar-type columns (Fig. 3.1), filled with the high porous limestone soil (**Fig. D-7 & D-8**) obtained from an agricultural land in Okinawa. Limestone is the second most abundant soil type there. This is a strong mucilaginous consolidated sedimentary rock, which is brownish yellow in color. It has a weak alkalinity. The bed rock can be found at 30-60 cm depth. The water holding capacity is low. The soil column experiment was conducted in the same way as the column experiment (chapter 3) on the low porous soil. However, since this was conducted after that, some modifications have been done, as well as some analyses have not been conducted. The *SRW* with the same characteristic was used as the influent. This chapter omits the repetition of some similar conditions as that of the chapter 3. The pore water, effluent, initial and final soil characteristics were studied to investigate the belowground dynamics of nitrogenous compounds.

4.1.2 Methodology

4.1.2.1 Soil column preparation

The soil columns were filled with soil up to 85 cm height. Very large clumps (diameter was 10-20 cm) of the soil were air-dried and crushed manually and passed through a 0.4-cm square screen. Crushed soil was mixed well and 10 samples, each having 100g soil, were grabbed from the soil mixture, for the analysis of the average moisture content. The average moisture content was 11.66 % and 29.9 kg of soil was weighed. It contained 26.78 kg oven-dry weight of soil. 5.2 kg of water was added on the uniformly spreaded soil on a mat, using a traditional watering can; and then soil was mixed well in order to achieve the homogeneity. Soil was filled in the columns as layers, each of 10 cm in thickness, so that a compaction density of 1.34 g/cm^3 on wet weight basis was

maintained in each layer. Therefore, the average bulk density of the soil inside the entire column was 1.34 g/cm^3. **Table 4.1** depicts the characteristics of the raw soil before it was filled in the column.

Table 4.1 Characteristics of raw limestone (high porous soil).

Description	Raw Soil (per kg of oven-dry soil)
NO_3^-+NO_2^-	0.068 cmole
NH_4^+	0.052 cmole
T-N	8.2 cmole
T-C	46.7 cmole
pH	6.25
Ca^{2+}	11.57 cmole
Mg^{2+}	0.98 cmole
Na^+	0.10 cmole
K^+	0.73 cmole
Fe^{2+} & Fe^{3+}	0.02 cmole
Ba^{2+}	0.02 cmole
ECEC	13.47 cmole

4.1.2.2 Experimental procedure and sampling

Initially, both the columns were leached with *DW* continuously at 450 mL/h (14 mm/h) for 25 days until both *PW* and *E* did not receive any readily flushable contaminants from soil. Then, *SRW* was irrigated on one column at a rate of 900 mL/h (28.65 mm/h) for 2 hours every week, while the other column was continuously irrigated at a rate of 11 mL/h (0.35 mm/h) so that both the columns received the same content of water every week. The application of *SRW* was continued for 150 days. No significant difference was observed in the total soil depth before and after leaching.

The effluents from both the columns were collected once every day during the course of experiment. *PW* was collected twice a week in *CA*, and on the previous and following days of each irrigation in *IA*. The wastewater samples were analyzed for nitrogenous $\{NO_3^- - N, NO_2^- - N$, NH_3-*N* and *T-N*$\}$ compounds, $PO_4^{3-} - P$, SO_4^{2-}, Cl^-, conductivity and pH and cations such as Ca^{2+}, Mg^{2+}, Na^+, K^+, Fe^{2+} and Fe^{3+}. At the end of the experimental run, the soil column was unloaded in 5cm thick-layers, without disturbing the orientation of the soil. Then, soil collected from each layer was mixed well and samples were grabbed for the analysis of the moisture content. Then, soil of each layer was characterized in terms of gravimetric moisture content, $NO_3^- - N$, NH_3-*N*, *T-N*, *T-C*, cations such as Ca^{2+}, Mg^{2+}, Na^+, K^+, Fe^{2+}, Fe^{3+} and Ba^{2+}. *ECEC* is the sum of Ca^{2+}, Mg^{2+}, Na^+, K^+, Fe^{2+}, Fe^{3+}, Ba^{2+} and NH_4^+.

At the end of the experiment, the calculations of the water balance, *T-N* and *T-C* mass balances were performed. In calculating the total cumulative mass of *T-N* and *T-C* discharged from each column as the effluent throughout the experimental period, both *T-N* and *T-C* concentrations, respectively, of each effluent sample was multiplied by the respective total volume of accumulated water in the effluent tank. To obtain the initial *T-N* and *T-C* content of soil, the total mass of *T-N* and *T-C* having flushed out with the effluent during the cleansing period was subtracted from the *T-N* and *T-C* of the raw soil, respectively. In calculating *T-N* and *T-C* of soil at the end of the experiment, it was assumed that the soil sample collected from each 5-cm thick layer had represented the total soil of that layer. *T-N* of soil at the end did not show any significant difference with that of raw soil. Therefore, the change of organic-N content in soil is negligible. The quantity of $NO_3^- - N$ and NH_3-*N* is only 1.5 % of *T-N* in raw soil. Therefore, it was very difficult to quantify the change of $NO_3^- - N$ and NH_3-*N* contents in soil at the end of the experimental run, using the final *T-N* value of soil. Hence, *T-N* of soil after leaching was considered equal to the *T-N* of raw soil plus the content of accumulated NH_3-*N* and $NO_3^- - N$ in soil at the end of the experiment.

4.1.2.3 Analyses

$NO_3^- - N$ and $NO_2^- - N$ of the wastewater were analyzed on a spectrophotometer (purchased from Shimadzu Corporation, Japan) and an ion chromatograph (purchased from Nihon DIONEX Corporation, Osaka, Japan). NH_3-*N* of the wastewater samples was analyzed on a spectrophotometer using the phenate method. The other analyses were similar to those described in the section 3.1.2.4.

4.1.3 Results & Discussion

4.1.3.1 Nitrogenous compounds dynamics due to CA

Figure 4.1 depicts the $NO_3^- - N$ and *T-N* profiles of *PW* and *E* due to *CA*. Upon receiving *SRW*, $NO_3^- - N$ concentration of *PW1*, *PW2*, *PW3*, *PW4*, *PW5*, *PW6* and *E* increased to a maximum in succession. The successive attainment of the steady state by *PW1*, *PW2*, *PW3*, *PW4*, *PW5*, *PW6* and *E* occurred within 75 days of the experimental run. At various depths, it exhibited similar profiles. The significant characteristics of these profiles are as follows: $NO_3^- - N$ concentration of *PW 1*-6 and effluent samples was

always less than 20 mg/L; and *T-N* concentration of the effluent never exceeded its value in the influent (approximately 23 mg/L).

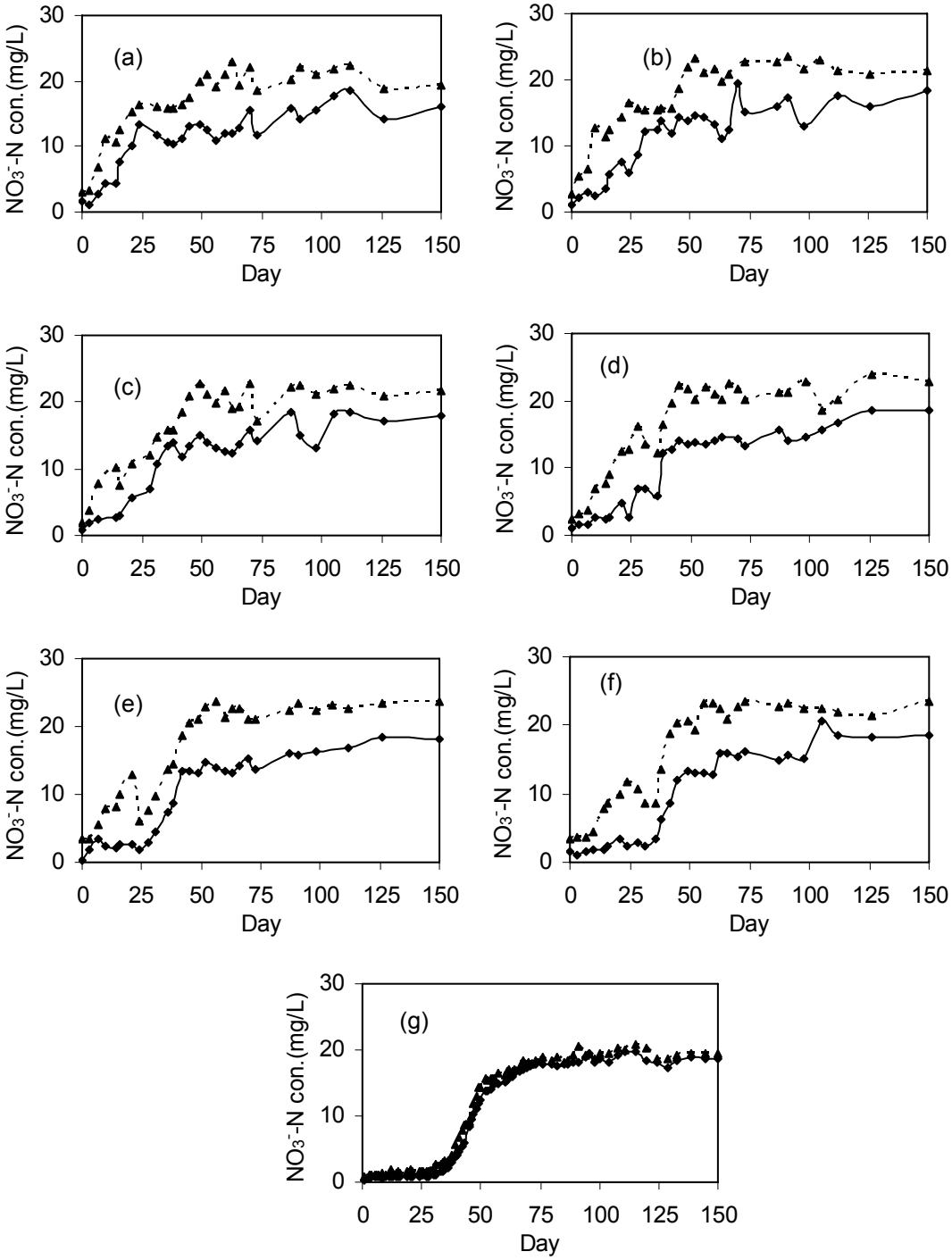

Fig. 4.1 Variation of NO_3^--N (diamonds with solid line) & T-N (triangles with dashed line) concentration of (a) PW1 (b) PW2 (c) PW3 (d) PW4 (e) PW5 (f) PW6 and (g) E, due to CA (high porous soil).

Figure 4.2 depicts the average *T-N*, $NO_3^- - N$ and NH_3-*N* distributions with depth during the steady state in *CA*. It is considered that the steady state existed 75 days onward. Transient and steady state NH_3-*N* concentrations of all *PW*s & *E* were almost invariant at

values less than 3.5 mg/L. **Figure A-5** shows the variation of NH_3-N concentration in PWs and E due to CA. Transient & steady state $NO_2^- - N$ concentration in both PW & E were negligible.

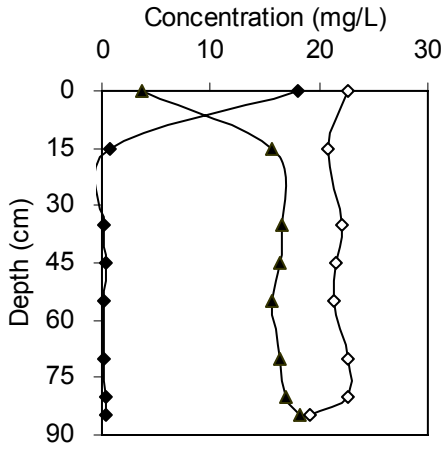

Fig. 4.2 Steady state T-N (hollow diamonds), NO_3^--N (triangles) & NH_3-N (solid diamonds) concentration distributions with soil depth due to CA (high porous soil).

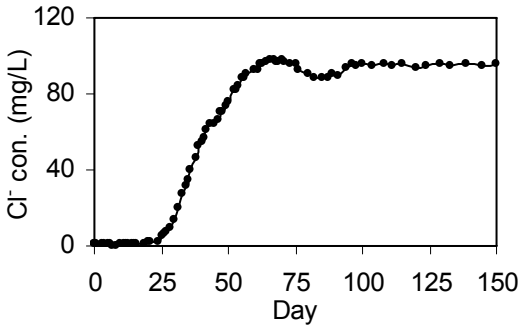

Fig. 4.3 Variation of Cl^- concentration in E due to CA (high porous soil).

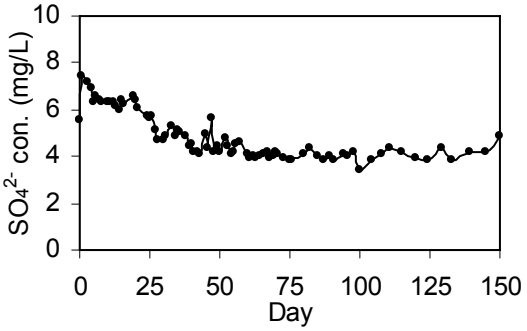

Fig. 4.4 Variation of SO_4^{2-} concentration in E due to CA (high porous soil).

4.1.3.2 Transient and steady state variations of the other contaminants due to CA

Figure 4.3 & **Fig. 4.4** denote the profiles of Cl^- and SO_4^{2-} in the effluent due to CA. The breakthrough of Cl^- occurred within 25 days of the experimental run, and Cl^- attained the steady state within 75 days of the experimental run. Eventually, Cl^- concentration reached the steady-state with the concentration equal to 90-100 mg/L, which is the range of Cl^- in the influent. Since, Cl^- has not undergone significant ion exchange reactions, its profile can be used as an indication of the flow path of the percolating water. Therefore, the percolating water seems not to have been influenced greatly by any preferential flow. **Figure A-7** & **Fig. A-8** show the variation of Cl^- and SO_4^{2-} in PW, with time. According to Fig. A-8 & Fig. 4.4, SO_4^{2-} contained in SRW (30-40 mg/L), has been greatly withdrawn by

soil. The withdrawn has greatly occurred below 15 cm depth. This result indicates that this soil has a great adsorption capacity of SO_4^{2-}. In addition, the existence of PO_4^{3-} in *PW* & *E* was insignificant.

Figure 4.5 & 4.6 show the variation of cations, Ca^{2+}, Mg^{2+},Na^{+}, K^{+}, Fe^{2+} and Fe^{3+} concentrations in the effluent, with time. Ca^{2+}, Mg^{2+} and K^{+} have increased upon receiving the *SRW*, and remained approximately constant after 75 days of the experimental run, while Na^{+} concentration fluctuates. Both Ca^{2+} and Mg^{2+} concentration have exceeded the respective values in the *SRW* whereas Na^{+} and K^{+} concentrations were less than those in the *SRW*.

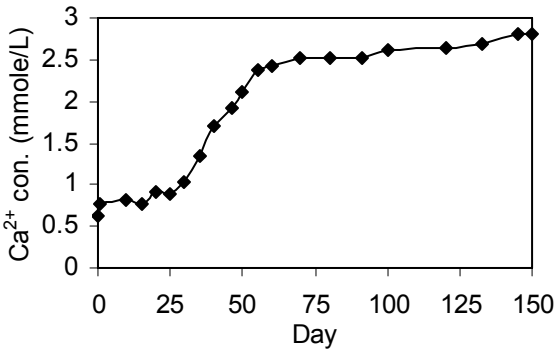

Fig. 4.5 Variation of Ca^{2+} concentration in E due to CA (high porous soil)

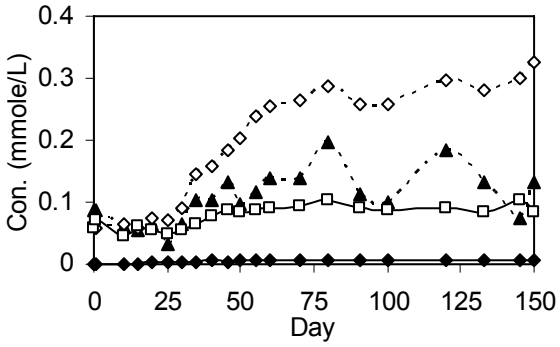

Fig. 4.6 Variation of Na^{+} (triangles), Mg^{2+} (hollow diamonds), K^{+} (hollow boxes) and Fe^{2+} & Fe^{3+} (solid diamonds) concentration in E due to CA (high porous soil)

Figure A-9 depicts the variation of *TOC* in both *PW* and *E* samples due to *CA*. The concentration in the pore water samples were manifold higher than the *TOC* concentration of the *SRW*. The concentration of *TOC* in the effluent was always very much less than that of the pore water. Steady state conductivity of the effluent due to *CA* ranged from 45-52 ms/m (**Fig. A-13**).

4.1.3.3 Nitrogenous compounds dynamics in IA

Figure 4.7 shows the profiles of $NO_3^- - N$ and *T-N* due to *IA*. $NO_3^- - N$ of the *PW* and *E* commenced increasing upon receiving *SRW*. Once received *SRW*, $NO_3^- - N$ concentration of *PW1*, *PW2*, *PW3*, *PW4*, *PW5*, *PW6* and *E* gradually increased to a maximum value in succession. Thereafter, the concentration has slightly decreased. The significant characteristics of these profiles are as follows: both $NO_3^- - N$ & *T-N*

concentrations of *PW 1*-6 & effluent exceeded 23 mg/L after about 75 days of the experimental run, and rose to elevated levels where *T-N* was close to 40 mg/L.

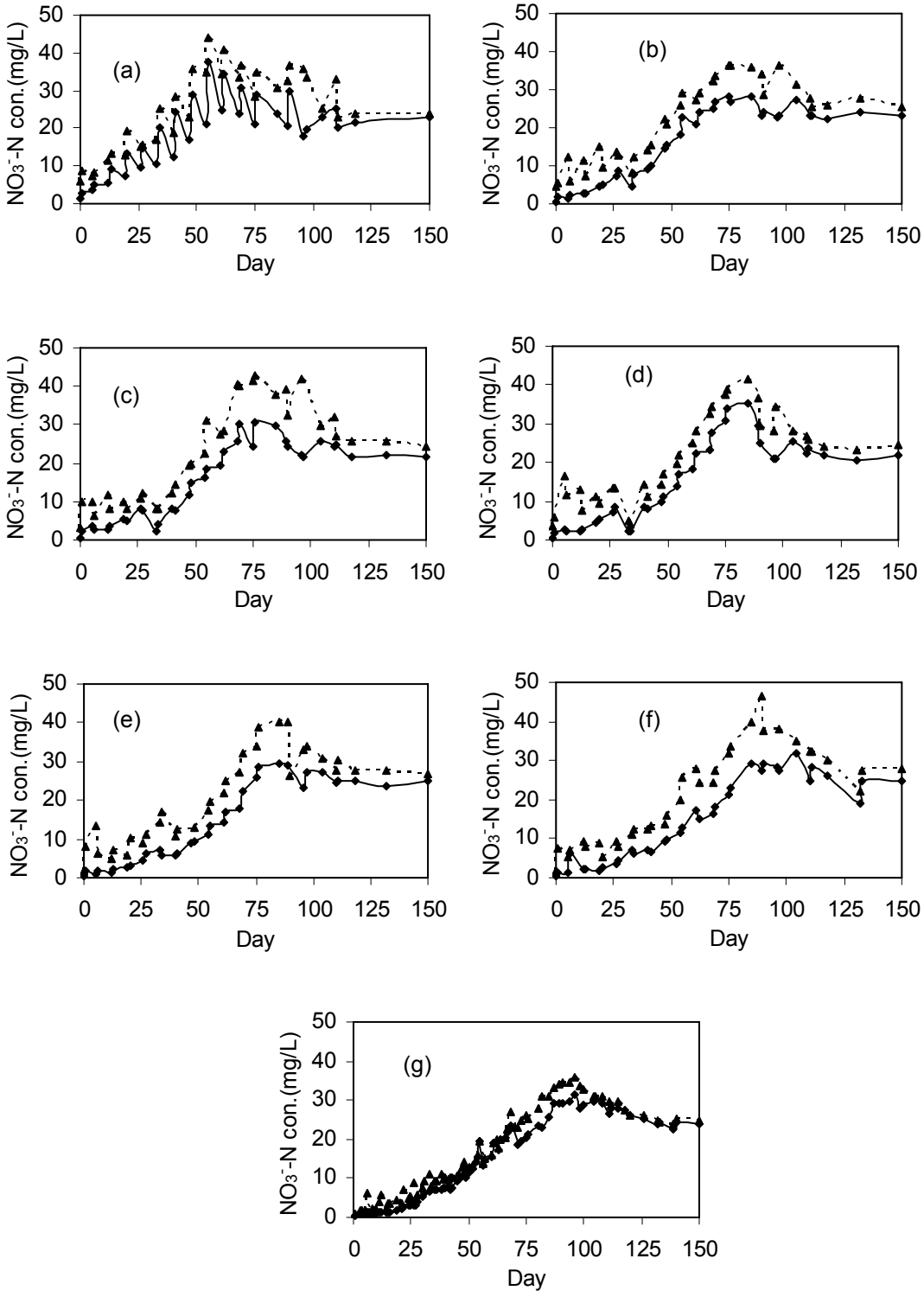

Fig. 4.7 Variation of NO_3^--*N* (diamonds with solid line) & *T-N* (triangles with dashed line) concentration of (a) *PW1* (b) *PW2* (c) *PW3* (d) *PW4* (e) *PW5* (f) *PW6* and (g) E, due to IA (high porous soil)

Figure 4.8 depicts the distribution of *T-N*, $NO_3^- - N$ and NH_3-*N* in the soil column due to *IA*, at the end of the experimental run. Transient and steady state NH_3-*N* concentrations of all *PW*s & *E* were always less than 2.5 mg/L. **Figure A-6** shows the variation of NH_3-*N* concentration in *PW*s and *E* due to *IA*. $NO_2^- - N$ never existed in significant concentrations in either *PW* or *E*.

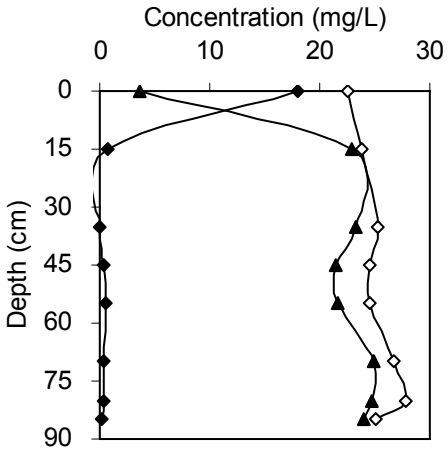

Fig. 4.8 T-N (hollow diamonds), NO_3^--N (triangles) & NH_3-N (solid diamonds) concentration distributions with soil depth in IA at the end of the experimental run (high porous soil)

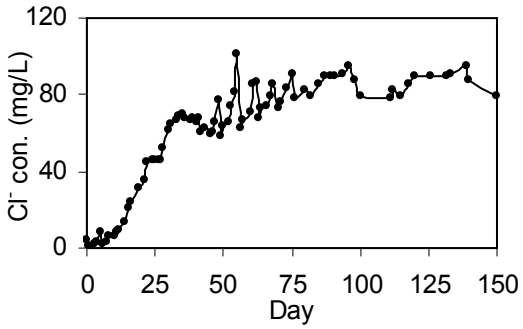

Fig. 4.9 Variation of Cl^- concentration in E due to IA (high porous soil)

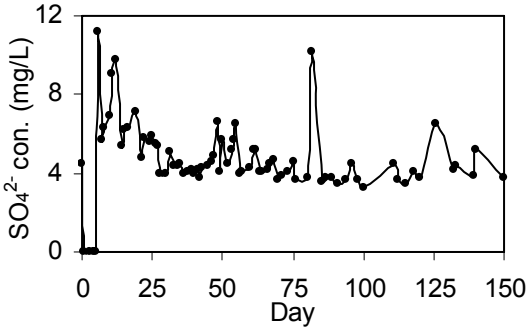

Fig. 4.10 Variation of SO_4^{2-} concentration in E due to IA (high porous soil)

4.1.3.4 Transient and steady state variations of the other contaminants due to IA

Figure 4.9 & **Fig. 4.10** denote the profiles of Cl^- and SO_4^{2-} in *E* due to *IA*. Cl^- concentration became approximately same as that in the influent, within 75 days of the experimental run. Since, Cl^- has not undergone significant ion exchange reactions, its profile can be used as an indication of the flow path of the percolating water. Therefore, the percolating water seems not to have been influenced greatly by any preferential flow.

Figure A-10 & **Fig. A-11** show the variation of Cl^- and SO_4^{2-} in *PW*, with time. According to Fig. A-11 & Fig. 4.10, SO_4^{2-} has been retained in the soil as was observed in *CA*. The great fluctuations of SO_4^{2-} profiles indicate that the retention of SO_4^{2-} in soil has been vastly influenced by the flow condition.

Figure 4.11 & 4.12 show the variation of cations, Ca^{2+}, Mg^{2+},Na^+, K^+, Fe^{2+} and Fe^{3+} concentrations in the effluent of *IA*, with time. Ca^{2+}, Mg^{2+} and K^+ have increased upon receiving the *SRW*, and remained approximately constant after 75 days of the experimental run, while Na^+ concentration fluctuates. Both Ca^{2+} and Mg^{2+} concentration have exceeded the respective values in the *SRW* whereas Na^+ and K^+ concentrations were less than those in the *SRW*.

Figure A-12 is the variation of *TOC* concentration in *PW* and *E* samples of *IA*. When Fig. A-9 and A-12 are compared, *TOC* concentration in the pore water of *CA* was higher than that of *IA*. Conductivity of *E* due to *IA* ranged from 50-55 ms/m toward the end of the experimental run (**Fig. A-14**).

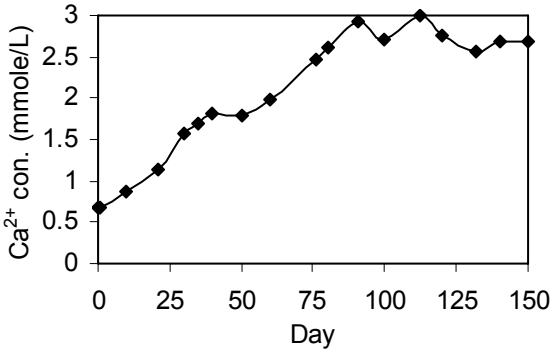

Fig. 4.11 Variation of Ca^{2+} concentration in E due to IA (high porous soil)

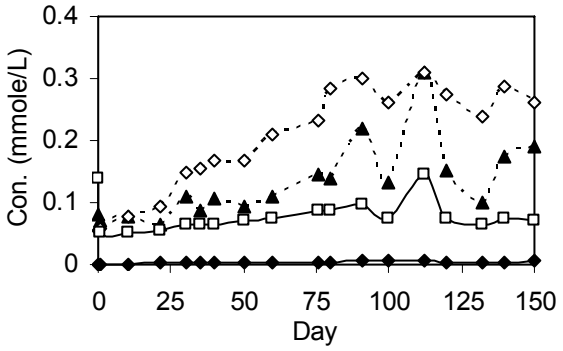

Fig. 4.12 Variation of Na^+ (triangles), Mg^{2+} (hollow diamonds), K^+ (hollow boxes) and Fe^{2+} & Fe^{3+} (solid diamonds) concentration in E due to IA (high porous soil)

4.1.3.5 Nitrogen, Carbon and Cation Mass Balance

Figure 4.13 (a & b) shows the variation of the cumulative volume of water applied on a column as influent and the cumulative volume of water discharged as effluent. Water lost in *IA* is lower than that of *CA*. This discrepancy may be attributed to the fact that the evaporation may have been higher in *CA* owing to the relatively high retention time.

Figure 4.14 (a & b) indicates the profiles of the cumulative mass of *T-N*, applied on each column via the influent and discharged from each column as the effluent. The

gradient of the effluent profile of *IA* is greater than that of *CA*, and the gap between the influent and effluent profiles of *IA* is smaller than that of *CA*. The gap between the cumulative mass of *T-N* in the influent and effluent indicates that the balance amount of *T-N* may have either accumulated on soil or off-gassed to the soil air, probably as N_2O, NO_x and N_2; or all.

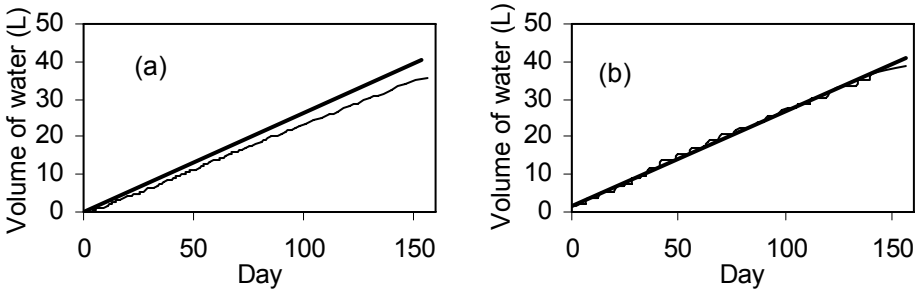

Fig. 4.13 Variation of the cumulative volume of water applied on the column via influent (thick line) and discharged as E (thin line), in (a) CA and (b) IA (high porous soil).

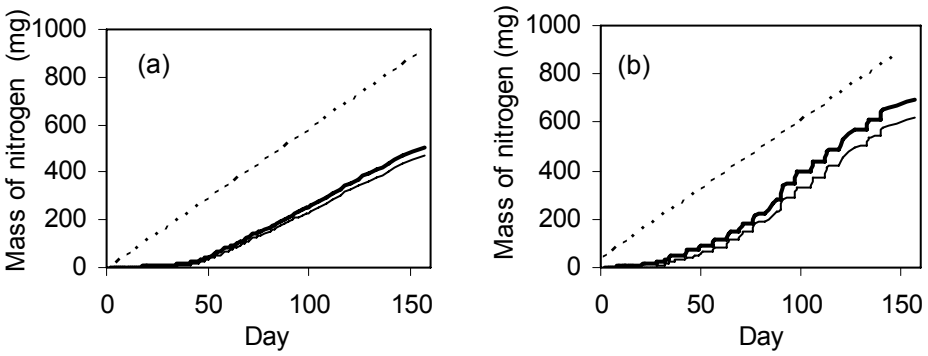

Fig. 4.14 Variation of the cumulative mass of T-N applied on the column via influent (dashed line), and the cumulative mass of T-N (thick solid line) and NO_3^--N (thin solid line) discharged as E, in (a) CA and (b) IA (high porous soil).

Table 4.2 depicts the total mass of $NO_3^- - N$, NH_3-*N*, *T-N* and *T-C*, which was initially in the columns before cleansing, and the mass of each component removed during the cleansing period. **Table 4.3 & 4.4** depict the mass of above-mentioned compounds and some cations in each 5cm layer of the column at the end of the experimental run on *CA* and *IA*, respectively.

Table 4.2 Soil characteristics before and after cleansing on high porous soil.

Description	CA				IA			
	NO_3^--N	NH_3-N	T-N	T-C	NO_3^--N	NH_3-N	T-N	T-C
Content in the column before cleansing (mg)	253.70	193.43	30560	15002	253.7	193.43	30560	15002
Content removed during cleansing (mg)	229.22	5.04	329.34	2650	225.14	4.41	315.53	3325
Content in the column before loading of SRW (mg)	24.48	188.39	30231	14735	28.56	189.02	30244	14670

Table 4.3 Final soil characteristics of CA on high porous soil.

Depth (cm)	Oven-dry weight (kg)	NO_3^--N (mg)	NH_3-N (mg)	T-N (g)	T-C (g)	Na^+ (mg)	Mg^{2+} (mg)	K^+ (mg)	Ca^{2+} (mg)
0-5	1.30	27.49	3.41	1.42	7.09	146.3	17.6	37.8	477.7
5-10	1.68	12.90	2.92	1.70	8.25	132.3	9.7	21.9	365.4
10-15	1.72	9.56	0.59	1.51	7.06	118.5	7.0	16.7	319.7
15-20	1.53	11.94	4.54	1.70	8.70	121.8	10.6	25.9	466.8
20-25	1.60	12.85	4.35	1.59	10.35	81.7	5.3	17.7	369.4
25-30	1.60	11.88	4.23	1.39	8.84	74.1	5.9	23.5	463.5
30-35	1.54	13.63	4.03	1.65	7.98	74.1	5.9	23.5	463.5
35-40	1.57	13.01	4.03	1.72	8.61	70.3	5.6	25.6	532.9
40-45	1.69	19.04	6.67	1.73	8.73	42.8	2.6	17.8	367.4
45-50	1.53	17.09	4.83	1.80	8.02	34.7	2.8	24.2	482.8
50-55	1.58	13.91	4.43	1.61	7.96	3.0	0.2	18.7	368.1
55-60	1.58	15.18	5.99	1.65	8.24	0.0	0.0	26.3	537.1
60-65	1.52	12.96	4.32	1.44	7.50	7.8	0.5	17.6	384.6
65-70	1.63	13.15	2.98	1.75	8.98	0.0	0.0	24.8	469.4
70-75	1.49	24.97	3.11	1.71	8.57	0.0	0.0	27.0	564.0
75-80	1.48	19.75	4.27	1.65	9.80	0.0	0.0	27.4	594.4
80-85	1.75	7.88	3.51	1.94	11.54	0.0	0.0	14.5	267.4
Total	26.78	257.21	68.22	27.99	146.23	907.2	73.9	390.9	7494.4

Table 4.5 shows the components of the input and output of each system, in terms of ultimate cumulative mass of *T-N*. It indicates that the gap between the influent and effluent profiles of Fig. 4.14(a & b) was caused by the off-gassing of *T-N* into the soil air. The ultimate cumulative mass of *T-N* lost by off- gassing is the ultimate cumulative *T-N* in the influent minus that in the effluent plus accumulated *T-N* in soil. The mass of *T-N* (N_2O,

NO_x and N_2) that has been lost by off-gassing to the soil air, for *CA* and IA are 30.0 % and 2.1 %, respectively, relative to the ultimate cumulative mass of *T-N* applied via the influent.

Table 4.4 Final soil characteristics of IA on high porous soil

Depth (cm)	Oven-dry weight (kg)	NO_3^--N (mg)	NH_3-N (mg)	T-N (g)	T-C (g)	Na^+ (mg)	Mg^{2+} (mg)	K^+ (mg)	Ca^{2+} (mg)
0-5	1.21	37.66	2.40	1.40	7.02	123.3	18.2	43.4	663.5
5-10	1.29	16.45	3.54	1.52	7.67	106.0	12.4	32.4	505.0
10-15	1.53	18.84	4.36	1.56	7.43	116.0	10.8	28.0	483.6
15-20	2.10	27.76	5.88	2.33	13.99	122.1	7.8	26.5	465.9
20-25	2.01	19.20	4.51	2.19	12.02	98.1	5.9	21.5	393.6
25-30	1.64	11.81	2.28	1.72	7.97	102.4	6.6	18.7	365.7
30-35	1.49	11.01	3.32	1.58	7.72	71.8	6.7	27.3	486.7
35-40	1.73	22.62	3.94	1.72	9.04	91.4	7.5	27.7	501.0
40-45	1.49	26.21	4.28	1.66	8.46	83.4	8.0	29.6	562.1
45-50	0.96	10.83	2.08	1.06	5.42	45.2	7.1	29.6	593.9
50-55	1.27	15.66	1.64	1.40	7.12	52.3	5.9	30.2	576.7
55-60	1.46	15.59	2.50	1.55	7.80	49.5	4.7	28.8	537.3
60-65	1.97	24.07	0.50	1.91	9.79	46.2	2.8	22.9	458.1
65-70	1.62	17.86	5.42	1.60	8.08	28.1	2.4	26.5	541.3
70-75	1.59	15.35	3.84	1.81	9.19	21.6	1.9	29.4	564.2
75-80	1.28	21.79	3.00	1.32	7.06	15.9	1.7	27.7	534.1
80-85	2.14	16.16	3.18	2.00	10.21	55.7	1.9	10.5	203.0
Total	26.78	328.87	56.69	28.34	146.01	1058.2	99.8	460.6	8435.7

Table 4.5 Nitrogen mass balance of the experiment on high porous soil

Description	CA	IA
Cumulative T-N supplied as influent (mg)	900.0	885.0
Accumulated T-N in soil after leaching (mg)	168.0	112.2
Cumulative T-N discharged as effluent (mg)	506.0	698.0
Cumulative NO_3^--N discharged as effluent (mg)	470.0	625.0
Cumulative T-N lost by off-gassing to the soil air (mg)	281.0	19.0

Figure 4.15 (a & b) indicates the profiles of the cumulative mass of *T-C* & *TOC*, applied on each column via the influent and discharged from each column as the effluent. The gap between the influent and effluent profiles of *TOC* of *IA* is smaller than that of *CA*. The gap between the cumulative mass of *TOC* in the influent and effluent indicates that the balance amount of *TOC* may have utilized by denitrification. The ultimate cumulative mass of *T-C* discharged as effluent in *IA* is more that that supplied via the influent.

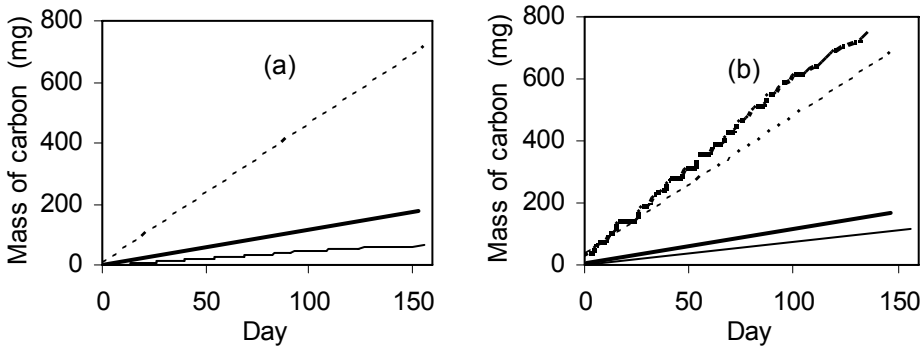

Fig. 4.15 Variation of the cumulative mass of T-C (thin dashed line) & TOC (thick solid line) applied on the column via influent, and the cumulative mass of T-C (thick dashed line) and TOC (thin solid line) discharged as E in (a) CA and (b) IA (high porous soil).

Table 4.6 shows the components of the input and output of each system, in terms of cumulative mass of *T-C* and *TOC*. The ultimate cumulative mass of *TOC*, supplied by the influent, that was lost in *CA* and *IA* are 62.9 % and 38.8 %, respectively, of the ultimate cumulative mass of *TOC* applied via the influent throughout the experimental run.

Table 4.6 Mass of cumulative carbon in the experiment on high porous soil.

Description	CA	IA
Cumulative T-C supplied as influent (mg)	697.2	683.3
Reduction T-C in soil after leaching (mg)	1150	700
Cumulative T-C discharged as effluent (mg)	695.1	765.0
Cumulative TOC supplied as influent (mg)	174.1	170.6
Cumulative TOC discharged as effluent (mg)	64.6	104.4

4.1.3.6 Nitrification, ion-exchange reactions and denitrification

The presence of nitrification in both *CA* & *IA* is confirmed by the obtained profiles of $NO_3^- - N$ (Fig. 4.1 & Fig.4.7) and NH_3-*N* (Fig. 4.2, 4.8, A-5 & A-6). Nitrification was greater above 15 cm depth, since concentration of $NO_3^- - N$ in the pore water samples at 15 cm exceeded the concentration of the influent within 7 days and 1-5 days of the commencement of the loading of *SRW*, in *CA* & *IA*, respectively. In addition, the transient and steady state NH_3-*N* concentrations of *PW* and *E* of both *CA* & *IA* were almost invariant at values less than 3.5 mg/L & 2.5 mg/L, respectively. The presence of NH_4^+ adsorption onto soil is also apparent. It is clear that the adsorbed NH_4^+ has also nitrified and leached into the solution because the average $NO_3^- - N$ concentration at the steady state of *CA* is

close to the concentration of NH_3-N in the influent. According to Fig. 4.5, 4.6, 4.11 & 4.12, overall, Ca^{2+} and Mg^{2+} have released from soil into the percolating water, while K^+ and Na^+ supplied by the *SRW* retained in soil. It shows that Na^+, K^+ and NH_4^+ contained in the *SRW* exchanged with Ca^{2+} and Mg^{2+} retained in the water film on the colloid surfaces due to their predominantly negative charge. When the mass of cations, namely Ca^{2+}, Mg^{2+}, Na^+ and K^+, present in raw soil and each column at the end of the experiment are compared, the following results are obtained: Na^+ content has increased by 12.4 and 14.8 % of dry soil in *CA* and *IA*, respectively; Ca^{2+}, Mg^{2+} and K^+ have decreased by 392.9%, 22.2% and 23.8%, respectively of the dry soil in *CA*; the decrease of Ca^{2+}, Mg^{2+} and K^+ contents in *IA* were 384.1%, 21.8% and 23.1% of the dry soil, respectively. The section 3.1.3.1 correlates several statements found in the literature with the results of the column experiment regarding nitrification and ion exchange reactions including the adsorption of NH_4^+. Since, that description is also valid to the observations described above, the reader is directed to the subsections 'nitrification' and 'ion exchange reactions' in the section 3.1.3.1.

Fig. 4.1 also indicates that the steady state concentrations of *PW* collected at depths greater than 70 cm and the effluent of *CA* were slightly higher than those of upper *PW* samples. Since *PW* does not necessarily represent the flowing water, a local condition may have been represented by this observation. Denitrification may have been high in those areas of the column. Denitrification is the microbial-mediated reduction of nitrogenous oxide to N_2 gas (DeBusk et al., 2001), and denitrifiers are known to exist in almost all soils and come from a wide range of genera (Tiedje, 1988). Shaffer et al. (2001) indicated that the key to understanding and simulating denitriifcation is the transient and localized nature of the anaerobic conditions; complete reduction of N_2O to N_2 is an anaerobic process, while partial or transient anaerobosis results in the production of N_2O and NO_x. Therefore, the presence of N_2O & NO_x are possible because the soil column, having a shallow depth and high porous unsaturated soil, do not ensure complete anaerobic environment. In accordance with Starr et al. (1974), N_2O is highly soluble in water, and there is a possibility that dissolved N_2O may have remained in the soil solution sufficiently long to be further reduced to N_2. Though, no measurement was made for dissolved N_2O, above hypothesis is quite possible because the nitrogen mass balance calculations explained above proved the significant existence of denitrification in *CA*.

In addition, according to Fig. 4.1, the gap between $NO_3^- - N$ and *T-N* profiles of pore water are quite high, whereas there is no such gap observed in the effluent. However, the concentration profiles of *NH₃-N* in *PW* are evident of that this high gap was not due to the contribution of *NH₃-N*. In addition, it can also be argued whether the nitrogen assimilated in cell tissues as a result of nitrification is represented by this gap. During the process of nitrification, some of the NH_4^+ is assimilated into cell tissues (Metcalf & Eddy, 1991). The fact that variations of *T-N* and *TOC* in *PW* samples of *CA* are quite similar to each other (Fig. 4.1 & A-9), slightly supports the above rationale. According to Eq. 3.1, during nitrification of 1 mole of NH_4^+, 0.105 mole of *C* and 0.021 mole of *N* are assimilated as microbial cells. Hence, 1 L of *SRW* can make 1.26 mg of *C* and 0.294 mg of *N* to assimilate in cell tissues. Though, these amounts are quite low compared to the *TOC* concentration in the pore water of *CA*, it is quite a rationale for the above-explained gap between $NO_3^- - N$ and *T-N* profiles.

Figure 4.7 depicts that when time progressed, both $NO_3^- - N$ and *T-N* concentrations of *PW* and *E* of *IA* first exceeded the influent *T-N* concentration by maximum 15 mg/L, before decreasing slightly. This observation is quite similar to the profiles of *CA* in the case of low porous soil, though the peak value of the profiles are not so high as those. This is an indication of the leaching of $NO_3^- - N$ from soil. Since, Fig.4.14b indicates that the ultimate total cumulative mass of *T-N* in *E* is well below that supplied by the influent, it hardly shows the presence of another source, except the influent, that supplied *N* into the percolating water. NH_4^+, which was adsorbed onto soil, would undergo nitrification on soil. Therefore, it is hypothesized that NH_4^+, which was adsorbed onto soil, would undergo nitrification on soil; however, leaching of NO_3^- takes place when there is a considerable water flow. In *IA*, a considerable water flow prevails only for less than 1 day. Therefore, during each irrigation, leaching of NO_3^- originating from the nitrification of earlier adsorbed NH_4^+,would take place in addition to the adsorption and nitrification processes of the NH_4^+ supplied by the influent at the time. This may have increased the *T-N* concentration in *PW 1*-6 and the effluent, more than that contained in the influent.

The nitrogen balance calculations of both *CA* and *IA* together with Fig.4.14 (a & b) & Fig.4.15 (a & b) ascertain that denitrification progressed in *CA* more rapidly than that of *IA*. The higher utilization of supplied *TOC* in *CA* than in *IA* supports the above statement.

As explained in the section 3.1.3.1 under the sub topic 'denitrification', the acceleration of denitrification in *CA* may have been attributed to the high retention time owing to the less percolation rate, and the possible water logged conditions that have created an anoxic environment. In addition, soil of *IA* remained relatively dry after first two days following each application of *SRW*, which may have caused an oxic environment. This provides evidence that the dissolved organic carbon in the soil solution may have been used for denitrification, and the consumption of that in *CA* may have been greater than that of *IA*. As stated by DeBusk et al. (2001), microbial utilization is one means of removing organic compounds during transportation. Also, Brye et al. (2001) mentioned that the dissolved organic carbon is considered to be a readily available substrate for soil microorganisms. Further, DeBusk et al. (2001) mentioned that the facultative anaerobic bacteria are capable of using NO_3^- or NO_2^- as terminal electron acceptors, coupled with the oxidation of organic carbon in the absence of oxygen gas. The denitrifcation equation can be represented by Eq. (4.1), in which CH_2O represents organic matter; (it is noted that the other organic compounds can also be oxidized).

$$CH_2O + \frac{4}{5}NO_3^- = \frac{2}{5}N_2(g) + HCO_3^- + \frac{1}{5}H^+ + \frac{2}{5}H_2O \text{ (Freeze et al., 1979)} \qquad (4.1)$$

According to the mass balance calculations, the mass of off-gassed nitrogen is 19 mg and 281 mg in *IA* and *CA*, respectively. Eq. (4.1) shows that the mass of organic carbon required to obtain 19 mg *N* & 281 mg *N* as N_2 gas due to denitrification is 20.4 mg and 301.1 mg, respectively. The reductions of dissolved organic carbon, which was originally contained in the influent, in the columns of *IA* and *CA* were 66.2 mg and 109.5 mg, respectively. These values show that though the reduction of supplied organic carbon in *IA* was enough for the existed denitrification, it was not enough for the denitrifcation that happened in *CA*. Therefore, it indicates that the soil too was a source of organic carbon. Carbon supplied by soil of *CA* was about 191.6 mg. There was a reduction of total carbon content in the soil at the end of the experiment.

4.2 BATCH SORPTION EXPERIMENTS

4.2.1 Introduction

Two series of batch sorption experiments were conducted using the high porous limestone soil. The particle size of soil was less than 2 mm square screen. *DW* and *SRW*

were used for the solvents. The objectives of experiment 1 and 2 can be found in the section 3.2.1.

4.2.2 Experiment 1

4.2.2.1 Methodology

This is similar to the procedure described in the section 3.2.3.1.

4.2.2.2 Result & Discussion

Figure 4.16 shows the equilibrium concentrations of *NH_3-N* vs. time of shaking. It clearly shows that nearly half the *NH_3-N* present in *SRW* (*NH_3-N* of *SRW* is 18 mg/L) was withdrawn from the solution. Results indicate that the equilibrium state reached less than 12h. **Figure 4.17** is the variation of increase of $NO_3^- - N$ concentration in the solution. It seems that $NO_3^- - N$ concentration has slightly increased in both *SRW* and *DW*. It is most probably due to the leaching of NO_3^- from soil. The increase is higher in *DW* than in *SRW*. It is because the ionic strength of *DW* is lower than that of *SRW*. The reader is directed to the discussion in the section 3.2.3.2. This indicates that both *NH_3-N* and $NO_3^- - N$ have not undergone any microbial transformation significantly. Therefore, it can be verified that the withdrawal of *NH_3-N* from the solution is mainly due to the adsorption. Also, leaching of $NO_3^- - N$ from soil is not so significant when the solvent is *SRW*.

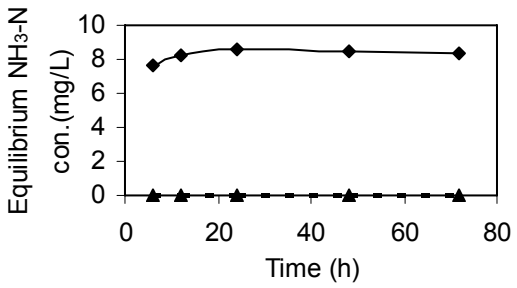

Fig. 4.16 Variation of equilibrium NH_3-N concentration in the supernatant of DW (triangles with dashed line) & SRW (diamonds with solid line) (high porous soil)

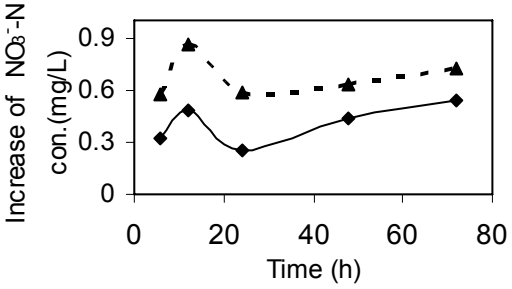

Fig. 4.17 Variation of increase of NO_3^- -N concentration in the supernatant of DW (triangles with dashed line) & SRW (diamonds with solid line) (high porous soil)

4.2.3 Experiment 2

4.2.3.1 Methodology

This is similar to the procedure described in the section 3.2.4.1.

4.2.3.2 Result & Discussion

Figure 4.18 is the solute (NH_3-N) concentration on soil (q) vs. the equilibrium concentration of solute in the solvent. The curve is non –linear. It can be excellently fit into a Freundlich isotherm with K_d = 2E-05 (L/mg)$^{1.3938}$ and n = 1.3938. If it is approximated to the linear form of Freundlich isotherm, R^2 still remains more than 0.9. Then, K_d is equal to 3E-05 (L/mg) (30 cm^3/g). It indicates that the sorption isotherm does not deviate much from the linearity.

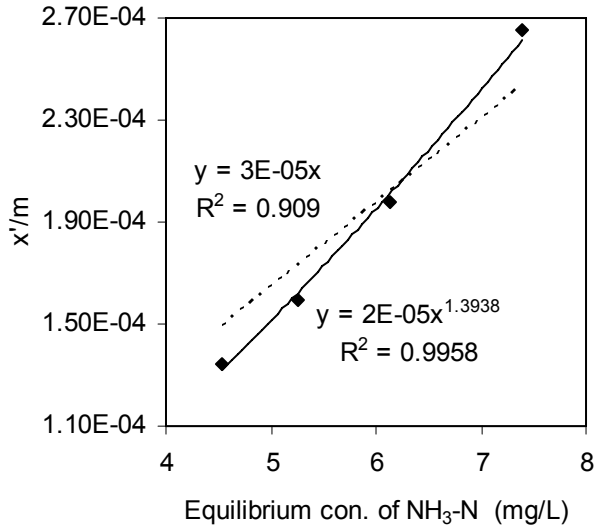

Fig. 4.18 Variation of NH_3-N concentration on the solid phase vs. equilibrium NH_3-N concentration in the supernatant (high porous soil).

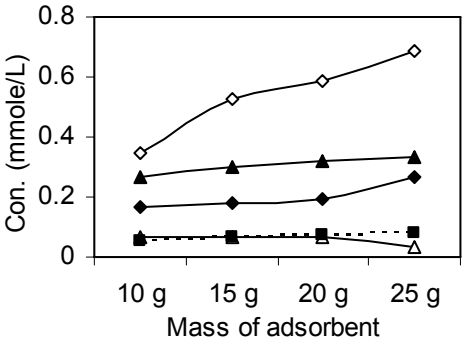

Fig. 4.19 Increase of Ca^{2+} (hollow diamonds), and decrease of NH_4^+ (triangles), Na^+ (solid diamond), K^+ (boxes) and Mg^{2+} (hollow triangles) in supernatant vs. mass of high porous soil.

Figure 4.19 shows that there was an increase of Ca^{2+} and decrease of Mg^{2+}, Na^+ and K^+ concentrations in the supernatant after shaking. Hence, Na^+ and NH_4^+ of the adsorbate have exchanged with soil- Ca^{2+} largely; and K^+ and Mg^{2+} of the adsorbate did the same slightly. This observation verifies that in the aforementioned soil column experiment, NH_4^+, Na^+ and K^+ contained in the *SRW* exchanged with Ca^{2+}, $Mg^{2+}$and K^+ from soil liquid interphase, however Mg^{2+} contained in *SRW* did not retain in soil in that case as is the case of batch experiment. The reader is directed to the 2nd paragraph of the section 3.2.4.2 for more explanation of the above behavior.

4.3 CONCLUSIONS

This study was conducted to investigate the dynamics of nitrogen in the high porous limestone soil, as a result of continuous and intermittent irrigation of *RWW*. Two laboratory scale unsaturated soil columns, loaded with the soil, were applied with the *SRW* continuously and intermittently for a period of 150 days. The simultaneous occurrence of nitrification, denitrification and adsorption of NH_4^+ on to soil was proved by the profiles of nitrogenous compounds and the nitrogen and carbon mass balances performed at the end of the experiment. More than 90% of *NH_3-N* in *SRW* diminished at the upper soil layers in both the columns, due to nitrification and adsorption. In *IA*, $NO_3^- - N$ concentration of the water samples obtained from various depths were characterized by a gradual increase to a peak followed by a slight decrease toward the end of the experiment. In *CA*, $NO_3^- - N$ concentration of all the water samples increased to a maximum before attaining the steady state successively. The nitrogen mass balance indicated that the mass of *T-N* that was lost by off-gassing to the soil air of *CA* and *IA* are 30.0 % and 2.1 %, respectively. The ultimate cumulative mass of *TOC*, supplied by the influent, that was lost in *CA* and *IA* are 62.9 % and 38.8 %, respectively. This provides evidence that the dissolved organic carbon in the soil solution may have been used for denitrification, and the consumption of that in *CA* may have been greater than that of *IA*. Therefore, the results concluded that *CA* has promoted denitrification in comparison to that of *IA*. In addition, the batch sorption experiments showed that the adsorption of NH_4^+ onto limestone soil is very quick and leaching of soil NO_3^- into the solution of *SRW* is negligible.

REFERENCES

Brye, K. R., J. M. Norman, L. G. Bundy, and S. T. Gower (2001), Nitrogen and carbon leaching in agro ecosystems and their role in denitrification potential, *J. Environ. Qual*., *30*, 58-70.

DeBusk, W.F., J.R. White, and K.R. Reddy (2001), Carbon and nitrogen dynamics in wetland soils, in *Modeling Carbon and Nitrogen Dynamics for Soil Management*, edited by M.J. Shaffer, Liwang Ma and S. Hansen, pp. 27-53, CRC Press LLC, 2000 N.W., Florida, USA.

Freeze, R. A., J. A. Cherry (1979), *Groundwater,* pp.118-119, Prentice-Hall, Inc., Englewood Cliffs, N. J. 07632.

Metcalf & Eddy, Inc. (1991), *Wastewater Engineering: Treatment, Disposal, and Reuse,* 3rd ed., McGraw-Hill.

Shaffer, M.J., and L. Ma (2001), Carbon and nitrogen dynamics in upland soils, in *Modeling Carbon and Nitrogen Dynamics for Soil Management*, edited by M.J. Shaffer, Liwang Ma and S. Hansen, pp. 11-26, CRC Press LLC, 2000 N.W., Florida, USA.

Starr, J. L., F. E. Broadbent, and D. R. Nielsen (1974), Nitrogen transformations during continuous leaching, *Soil.Sci.Soc.Amer.Proc*, *38*, 283-289.

Tiedje, J.M. (1988), Ecology of denitrification and dissimilatory nitrate reduction to ammonium, in *Biology of Anaerobic Microorganisms*, edited by A.J.B. Zehnder, pp. 179-245, John Wiley & Sons, New York.

CHAPTER 5

ANALYTICAL MODELING OF NITROGEN DYNAMICS IN SOIL DUE TO CONTINUOUS IRRIGATION OF RECLAIMED WASTEWATER

5.1 INTRODUCTION

This chapter describes about two types of analytical models developed to simulate the NO_3^- dynamics due to *CA*, which are presented in chapter 3 & 4. Because the characteristics of the *PW* at different depths & effluent, initial and final soil indicated the simultaneous occurrence of nitrification, denitrification and adsorption of NH_4^+ on to soil, these were the processes that interpret the developed models. The coupled material balance equations for both *NH3-N* and $NO_3^- - N$ on entire soil volume were solved analytically to simulate the distributions of $NO_3^- - N$ concentration with time along the soil depth. As a result of the concentration of *NH3-N* being negligible and possesses no particular pattern, the calibration of the models were done with $NO_3^- - N$ concentrations. It is assumed that the process of oxidation of NH_4^+ to NO_2^- is very quick and therefore, that process has been omitted from the transformation terms. According to the results, NO_2^- never existed in significant concentrations. The material balance equations were modified by changing the sink-source term to address the dominating mechanisms of each column experiment. In each case, both nitrification and denitrification rate constants were varied within a wide range until the simulated $NO_3^- - N$ concentrations fit properly with the measured values, in order to obtain optimized rate constants for each case.

These models represent a simplified version for the heterogeneity of the unsaturated porous media in the column. Since, the overall material balance equations of *NH3-N* and $NO_3^- - N$ were solved using analytical techniques, it was important to preserve the linearity of the equations. In addition, analytical solutions are possible for these equations because they have relatively simple initial conditions and boundary conditions. In order to preserve the linearity of the equations and making the analytical solutions, a number of simplifying assumptions were made such as steady state water flow was assumed; a

uniform hydrogeologic condition were assumed in the soil column whereas it is different from the reality. The interstitial pore water velocity was most likely not uniform in the column because of unsaturated conditions. As stated by Lafolie et al. (1991), a better prediction of the water flow including macropore and soil structure effects is probably a major challenge in modeling not only water flow but also the transport of fertilizer and chemical substances.

Another important assumption was first-order kinetics for the microbial transformation of nitrogen compounds. McLaren (1976) stated that in order to construct predictive mathematical models for microbial transformations of elements such as *N* in flowing systems in nature, it is essential to have realistic rate constants. According to Starr et al. (1974), many factors such as microbial growth kinetics, temperature, *pH*, and the supply of oxygen and carbon and a host of other environmental parameters are implicitly included in the rate coefficients. Starr et al. (1974) describes that under steady-state conditions, the transformations are generally zero or first-order rate reactions for relatively large or small concentrations, respectively. According to the same author, for more dilute solutions and/or where oxygen or carbon supplies are limited, the net rate of oxidation of NH_4^+, oxidation of NO_2^- and reduction of NO_3^- can be given by first order kinetics. Further, Kumar et al. (1984) stated that it can be assumed that nitrification can be expressed with first-order reaction kinetics. McLaren (1976) mentioned that the rate constants obtained in the field or laboratory soil studies depend on both time and biomass or microbial number, and Doner et al. (1974) indicated that the microbial numbers are as important as are other parameters including flow rates, organic matter content, soil *pH* and redox potential etc. These facts show that the estimated rate constants, k_1 and k_2, in this study are subject to some limitations. However, these values may represent the apparent constants, into which the aforementioned various factors have been lumped together. In addition, the models presented in this chapter are oriented toward a simple simulation using physico-chemical aspects rather than microbial processes. If microbial dynamics were taken into account, the models would be non-linear, and would unable to be solved analytically. In addition, the models would also require more input parameters.

In this study, a unique approach was followed in order to estimate the apparent rate constants, which are the calibration parameters of the developed models. As stated by Odencrantz et al. (2003), modelers using the first-order decay expression typically use the rate coefficient as a calibration parameter and adjust it until the transport model results

match field data, and with this approach, uncertainties with a number of parameters (dispersion, sorption, biodegradation, etc.) are lumped together in a single calibration parameter. In this study, the same method was used in a unique style to optimize the calibration parameters. That is to optimize the rate constants using a huge database of simulated $NO_3^- - N$, with the aid of computer programs and statistics. The traditional method of estimating the rate constant is to use the curve fitting techniques. According to Kumar et al. (1984), usually, all parameters other than the kinetic rate coefficients are independently known or measured, and the rate coefficients are determined by a curve fitting process.

In the developed models, sorption was subject to several simplified assumptions. It was further assumed that the NH_4^+ on both solid and solution phases would undergo nitrification. Krupp et al. (1972) stated that the microbial oxidation can involve NH_4^+ ions on both phases, together with the existence of both mobile and immobile soil water. The measured data support this statement. It is considered that the adsorbates both on the adsorbent and in solution are in local equilibrium with each other. However, in reality, initially it tends to be sorbed irreversibly, only after some time a reversible sorption-desorption equilibrium is potentially established. However, it is worth mentioning here that the model developed on *CA* of low porous soil is subject to different adsorption phenomena as appropriate.

The predictive capability of the developed models also depends on the accuracy and relevance of the input parameters such as apparent molecular diffusion and the sorption partition coefficient.

5.2 HIGH POROUS SOIL

5.2.1 Model development

5.2.1.1 Simplified materials-balance equation

Contaminant transport in porous media is influenced by advection, molecular diffusion, hydrodynamic dispersion, sorption and transformation processes (Nazaroff et al., 2001). Therefore, a simplified material balance equation for a contaminant transporting in an unsaturated soil column can be given by the equation:

$$\frac{\partial C_i}{\partial t} + \frac{(1-\phi)\rho_b}{\phi_w}\frac{\partial q_i}{\partial t} + v\frac{\partial C_i}{\partial x} - \varepsilon_h \frac{\partial^2 C_i}{\partial x^2} - r_i = 0 \qquad (5.1)$$

The derivation of Eq. (5.1) is explained in Appendix C. Each term in this equation has dimensions of contaminant quantity per unit total volume of the medium (including pores and soil grains) per unit time. Eq. (5.1) is subject to the following assumptions: soil column is homogeneous; the fluid flow field is uniform and steady in time; the fluid flows with a velocity parallel to the *x* axis and is in the direction of increasing *x*; and the effect of lateral dispersion is neglected.

5.2.1.2. Linear Form of Freundlich isotherm for sorption

The sorption process was represented by the linear form of Freundlich isotherm, in which sorption was assumed to be reversible and rapid relative to the advective and dispersive transport. It means that the sorption–desorption reactions quickly transforms into a reversible equilibrium state. Hence, q_i is given by:

$q_i = K_d C_i$ (Bohn et al., 1985) (5.2)

Then, Eq. (5.1) can be written as:

$$R\frac{\partial C_i}{\partial t} + v\frac{\partial C_i}{\partial x} - \varepsilon_h \frac{\partial^2 C_i}{\partial x^2} - r_i = 0 \quad (5.3)$$

$$R = \left\{1 + (1-\phi)K_d \frac{\rho_b}{\phi_w}\right\} \quad (5.4)$$

where R = retardation factor (Kinzelbach, 1986).

5.2.1.3 Kinetics of microbial transformation of nitrogen

In this analytical model, first order kinetics were assumed for both nitrification and denitrification. Therefore, the net rates of transformation of NH_4^+ (r_1) and NO_3^- (r_2) can be given by:

$$r_1 = -Rk_1C_1 \quad (5.5)$$

$$r_2 = Rk_1C_1 - k_2C_2 \quad (5.6)$$

It was assumed that there was an instantaneous equilibrium between the NH_4^+ on the solid and liquid phases. Therefore, r_1 contains R that depicts adsorbed NH_4^+ also undergoes nitrification. In this model, NO_3^- was not subject to sorption. Therefore, the governing equations for NH_3-N and $NO_3^- - N$ dynamics that incorporates the advection, dispersion, sorption and transformation are given by:

$$R\frac{\partial C_1}{\partial t}+v\frac{\partial C_1}{\partial x}-D_1\frac{\partial^2 C_1}{\partial x^2}+Rk_1C_1=0 \tag{5.7}$$

$$\frac{\partial C_2}{\partial t}+v\frac{\partial C_2}{\partial x}-D_2\frac{\partial^2 C_2}{\partial x^2}-Rk_1C_1+k_2C_2=0 \tag{5.8}$$

ε_h was replaced with D_1 and D_2 by considering that the dispersive effect is negligible due to the very low pore water velocity.

5.2.1.4 Analytical solutions for the governing equations

The following boundary conditions were considered. The duration of the entire course of experimental run is equal to T.

$C_1 = C_1^0 = C_2^0$ $\quad x=0$ $\quad 0 < t < T$ (a)

$C_1 = C_2 = 0$ $\quad x=0$ $\quad t > T$ (b)

$C_1 = C_2 = 0$ $\quad x \geq 0$ $\quad t = 0$ (c)

$C_1 = C_2 = 0$ $\quad x \to \infty$ $\quad t \geq 0$ (d)

Eq. (5.7) and (5.8) were solved using the Laplace transformation techniques (Riley et al., 1998; Schiff, 1999; Abramowitz and Stegun, 1972) subject to above-mentioned boundary conditions as:

$$C_1(x,t) = C_0^1 F(x,t) \tag{5.9}$$

$$C_2(x,t) = C_2^0 Q(x,t) + \frac{Rk_1C_1^0}{(k_1R-k_2)}\left[Q(x,t)-P(x,t)+S(x,t)-F(x,t)\right] \tag{5.10}$$

Where

$$F(x,t)=\frac{1}{2}\left[\begin{array}{l}\exp\left\{\frac{x}{2D}\left(v-\sqrt{\left(v^2+4Dk_1R\right)}\right)\right\}erfc\left(\frac{x-t\sqrt{\left(v^2+4Dk_1R\right)}/R}{\sqrt{(4Dt/R)}}\right)+\\ \exp\left\{\frac{x}{2D}\left(v+\sqrt{\left(v^2+4Dk_1R\right)}\right)\right\}erfc\left(\frac{x+t\sqrt{\left(v^2+4Dk_1R\right)}/R}{\sqrt{(4Dt/R)}}\right)\end{array}\right] \tag{5.11}$$

$$Q(x,t)=\frac{1}{2}\left[\begin{array}{l}\exp\left\{\frac{x}{2D}\left(v-\sqrt{\left(v^2+4Dk_2\right)}\right)\right\}erfc\left(\frac{x-t\sqrt{\left(v^2+4Dk_2\right)}}{\sqrt{4Dt}}\right)+\\ \exp\left\{\frac{x}{2D}\left(v+\sqrt{\left(v^2+4Dk_2\right)}\right)\right\}erfc\left(\frac{x+t\sqrt{\left(v^2+4Dk_2\right)}}{\sqrt{4Dt}}\right)\end{array}\right] \tag{5.12}$$

$$P(x,t)=\frac{1}{2}\left[\begin{array}{l}\exp\{-At\}\exp\left\{\frac{x}{2D_2}\left(v-\sqrt{\left(v^2+4Dk_2-4DA\right)}\right)\right\}\\ erfc\left(\frac{x-t\sqrt{\left(v^2+4Dk_2-4DA\right)}}{\sqrt{(4Dt)}}\right)+\\ \exp\{-At\}\exp\left\{\frac{x}{2D}\left(v+\sqrt{\left(v^2+4Dk_2-4DA\right)}\right)\right\}\\ erfc\left(\frac{x+t\sqrt{\left(v^2+4Dk_2-4DA\right)}}{\sqrt{(4Dt)}}\right)\end{array}\right] \tag{5.13}$$

$$S(x,t)=\frac{1}{2}\left[\begin{array}{l}\exp\{-At\}\exp\left\{\frac{x}{2D_1}\left(v-\sqrt{\left(v^2+4Dk_1R-4DAR\right)}\right)\right\}\\ erfc\left(\frac{x-t\sqrt{\left(v^2+4Dk_1R-4DAR\right)}/R}{\sqrt{(4Dt/R)}}\right)+\\ \exp\{-At\}\exp\left\{\frac{x}{2D_2}\left(v+\sqrt{\left(v^2+4Dk_1R-4DAR\right)}\right)\right\}\\ erfc\left(\frac{x+t\sqrt{\left(v^2+4Dk_1R+4DAR\right)}/R}{\sqrt{(4Dt/R)}}\right)\end{array}\right] \tag{5.14}$$

$$A=\left(\frac{k_1R-k_2}{R-1}\right) \tag{5.15}$$

It was assumed that $D=D_1=D_2$ for the simplicity of the solutions.

The steady state solutions are given by Eq. (5.16) and (5.17).

$$C_1(x,t)=C_1^0F_1'(x) \tag{5.16}$$

$$C_2(x,t)=C_2^0F_2'(x)+\frac{Rk_1C_1^0}{\left(r^2D_2-vr-k_2\right)}\left[F_2'(x)-F_1'(x)\right] \tag{5.17}$$

Where $r=\dfrac{v-\sqrt{v^2+4k_1RD_1}}{2D_1}$; $F_1'(x)=\exp\left(\dfrac{x}{2D_1}\left\{v-\sqrt{v^2+4k_1RD_1}\right\}\right)$ &

$F_2'(x)=\exp\left(\dfrac{x}{2D_2}\left\{v-\sqrt{v^2+4k_2D_2}\right\}\right)$

The complete procedures of the solutions for Eq. (5.9), (5.10), (5.16) and (5.17) can be found in Appendix C.

5.2.1.5 Model application

Input data

A computer program (**Fig. C-1**) was developed to incorporate equations (5.9) and (5.10) using Microsoft Visual Basic. The 'erfc' was computed using a numerical approximation given by Abramowitz and Stegun (1972). **Table 5.1** shows the input parameters in the model. The soil parameters shown in Table 5.1 are the average values of the soil before and after leaching the SRW through soil. The particle density of soil was assumed as 2.65 mg/cm^3 (GLOBE, 2002) in calculating the air-filled porosity. The average effluent rate of the entire course of experiment (9.98 mL/h) was divided by the cross sectional area of the column and ϕ_w, to obtain v. The daily discharge rates of effluent over the course of experimental run were averaged out to compute the average effluent rate. R obtained using the results (K_d = 30 cm^3/g) of batch experiment, described in the section 4.2.3.2, is 68.3. If this value had been used as R, NH_3-N concentration would have become 0 at greater depths. But, according to measured results, it is not 0 at greater depths. So, R was calculated using a value of K_d mentioned in the literature.

Table 5.1 Input data of the model on high porous soil.

Parameter	Value	Note
D	1.4 cm^2/ d	Reference: Odencrantz et. al. (1990)
K_d	2 cm^3/g	Reference: Gusman et. al. (1999)
ϕ	0.62	Average of initial and final soil
ϕ_w	0.375	Average of initial and final soil
ρ_b	1.378 g/cm^3	Average of initial and final soil
R	3.79	Calculated
v	2.033 cm/d	Calculated using average effluent rate
C_1^0	18 mg/L	Measured
C_2^0	3 mg/L	Measured

Calibration of the model

The model was calibrated in terms of k_1 and k_2, by applying it to the experimental results of the soil column. Transient and steady state $NO_3^- - N$ concentrations at depths, 15 cm, 35 cm, 45 cm, 55 cm, 70 cm, 80 cm and 85 cm, were computed for each 0.01 d^{-1} increment of k_1 from 0.01 to 0.7 d^{-1} and k_2 from 0.001-0.1 d^{-1}. These ranges are the common ranges, in which existing k_1 and k_2 values lie. Then, the optimum k_1 and k_2 were

obtained for each depth using the sum of squares of error between each estimated and measured $NO_3^- - N$ concentration. When applying the model to optimize the rate constants at each depth, it was considered that the control volume was from the soil surface to each depth. Then, the optimized k_1 and k_2 per each depth, except 85 cm, were averaged out. These average k_1 and k_2 represent the *PW* inside the soil column, since measured $NO_3^- - N$ concentrations in the *PW* samples were used for the initial optimization. The k_1 and k_2 at 85 cm depth were considered as the global averages of k_1 and k_2 in the soil column because those values were optimized using the measured $NO_3^- - N$ concentrations in *E* samples. The average k_1 and k_2 of *PW* and the global averages were considered as the calibration parameters of the model.

5.2.2 Results and Discussion

5.2.2.1 Model simulations of experimental results

Table 5.2 is a list of k_1 and k_2 at each depth, which were optimized using the measured data of *PW* samples, and the results of the goodness of the simulations in terms of the correlation coefficient. The global averages of k_1 and k_2 were 0.09 d^{-1} and 0.003 d^{-1}, respectively. The average k_1 and k_2 that represent the pore water in the soil column were 0.045 d^{-1} and 0.011 d^{-1}, respectively. **Table 5.3** and **Fig. 5.1** show the description of the simulation of $NO_3^- - N$ concentrations for pore water samples and the effluent.

Table 5.2 Optimum k_1 and k_2 for each depth of the model on high porous soil

Depth (cm)	k_1 (d^{-1})	k_2 (d^{-1})	R^2	Sum of squares of errors
0-15	0.04	0.02	0.69	116
0-35	0.05	0.02	0.86	144
0-45	0.05	0.01	0.89	120
0-55	0.03	0.006	0.88	149
0-70	0.04	0.005	0.88	186
0-80	0.06	0.005	0.92	111

Table 5.3 Calibration data of the model on high porous soil

Depth (cm)	k_1(d^{-1})	k_2 (d^{-1})	R^2	Sum of squares of errors
15	0.045	0.011	0.64	166
35			0.86	169
45			0.87	127
55			0.90	120
70			0.88	261
80			0.91	378
85 (Effluent)	0.09	0.003	0.99	20

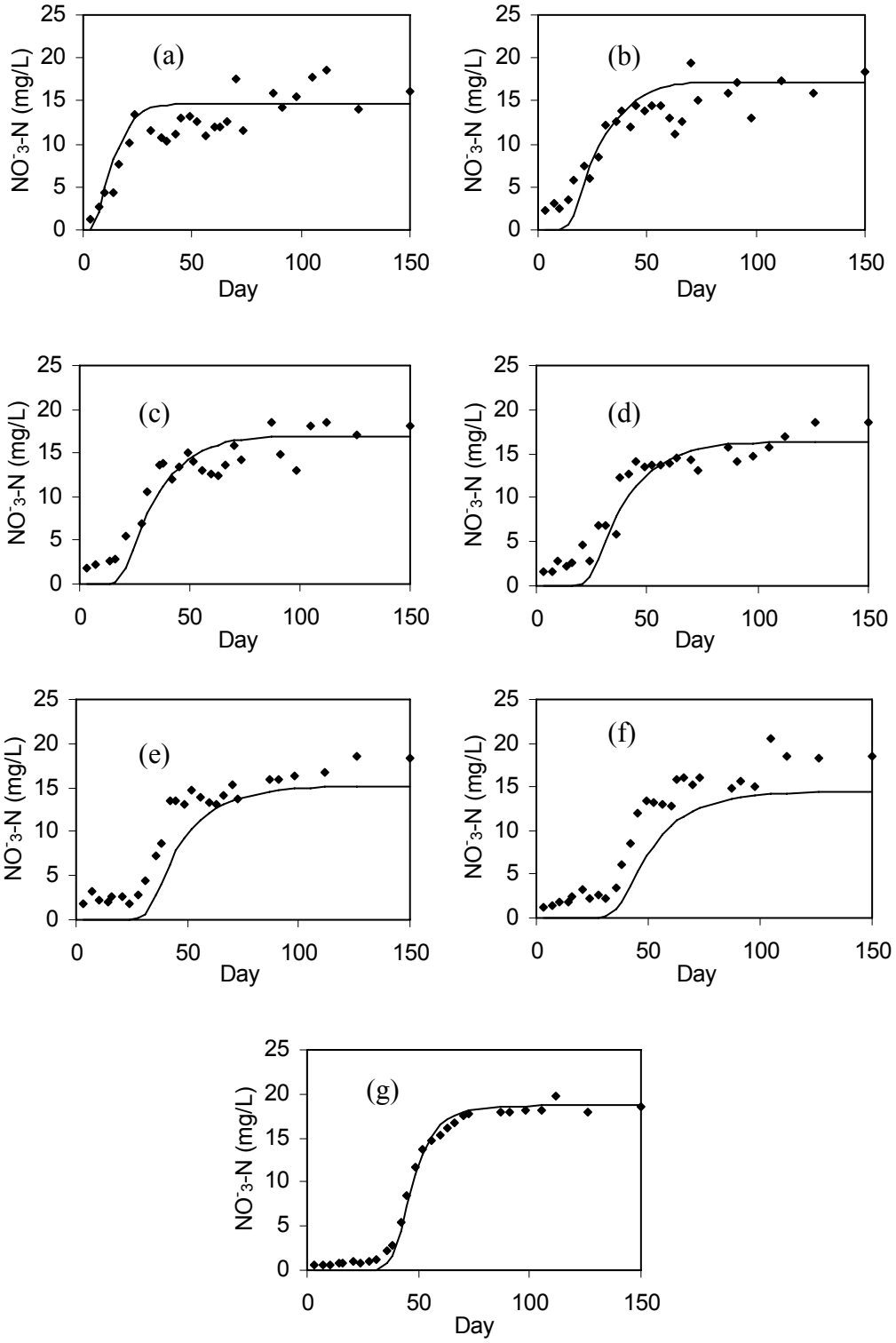

Fig. 5.1 Simulated (lines) and measured (diamonds) NO_3^-N concentrations in (a) PW1, (b) PW2, (c) PW3, (d) PW4, (e) PW5, (f) PW6 and (g) Effluent.

As shown in Table 5.3, there is a significant difference between the constants optimized using the pore water and effluent. The heterogeneous nature and sampling

techniques in the column are the main candidates in explaining the variation. Pore water samples were collected at the vertical centre line of the column. Each pore water sample represents only one point of the column. In addition, the pore water represents both mobile and immobile water. Therefore, the $NO_3^- - N$ concentration of pore water samples largely represents local conditions. However, the effluent represents the total percolated water. Hence, the constants derived using the measured data of the effluent samples are referred to as the global average of the rate constants, k_1 and k_2, that represent the percolating water downward.

5.2.2.2 Sensitivity analysis

In order to investigate the degree of contribution of each input parameter in the model, a sensitivity analysis was carried out for D, R, v, k_1 and k_2. The range, for which each parameter was varied, depended on the existing range as well as the applicability of the value in the model so that the model did not compute indefinite answers. When the parameter of concern for the sensitivity analysis was varied, all the other parameters were kept constants, and the constant values of D, R, v and other input parameters were similar to those of Table 5.1. The varying interval depended on the order of magnitude of the parameter. $NO_3^- - N$ concentration was computed at the 85 cm depth and for the experimental period. Hence, constant k_1 and k_2 were the optimum rate constants that represent the effluent, i.e. 0.09 d^{-1} and 0.003 d^{-1}, respectively.

Fig. 5.2 shows the results of the sensitivity analysis. The least sensitive input parameter is R. The effect of change of R within a range from 3.79-40 is negligible (Fig. 5.2b). Though, R is insentive for the $NO_3^- - N$ model, it is extremely sensitive on the NH_3-N model. According to the discussion in chapter 4, applied NH_4^+ via the influent is converted to NO_3^- by both direct nitrification and nitrification after adsorption on to soil. R equal to 3.79 is enough to cause a large portion of applied ammonium to convert into $NO_3^- - N$. Therefore, R being greater in any amount than 3.79 would not affect NO_3^- concentration.

D was varied within a range from 0.5 to 5.0cm^2/d. This is the common range, in which D varies according to the past research. Because, this model deals with low v values, mechanical dispersive effect is negligible. The effect of change of D is not so significant (Fig. 5.1a).

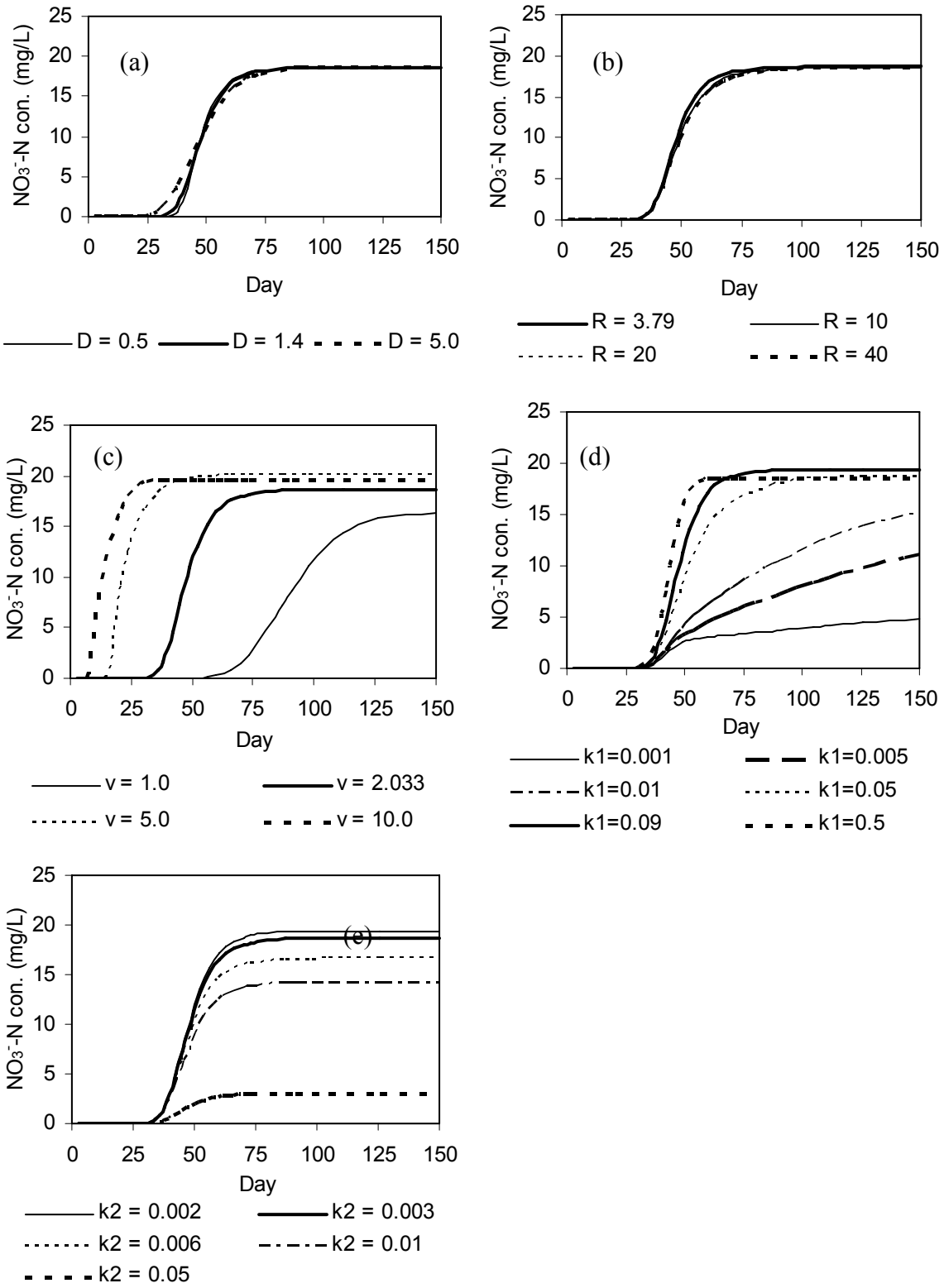

Fig. 5.2 Sensitivity analysis on high porous soil-model (a) D, (b) R, (c) v, (d) k_1, and (e) k_2.

v was varied from 1 -10 cm/d, and the effect of change is significant. *v* is the main factor to determine the duration of the transient period before attaining the steady state. The time taken for the steady state to occur greatly increases with the decrease of *v*. Not

only does *v* affect the time for the steady state, but also it affects the steady state concentration of NO_3^- -*N* (Fig. 5.2c). The reason for the latter is that the retention time decreases with the increase of *v*, which in turn decreases the degree of denitrification.

When k_1 is varied from 0.001-0.09 d^{-1}, the steady-state NO_3^- -*N* concentration increases. However, when k_1 is equal to 0.5 d^{-1}, the steady-state NO_3^- -*N* concentration is less than that when it is equal to 0.09 d^{-1}, and the steady state occurred a little earlier than that when k_1 = 0.09 d^{-1}. This implies that k_1 mainly affects the peak concentration while change by 1-2 order of magnitude causes the transient period shorter (Fig. 5.2d). k_2 was varied from 0.002 - 0.05 d^{-1}. Variation affects the peak concentration. When the value increases, the peak concentration decreases. It means increased denitrification decreases the nitrate concentration fast.

5.2.2.3 Evaluation of the model

The model simulates the measured values quite well and consistently throughout the column. All simulations of $NO_3^- - N$ showed a reasonable agreement with the experimental results. In particular, the shapes of the profiles are represented with the model. Although, this model suffers from some limitations, $NO_3^- - N$ dynamics are satisfactorily described. The measured data verified that the nitrification, denitrification and adsorption of NH_4^+ processes dominate the nitrogen dynamics in the soil column. The calibration data of the model also indicate that the nitrification and denitrification both had a significant effect on the nitrate dynamics. Hence, the estimated rate constants in this text represent the nitrogen dynamics quite well. The correlation coefficients between the measured and simulated concentrations of the pore water at all depths were more than 0.85, but 15 cm. It was 0.99 for the effluent.

5.3 LOW POROUS SOIL

5.3.1 Model Development

5.3.1.1 Derivation of the governing equations

As described in Chapter 3, $NO_3^- - N$ concentration of *PW* and the effluent of this column experiment increased to very high levels. It exceeded the *T-N* concentration in the influent by manifold. It implies that there may have been another source that supplied *N*.

However, according to Fig.3.18a, ultimate cumulative *T-N* supplied by the influent was higher than that discharged as the effluent. Therefore, this additional source has gained nitrogenous compounds supplied by the influent. The reader is directed to the sub section 'Ion exchange reactions' under the section 3.1.3.1. in order to get a clear understanding of this. Initially, until about two weeks, $NO_3^- - N$ concentration was below 3 mg/L even in *PW1*, whereas NH_3-*N* concentration of *PW1* had almost become negligible.

Therefore, based on above-mentioned discussion, the below-mentioned interpretation was adopted in the developed model. No oxidation of adsorbed NH_4^+ happened, until sufficient number of nitrifiers grew for oxidation to take place (Until $t = T_1$). Therefore, two sets of governing equations were derived for this model. The total duration of the experimental run was divided into two time zones. It was assumed that the nitrifiers took 15 days to grow into a satisfied number. Normally, nitrifiers require14 days to get their number doubled. Therefore, until 15 days, only the NH_4^+, supplied by the influent at the time, would undergo nitrification at low rates. In addition, NH_4^+ supplied thus would largely be adsorbed onto the soil. The adsorbed NH_4^+ would not nitrify until a satisfied number of nitrifiers grew. After 15 d, the adsorbed NH_4^+ would start nitrification. Then, NO_3^- produced as thus, would leach into the soil solution to make the balance of negative charge between soil and soil solution. This leaching of NO_3^- is considered as an additional source to the general material balance given by Eq. 5.8. In addition, NH_4^+ supplied by the influent at the time, would be subject to the sorption assumptions described under the section 5.2.1.2. Therefore, following are the respective governing equations for each parameter at each time zone.

NH_3-N ($0 < t < T_1$)

$$R\frac{\partial C_1^p}{\partial t} + v\frac{\partial C_1^p}{\partial x} - D\frac{\partial^2 C_1^p}{\partial x^2} + k_1 C_1^p = 0 \qquad (5.18)$$

NO_3-N ($0 < t < T_1$)

$$\frac{\partial C_2^p}{\partial t} + v\frac{\partial C_2^p}{\partial x} - D_2\frac{\partial^2 C_2^p}{\partial x^2} - k_1 C_1^p + k_2 C_2^p = 0 \qquad (5.19)$$

NH_3-N ($t > T_1$)

It was assumed that the desorbed NH_4^+ (additional source) would quickly nitrify and the rate constant would be high. Therefore, the additional source only supplies NO_3^- into the soil solution. So, the effect of desorbed NH_4^+ on its concentration in the solution would be neglected. Therefore, *NH_3-N* during $t > T_1$ becomes:

$$R\frac{\partial C_1}{\partial t} + v\frac{\partial C_1}{\partial x} - D_1\frac{\partial^2 C_1}{\partial x^2} + Rk_1C_1 = 0 \qquad (5.7)$$

NO_3-N ($t > T_1$)

In Eq. (5.20), the leaching of $NO_3^- - N$, which originated as a result of delayed nitrification of earlier adsorbed NH_4^+, is represented as an additional source term by $(R-1)\times k_1' \times \left(C_1^p\right)^1$. In the above source term, nitrification was assumed to be proportional to the *NH_3-N* concentration of the soil solution during the period $0 < t < T_1$, which is represented by $C_1^p(x,t)$. However, the term $C_1^p(x,t)$ cannot be input in Eq. (5.20), in the same form, because Eq. (5.20) represents the period $t > T_1$. Hence, $C_1^p(x,t)$ was considered as one period of a periodic function with period T_1, which is denoted by $\left(C_1^p\right)^1$. This is how the effect of previously happened $C_1^p(x,t)$ was brought into the present equation mathematically. Then, the Laplace transformation of $\left(C_1^p\right)^1(x,t)$ is given by $\left(\overline{C}_1^p\right)^1(s) = \int_0^{T_1} e^{-st} C_1^p(x,t)dt$, which is the Laplace transform of the function denoting the first period and zero elsewhere (Schiff, 1999). According to this mathematical interpretation, this additional source term functions only for a limited time period. The capacity of that source depends on how much NH_4^+ was adsorbed onto soil during $0 < t < T_1$. The portion of each $NO_3^- - N$ profile, which is higher than *T-N* concentration of the influent, was simulated when this term functioned. It brings the $NO_3^- - N$ concentration to the peak and then makes it fade. When this source term terminates functioning, the simulated $NO_3^- - N$ becomes less than *T-N* concentration of the influent. Therefore, during the steady state, this additional source term does not function in the equation.

$$\frac{\partial C_2}{\partial t}+v\frac{\partial C_2}{\partial x}-D_2\frac{\partial^2 C_2}{\partial x^2}-Rk_1C_1+k_2C_2-(R-1)\times k_1'\times\left(C_1^p\right)^1=0 \tag{5.20}$$

5.3.1.2 Analytical solutions for the governing equations

NH_3-N ($0 < t < T_1$)

Eq. (5.18) can be solved using the same procedure described in Appendix C under the solution for the governing equation of *NH_3-N* for *CA* of high porous soil. Then;

$$C_1^p(x,t)=C_0^1F'(x,t) \tag{5.21}$$

$$F'(x,t)=\frac{C_0^1}{2}\left[\begin{array}{l}\exp\left\{\frac{x}{2D}\left(v-\sqrt{\left(v^2+4Dk_1\right)}\right)\right\}erfc\left(\frac{x-t\sqrt{\left(v^2+4Dk_1\right)}/R}{\sqrt{4DRt}}\right)+\\ \exp\left\{\frac{x}{2D}\left(v+\sqrt{\left(v^2+4Dk_1\right)}\right)\right\}erfc\left(\frac{x+t\sqrt{\left(v^2+4Dk_1\right)}/R}{\sqrt{4DRt}}\right)\end{array}\right] \tag{5.22}$$

NO_3-N ($0 < t < T_1$)

Eq. (5.19) can be solved using the same procedure described in Appendix C, under the solution of the governing equation for $NO_3^- - N$ of high porous soil. Then;

$$C_2^p(x,t)=C_2^0\times Q(x,t)+\frac{k_1C_1^0}{(k_1-k_2)}\left[Q(x,t)-P'(x,t)+S'(x,t)-F'(x,t)\right] \tag{5.23}$$

$$P'(x,t)=\frac{1}{2}\left[\begin{array}{l}\exp\{-Bt\}\exp\left\{\frac{x}{2D}\left(v-\sqrt{\left(v^2+4Dk_2-4DB\right)}\right)\right\}\\ erfc\left(\frac{x-t\sqrt{\left(v^2+4Dk_2-4DB\right)}}{\sqrt{(4Dt)}}\right)+\\ \exp\{-Bt\}\exp\left\{\frac{x}{2D}\left(v+\sqrt{\left(v^2+4Dk_2-4DB\right)}\right)\right\}\\ erfc\left(\frac{x+t\sqrt{\left(v^2+4Dk_2-4DB\right)}}{\sqrt{(4Dt)}}\right)\end{array}\right] \tag{5.24}$$

$$S'(x,t)=\frac{1}{2}\left[\begin{array}{l}\exp\{-Bt\}\exp\left\{\dfrac{x}{2D}\left(v-\sqrt{\left(v^2+4Dk_1-4DBR\right)}\right)\right\}\\ erfc\left(\dfrac{x-t\sqrt{\left(v^2+4Dk_1-4DBR\right)}/R}{\sqrt{(4Dt/R)}}\right)+\\ \exp\{-Bt\}\exp\left\{\dfrac{x}{2D_2}\left(v+\sqrt{\left(v^2+4Dk_1-4DBR\right)}\right)\right\}\\ erfc\left(\dfrac{x+t\sqrt{\left(v^2+4Dk_1+4DBR\right)}/R}{\sqrt{(4Dt/R)}}\right)\end{array}\right] \tag{5.25}$$

$$B=\left(\frac{k_1-k_2}{R-1}\right) \tag{5.26}$$

NH_3-N ($t > T_1$)

$$C_1(x,t)=C_0^1F(x,t) \tag{5.27}$$

NO_3-N ($t > T_1$)

The procedure of solving Eq. (5.20) can be found in the Appendix C. The solution is as follows:

$$\begin{array}{l}C_2(x,t)=C_2^0Q(x,t)+\dfrac{Rk_1C_1^0}{(k_1R-k_2)}\left[Q(x,t)-P(x,t)+S(x,t)-F(x,t)\right]\\ +\dfrac{(R-1)k_1'C_1^0}{(k_1-k_2)}\left[\begin{array}{l}Q(x,t)-Q(x,(t-T_1))+P_1(x,(t-T_1))-P_1(x,t)+\\ S_3(x,t)-S_3(x,(t-T_1))-F_3(x,t)+F_3(x,(t-T_1))\end{array}\right]\end{array} \tag{5.28}$$

Where;

$$P_1(x,t)=\frac{1}{2}\left[\begin{array}{l}\exp\{-Bt\}\exp\left\{\dfrac{x}{2D}\left(v-\sqrt{\left(v^2+4Dk_2-4DB\right)}\right)\right\}\\ erfc\left(\dfrac{x-t\sqrt{\left(v^2+4Dk_2-4DB\right)}}{\sqrt{(4Dt)}}\right)+\\ \exp\{-Bt\}\exp\left\{\dfrac{x}{2D}\left(v+\sqrt{\left(v^2+4Dk_2-4DB\right)}\right)\right\}\\ erfc\left(\dfrac{x+t\sqrt{\left(v^2+4Dk_2-4DB\right)}}{\sqrt{(4Dt)}}\right)\end{array}\right] \tag{5.29}$$

$$S_3(x,t)=\frac{1}{2}\left[\begin{array}{l}\exp\{-Bt\}\exp\left\{\frac{x}{2D}\left(v-\sqrt{\left(v^2+4Dk_1-4DBR\right)}\right)\right\}\\ erfc\left(\frac{x-t\sqrt{\left(v^2+4Dk_1-4DBR\right)}/R}{\sqrt{(4Dt/R)}}\right)+\\ \exp\{-Bt\}\exp\left\{\frac{x}{2D}\left(v+\sqrt{\left(v^2+4Dk_1-4DBR\right)}\right)\right\}\\ erfc\left(\frac{x+t\sqrt{\left(v^2+4Dk_1+4DBR\right)}/R}{\sqrt{(4Dt/R)}}\right)\end{array}\right] \quad (5.30)$$

$$F_3(x,t)=\frac{1}{2}\left[\begin{array}{l}\exp\left\{\frac{x}{2D}\left(v-\sqrt{\left(v^2+4Dk_1\right)}\right)\right\}erfc\left(\frac{x-t\sqrt{\left(v^2+4Dk_1\right)}/R}{\sqrt{(4D_1t/R)}}\right)+\\ \exp\left\{\frac{x}{2D}\left(v+\sqrt{\left(v^2+4Dk_1\right)}\right)\right\}erfc\left(\frac{x+t\sqrt{\left(v^2+4Dk_1\right)}/R}{\sqrt{(4Dt/R)}}\right)\end{array}\right] \quad (5.31)$$

The steady state solutions are given by Eq. (5.16) and (5.17).

5.3.1.3 Model application

Input data

A computer program (**Fig. C-2**) was developed to incorporate equations (5.21), (5.23), (5.27) and (5.28) using Microsoft Visual Basic. **Table 5.4** shows the input parameters in the model. The derivation of all the input parameters are similar to that of the section 5.2.1.5. *R* obtained using the results (40 cm^3/g) of batch experiments, described in the section 3.2.3.4, is 78.65. If this value has been substituted as *R*, *NH_3-N* concentration would have become 0 at greater depths. But, according to measured results, it is not 0 at greater depths. So, *R* was calculated using a value of K_d mentioned in the literature.

Table 5.4 Input data of the model on low porous soil

Parameter	Value	Note
D	1.4 cm^2/ d	Reference: Odencrantz et. al. (1990)
K_d	2 cm^3/g	Reference: Gusman et. al. (1999)
ϕ	0.56	Average of initial and final soil
ϕ_w	0.34	Average of initial and final soil
ρ_b	1.5 g/cm^3	Average of initial and final soil
R	4.88	Calculated
v	2.037 cm/d	Calculated using average effluent rate
C_1^0	18 mg/L	Measured
C_2^0	3 mg/L	Measured
T_1	15 d	From observation

Calibration of the model

The model was calibrated in terms of k_1, k_2 and k_1', by applying it to the experimental results of the soil column. Transient and steady state $NO_3^- - N$ concentrations at depths, 15 cm, 35 cm, 45 cm, 55 cm, 70 cm, 80 cm and 85 cm, were computed for each 0.01 d^{-1} increment of k_1 and k_1' from 0.01 to 0.6 d^{-1} and k_2 from 0.001-0.1 d^{-1}. These ranges are the common ranges, in which existing k_1, k_1' and k_2 values lie. Then, the optimum k_1, k_2 and k_1' were obtained for each depth using the sum of squares of error between each estimated and measured $NO_3^- - N$ concentration. When applying the model to optimize the rate constants at each depth, it was considered that the control volume was from the soil surface to each depth. Then, the optimized k_1, k_2 and k_1' per each depth, except 85 cm, were averaged out. These average k_1, k_2 and k_1' represent the pore water inside the soil column. The k_1, k_2 and k_1' at 85 cm depth were considered as the global averages of k_1, k_2 and k_1' in the soil column. The average k_1, k_2 and k_1' of the pore water and the global averages were considered as the calibration parameters of the model.

5.3.2 Results and Discussion

5.3.2.1 Model simulations of experimental results

The optimized k_1' for each depth is 1 d^{-1}. **Table 5.5** is a list of k_1 and k_2 at each depth, which were optimized using the measured data of pore water samples, and the correlation coefficients. The global averages of k_1, k_2, k_1' were 0.4 d^{-1}, 0.03 d^{-1} and 1 d^{-1}, respectively. The average k_1, k_2 and k_1' that represent the pore water in the soil column were 0.317 d^{-1}, 0.011 d^{-1} and 1 d^{-1}, respectively. **Table 5.6** and **Fig. 5.2** show the description of the simulation of $NO_3^- - N$ concentrations for pore water samples and the effluent.

Table 5.5 Optimum k_1 and k_2 for each depth of the model on low porous soil.

Depth (cm)	k_1 (d^{-1})	k_2 (d^{-1})	R^2
0-15	0.5	0.001	0.74
0-35	0.2	0.001	0.76
0-45	0.3	0.001	0.8
0-55	0.3	0.001	0.74
0-70	0.3	0.03	0.79
0-80	0.3	0.03	0.63

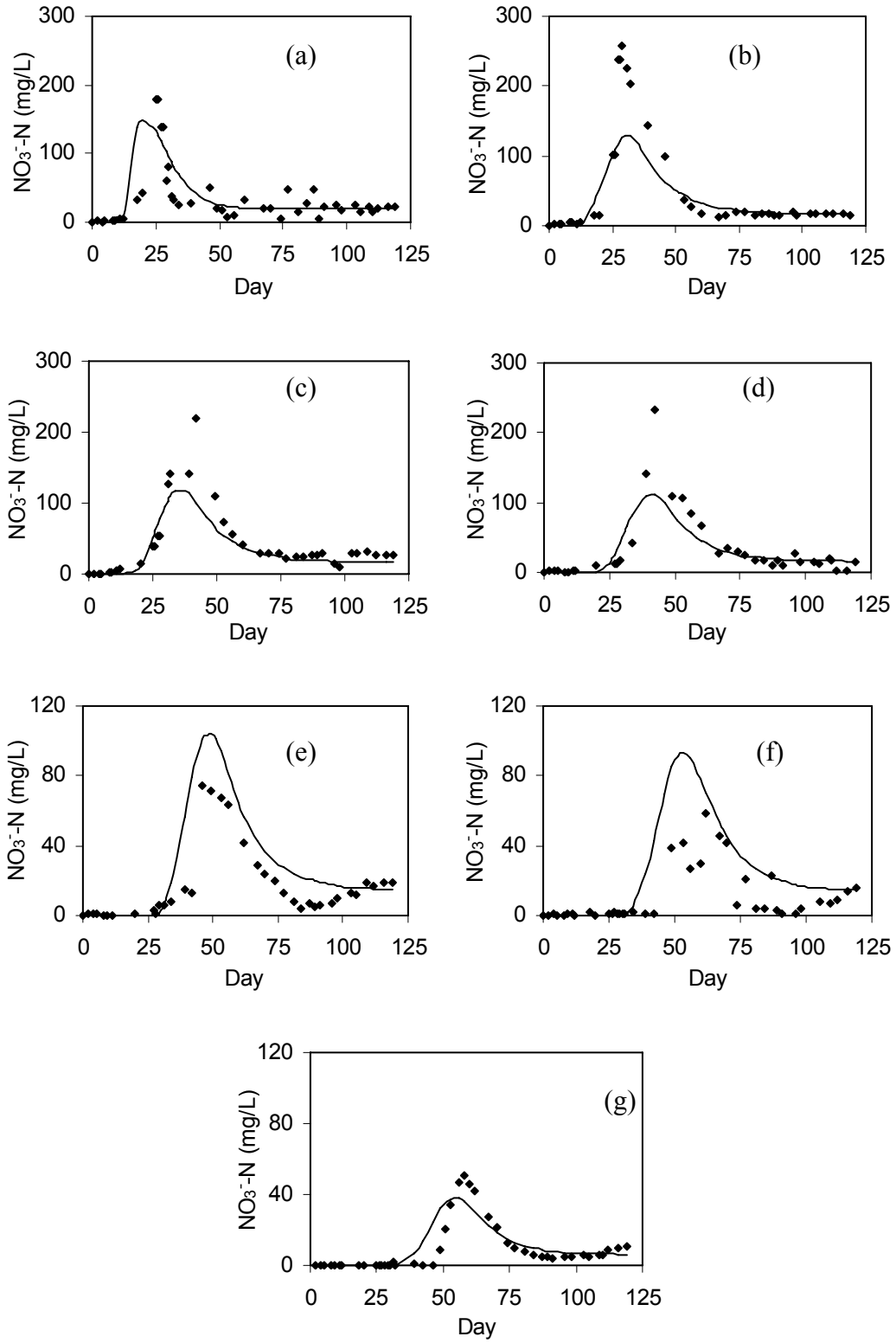

Fig. 5.3 Simulated (lines) and measured (diamonds) NO_3^--N concentrations in (a) PW1, (b) PW2, (c) PW3, (d) PW4, (e) PW5, (f) PW6 and (g) Effluent.

As indicated by **Table 5.6**, there is a significant difference between the constants optimized using the pore water and the effluent.

The reader is directed to the section 5.2.2.1 for the rationale of this discrepancy.

Table 5.6 Calibration data of the model on low porous soil.

Depth (cm)	$k_1(d^{-1})$	$k_2(d^{-1})$	R^2
15			0.72
35			0.83
45			0.79
55	0.317	0.011	0.72
70			0.8
80			0.64
85 (Effluent)	0.4	0.03	0.68

5.3.2.2 Sensitivity analysis

The sensitivity analysis on the low porous soil model was carried out in the same way as described in the section 5.2.2.2. When the parameter of concern for the sensitivity analysis was varied, the values of all the other parameters were similar to those in Table 5.4. The varying interval depended on the order of magnitude of the parameter. $NO_3^- - N$ concentration was computed at the 85 cm depth and for the entire experimental period. Hence, constant k_1 and k_2 were the optimum rate constants that represent the effluent, i.e. 0.4 d^{-1} and 0.03 d^{-1}, respectively.

Fig. 5.4 shows the results of the sensitivity analysis. The least sensitive input parameter is D (Fig. 5.4a). D was varied within a very short span from 0.5 to 2 cm^2/d because D being greater than 2 cm^2/d with the values of the other parameters such as v and k_1, makes the output of the model indefinite as the complementary error function goes to the infinity.

The effect of change of R in this model is significant because it directly affects the additional source term described in the section 5.3.1.1. The more the R is the more the peak concentration is. R slightly affects the time taken for the peak to occur as well. R greatly affects the duration of the transient period. The more the R is, the less the gradient of the profile in the downward direction prior to the steady state is (Fig.5.4b). v was varied from 1 -10 cm/d, and the effect of change is significant. Not only does v affect the duration of the transient period, but also it affects the peak concentration significantly. (Fig. 5.4c). The reduction of the degree of denitrifcation with the increase of v causes the latter.

When k_1 is varied from 0.05-0.6 d^{-1}, the peak $NO_3^- - N$ concentration decreases (Fig. 5.4d). When k_1 increases, the instantaneous nitrification of the adsorbed ammonium

on soil is rapid, which in turn causes the accumulated ammonium on soil (additional source of NO_3^-) to decrease. In this model, k_1 greatly affects the duration of the transient period as well as the peak concentration. k_2 was varied from 0.002 - 0.08 d^{-1}. Variation affects the peak concentration. When the value increases, the peak concentration decreases. It means increased denitrification decreases the nitrate concentration fast.

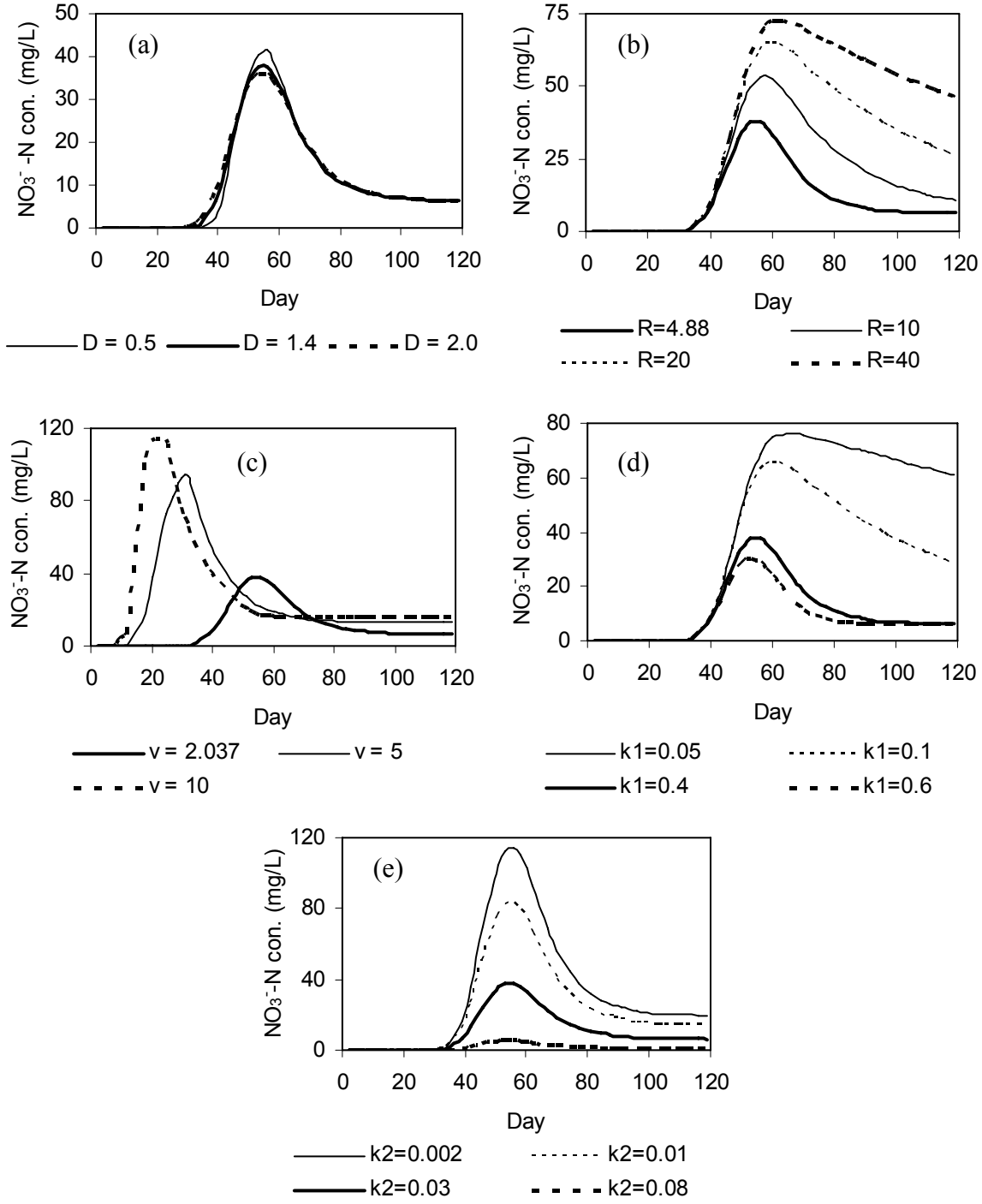

Fig. 5.4 Sensitivity analysis on low porous soil- model (a) D, (b) R, (c) v, (d) k_1, and (e) k_2.

5.3.2.3 Evaluation of the model

The measured data verified that the processes of nitrification, denitrification and adsorption of NH_4^+ dominate the nitrogen dynamics in the soil column. The calibration data of the model also indicate that the nitrification and denitrification both had a significant effect on the NO_3^- dynamics. The simulations of $NO_3^- - N$ during the steady state showed a good agreement with the experimental results. The steady-state measured values for *PW2*, *PW3*, *PW4* and E were very well simulated while those for *PW1* and *PW5* were simulated quite well. In particular, the shapes of the profiles are represented with the model. The R^2 between the measured and simulated $NO_3^- - N$ concentrations of the pore water at all depths were more than 0.72, but 80 cm. It was 0.68 for the effluent. The low R^2 for the effluent and *PW6* are attributed to the fact that the measured values apparently lagged the simulated curves during the period from day 35 to 75. The goodness of the simulations largely depend on the model's under estimation of the peak values for *PW* 1-4 and the over estimation of the peak values for *PW5* and *PW6*. This under estimation and over estimation largely depend on T_1 as it determines the capacity of the additional source term. The value of T_1 was obtained using the observations as well as considering the time for doubling the microbial growth that is about 14 d. Therefore, the term k_1' is a factor that lumps together all the discrepancies involved in the assumptions made for this additional source term. The rates of ascending to the peak and descending from the peak of the simulated profiles are lower than those of measured profiles. It caused the deviations of simulated profiles with the measured profiles around the peak concentrations. In addition, as explained in chapter 3, the observed data clearly indicated the acceleration of denitrification at the lower layers of this column. It is clearly visible in the denitrification coefficients derived using the control volumes to each depth (Table 5.5). In this experiment, k_2 largely varies with the soil depth.

Therefore, this analytical model, in which rate constants are considered as constants, have limited capacity to be perfectly fitted with the measured data. An approach of analytical-numerical combination would be better to address this kind of complex dynamics. However, it would require more input parameters. Unless those additional input parameters are measured, the model would not be more accurate than the developed model. Although, this model suffers from some limitations, it is capable of simulating $NO_3^- - N$ dynamics quite satisfactorily in this kind of complex system, using less number of inputs.

5. 4 CONCLUSIONS

Two simple analytical models were developed to simulate the $NO_3^- - N$ dynamics, which were demonstrated by the simultaneous occurrence of nitrification, denitrification and sorption of ammonium in the measured data of continuous irrigation for high and low porous soils. The models incorporate all the aforesaid processes with several assumptions used to preserve the linearity of the models. A simple linear Freundlich isotherm was used to address the sorption process of NH_4^+. The transformation processes such as nitrification and denitriifcation were interpreted using first-order rate constants. The parameters such as diffusion coefficients and K_d were obtained from the literature. Though, K_d of each soil was obtained using batch sorption experiments, the use of those K_d values leads measured data to immensely deviate from the simulated data. Batch experiments results usually overestimate the real situation inside a soil column.

The model developed for the high porous soil was calibrated in terms of the nitrification and denitrification rate constants. $NO_3^- - N$ concentration at each depth was obtained using a range of nitrification and denitrification rate constants. Then, both the rate constants were optimized using the sum of the squares of the error between each measured and simulated value. The average nitrification and denitrification rate constants that represent the pore water were 0.045 d^{-1} and 0.011 d^{-1}, respectively. The nitrification and denitrification rate constants derived using the measured data of the effluent samples, which represent the global averages, were 0.09 d^{-1} and 0.003 d^{-1}.

In order to simulate the high peaks of the measured profiles of $NO_3^- - N$ concentration of the pore water and effluent of *CA* of low porous soil, an additional source term was applied in the governing mass balance equation of $NO_3^- - N$. This source term represents the leaching of $NO_3^- - N$, which was initially adsorbed onto soil before nitrification. This model was calibrated in terms of the nitrification rate constants both on soil and solution, and denitrification rate constant. $NO_3^- - N$ concentration at each depth was obtained using a range of these constants. Then, all the rate constants were optimized using the sum of the squares of the error between each measured and simulated value. The average nitrification rate constants on soil and solution, and denitrification rate constant that represent the pore water were 1.0 d^{-1}, 0.317 d^{-1} and 0.011 d^{-1}, respectively. The nitrification rate constant on soil and solution and

denitrification rate constants derived using the measured data of the effluent samples, which represent the global averages, were 1.0 d^{-1}, 0.4 d^{-1} and 0.03 d^{-1},respectively.

The constants representing the pore water may have been largely influenced by the heterogeneity of the soil column and sampling. Therefore, with the global averages of the rate constants, the models can be used to make reasonable predictions of NO_3^- leaching to the groundwater. It can also be good enough to predict the NO_3^- concentration due to a continuous irrigation. Therefore, the models can be used as a means of testing strategies and assessing risks.

REFERENCES

Abramowitz, M., and I.A. Stegun (1972), *Handbook of Mathematical Functions: with Formulas, Graphs and Mathematical Tables*, Dover Publications, Inc., New York.

Bohn, H. L., B. L. McNeal, G. A. O'Connor (1985), *Soil Chemistry*, John Wiley & Sons, Inc., New York.

Doner, H. E., M. G. Volz, and A. D. McLaren (1974), Column studies of denitrification in soil, *Soil Biol. Biochem., 6*, 341-346.

GLOBE, Soil Particle Density Pro*toco*l, http://archive.globe.gov/sda/tg/pardensity.pdf, (2002).

Gusman, A.J., and M. A. Marino (1999), Analytical modeling of nitrogen dynamics in soils and groundwater, *Journal of Irrigation and Drainage Engineering, 125*(6), 330-337.

Kinzelbach (1986), W., *Groundwater Modelling: An Introduction with Sample Programs in BASIC*, Elsevier.

Krupp, H. K., J. W. Biggar, and D.R. Nielsen (1972), Relative flow rates of salt and water in soil, *Soil Sci. Soc. Amer. Proc.*, *36*, 412-417.

Kumar, V., R.J. Wagenet (1984), Salt effects on urea hydrolysis and nitrification during leaching through laboratory soil columns, *Plant and Soil 85*, pp. 219-227, Martinus Nihoff/Dr. W. Junk publishers, The Nethrlands.

Lafolie, F. (1991), Modelling water flow, nitrogen transport and root uptake including physical non-equilibrium and optimization of the root water potential, *Fertilizer Research*, *27*, 215-231.

McLaren, A. D. (1976), Rate constants for nitrification and denitrification in soils, *Rad. and Environm. Biophys.*, *13*, 43-48.

Nazaroff, W.W., and L. Alvarez-Cohen (2001), *Environmental Engineering Science*, John Wiley &sons, Inc., New York, NY.

Odencrantz, J. E., B. Wookeun, A. J. Valocchi, and B. E. Rittmann (1990), Stimulation of biologically active zones (BAZ's) in porous media by electron-acceptor injection, *J. Contam. Hydrol.*, *6*, 37-52.

Odencrantz, J.E., R. A. Vogl, and M.D. Varljen (2003), Natural attenuation rate clarifications: The true picture is in the details. *Soil and Sediment Contamination Journal*, *Amherst Scientific Publications*, *12*, 663-672.

Riley, K.F., M. P. Hobson, and S.J. Bence (2003), *Mathematical methods for Physics and Engineering,* Cambridge University Press, Cambridge, UK.

Schiff, J.L. (1999), *The Laplace Transform: Theory and Applications*, Springer-Verlag, New York, NY 10010.

Starr, J. L., F. E Broadbent, and D. R. Nielsen (1974), Nitrogen transformations during continuous leaching, *Soil Sci. Soc. Amer. Proc*., *38*, 283-289.

CHAPTER 6

DISCUSSION OF PRECAUTIONARY MEASURES FOR NITRATE POLLUTION IN OKINAWA

6.1 INTRODUCTION

This chapter discusses about possible precautionary measures to prevent NO_3^- pollution due to the RWW irrigation based on the laboratory soil column experiments, batch sorption experiments and developed analytical models along with the optimized average apparent nitrification and denitrification rate constants. It also contrasts the continuous irrigation of *RWW* with that of intermittent focusing the characteristics of each soil type. Further, the chapter presents the calculations of possible steady-state $NO_3^- - N$ concentrations that may exist in the groundwater due to the continuous irrigation of *RWW*, on both low and high porous soils.

6.2 COMPARISON OF NITROGEN DYNAMICS DUE TO CONTINUOUS AND INTERMITTENT IRRIGATION ON LOW AND HIGH POROUS SOILS

According to four soil column experiments conducted on two types of soils, the dynamics of nitrogen are different among each another. *CA* on low porous mudstone soil caused the acceleration of denitrification the most. Especially, when *CA* and *IA* on one soil type are contrasted, *CA* promotes denitrification. The dynamics of nitrogen compounds in mudstone is more complicated than those of high porous limestone. The dynamics of NO_3^- in *CA* on limestone is the simplest of all, and those dynamics could be easily interpreted by conventional advective, dispersive equation incorporating sorption and transformation. However, the dynamics of NO_3^- in *CA* on mudstone could not be described in the same way. Therefore, that equation had to be modified by incorporating an additional source of NO_3^-.

Low porosity makes the specific surface area of the soil grains large. Various physical and chemical properties including water retention and cation exchange capacity, have been shown to be highly correlated with the surface area of soils (Bohn et al., 1985). Therefore, owing to the higher specific surface area, the mudstone has the higher water holding and the adsorption capacities. The batch sorption experiments confirmed the comparatively high adsorption capacity of mudstone over limestone, as well. In addition, the soil analyses conducted by the Okinawa reclamation unit indicate that mudstone possess high water holding capacity whereas it is weak in limestone. High water retention allows the contaminants of water to involve with many biochemical reactions, which results in complex web of characteristics in pore water and the effluent. Though the similar types of pre-treatments were applied on both types of soils, once the soil receives water, all particles of the low porous soil tend to stick together and attain its original characteristic. Mudstone has strong physical characteristics such as stickiness and high plasticity. Moreover, the infiltration rate of mudstone is comparatively low. On a flat ground, it may range from 10-15 mm/h. For limestone, it may range from 15-30 mm/h. However, the difference between the infiltration rates has not affected the results of two soil columns irrigated continuously, since the application rate met with the allowable infiltration capacities of both the soils. The time spent to attain the steady state in *CA* of low and high porous soils were 80 and 75 days, respectively. The superficial pore water velocity of both the cases are approximately equal. Even so, the less infiltration capacity of the low porous mudstone may have affected the results of the intermittent applications. Though, the irrigation period is 2h every week, there was a free board that prevailed for about several hours (9 h) once it was irrigated for 2h. On contrary, water rapidly infiltrated into the high porous limestone leaving no free board even for a very short time.

Therefore, this study revealed that nitrogen dynamics in soil due to the RWW irrigation depend on many factors such as the application frequency and rate, characteristics of *RWW*, soil type and the climatic conditions such as rainfall and temperature. It postulates that a thorough study of nitrogen dynamics in soil due to *RWW* irrigation should be individually conducted based on the soil, characteristic of *RWW*, rate and frequency of application and etc, of concern.

6.3 DISCUSSION OF LOW-COST PRECAUTIONARY MEASURES FOR NITRATE POLLUTION IN OKINAWA

The results indicate that NO_3^- concentration that may leach into the groundwater is less in *CA* than in *IA*, and denitrification is accelerated in *CA*. Denitrification is the primary mechanism for the removal of inorganic nitrogen from the soil (DeBusk et al., 2001). The aforementioned phenomenon coupled with above results can be used to evaluate the best irrigation system in terms of prevention of NO_3^- pollution due to the *RWW*. Then, the continuous irrigation is preferred to the intermittent irrigation.

The above results indicate that the velocity of the flow has a significant influence on the NO_3^- pollution in subsurface water. Therefore, the *RWW* should be applied in small quantities at shorter intervals, if the continuous irrigation is difficult to be applied on large scale in real practice. Hence, in order to mitigate NO_3^- pollution caused by the *RWW* irrigation, the surface drip irrigation system is suggested because even continuous irrigation is possible in such a system, which is classified as a system, which applies water on a part of the surface with low velocities. In this system, small quantities of water is applied near the roots of crops as drops. Moreover, the cultivation under a greenhouse would be more effective because the rainfall experiment suggested that the rainfall can accelerate the leaching of accumulated NO_3^- in soil.

When using *RWW* as the irrigation source, other factors which are normally not concerned in selecting a proper irrigation system, should be considered, such as contamination of plants and harvested products, farm workers or the environment, as well as salinity and toxicity hazards (Lazarova et al., 2005). Lazarova et al. (2005) stated that ideally, *RWW* should be applied closely to the root zone using micro-sprayers or drip emitters. Further, certainly, leaching is essential to prevent salinization of the root zone, but because there can be excess NO_3^- in this zone, leaching will result in the movement of NO_3^- and salts to the groundwater. Also, the same authors insisted that in irrigation, especially with *RWW*, it is important to apply an appropriate, well - controlled quantity of water sufficient to meet the crop requirements and to prevent accumulation of salts in the soil. Excessive flooding can be more harmful as it saturates the soil for a long time, inhibiting aeration, leaching nutrients, including salinization and polluting underground water. The drip irrigation system meets with all the above-mentioned requirements for

RWW irrigation. It is also recommended to apply *RWW* only under dry weather conditions, with regular inspections to avoid ponding of *RWW* or run off water (Lazarova et al., 2005). This statement supports the idea of using a green house.

In accordance with both Asano et al. (2006) and Lazarova et al. (2005), the drip irrigation system also boasts the following advantages over the other systems. It possesses high irrigation efficiency (about 70-90%), high yields and the highest level of health protection such as minimal contact between farm workers and effluent. From the point view of water quality, drip irrigation systems have the advantage to allow using *RWW* with high salinity or high *BOD*, because the entire root zone is not saturated, thus providing good soil aeration. Drip irrigation is most suitable for row crops (vegetables, soft fruits). Nevertheless, drip irrigation is effectively applied for a wide range of crops, low energy requirement, low labor requirement and etc. Among the numerous benefits of this system is the ability to be used with all types of soils and topography without special land preparation and the ability to be adjusted well to the crop irrigation requirements. In this case, storage capacity and soil capability to retain moisture are no longer decisive as well. Moreover, the water quality restrictions for the prevention of emitter clogging meet with the quality of the reclaimed water produced in Okinawa. There are no special protection measures required in the use of this system as well. Besides, the most important management practices recommended to overcome boron toxicity are frequent irrigation and the appropriate choice of micro irrigation. In summary, drip irrigation is best suited to areas where water is scarce, land is steepy, sloping or undulating, water and/or labor are expensive, reclaimed water has high salinity, or production of high – value crops that require frequent water applications (Lazarova et al., 2005).

Nonetheless, Asano et al. (2006) and Lazarova et al. (2005) pointed out the following demerits associated with the drip irrigation system. The salt movement is radial along the direction of water movement, a salt wedge is formed between drip points. Another major constraint is the need for continuous operation, because any short-term interruption can quickly result in plantation damage. Clogging of drip irrigation system is likely to occur. The equipment and the installation demand high costs and maintenance is a must. However, the operational and management costs are moderate. The capital and the operation costs of drip system falls generally somewhere between flood and sprinkler irrigation. Compared to the sprinkler irrigation, which is associated with a number of negative points regarding the health risks and adverse environmental issues, the drip irrigation is cheap. Thus the merits associated with the surface drip irrigation system more

than compensate for its comparatively high cost and very few demerits. In Okinawa, the major irrigation system is sprinkler irrigation according to the planned project. Even so, the drip irrigation is already introduced in the agricultural field. Greenhouse cultivation is very common in Okinawa. Thus, the importance of increasing the use of drip irrigation under greenhouses is highlighted.

6.4 PREDICTION OF NITRATE NITROGEN CONCENTRATION IN GROUNDWATER DUE TO RECLAIMED WASTEWATER IRRIGATION IN OKINAWA

The following section demonstrates how the steady state solutions of the developed models with the estimated apparent rate constants are used to predict the concentration of $NO_3^- - N$ in the groundwater due to the nitrogen contained in the *RWW*. The designed net irrigation rate (*NR*) of the Okinawa-project, which has been designed considering the crop water requirement of each month and the allowable infiltration rate for no run off, is 30 mm/h for 2h every week. It is noted that the rainfall effect has not been considered in determining this value. The irrigation hydraulic loading rate (L_w) is given by:

$$L_w = \frac{NR}{E_i/100} \quad \text{(Asano et al., 2006)} \qquad (6.1)$$

Since E_i of the drip irrigation system is 70-90 %, designed L_w in Okinawa-project is equal to 10.72 mm/d, considering E_i= 80%. The average crop water requirement (ET_c) of each month for the expected types of crops such as sugar cane, vegetables, fruits and flowers in Okinawa is 2.75 mm/d. If *RWW* is applied continuously with no precipitation; quantity of water infiltrates into the soil is 7.97 mm/d. If assumed water percolates downward without any losses at this rate, the Darcy velocity is 7.97 cm/d. The water table of mudstone and limestone should lie above 90 cm and 60 cm depths, respectively (bed rock levels). Therefore, $NO_3^- - N$ concentration was calculated at 90 cm and 60 cm depths in mudstone and limestone, respectively. The input parameters shown by **Table 6.1** were substituted in Eq. 5.17 to compute the steady state $NO_3^- - N$ concentration that may leach into the groundwater due to the continuous drip irrigation of *RWW*, under a greenhouse, on both high and low porous soils in Okinawa. Steady state $NO_3^- - N$ concentration at 60 cm of high porous soil is 19.4 mg/L, while that at 90 cm of low porous soil is 6.8 mg/L.

Therefore, it is evident that the $NO_3^- - N$ concentration that leaches into the groundwater in high porous soil is greater than 10 mg/L, the maximum permissible concentration for drinking purposes. $NO_3^- - N$ concentration in low porous soil may exceed 10 mg/L if the groundwater table is above 60 cm depth.

Table 6.2 Input parameters to obtain steady state NO_3^- -N concentration at the water table in Okinawa

Input parameters	High-porous soil	Low porous soil
x	60 cm	90 cm
D_1 & D_2	1.4 cm^2/d	1.4 cm^2/d
v	0.797 cmd^{-1}/0.375=2.12 cmd^{-1}	0.797 cmd^{-1}/0.34= 2.34 cmd^{-1}
k_1	0.09	0.4
k_2	0.003	0.03
R	3.79	4.88
C_0^1	18 mg/L	18 mg/L
C_0^2	3 mg/L	3 mg/L
ϕ_w	0.375	0.340

The depth of the water table will affect the time delay before the effects of effluent irrigation are seen at the water table. This may also provide the opportunity for further denitriifcation to occur if the soil is wet enough and there is a suitable carbon source (Lazarova et al., 2005). Further, the same authors mentioned that the extent of dilution of salt and NO_3^- when reaching the groundwater will depend on the rate of recharge and the rate of flow of groundwater beneath the irrigation site, which in turn depends on aquifer permeability and hydraulic gradient. The amount of dilution will also depend on the size of the irrigated area. Hence, the above-estimated values are subject to limitations. Even so, the estimated values are quite reasonable to represent shallow groundwater tables with a drip irrigation system under a greenhouse, which may not cause high variations.

6.5 CONCLUSIONS

The results of the experiments and the models verify that denitrification is accelerated in the continuous irrigation compared to the intermittent irrigation. Therefore, the continuous irrigation of *RWW* is preferred to the intermittent irrigation in the standpoint of mitigating the NO_3^- pollution. The continuous irrigation can be applied practically using

the surface drip irrigation system. Hence, it can be concluded that the irrigation of *RWW*, either continuously or at shorter intervals with low rates, using the surface drip irrigation method, under a greenhouse, would mitigate the NO_3^- pollution.

In addition, the steady state $NO_3^- - N$ that may exist in the groundwater in the fields containing high porous limestone in Okinawa would exceed 10 mg/L, the maximum permissible limit of $NO_3^- - N$ for the drinking purposes, even due to the continuous drip irrigation under a green house. It would exceed 10 mg/L in the case of low porous mudstone, if the groundwater table is above 60 cm depth. In order to minimize NO_3^- contamination with groundwater, it is suggested to reduce the Okinawa proposed irrigation rate appropriately or blend *RWW* with other types of water, while adopting the drip irrigation under a greenhouse.

REFERENCES

Asano T., F.L. Burton, H.L. Leverenz, and G. Tchobanoglous (2006), *Water Reuse: Issues, Technologies, and Applications*, McGraw-Hill Professional, New York.

Bohn, H. L., B. L. McNeal, G. A. O'Connor (1985), *Soil chemistry*, John Wiley & Sons, Inc., New York.

Lazarova, V., A. Bahri (2005), *Water Reuse for Irrigation: Agriculture, Landscape, and Turf Grass*, CRC Press, Florida, USA.

DeBusk, W.F., J.R. White, and K.R. Reddy (2001), Carbon and nitrogen dynamics in wetland soils, in *Modeling Carbon and Nitrogen Dynamics for Soil Management*, edited by M.J. Shaffer, Liwang Ma and S. Hansen, pp. 27-53, CRC Press LLC, 2000 N.W., Florida, USA.

CHAPTER 7

CONCLUSIONS AND FURTHER RECOMMENDATIONS

7.1 CONCLUSIONS

Reclaimed wastewater has become an unavoidable water resource with the growing population and increasing urbanization that lead to deficiency of water in many areas of water usage. The reclaimed wastewater is highly demanded for the agricultural irrigation. Okinawa, Japan suffers from water scarcity, especially for the agricultural irrigation. The government authorities have paid their attention on this issue, and have introduced reclaimed wastewater as a potential water source. As a result, reclaimed wastewater will be applied for the agricultural irrigation in Okinawa on large-scale in the next few years, under an already planned project. However, the proposed treatment train of the reclaimed wastewater does not contain an advanced unit process (ex: nitrification/denitrification process) to treat excess nitrogen in the secondary treated wastewater. The absence of the advanced unit process of nitrification and denitrification in the reclamation unit in Okinawa is a direct result the cost-prohibitive treatment cost of RWW. However, the targeted secondary treated wastewater to produce reclaimed wastewater contains ammonium in high concentrations, which is likely to contribute to the nitrate pollution in the subsurface water. Therefore, the primary objective of this dissertation was to analyze belowground dynamics of nitrogenous compounds, qualitatively and quantitatively, in order to evaluate the nitrate pollution due to the reclaimed wastewater irrigation.

This study consists of four major components, namely: a case study, laboratory scale soil column experiments, batch sorption experiments and analytical model development. The latter three studies were conducted each in a unique way. Though, the behavior of nitrogenous compounds in the underground have been simulated using laboratory soil columns in numerous studies to date, there are very few researches, in which laboratory soil column studies are coupled with the reclaimed wastewater irrigation. Much research has focused on modeling nitrogen dynamics in soil, and many of these models incorporate the nitrogen dynamics due to fertilizer. Most of such attempts have been taken by the agriculture-based researches. It is very rare that there is an attempt of modeling nitrogen dynamics in soil due to *RWW* irrigation. Therefore, this research is significant because it is about two aspects which rare attention has been paid on so far.

The initiating step of this dissertation, which is described in **Chapter 2,** was to conduct a case study on the utilization of reclaimed wastewater for irrigation and urban activities in Okinawa. At present, in order to investigate the soil and subsurface water pollution due to reclaimed wastewater irrigation, several experiments are being conducted on field lysimeters. The case study revealed that the assessment of the experiments, so far conducted on these field lysimeters, hold inaccuracies. The nitrogenous compounds have leached into the percolating water of the lysimeters in large quantities so that the characteristics of the percolating water were dominated by leached nitrogen from soil. Therefore, the fate of nitrogenous compounds, which reclaimed wastewater itself contains, was not assessed properly. Therefore, the importance of conducting laboratory soil column experiments were highlighted because such an experiment can be easily managed so that these kinds of barriers are eliminated.

As the second step of this dissertation, the belowground dynamics of nitrogenous compounds were qualitatively analyzed using two laboratory scale unsaturated soil column experiments and batch sorption experiments, on two most abundant soil types in Okinawa, namely low porous mudstone and high porous limestone.

Chapter 3 presents the experiments on low porous soil. The soil column experiment was first conducted by continuous and intermittent irrigation of the two soil columns for 120 days with the simulated reclaimed wastewater. Then, the effects of the concurrent applications of simulated rainwater and the application of simulated reclaimed wastewater intermittently were also studied. The simultaneous occurrence of nitrification, denitrification and adsorption of ammonium on to soil was proved by the results. NH_3-N profiles representing all the pore water and effluent of both continuous and intermittent applications never exceeded 3.5 mg/L though the influent contained 18 mg/L of NH_3-N. In the intermittent application, $NO_3^- - N$ of all the pore water and effluent gradually increased to a peak value in secession. Thereafter, the concentration remained approximately constant. At various depths, it exhibited similar profiles. In the continuous application, $NO_3^- - N$ profile of each pore water & effluent increased to a maximum in succession, preceding a decrease toward the steady state. The peak $NO_3^- - N$ concentrations of the profiles representing the pore water collected from above 55 cm depth were considerably higher than those from below 55 cm depth and the effluent. In addition, $\delta^{15} N$ ‰ (of NO_3^-) in 6 effluent samples increased from 30 to 50, while $NO_3^- - N$ concentration dropped from

the peak at the same time. The cumulative mass of *T-N* that was lost by off-gassing to the soil air of the continuous and intermittent applications were 41.5% and 13.0%, respectively. The results concluded that the lower soil layers of the continuous column promoted denitrification in comparison to that of the intermittent application. Moreover, the results of the variation of $\delta^{15} N$ postulates that the analysis of nitrogen stable isotopes is an effective tool to understand nitrogen dynamics in the soil. According to the steady state profiles of $NO_3^- - N$, the concentration of $NO_3^- - N$ that may transport toward the groundwater is less in the continuous application than that in the intermittent application. In addition, the experiment of the simulated rainwater proved that the leaching of accumulated NO_3^- in soil, into the percolating water would be enhanced with the dilution effect of rainfall. The batch sorption experiments showed that the adsorption of NH_4^+ onto mudstone soil was very quick and leaching of soil-NO_3^- into the supernatant of reclaimed wastewater was negligible.

Chapter 4 presents the experiments on the high porous soil. The soil column experiment was conducted by continuous and intermittent irrigation of two similar-type soil columns for 150 days with the simulated reclaimed wastewater. The soil column experimental set up was exactly similar to the previous case on low porous soil. The application rates of simulated reclaimed wastewater were also exactly the same as that. The simultaneous occurrence of nitrification, denitrification and adsorption of ammonium on to soil was proved by the results. *NH_3-N* profiles representing all the pore water and effluent of both continuous and intermittent applications never exceeded 3.5 mg/L though the influent contained 18 mg/L of *NH_3-N*. The nitrogen dynamics in terms of $NO_3^- - N$ and *T-N* of both the applications were different from those of respective applications on low porous mudstone. In continuous application, the variation of $NO_3^- - N$ of pore water and effluent follows simple profiles, which could be easily described by the convective-dispersive equation. According to the transient and steady state profiles of $NO_3^- - N$, the concentration of $NO_3^- - N$ that may transport toward the groundwater is less in the continuous application than that in the intermittent application. The nitrogen mass balance indicated that the mass of total nitrogen that was lost by off-gassing to the soil air of *CA* and *IA* were 30.0 % and 2.1 %, respectively. The cumulative mass of *TOC*, supplied by the influent that was lost in *CA* and *IA* were 62.9 % and 38.8 %, respectively. This result provides evidence that the dissolved organic carbon in the soil solution may have been

used for denitrification, and the consumption of that in *CA* may have been greater than that of *IA*. The major conclusion of this experiment was that denitrifciation has been accelerated in *CA* when compared to *IA*. The batch sorption experiments showed that the adsorption of ammonium onto limestone soil was very quick and leaching of soil nitrate into the supernatant of reclaimed wastewater was negligible. The ammonium adsorption capacity of low porous mudstone is higher than that of the high porous limestone.

Chapter 5 presents the quantitative analyses of the obtained nitrogen dynamics on two soil types. The dynamics of ammonium and nitrate due to the continuous irrigation on high and low porous soils were simulated using two simple analytical models. The models were developed using the coupled material balance equations for NH_3-N and $NO_3^- - N$ on entire soil volume that incorporate convection, dispersion, adsorption and biological transformation of the solute. The transformation processes incorporate nitrification, denitrification and adsorption of ammonium onto soil as those were the dominating processes in determining the fate of nitrogen in those experiments. In order to preserve the linearity of equations, several assumptions were used to interpret the above processes in the models. First-order rate constants were assumed for nitrification and denitrification. The linear form of Freundlich equation was used to address the sorption process of ammonium. However, the model developed on *CA* of low porous soil was subject to different adsorption phenomena as appropriate. The calibration parameters of the models were apparent rate constants of nitrification and denitriifcation. In this study, a unique approach was followed in order to estimate the apparent rate constants. That is to optimize the rate constants using a huge database of simulated $NO_3^- - N$, with the aid of a computer program and statistics. The models simulate the respective measured values quite well and consistently throughout the column. In particular, the shapes of the profiles are represented with the models. The calibration data of the models indicate that the nitrification and denitrification both had a significant effect on the nitrate dynamics of these soil column experiments. In the continuous application of high porous soil, the nitrification and denitrification rate constants derived using the measured data of the effluent samples, which represent the global averages, were 0.09 d^{-1} and 0.003 d^{-1}. The model on the continuous application of low porous soil was calibrated in terms of the nitrification rate constants both on soil and solution, and denitrification rate constants. The nitrification rate constant on soil and solution and denitrification rate constants derived using the measured data of the effluent samples, which represent the global averages, were 1.0 d^{-1}, 0.4 d^{-1} and

0.03 d^{-1}. With the global averages of the rate constants, the models can be used to make reasonable predictions of nitrate leaching to the groundwater. They can also be good enough to predict the nitrate concentration due to a continuous irrigation in a porous soil. Therefore, the models can be used as a means of testing strategies and assessing risks. These models represent a simplified version for the heterogeneity of the unsaturated porous media in the column. In addition, these models are oriented toward a simple simulation using physico-chemical aspects rather than microbial processes. If microbial dynamics were taken into account, the models would be non-linear, and would unable to be solved analytically. In addition, the models would also require more input parameters. The other significance of these models was that the adsorption of NH_4^+ is addressed using the linear form of Freundlich equation, which is very rare case for this kind of simple analytical modeling approach.

Chapter 6 presents a discussion of precautionary measures for nitrate pollution in Okinawa based on the above-mentioned results. The above results indicate that the velocity of the flow has a significant influence on the NO_3^- pollution in subsurface water. The continuous irrigation of reclaimed wastewater is preferred to the intermittent irrigation in the standpoint of mitigating the nitrate pollution. The reclaimed wastewater should be applied in small quantities at shorter intervals, if the continuous irrigation is difficult to be applied on large scale in real practice. Hence, in order to mitigate NO_3^- pollution caused by the reclaimed water irrigation, the surface drip irrigation system is suggested because even continuous irrigation is possible in such a system. Moreover, the continuous drip irrigation under a greenhouse would be more effective because rainfall can accelerate the leaching of accumulated NO_3^- in soil. The steady state solutions of the developed models with the estimated apparent rate constants were used to predict the concentration of $NO_3^- - N$ in the groundwater due to the continuous drip irrigation of *RWW* under a green house. $NO_3^- - N$ concentration that may exist in the groundwater in the fields containing high porous limestone in Okinawa would exceed 10 mg/L, the maximum permissible limit of $NO_3^- - N$ for the drinking purposes. It would exceed 10 mg/L in the case of low porous mudstone, if the groundwater table is above 60 cm depth. Though, the above predictions are subject to certain limitations, they are reasonable for shallow depths with a system like drip irrigation with no effect of rainfall, which do not undergo much variations. In order to minimize NO_3^- contamination with groundwater, it is suggested to reduce the Okinawa

proposed irrigation rate appropriately or blend *RWW* with other types of water, while adopting the drip irrigation under a greenhouse.

7.2 FURTHER RECOMMENDATIONS

In order to improve the laboratory soil column experiments, the following analyses are suggested: the soil atmosphere measurement in terms of N_2O, N_2, O_2 and CO_2 to make sure the existence of denitrification; the in-situ measurement of the oxidation reduction potential of percolating water to understand the potential of redox reactions that involve nitrogenous compounds; and the variation of dissolved oxygen concentration in pore water. According to Donn et al. (2005), this kind of system may be influenced by the presence of macro flow and inconsistencies in the hydrological conditions and number of other parameters not investigated yet. Hence, in order to understand the interrelation of the mechanisms properly, a model that incorporates the synchronization of all these mechanisms would be essential. The developed models can be modified incorporating numerical techniques to address the non-linear processes more accurately than the analytical solutions.

The use of reclaimed wastewater has the potential for both positive and negative environmental consequences as well as human health risks. The issues of the contaminants, other than nutrients, are potential candidates to focus on as a continuation of the present study in a broader perspective. Pathogenic issues are a major threat to the sustainability of water resources. From a health perspective, pathogens in the reclaimed wastewater are generally considered to be the most important risk issue. This may effect adversely on fieldworkers and the environment. In addition, the contamination due to micro pollutants has so far been less focused on. In fact, specific attention on the presence of micro pollutants in reclaimed wastewater are rare or none. In the reclaimed wastewater, large varieties of toxic micro pollutants may be present. Emerging *PPCPs*, *PCBs*, *EDCs* are suspected to remain in the reclaimed wastewater. Lazarova et al. (2005) indicated the effects of disinfection by-products and *PPCPs* on groundwater via the reclaimed wastewater irrigation. *NDMA*, too, is an emerging contaminant, which has been first detected during an investigation of groundwater contamination, and has also been reported as a new disinfection by-product. Although, *NDMA* is listed as a priority pollutant, the maximum contaminant level has not yet been established. Many are difficult to be detected due to the lack of analytical techniques. Therefore, risks associated with these

contaminants should be extensively assessed in order to develop economically feasible precautionary strategies. In extending the present study, addressing the issues of aforesaid micro pollutants and pathogens in reclaimed wastewater is imperative as they are key concerns to both developed and developing countries, and directly affects the human health.

Findings of the present study postulate some valuable insights that the pollution due to nitrate can be mitigated by altering the existing irrigation scenarios. Therefore, it is expected that the issues of pathogens and micro pollutants can also be solved to greater extent by simple precautionary measures. With proper treatment techniques and careful planning and management, the use of reclaimed wastewater can be beneficial to the environment. If caution is exercised in the irrigation scenarios as suggested by the findings of the present study, the risks can be reduced to greater extent. In particular, proper management is preferred to the treatment techniques in the view point of developing countries.

Hence, the following aspects are recommended as the further expansion of this study:

- Estimation of the concentration levels of pathogens and the afore-mentioned contaminants in the reclaimed wastewater at different treatment levels.
- Investigation of the alternative methods for the analyses of *PPCPs*, *NDMA*, *PCBs*, and *EDCs* in the reclaimed wastewater.
- Investigation of the fate and transport of the above contaminants through soil.
- Removal and destruction of *NDMA* and *PPCPs* together with respective precursors, during the wastewater treatment using membrane filtration, ozonation or *A/O* processes.
- Investigation of the ways of achieving allowable risks in wastewater reclamation and reuse by altering the treatment techniques, and application scenarios of reclaimed wastewater for many reuse-goals.

REFERENCES

Donn, M. J., and N. W. Menzies (2005), Simulated rainwater effects on anion exchange capacity and nitrate retention in ferrosols, *Australian Journal of Soil Research, 43*, 33-42.

Lazarova, V., and A. Bahri (2005), *Water Reuse for Irrigation: Agriculture, Landscape, and Turf Grass*, CRC Press, Florida, USA.

APPENDIX A

GRAPHS ON SOIL COLUMN EXPERIMENTS AND BATCH SORPTION EXPERIMENTS

Soil column Experiment on Low Porous Soil (Mudstone)

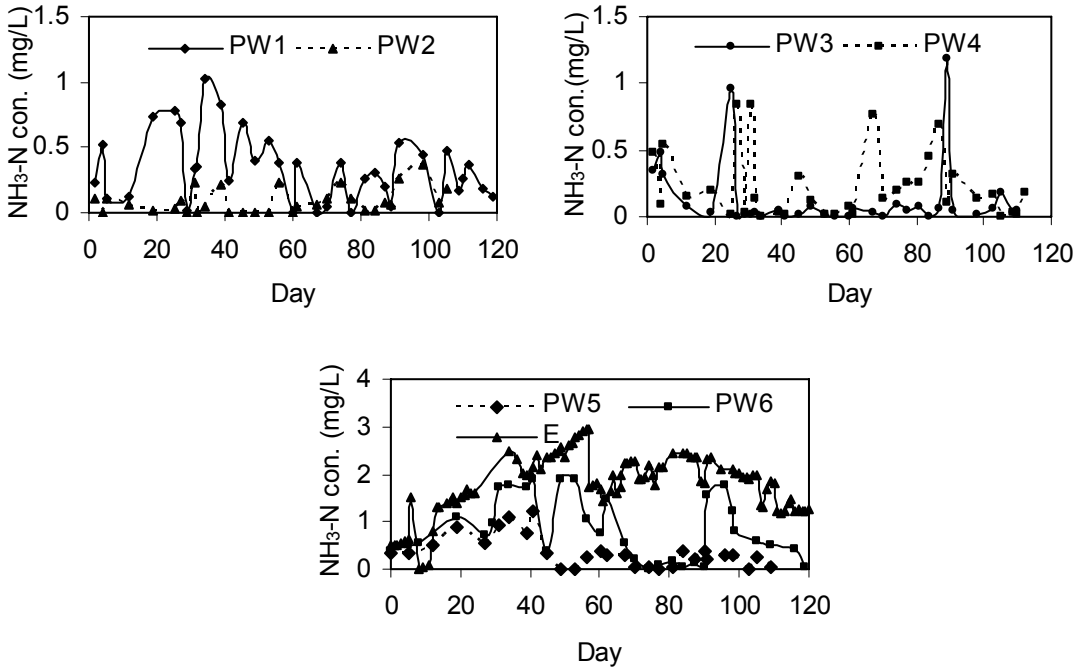

Fig. A-1 Variation of NH_3-N concentration of PWs and E due to CA (low porous soil).

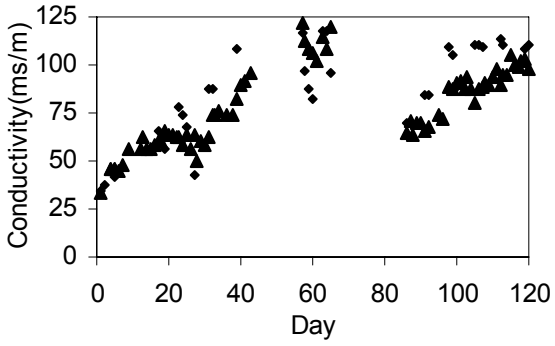

Fig. A-2 Variation of conductivity of E due to CA & IA (low porous soil).

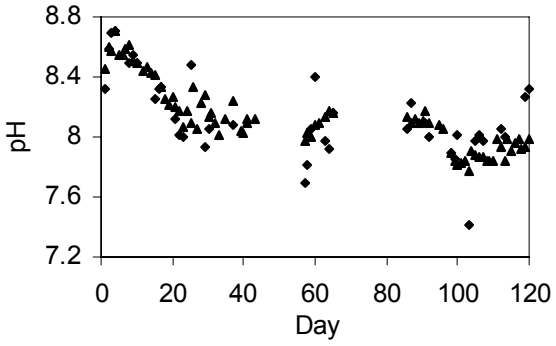

Fig. A-3 Variation of pH of E due to CA & IA (low porous soil).

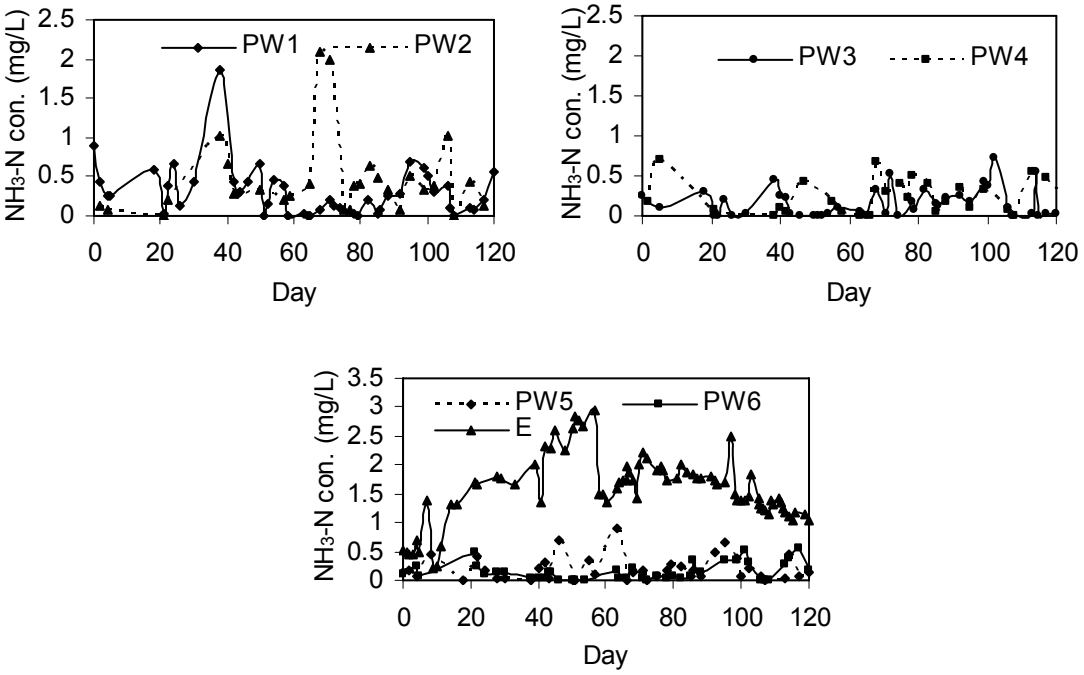

Fig. A-4 Variation of NH_3-N concentration of PWs and E due to IA (low porous soil).

Soil column Experiment on High Porous Soil (Limestone)

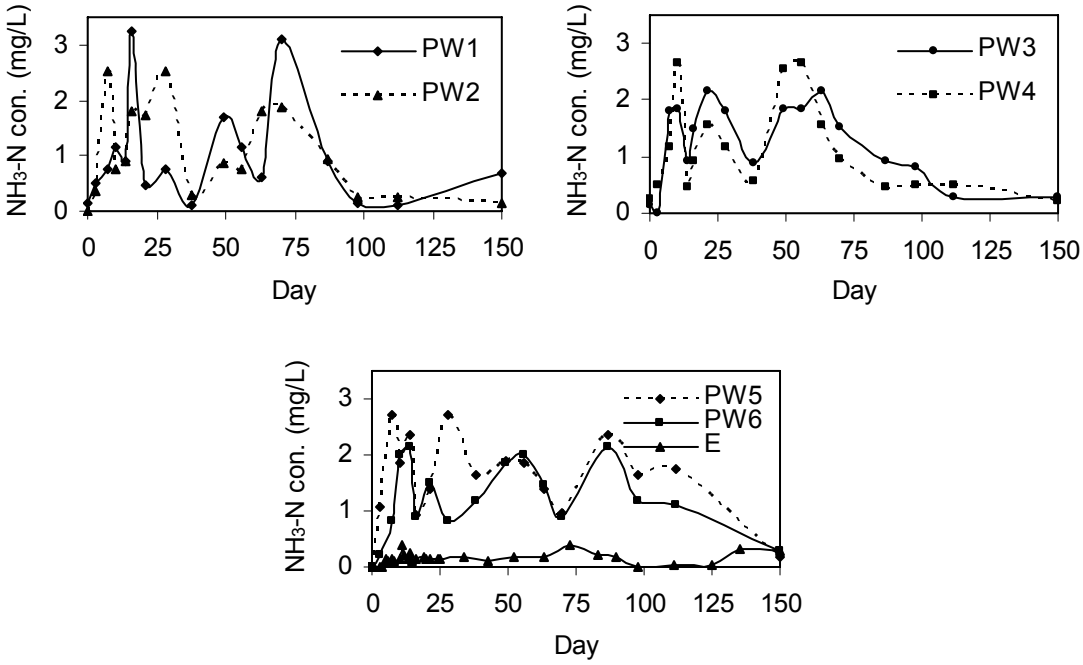

Fig. A-5 Variation of NH_3-N concentration of PWs and E due to CA (high porous soil).

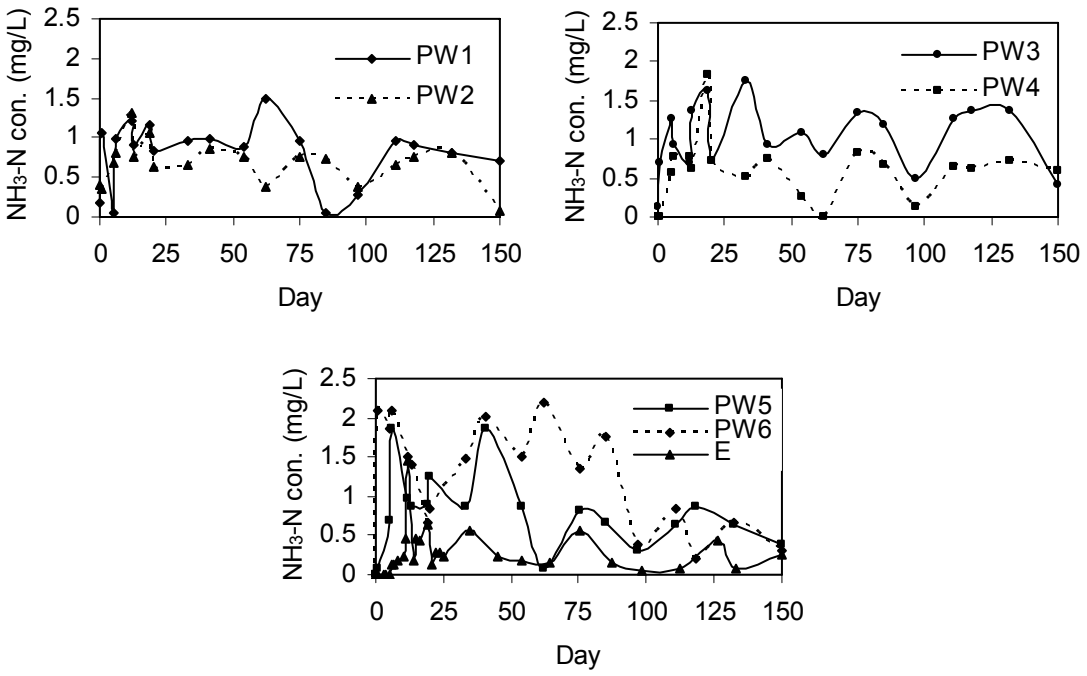

Fig. A-6 Variation of NH_3-N concentration of PWs and E due to IA (high porous soil).

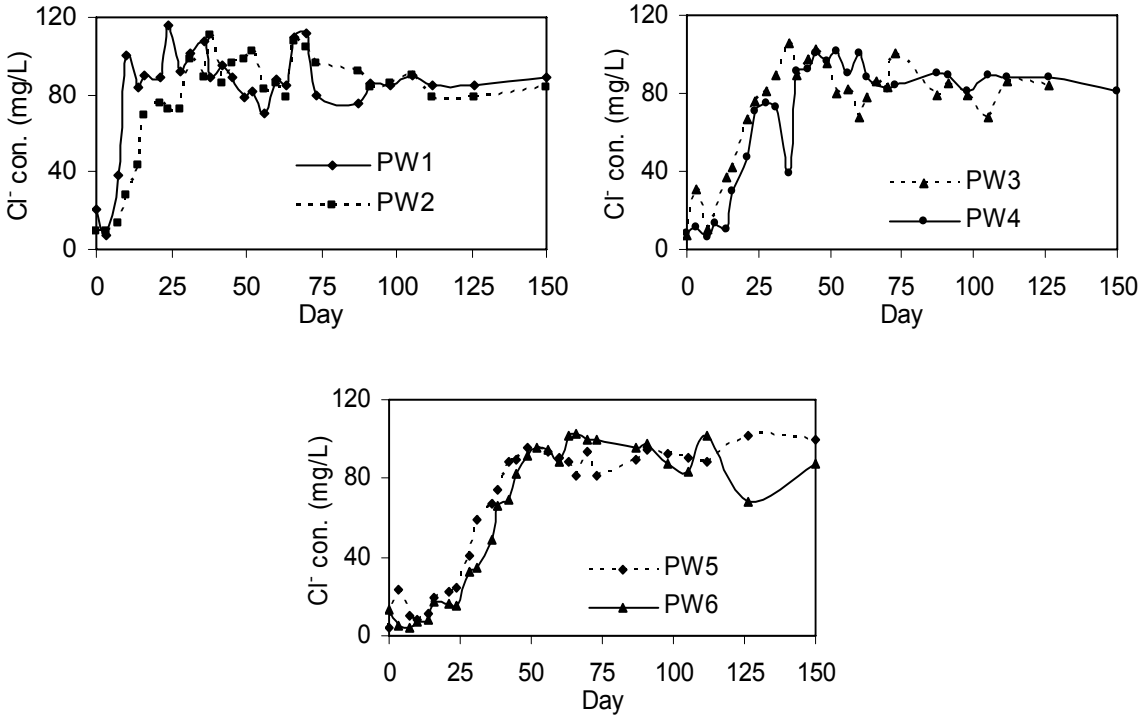

Fig. A-7 Variation of Cl^- concentration in PWs due to CA (high porous soil).

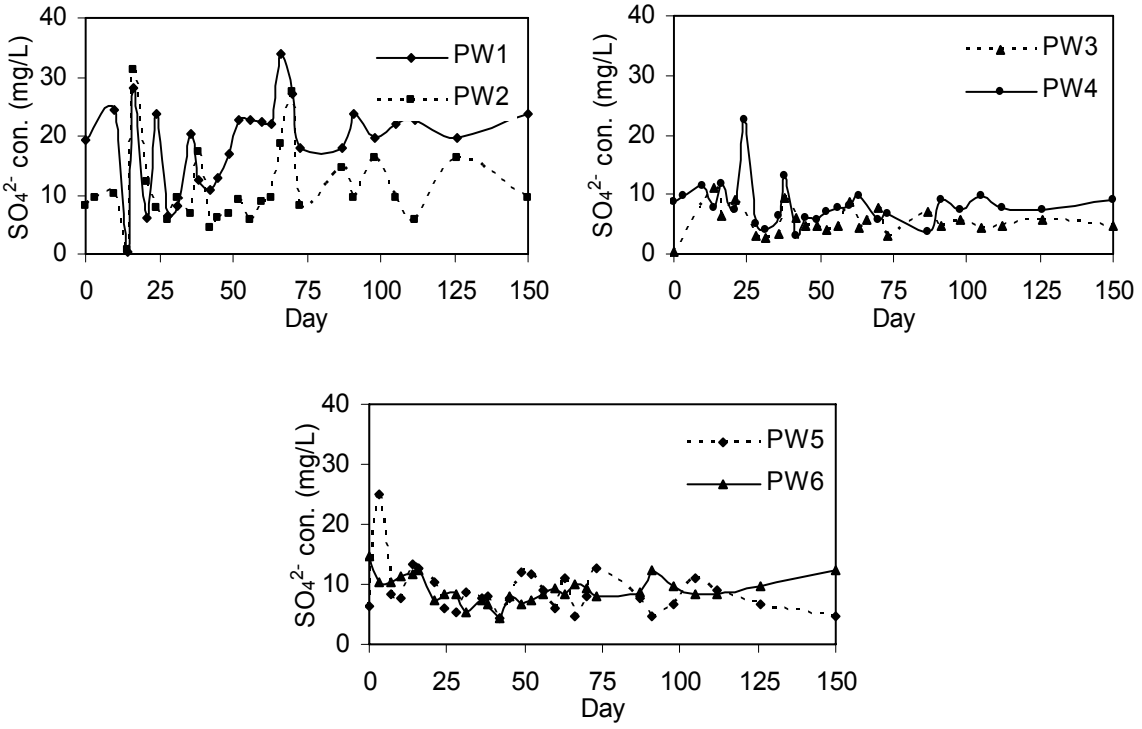

Fig. A-8 Variation of SO_4^{2-} concentration in PWs due to CA (high porous soil).

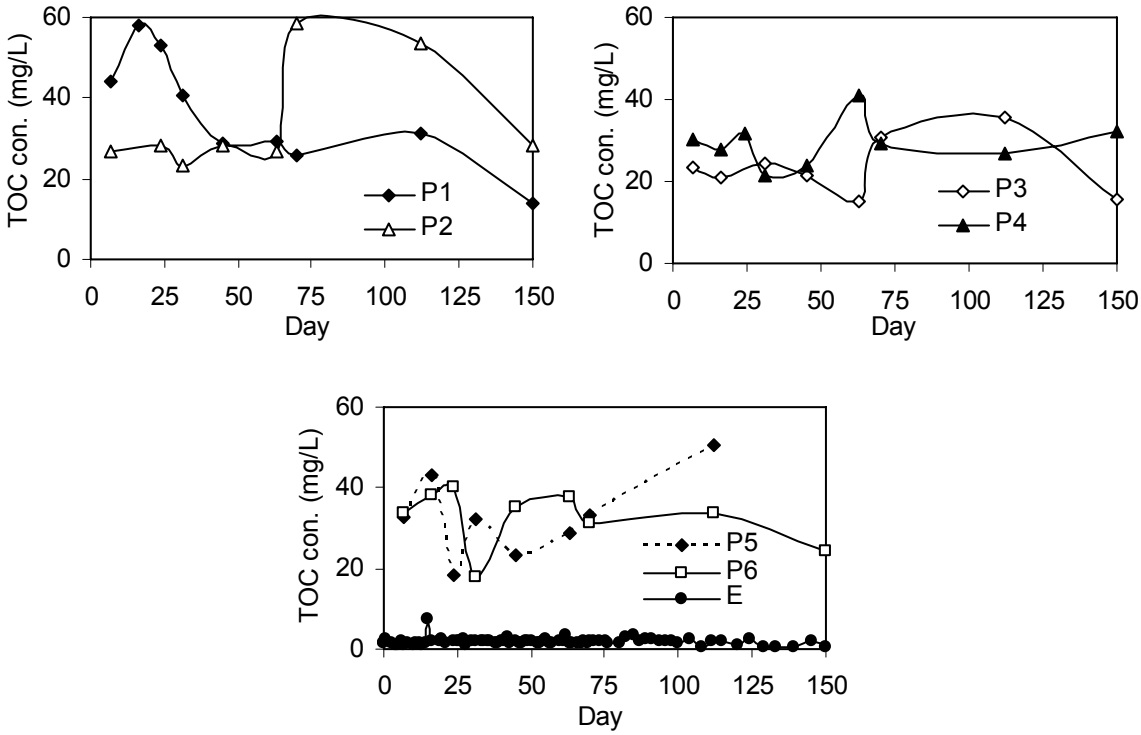

Fig. A-9 Variation of TOC concentration in PWs and E due to CA (high porous soil).

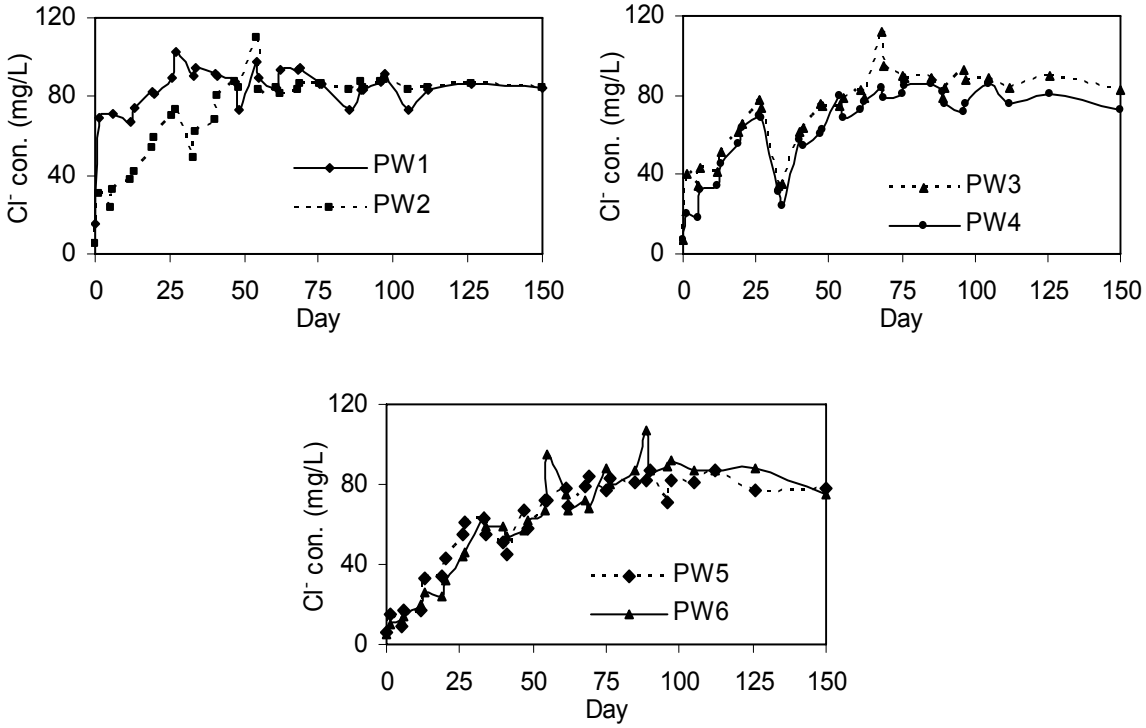

Fig. A-10 Variation of Cl^- concentration in PWs due to IA (high porous soil).

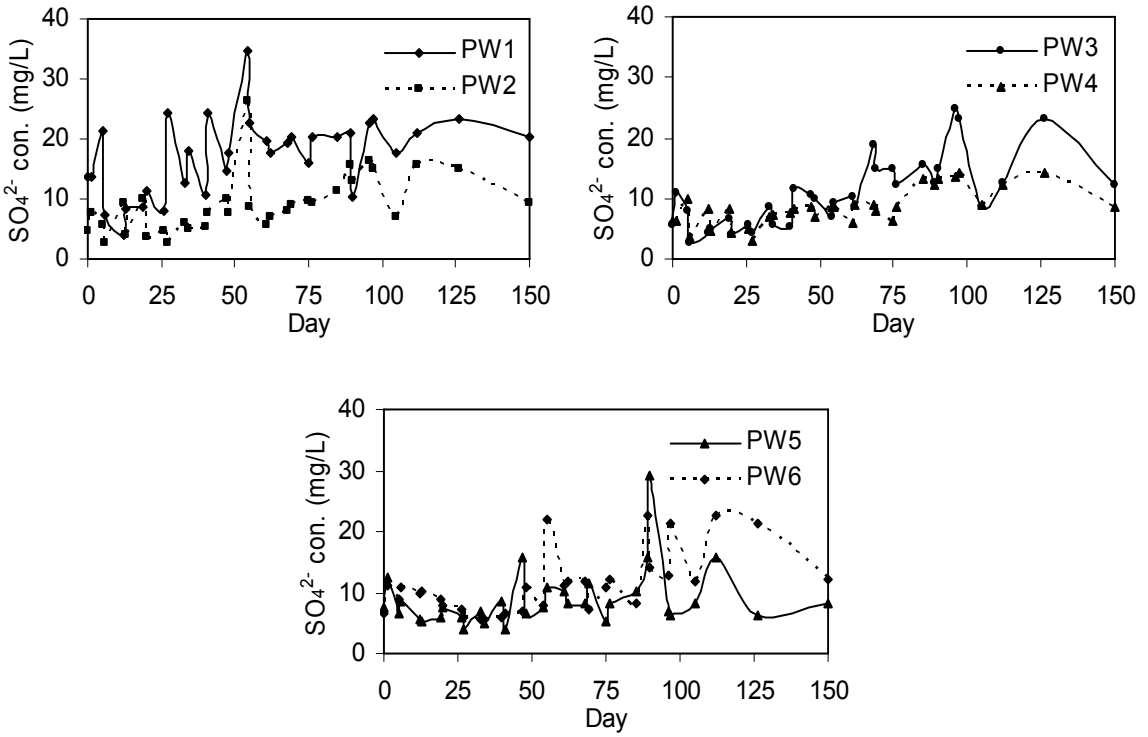

Fig. A-11 Variation of SO_4^{2-} concentration in PWs due to IA (high porous soil).

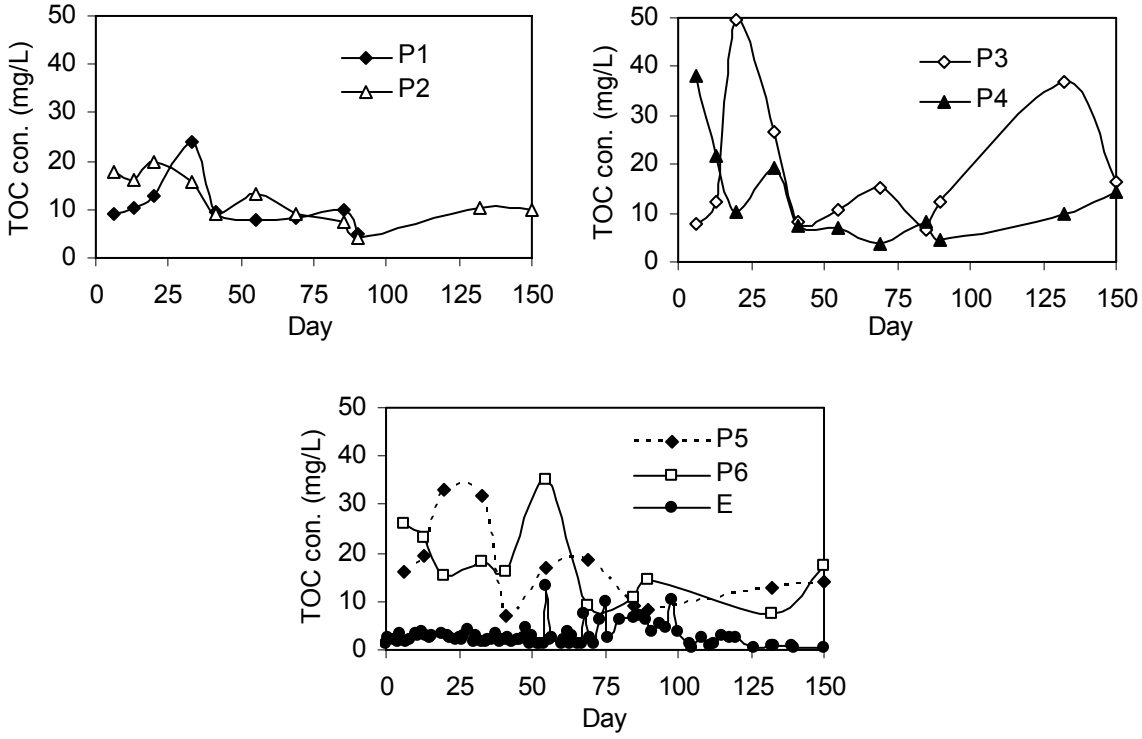

Fig. A-12 Variation of TOC concentration in PWs and E due to IA (high porous soil).

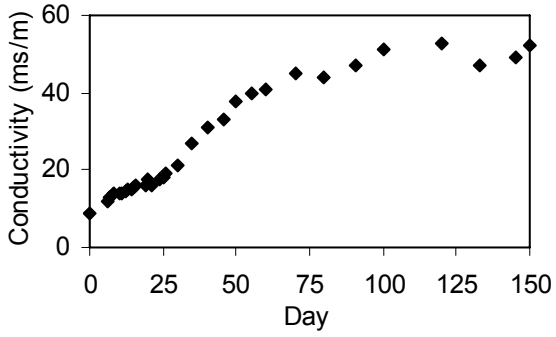

Fig. A-13 Variation of conductivity due to CA in high porous soil.

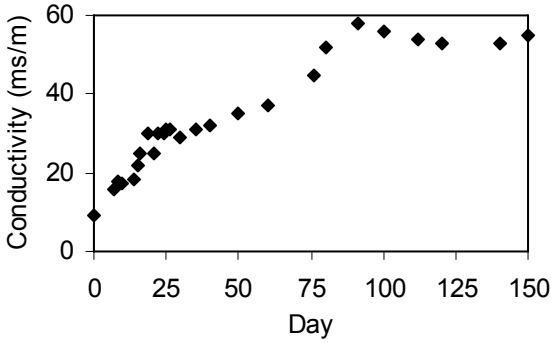

Fig. A-14 Variation of conductivity due to IA in high porous soil.

APPENDIX B

PHYSICAL CHARACTERISTICS OF SOIL

Physical Characteristics Before and After Loading of *SRW*

Table B-1 Physical characteristics of high porous soil due to CA.

Parameter	Before loading SRW (after cleansing)	After loading SRW
Total weight of soil column (kg)	46.4	45.475
Empty column (kg)	9.15	9.15
Oven dry weight of soil (kg)	26.78	26.78
Weight of water (kg)	10.47	9.545
Volume of soil (L)	10.1	10.1
Volume of water (L)	10.47	9.545
Volume of voids (L)	6.13	7.055
ϕ	0.62	0.62
Air-filled porosity	0.23	0.26
ϕ_w	0.39	0.36
ρ_b (g/cm^3)	1.395	1.360

Table B-2 Physical characteristics of low porous soil due to CA.

Parameter	Before loading SRW (After cleansing)
Oven dry weight of soil (kg)	30.887
Weight of water (kg)	9.17
Volume of soil (L)	11.66
Volume of water (L)	9.17
Volume of voids (L)	5.87
ϕ	0.56
Air-filled porosity	0.22
ϕ_w	0.34
ρ_b (g/cm^3)	1.5

Table B-3 Physical characteristics of high porous soil due to IA.

Parameter	Before loading SRW (After cleansing)	After loading SRW
Total weight of soil column (kg)	46.4	45.375
Empty column (kg)	9.4	9.4
Oven dry weight of soil (kg)	26.78	26.78
Weight of water (kg)	10.22	9.195
Volume of soil (L)	10.1	10.1
Volume of water (L)	10.22	9.195
Volume of voids (L)	6.38	7.405
ϕ	0.62	0.62
Air-filled porosity	0.24	0.28
ϕ_w	0.38	0.34
ρ_b (g/cm^3)	1.386	1.347

Table B-4 Physical characteristics of low porous soil due to IA.

Parameter	Before loading SRW (After cleansing)
Oven dry weight of soil (kg)	30.887
Weight of water (kg)	9.17
Volume of soil (L)	11.66
Volume of water (L)	9.17
Volume of voids (L)	5.87
ϕ	0.56
Air-filled porosity	0.22
ϕ_w	0.34
ρ_b (g/cm^3)	1.5

Equations Used for Calculation of the Physical Characteristics of Soil

$$\phi = \frac{V_w + V_v}{V_t} \qquad \text{(B-1)}$$

$$\phi_w = \frac{V_w}{V_t} \qquad \text{(B-2)}$$

$$\rho_b = \frac{m_s + m_w}{V_t} \qquad \text{(B-3)}$$

$$V_s = \frac{m_s}{2.65} \qquad \text{(B-4)}$$

Calculation of Interstitial Pore Water Velocity (v)

Continuous Irrigation

High porous soil

Average effluent rate = 9.98 mL/h

$$v = {9.98 \times 4} \Big/ {\left(\pi \times 20^2 \times 0.375\right)} = 0.085 cm/h = 2.033 cm/d$$

Low porous soil

Average effluent rate = 9.065 mL/h

$$v = {9.065 \times 4} \Big/ {\left(\pi \times 20^2 \times 0.34\right)} = 0.085 cm/h = 2.037 cm/d$$

APPENDIX C

SOLUTION PROCEDURE OF MODEL EQUATIONS

Derivation of the One-Dimensional General Material Balance Equation for a System Containing only Fluid

The material balance equation for a control volume of $\Delta x \times \Delta y \times \Delta z$ is written as (Nazaroff et al., 2001):

$$C_i(x,t+\Delta t)A_c\Delta x - C_i(x,t)A_c\Delta x = J_x(x,t)A_c\Delta t - J_x(x+\Delta x,t)A_c\Delta t + r_i A_c \Delta x \Delta t$$

$$\frac{[C_i(x,t+\Delta t)-C_i(x,t)]}{\Delta t} = \frac{[J_x(x,t)-J_x(x+\Delta x,t)]}{\Delta x} + r_i$$

when $\Delta x \to 0$ and $\Delta t \to 0$, the general material balance equation for a one-dimensional system:

$$\frac{\partial C_i}{\partial t} + \frac{\partial J_x}{\partial x} - r_i = 0 \qquad \text{(C-1)}$$

where $\frac{\partial C_i}{\partial t} =$ accumulation term; change in species concentration with time; $\frac{\partial J_x}{\partial x} =$ net effect of transport.

Derivation of the Material Balance Equation for an Unsaturated Porous Media

Contaminant flux in the direction of flow can be given as:

$$J_x = UC - \varepsilon_h \frac{\partial C_i}{\partial x} \qquad \text{(C-2)}$$

where $U=Q/A_c$

Therefore, Eq. (C-1) for a saturated flow in porous media can be written as:

$$\frac{\partial C_i}{\partial t} + \frac{(1-\phi)\rho_b}{\phi}\frac{\partial q_i}{\partial t} + \frac{U}{\phi}\frac{\partial C_i}{\partial x} - \varepsilon_h \frac{\partial^2 C_i}{\partial x^2} - r_i = 0 \qquad \text{(C-3)}$$

Eq. (C-3) can be approximately converted to the following equation to describe an unsaturated flow in a porous media based on the assumptions described in the text.

$$\frac{\partial C_i}{\partial t} + \frac{(1-\phi)\rho_b}{\phi_w}\frac{\partial q_i}{\partial t} + v\frac{\partial C_i}{\partial x} - \varepsilon_h \frac{\partial^2 C_i}{\partial x^2} - r_i = 0 \qquad \text{(5.1)}$$

where $v = U/\phi_w$

Incorporation of linear Freundlich isotherm for sorption

$$q_i = K_d C_i \tag{5.2}$$

$\frac{\partial q_i}{\partial t} = \frac{\partial q_i}{\partial C_i}\frac{\partial C_i}{\partial t}$ and therefore, $\frac{\partial q_i}{\partial C_i} = K_d$

Therefore, Eq. (5.1) is written as: $R\frac{\partial C_i}{\partial t} + v\frac{\partial C_i}{\partial x} - \varepsilon_h \frac{\partial^2 C_i}{\partial x^2} - r_i = 0$ (5.3)

where $R = \left\{1 + (1-\phi)K_d \frac{\rho_b}{\phi_w}\right\}$ (5.4)

Continuous Irrigation- High Porous Soil

Solution of the governing equation for *NH_3-N* (Transient state)

$$R\frac{\partial C_1}{\partial t} + v\frac{\partial C_1}{\partial x} - D_1\frac{\partial^2 C_1}{\partial x^2} + Rk_1 C_1 = 0 \tag{5.7}$$

Since, we are interested only in *t>0*, the use of Laplace transform is suggested. Taking the Laplace transformation, Eq. (5.7) becomes:

$$\int_0^\infty R\frac{\partial C_1}{\partial t}\exp(-st)dt + \int_0^\infty v\frac{\partial C_1}{\partial x}\exp(-st)dt - \int_0^\infty D_1\frac{\partial^2 C_1}{\partial x^2}\exp(-st)dt + \int_0^\infty Rk_1 C_1\exp(-st)dt = 0$$

When differentiation is with respect to 'x' and the integration is with respect to't', the derivative can be taken outside the integral. Then;

$s\overline{C}_1(x,s) - C_1(x,0) + \frac{v}{R}\frac{\partial \overline{C}_1}{\partial x} - \frac{D_1}{R}\frac{\partial^2 \overline{C}_1}{\partial x^2} + k_1\overline{C}_1(x,s) = 0$ where the Laplace transform of $C_1(x, t)$ is given by $\overline{C}_1(x,s)$.

According to the boundary conditions (c); $C_1(x, 0) = 0$. Then;

$$\frac{\partial^2 \overline{C}_1}{\partial x^2} - \frac{v}{D_1}\frac{\partial \overline{C}_1}{\partial x} - \frac{R}{D_1}(s + k_1)\overline{C}_1 = 0 \tag{C-4}$$

This is a linear homogeneous ordinary differential equation (*ODE*). So, $\overline{C}_1(x) = \overline{C}_{1c}(x)$

Complementary function:

$\overline{C}_{1c}(x) = \mu e^{\lambda x}$; $\frac{d\overline{C}_{1c}(x)}{dx} = \mu\lambda e^{\lambda x}$; $\frac{d^2\overline{C}_{1c}(x)}{dx^2} = \mu\lambda^2 e^{\lambda x}$

Substituting in (C-4):

$\mu\lambda^2 e^{\lambda x} - \frac{v}{D_1}\mu\lambda e^{\lambda x} - \frac{R(k_1+s)\mu e^{\lambda x}}{D_1} = 0$ and dividing by $\mu e^{\lambda x}$: $\lambda^2 - \frac{v}{D_1}\lambda - \frac{R(k_1+s)}{D_1} = 0$

Therefore; $\lambda = \frac{v \pm \sqrt{v^2 + 4R(k_1+s)D_1}}{2D_1}$

$$\overline{C_1} = A_1 \exp\left(\frac{x}{2D_1}\left(v + \sqrt{v^2 + 4R(k_1+s)D_1}\right)\right) + A_2 \exp\left(\frac{x}{2D_1}\left(v - \sqrt{v^2 + 4R(k_1+s)D_1}\right)\right)$$

According to the boundary conditions (d),

$C_1(x,t) \to 0$ *as* $x \to \infty$*; so* $\overline{C_1}(\infty,s) = 0 \quad \therefore A_1 = 0$

$$\overline{C_1} = A_2 \exp\left(\frac{x}{2D_1}\left(v - \sqrt{v^2 + 4R(k_1+s)D_1}\right)\right)$$

From the boundary conditions (1), $C_1\,(0,\,t) = C_1^0$; $\therefore \overline{C_1}(0,s) = \int_0^\infty C_1^0 \exp(-st)dt = \frac{C_1^0}{s}$

Then $\overline{C_1}(x,s) = \frac{C_1^0}{s}\exp\left(\frac{x}{2D_1}\left(v - \sqrt{v^2 + 4R(k_1+s)D_1}\right)\right)$ (C-5)

$$z_1 = \left(\frac{1}{2D_1}\left(v - \sqrt{v^2 + 4R(k_1+s)D_1}\right)\right)$$

$$\exp(z_1 x) = \exp\left(\frac{xv}{2D_1}\right)\exp\left(-\frac{x}{2D_1}\sqrt{v^2 + 4D_1R(k_1+s)}\right)$$

$$\exp(z_1 x) = \exp\left(\frac{xv}{2D_1}\right)\exp\left(-x\sqrt{\frac{R}{D_1}}\sqrt{\left(\frac{v^2}{4D_1R} + k_1\right) + s}\right)$$

The inverse of $\exp(z_1 x)$ is:

$$L^{-1}(\exp(z_1 x)) = \exp\left(\frac{xv}{2D_1}\right)x\left(\frac{R}{4\pi D_1 t^3}\right)^{1/2}\exp\left[-\left(\frac{v^2}{4D_1R} + k_1\right)t - \frac{x^2R}{4D_1 t}\right]$$

In order to obtain the inverse of Eq. (B-5), a convolution theorem is applied. Thus,

$f(t) = \exp\left(\frac{xv}{2D_1}\right)x\left(\frac{R}{4\pi D_1 t^3}\right)^{1/2}\exp\left[-\left(\frac{v^2}{4D_1R} + k_1\right)t - \frac{x^2R}{4D_1 t}\right]$ and $g(t) = 1$ since

$L^{-1}\left(\frac{1}{s}\right) = 1$

By applying the convolution theorem:

$$L^{-1}\left[\frac{1}{s}\exp\left(\frac{x}{2D_1}\left(v-\sqrt{v^2+4R(k_1+s)D_1}\right)\right)\right]=\int_0^t \exp\left(\frac{xv}{2D_1}\right)x\left(\frac{R}{4\pi D_1\tau^3}\right)^{1/2}\exp\left[-\left(\frac{v^2}{4D_1R}+k_1\right)\tau-\frac{x^2R}{4D_1\tau}\right]d\tau$$

where $f(\tau)=\exp\left(\frac{xv}{2D_1}\right)x\left(\frac{R}{4\pi D_1\tau^3}\right)^{1/2}\exp\left[-\left(\frac{v^2}{4D_1R}+k_1\right)\tau-\frac{x^2R}{4D_1\tau}\right]$

$$C_1(x,t)=C_1^0\exp\left(\frac{xv}{2D_1}\right)\int_0^t x\left(\frac{R}{4\pi D_1\tau^3}\right)^{1/2}\exp\left[-\left(\frac{v^2}{4D_1R}+k_1\right)\tau-\frac{x^2R}{4D_1\tau}\right]d\tau \qquad \text{(C-6)}$$

Eq. (B-6) can be rearranged as:

$$C_1(x,t)=C_1^0\exp\left(\frac{xv}{2D_1}\right)x\left(\frac{R}{4\pi D_1}\right)^{1/2}\int_0^t\exp\left[-\left(\frac{v^2}{4D_1R}+k_1\right)\tau-\frac{x^2R}{4D_1\tau}\right]\frac{d\tau}{\tau^{3/2}}$$

$$C_1(x,t)=\exp\left(\frac{xv}{2D_1}\right)2x\left(\frac{R}{4\pi D_1}\right)^{1/2}\int_0^{t^{-1/2}}\exp\left[-\frac{x^2Ru^2}{4D_1}-\left(\frac{v^2}{4D_1R}+k_1\right)\frac{1}{u^2}\right]du \qquad \text{(C-7)}$$

where $u=\tau^{-1/2}$; $du=-0.5\tau^{(-3/2)}d\tau$; $u^{-2}=\tau$

To carry out the integral of Eq. (C-7); Eq. (C-8) (Abramowitz and Stegun, 1972) is used.

$$\int\exp\left(-a^2x^2-b^2/x^2\right)dx=\frac{\sqrt{\pi}}{4a}\left\{\exp(2ab)erf(ax+b/x)+\exp(-2ab)erf(ax-b/x)\right\} \qquad \text{(C-8)}$$

Considering $a^2=\frac{Rx^2}{4D_1}$; $b^2=\left(\frac{v^2}{4D_1R}+k_1\right)$;

$$C_1(x,t)=\exp\left(\frac{xv}{2D_1}\right)2x\left(\frac{R}{4\pi D_1}\right)^{1/2}\frac{\sqrt{(4D_1\pi)}}{4\sqrt{R}x}\left[\begin{array}{l}\exp\left(\frac{x}{2D_1}\sqrt{\left(v^2+4D_1Rk_1\right)}\right)\\ erfc\left(\frac{\sqrt{R}xu}{2\sqrt{(D_1)}}+\frac{\sqrt{\left(v^2+4k_1RD_1\right)}}{2\sqrt{D_1Ru}}\right)\\ +\exp\left(-\frac{x}{2D_1}\sqrt{\left(v^2+4D_1Rk_1\right)}\right)\\ erfc\left(\frac{\sqrt{R}xu}{2\sqrt{D_1}}-\frac{\sqrt{\left(v^2+4k_1RD_1\right)}}{2\sqrt{D_1Ru}}\right)\end{array}\right]_0^{t^{-1/2}}$$

$$C_1(x,t)=\frac{1}{2}\exp\left(\frac{xv}{2D_1}\right)\left[\begin{array}{l}\exp\left(\frac{x}{2D_1}\sqrt{\left(v^2+4D_1Rk_1\right)}\right)erfc\left(\frac{\sqrt{R}x}{2\sqrt{D_1t}}+\frac{\sqrt{t}\sqrt{\left(v^2+4k_1RD_1\right)}}{2\sqrt{D_1R}}\right)\\+\exp\left(-\frac{x}{2D_1}\sqrt{\left(v^2+4D_1Rk_1\right)}\right)erfc\left(\frac{\sqrt{R}x}{2\sqrt{D_1t}}-\frac{\sqrt{t}\sqrt{\left(v^2+4k_1RD_1\right)}}{2\sqrt{D_1R}}\right)\end{array}\right]$$

$$C_1(x,t)=\frac{C_0^1}{2}\left[\begin{array}{l}\exp\left\{\frac{x}{2D_1}\left(v-\sqrt{\left(v^2+4D_1k_1R\right)}\right)\right\}erfc\left(\frac{x-t\sqrt{\left(v^2+4D_1k_1R\right)}/R}{\sqrt{\left(4D_1t/R\right)}}\right)+\\\exp\left\{\frac{x}{2D_1}\left(v+\sqrt{\left(v^2+4D_1k_1R\right)}\right)\right\}erfc\left(\frac{x+t\sqrt{\left(v^2+4D_1k_1R\right)}/R}{\sqrt{\left(4D_1t/R\right)}}\right)\end{array}\right]$$

Therefore, $C_1(x,t)=C_0^1F(x,t)$ (5.9)

where $F(x,t)=\frac{1}{2}\left[\begin{array}{l}\exp\left\{\frac{x}{2D}\left(v-\sqrt{\left(v^2+4Dk_1R\right)}\right)\right\}erfc\left(\frac{x-t\sqrt{\left(v^2+4Dk_1R\right)}/R}{\sqrt{\left(4Dt/R\right)}}\right)+\\\exp\left\{\frac{x}{2D}\left(v+\sqrt{\left(v^2+4Dk_1R\right)}\right)\right\}erfc\left(\frac{x+t\sqrt{\left(v^2+4Dk_1R\right)}/R}{\sqrt{\left(4Dt/R\right)}}\right)\end{array}\right]$ (5.11)

D_1 was replaced with D.

Solution of the governing equation for NO_3^--N (Transient state)

$$\frac{\partial C_2}{\partial t}+v\frac{\partial C_2}{\partial x}-D_2\frac{\partial^2C_2}{\partial x^2}-Rk_1C_1+k_2C_2=0 \quad (5.8)$$

The Laplace transformation of Eq. (5.8) can be written as:

$$\int_0^\infty\frac{\partial C_2}{\partial t}\exp(-st)dt+\int_0^\infty v\frac{\partial C_2}{\partial x}\exp(-st)dt-\int_0^\infty D_2\frac{\partial^2C_2}{\partial x^2}\exp(-st)dt+\int_0^\infty k_2C_2\exp(-st)dt-Rk_1\overline{C}_1=0$$

$sC_2(x,s)-C_2(x,0)+v\frac{\partial\overline{C}_2}{\partial x}-D_2\frac{\partial^2\overline{C}_2}{\partial x^2}+k_2\overline{C}_2(x,s)-Rk_1\overline{C}_1=0$ where the Laplace transform of $C_2(x, t)$ is denoted as $\overline{C}_2(x,s)$.

According to the boundary conditions (c); $C_1(x, 0) = 0$. Then;

$$D_2\frac{\partial^2\overline{C}_2}{\partial x^2}-v\frac{\partial\overline{C}_2}{\partial x}-(s+k_2)\overline{C}_2=Rk_1\overline{C}_1$$

$$\frac{\partial^2 \overline{C}_2}{\partial x^2} - \frac{v}{D_2}\frac{\partial \overline{C}_2}{\partial x} - \frac{1}{D_2}(s + k_2)\overline{C}_2 = \frac{Rk_1}{D_2}\frac{C_1^0}{s}\exp(z_1 x) \qquad \text{(C-9)}$$

This is a linear inhomogeneous *ODE*. So, $\overline{C}_2(x) = \overline{C}_{2c}(x) + \overline{C}_{2p}(x)$.

Complementary function: $\overline{C}_{2c}(x) = \eta e^{\delta x}$; $\frac{d\overline{C}_{2c}(x)}{dx} = \eta\delta e^{\delta x}$; $\frac{d^2\overline{C}_{2c}(x)}{dx^2} = \eta\delta^2 e^{\delta x}$

Substituting in (C-9);

$$\eta\delta^2 e^{\delta x} - \frac{v}{D_2}\eta\delta e^{\delta x} - \frac{(k_2 + s)\eta e^{\delta x}}{D_2} = 0$$

Dividing by $\eta e^{\delta x}$;

$$\delta^2 - \frac{v}{D_2}\delta - \frac{(k_2 + s)}{D_2} = 0 \text{ and } \delta = \frac{v \pm \sqrt{v^2 + 4(k_2 + s)D_2}}{2D_2}$$

$$\overline{C}_{2c} = A_3 \exp\left(\frac{x}{2D_2}\left(v + \sqrt{v^2 + 4(k_2 + s)D_2}\right)\right) + A_3 \exp\left(\frac{x}{2D_2}\left(v - \sqrt{v^2 + 4(k_2 + s)D_2}\right)\right)$$

In order to obtain the particular function, the method of undetermined coefficient is used.

Trial function; $C_{2p}(x) = \alpha e^{Z_1 x}$

$$\frac{d(\overline{C}_{2p}(x))}{dx} = \alpha z_1 e^{rx}; \quad \frac{d^2(\overline{C}_{2p}(x))}{dx^2} = \alpha {z_1}^2 e^{rx}$$

Substituting in equation (C-9);

$$\alpha {z_1}^2 e^{z_1 x} - \frac{v}{D_2}\alpha z_1 e^{z_1 x} - \frac{(k_2 + s)}{D_2}\alpha e^{z_1 x} = -\frac{Rk_1 C_1^0}{D_2 s}e^{z_1 x}$$

$$\alpha {z_1}^2 - \frac{v}{D_2}\alpha z_1 - \frac{(k_2 + s)}{D_2}\alpha = -\frac{Rk_1 C_1^0}{D_2 s} \text{ and } \alpha = \frac{Rk_1 C_1^0}{s\{vz_1 + (k_2 + s) - {z_1}^2 D_2\}}$$

For the simplicity, it is considered that $D=D_1= D_2$;

$$\therefore \{{z_1}^2 D_2 - vz_1 - (k_2 + s)\} = k_1 R - k_2 + (R - 1)s$$

Then; $\overline{C}_{2p}(x) = \frac{Rk_1 C_1^0}{-\{k_1 R - k_2 + (R-1)s\}}$

$$\overline{C}_2(x) = A_3 \exp\left(\frac{x}{2D}\left(v + \sqrt{v^2 + 4(k_2 + s)D}\right)\right) + A_4 \exp\left(\frac{x}{2D}\left(v - \sqrt{v^2 + 4(k_2 + s)D}\right)\right)$$

$$- \frac{Rk_1 C_1^0}{s\{k_1 R - k_2 + (R-1)s\}}e^{z_1 x}$$

According to the boundary conditions (d),

$C_2(x,t) \to 0$ *as* $x \to \infty$*; so* $\overline{C}_2(\infty,s) = 0 \quad \therefore\ A_3 = 0$

$$\overline{C}_2(x) = A_4 \exp\left(\frac{x}{2D}\left\{v - \sqrt{v^2 + 4(k_2 + s)D}\right\}\right) -$$

$$\frac{Rk_1C_1^0}{s\{k_1R - k_2 + (R-1)s\}} \exp\left(\frac{x}{2D}\left\{v - \sqrt{v^2 + 4(k_1 + s)RD}\right\}\right)$$

When x=0; $\overline{C}_2 = \dfrac{C_2^0}{s}$; $\therefore \dfrac{C_2^0}{s} = A_4 - \dfrac{Rk_1C_1^0}{s\{k_1R - k_2 + (R-1)s\}}$

Then; $A_4 = \dfrac{C_2^0}{s} + \left[\dfrac{Rk_1C_1^0}{s\{k_1R - k_2 + (R-1)s\}}\right]$

Then;
$$\overline{C}_2(x,s) = \left[\frac{C_2^0}{s} + \left\{\frac{Rk_1C_1^0}{s\{k_1R - k_2 + (R-1)s\}}\right\}\right] \exp\left(\frac{x}{2D}\left(v - \sqrt{v^2 + 4(k_2 + s)D}\right)\right) -$$
$$\frac{Rk_1C_1^0}{s\{k_1R - k_2 + (R-1)s\}} \exp\left(\frac{x}{2D}\left\{v - \sqrt{v^2 + 4(k_1 + s)RD}\right\}\right) \qquad \text{(C-10)}$$

$$\overline{C}_2(x) = \frac{C_2^0}{s}\overline{q}(x,s) + \frac{Rk_1C_1^0}{s\{k_1R - k_2 + (R-1)s\}}\left[\overline{q}(x,s) - \bar{f}(x,s)\right] \qquad \text{(C-11)}$$

where $\bar{f}(x,s) = \exp\left(\dfrac{x}{2D}\left\{v - \sqrt{v^2 + 4(k_1 + s)RD}\right\}\right) = \exp(z_1 x)$ &

$$\overline{q}(x,s) = \exp\left(\frac{x}{2D}\left\{v - \sqrt{v^2 + 4(k_2 + s)D}\right\} = \exp(z_2 x)\right)$$

Taking the inverse of $\overline{q}(x,s)\ \&\ \bar{f}(x,s)$;

$$L^{-1}\{\exp(z_2 x)\} = q(x,t) = \exp\left(\frac{xv}{2D}\right)\left(\frac{x}{\left(4\pi Dt^3\right)^{1/2}}\right)\exp\left[-\left(\frac{v^2}{4D} + k_2\right)t - \frac{x^2}{4Dt}\right]$$

$$q(x,\tau) = \exp\left(\frac{xv}{2D}\right)\left(\frac{x}{\left(4\pi D\tau^3\right)^{1/2}}\right)\exp\left[-\left(\frac{v^2}{4D} + k_2\right)\tau - \frac{x^2}{4D\tau}\right]$$

$$f(x,\tau) = \exp\left(\frac{xv}{2D}\right)x\left(\frac{R}{4\pi D\tau^3}\right)^{1/2}\exp\left[-\left(\frac{v^2}{4DR} + k_1\right)\tau - \frac{x^2R}{4D\tau}\right]$$

In order to invert Eq. (C-11), the convolution theorem is applied.

$$C_2(x,t) = C_2^0\int_0^t q(\tau)d\tau + Rk_1C_1^0\int_0^t q(\tau)\times G(t-\tau)d\tau - Rk_1C_1^0\int_0^t f(\tau)\times G(t-\tau)d\tau \qquad \text{(C-12)}$$

where; $G(t) = L^{-1}\left(\frac{1}{s(k_1R - k_2 + (R-1)s)}\right) = \frac{\exp\left\{\left(\frac{k_2 - k_1R}{R-1}\right)t\right\} - 1}{(R-1)\left(\frac{k_2 - k_1R}{R-1}\right)}$ &

$$G(t-\tau) = \frac{\exp\left\{\left(\frac{k_2 - k_1R}{R-1}\right)(t-\tau)\right\} - 1}{(R-1)\left(\frac{k_2 - k_1R}{R-1}\right)} = \frac{\exp\left\{\left(\frac{k_1R - k_2}{R-1}\right)(\tau - t)\right\} - 1}{(1-R)\left(\frac{k_1R - k_2}{R-1}\right)}$$

because $L^{-1}\frac{1}{s(s-a)} = \frac{1}{a}\left(e^{at} - 1\right)$

$$G(t-\tau) = \frac{\exp\{A(\tau - t)\} - 1}{A} \quad \text{where } A = \left(\frac{k_1R - k_2}{R-1}\right)$$

Therefore, Eq. (C-12) can be written as:

$$C_2(x,t) = C_2^0\int_0^t q(\tau)d\tau + \frac{Rk_1C_1^0}{(1-R)A}\exp(-At)\int_0^t q(\tau)\times\exp(A\tau)d\tau - \frac{Rk_1C_1^0}{(1-R)A}\int_0^t q(\tau)d\tau -$$
$$\frac{Rk_1C_1^0}{(1-R)A}\exp(-At)\int_0^t f(\tau)\times\exp(A\tau)d\tau + \frac{Rk_1C_1^0}{(1-R)A}\int_0^t f(\tau)d\tau \qquad \text{(C-13)}$$

To solve the integrals in Eq. (C-13), the formula given by Abramowitz and Stegun, (1972) described in the above section is used. Then Eq. (C-13) becomes:

$$C_2(x,t) = C_2^0Q(x,t) + \frac{Rk_1C_1^0}{(k_1R - k_2)}\left[Q(x,t) - P(x,t) + S(x,t) - F(x,t)\right] \qquad (5.10)$$

Where;

$$F(x,t) = \int_0^t f(\tau)d\tau = \frac{1}{2}\left[\begin{array}{l}\exp\left\{\frac{x}{2D}\left(v - \sqrt{\left(v^2 + 4Dk_1R\right)}\right)\right\}erfc\left(\frac{x - t\sqrt{\left(v^2 + 4Dk_1R\right)}/R}{\sqrt{(4Dt/R)}}\right) + \\ \exp\left\{\frac{x}{2D}\left(v + \sqrt{\left(v^2 + 4Dk_1R\right)}\right)\right\}erfc\left(\frac{x + t\sqrt{\left(v^2 + 4Dk_1R\right)}/R}{\sqrt{(4Dt/R)}}\right)\end{array}\right] \qquad (5.11)$$

$$Q(x,t)=\int_0^t q(\tau)d\tau=\frac{1}{2}\left[\begin{array}{l}\exp\left\{\frac{x}{2D}\left(v-\sqrt{\left(v^2+4Dk_2\right)}\right)\right\}erfc\left(\frac{x-t\sqrt{\left(v^2+4Dk_2\right)}}{\sqrt{4Dt}}\right)+\\ \exp\left\{\frac{x}{2D}\left(v+\sqrt{\left(v^2+4Dk_2\right)}\right)\right\}erfc\left(\frac{x+t\sqrt{\left(v^2+4Dk_2\right)}}{\sqrt{4Dt}}\right)\end{array}\right] \quad (5.12)$$

$$P(x,t)=\exp(-At)\int_0^t q(\tau)\times\exp(A\tau)d\tau=\frac{1}{2}\left[\begin{array}{l}\exp\{-At\}\exp\left\{\frac{x}{2D}\left(v-\sqrt{\left(v^2+4Dk_2-4DA\right)}\right)\right\}\\ erfc\left(\frac{x-t\sqrt{\left(v^2+4Dk_2-4DA\right)}}{\sqrt{(4Dt)}}\right)+\\ \exp\{-At\}\exp\left\{\frac{x}{2D}\left(v+\sqrt{\left(v^2+4Dk_2-4DA\right)}\right)\right\}\\ erfc\left(\frac{x+t\sqrt{\left(v^2+4Dk_2-4DA\right)}}{\sqrt{(4Dt)}}\right)\end{array}\right]$$

(5.13)

$$S(x,t)=\exp(-At)\int_0^t f(\tau)\times\exp(A\tau)d\tau=\frac{1}{2}\left[\begin{array}{l}\exp\{-At\}\exp\left\{\frac{x}{2D}\left(v-\sqrt{\left(v^2+4Dk_1R-4DAR\right)}\right)\right\}\\ erfc\left(\frac{x-t\sqrt{\left(v^2+4Dk_1R-4DAR\right)}/R}{\sqrt{(4Dt/R)}}\right)+\\ \exp\{-At\}\exp\left\{\frac{x}{2D}\left(v+\sqrt{\left(v^2+4Dk_1R-4DAR\right)}\right)\right\}\\ erfc\left(\frac{x+t\sqrt{\left(v^2+4Dk_1R+4DAR\right)}/R}{\sqrt{(4Dt/R)}}\right)\end{array}\right]$$

(5.14)

Solution of the governing equation for *NH_3-N* (Steady state)

For steady state Eq. (5.7) becomes:

$$v\,dC_1/dx-D_1\,d^2C_1/dx^2+Rk_1C_1=0 \quad \text{(C-14)}$$

This is a linear homogeneous equation. So, $C_1(x)=C_{1c}(x)+C_{1p}(x);\ C_{1p}(x)=0$

Complementary function: $C_{1c}(x)=A^0e^{\lambda' x}$; $\frac{dC_{1c}(x)}{dx}=A^0\lambda' e^{\lambda' x}$; $\frac{d^2C_{1c}(x)}{dx^2}=A^0\lambda'^2e^{\lambda' x}$

Substituting in (C-14); $\lambda'^2-\frac{v}{D_1}\lambda'-\frac{Rk_1}{D_1}=0$; $\lambda'=\frac{v\pm\sqrt{v^2+4k_1RD_1}}{2D_1}$

$$C_1 = A_1^0 \exp\left(\frac{x}{2D_1}\left(v+\sqrt{v^2+4k_1RD_1}\right)\right) + A_1^0 \exp\left(\frac{x}{2D_1}\left(v-\sqrt{v^2+4k_1RD_1}\right)\right)$$

$C_1(x) \to 0$ as x $\to \infty; \therefore A_1^0 = 0$

$$C_1 = C_1^0 F_1(x) \qquad (5\text{-}16)$$

Where $F_1'(x) = \exp\left(\frac{x}{2D_1}\left\{v-\sqrt{v^2+4k_1RD_1}\right\}\right)$

For steady state Eq. (5.8) becomes:

$$\partial C_2/\partial t + v\,\partial C_2/\partial x - D_2\,\partial^2 C_2/\partial x^2 - Rk_1C_1 + k_2C_2 = 0$$

$$d^2C_2/dx^2 - \frac{v}{D_2}\,dC_2/dx - \frac{k_2}{D_2}C_2 = -\frac{Rk_1C_1^0}{D_2}e^{rx} \qquad (C\text{-}15)$$

where $r = \dfrac{v-\sqrt{v^2+4k_1RD_1}}{2D_1}$

This is a linear inhomogeneous equation. So, $C_2(x) = C_{2c}(x) + C_{2p}(x)$

$$C_{2c}(x) = B_1^0 \exp\left(\frac{x}{2D_2}\left(v+\sqrt{v^2+4k_2D_2}\right)\right) + B_2^0 \exp\left(\frac{x}{2D_2}\left(v-\sqrt{v^2+4k_2D_2}\right)\right)$$

In order to find the particular integral, the method of undetermined coefficient is used.

Trial function, $C_{2p}(x) = \alpha' e^{rx}$; $\dfrac{d(C_{2p}(x))}{dx} = \alpha' r e^{rx}$; $\dfrac{d^2(C_{2p}(x))}{dx^2} = \alpha' r^2 e^{rx}$

Substituting in Eq. (C-15):

$$\alpha' r^2 - \frac{v}{D_2}\alpha' r - \frac{k_2}{D_2}\alpha' = -\frac{Rk_1C_1^0}{D_2}; \alpha' = \frac{Rk_1C_1^0}{\left(vr+k_2-r^2D_2\right)}; C_{2p}(x) = \frac{Rk_1C_1^0}{\left(vr+k_2-r^2D_2\right)}e^{rx}$$

$$C_2(x) = B_1^0 \exp\left(\frac{x}{2D_2}\left(v+\sqrt{v^2+4k_2D_2}\right)\right) + B_2^0 \exp\left(\frac{x}{2D_2}\left(v-\sqrt{v^2+4k_2D_2}\right)\right)$$

$$+ \frac{Rk_1C_1^0}{\left(vr+k_2-r^2D_2\right)}e^{rx}$$

$C_2(x) \to 0$ *as* $x \to \infty$; $\therefore\ B_1^0 = 0$

$$C_2(x) = B_2^0 \exp\left(\frac{x}{2D_2}\left(v-\sqrt{v^2+4k_2D_2}\right)\right) + \frac{Rk_1C_1^0}{\left(vr+k_2-r^2D_2\right)}\exp\left(\frac{x}{2D_1}\left\{v-\sqrt{v^2+4k_1RD_1}\right\}\right)$$

When x=0; $C_2 = C_2^0$; $\quad B_2^0 = C_2^0 - \left[\dfrac{Rk_1C_1^0}{\left(vr+k_2-r^2D_2\right)}\right]$

$$C_2(x,t) = C_2^0 F_2'(x) + \frac{Rk_1 C_1^0}{\left(r^2 D_2 - vr - k_2\right)}\left[F_2'(x) - F_1'(x)\right] \tag{5.17}$$

where $r = \dfrac{v - \sqrt{v^2 + 4k_1 RD_1}}{2D_1}$; $F_1'(x) = \exp\left(\dfrac{x}{2D_1}\left\{v - \sqrt{v^2 + 4k_1 RD_1}\right\}\right)$ **&**

$F_2'(x) = \exp\left(\dfrac{x}{2D_2}\left\{v - \sqrt{v^2 + 4k_2 D_2}\right\}\right)$

Continuous Irrigation- Low Porous Soil

Solution of the governing equation for NO_3^--N ($t > T_1$)

$$\frac{\partial C_2}{\partial t} + v\frac{\partial C_2}{\partial x} - D_2\frac{\partial^2 C_2}{\partial x^2} - Rk_1 C_1 + k_2 C_2 - (R-1)\times k_1' \times \left(C_1^p\right)^1 = 0 \tag{5.20}$$

Consider $\left(C_1^p\right)^1$ is one period of a periodic function with period 'T_1'.

Then, $\left(\overline{C}_1^{\,p}\right)^1(s) = \int_0^{T_1} e^{-st} C_1^p(x,t)dt$, which is the Laplace transform of the function denoting the first period and zero elsewhere.

$$\left(\overline{C}_1^{\,p}\right)^1(s) = \int_0^{T_1} e^{-st} C_1^p(x,t)dt = \int_0^{\infty} e^{-st} C_1^p(x,t)dt - \int_{T_1}^{\infty} e^{-st} C_1^p(x,t)dt$$

Changing variables with $\tau = t - T_1; d\tau = dt$;

$$\left(\overline{C}_1^{\,p}\right)(s) = \int_0^{T_1} e^{-st} C_1^p(x,t)dt = \int_0^{\infty} e^{-st} C_1^p(x,t)dt - e^{-sT_1}\int_0^{\infty} e^{-s\tau} C_1^p(x,\tau)d\tau = \overline{C}_1^{\,p}\left(1 - e^{-sT_1}\right)$$

Taking the Laplace transform of Eq. (5.20);

$$\int_0^{\infty}\frac{\partial C_2}{\partial t}\exp(-st)dt + \int_0^{\infty} v\frac{\partial C_2}{\partial x}\exp(-st)dt - \int_0^{\infty} D_2\frac{\partial^2 C_2}{\partial x^2}\exp(-st)dt + \int_0^{\infty} k_2 C_2\exp(-st)dt - Rk_1\overline{C}_1 -$$
$$(R-1)k_1'\left(1 - e^{-sT_1}\right)\overline{C}_1^{\,p} = 0$$

$$sC_2(x,s) - C_2(x,0) + v\frac{\partial \overline{C}_2}{\partial x} - D_2\frac{\partial^2 \overline{C}_2}{\partial x^2} + k_2\overline{C}_2(x,s) - Rk_1\overline{C}_1 - (R-1)k_1'\left(1 - e^{-sT_1}\right)\overline{C}_p = 0$$

where the Laplace transform of $C_2(x, t)$ is $\overline{C}_2(x,s)$.

According to the boundary conditions (c); $C_1(x, 0) = 0$. Then;

$$D_2\frac{\partial^2 \overline{C}_2}{\partial x^2} - v\frac{\partial \overline{C}_2}{\partial x} - (s + k_2)\overline{C}_2 = -Rk_1\overline{C}_1 - (R-1)k_1'\left(1 - e^{-sT_1}\right)\overline{C}_1^{\,p}$$

$$\frac{\partial^2 \overline{C}_2}{\partial x^2} - \frac{v}{D_2}\frac{\partial \overline{C}_2}{\partial x} - \frac{1}{D_2}(s+k_2)\overline{C}_2 = -\frac{Rk_1C_1^0}{D_2 s}\exp\left(\frac{x}{2D_1}\left\{v - \sqrt{v^2 + 4R(k_1+s)D_1}\right\}\right) -$$

$$\frac{(R-1)k_1'C_1^0}{D_2 s}\left(1-e^{-sT_1}\right)\exp\left(\frac{x}{2D_1}\left\{v - \sqrt{v^2 + 4D_1(k_1+Rs)}\right\}\right)$$

$$z_1 = \frac{1}{2D_1}\left\{v - \sqrt{v^2 + 4R(k_1+s)D_1}\right\};\ z_3 = \frac{1}{2D_1}\left\{v - \sqrt{v^2 + 4D_1(k_1+Rs)}\right\}$$

$$\frac{Rk_1C_1^0}{D_2} = M';\ \frac{(R-1)k_1'C_1^0}{D_2} = N'$$

$$\frac{\partial^2 \overline{C}_2}{\partial x^2} - \frac{v}{D_2}\frac{\partial \overline{C}_2}{\partial x} - \frac{1}{D_2}(s+k_2)\overline{C}_2 = -\frac{M'}{s}\exp(z_1 x) - \frac{N'}{s}\left(1-e^{-sT_1}\right)\exp(z_3 x) \qquad \text{(C-16)}$$

This is a linear inhomogeneous equation. So, $\overline{C}_2(x) = \overline{C}_{2c}(x) + \overline{C}_{2p}(x)$

Complementary function: $\overline{C}_{2c}(x) = \xi e^{\varepsilon x};\ \frac{d\overline{C}_{2c}(x)}{dx} = \xi\varepsilon e^{\varepsilon x};\ \frac{d^2\overline{C}_{2c}(x)}{dx^2} = \xi\varepsilon^2 e^{\varepsilon x}$

Substituting in Eq. (B-16); $\xi\varepsilon^2 e^{\varepsilon x} - \frac{v}{D_2}\xi e^{\varepsilon x} - \frac{(k_2+s)\xi e^{\varepsilon x}}{D_2} = 0$

Dividing by $\xi e^{\varepsilon x}$; $\varepsilon^2 - \frac{v}{D_2}\varepsilon - \frac{(k_2+s)}{D_2} = 0$ and $\varepsilon = \frac{v \pm \sqrt{v^2 + 4(k_2+s)D_2}}{2D_2}$

$$\therefore \overline{C}_{2c} = A_5\exp\left(\frac{x}{2D_2}\left(v + \sqrt{v^2 + 4(k_2+s)D_2}\right)\right) + A_6\exp\left(\frac{x}{2D_2}\left(v - \sqrt{v^2 + 4(k_2+s)D_2}\right)\right)$$

In order to find the particular function, the method of undetermined coefficient is used.

Trial function: $C_{2p}(x) = \gamma e^{Z_1 x} + \beta e^{z_3 x}$

$$\frac{d\left(C_{2p}(x)\right)}{dx} = \gamma z_1 e^{z_1 x} + \beta z_3 e^{z_3 x};\ \frac{d^2\left(C_{2p}(x)\right)}{dx^2} = \gamma {z_1}^2 e^{z_1 x} + \beta {z_3}^2 e^{z_3 x}$$

Substituting in Eq. (C-16);

$$\gamma {z_1}^2 e^{z_1 x} - \frac{v}{D_2}\gamma z_1 e^{z_1 x} - \frac{(k_2+s)}{D_2}\gamma e^{z_1 x} + \beta {z_3}^2 e^{z_3 x} - \frac{v}{D_2}\beta z_3 e^{z_3 x} - \frac{(k_2+s)}{D_2}\beta e^{z_3 x} =$$

$$-\frac{M'}{s}e^{z_1 x} - \frac{N'}{s}\left(1-e^{-sT_1}\right)e^{z_3 x}$$

$$\gamma {z_1}^2 - \frac{v}{D_2}\gamma z_1 - \frac{(k_2+s)}{D_2}\gamma = -\frac{M'}{s};\ Rk_1C_1^0 = M;\ (R-1)k_1'C_0^1 = N$$

$$\therefore \gamma = \frac{M}{s\left(vz_1 + (k_2+s) - {z_1}^2 D_2\right)}\ \&\ \beta = \frac{N\left(1-e^{-sT_1}\right)}{s\left(vz_3 + (k_2+s) - {z_3}^2 D_2\right)}$$

Therefore; $\overline{C}_{2p}(x)=\dfrac{M}{s\left(vz_1+(k_2+s)-z_1{}^2D_2\right)}e^{z_1x}+\dfrac{N\left(1-e^{-sT_1}\right)}{s\left(vz_2+(k_2+s)-z_2{}^2D_2\right)}e^{z_3x}$

$$\overline{C}_2(x)=A_5\exp\left(\frac{x}{2D_2}\left(v+\sqrt{v^2+4(k_2+s)D_2}\right)\right)+A_6\exp\left(\frac{x}{2D_2}\left(v-\sqrt{v^2+4(k_2+s)D_2}\right)\right)+$$
$$\frac{M}{s\left(vz_1+(k_2+s)-z_1{}^2D_2\right)}e^{z_1x}+\frac{N\left(1-e^{-sT_1}\right)}{s\left(vz_2+(k_2+s)-z_2{}^2D_2\right)}e^{z_3x}$$

(C-17)

It is considered that $D= D_1= D_2$ for the simplicity of Eq. (C-17).

$\therefore \left(z_1{}^2D_2-vz_1-(k_2+s)\right)=k_1R-k_2+(R-1)s$ & $\left(z_3{}^2D_2-vz_3-(k_2+s)\right)=k_1-k_2+(R-1)s$

Therefore Eq. (C-17) becomes:

$$\overline{C}_2(x)=A_5\exp\left(\frac{x}{2D}\left(v+\sqrt{v^2+4(k_2+s)D}\right)\right)+A_6\exp\left(\frac{x}{2D}\left(v-\sqrt{v^2+4(k_2+s)D}\right)\right)-$$
$$\frac{M}{s\left(k_1R-k_2+(R-1)s\right)}e^{z_1x}-\frac{N\left(1-e^{-sT_1}\right)}{s\left(k_1-k_2+(R-1)s\right)}e^{z_3x}$$

According to the boundary conditions (d);

$C_2(x,t)\to 0$ *as* $x\to\infty$*; so* $\overline{C}_2(\infty,s)=0 \quad \therefore\ A_5=0$.

When *x=0*; $\overline{C}_2=\dfrac{C_2^0}{s}$; $\therefore A_6=\dfrac{C_2^0}{s}+\left(\dfrac{M}{s\left(k_1R-k_2+(R-1)s\right)}+\dfrac{N\left(1-e^{-sT_1}\right)}{s\left(k_1-k_2+(R-1)s\right)}\right)$

$$\overline{C}_2(x,s)=\frac{C_2^0}{s}\exp\left(\frac{x}{2D}\left(v-\sqrt{v^2+4(k_2+s)D}\right)\right)+\left(\frac{M}{s\left(k_1R-k_2+(R-1)s\right)}+\frac{N\left(1-e^{-sT_1}\right)}{s\left(k_1-k_2+(R-1)s\right)}\right)$$
$$\exp\left(\frac{x}{2D}\left(v-\sqrt{v^2+4(k_2+s)D}\right)\right)-\frac{M}{s\left(k_1R-k_2+(R-1)s\right)}e^{z_1x}-\frac{N\left(1-e^{-sT_1}\right)}{s\left(k_1-k_2+(R-1)s\right)}e^{z_3x}$$

(C-18)

$$\bar{f}(x)=\exp\left(\frac{x}{2D}\left\{v-\sqrt{v^2+4(k_1+s)RD}\right\}\right)=\exp(z_1x)\ \&$$

$$\bar{f}'(x)=\exp\left(\frac{x}{2D}\left\{v-\sqrt{v^2+4(k_1+Rs)D}\right\}=\exp(z_3x)\right)$$

$$\bar{q}(x,s)=\exp\left(\frac{x}{2D}\left\{v-\sqrt{v^2+4(k_2+s)D}\right\}=\exp(z_2x)\right)$$

Taking the inverse of $\bar{f}(x,s), \bar{f}'(x,s), q(x,s)$;

$$f(\tau) = \exp\left(\frac{xv}{2D}\right) x\left(\frac{R}{4\pi D\tau^3}\right)^{1/2} \exp\left[-\left(\frac{v^2}{4DR}+k_1\right)\tau - \frac{x^2R}{4D\tau}\right]$$

$$f'(\tau) = \exp\left(\frac{xv}{2D}\right) x\left(\frac{R}{4\pi D\tau^3}\right)^{1/2} \exp\left[-\left(\frac{v^2}{4DR}+\frac{k_1}{R}\right)\tau - \frac{x^2R}{4D\tau}\right]$$

$$q(\tau) = \exp\left(\frac{xv}{2D}\right)\left(\frac{x}{\left(4\pi D\tau^3\right)^{1/2}}\right) \exp\left[-\left(\frac{v^2}{4D}+k_2\right)\tau - \frac{x^2}{4D\tau}\right]$$

In order to invert Eq. (C-18), the convolution theorem is applied.

$$C_2(x,t) = C_2^0 \int_0^t q(\tau)d\tau + M\int_0^t q(\tau)\times G(t-\tau)d\tau - M\int_0^t f(\tau)\times G(t-\tau)d\tau + N\int_0^t q(\tau)\times H_1(t-\tau)d\tau -$$

$$N\int_0^t q(t-\tau)\times H_2(\tau)d\tau - N\int_0^t f'(\tau)\times H_1(t-\tau)d\tau + N\int_0^t f'(t-\tau)\times H_2(\tau)d\tau$$

(C-19)

Where $G(t) = L^{-1}\left(\frac{1}{s(k_1R-k_2+(R-1)s)}\right) = \frac{\exp\left\{\left(\frac{k_2-k_1R}{R-1}\right)t\right\}-1}{(R-1)\left(\frac{k_2-k_1R}{R-1}\right)}$ &

$$G(t-\tau) = \frac{\exp\left\{\left(\frac{k_1R-k_2}{R-1}\right)(\tau-t)\right\}-1}{(1-R)\left(\frac{k_1R-k_2}{R-1}\right)}$$

$$A = \left(\frac{k_1R-k_2}{R-1}\right) \qquad (5.14)$$

$$H_1(t) = L^{-1}\left(\frac{1}{s(k_1-k_2+(R-1)s)}\right) = \frac{\exp\left\{\left(\frac{k_2-k_1}{R-1}\right)(t)\right\}-1}{(R-1)\left(\frac{k_2-k_1}{R-1}\right)}$$ &

$$B = \left(\frac{k_1-k_2}{R-1}\right) \qquad (5.26)$$

Using the second translation theorem of Laplace transformation

$\{ L^{-1}\left(e^{-as}F(s)\right) = u_a(t)f(t-a)$ where $F(s) = L(f(t)), a \geq 0 \}$;

$$H_2(t) = L^{-1}\left(\frac{e^{-sT_1}}{s(k_1 - k_2 + (R-1)s)}\right) = u_T(t)\frac{\exp\left\{\left(\frac{k_2 - k_1}{R-1}\right)(t - T_1)\right\} - 1}{(R-1)\left(\frac{k_2 - k_1}{R-1}\right)}$$

$$H_2(\tau) = u_T(\tau)\frac{\exp\left\{\left(\frac{k_2 - k_1}{R-1}\right)(\tau - T_1)\right\} - 1}{(R-1)\left(\frac{k_2 - k_1}{R-1}\right)}$$

Eq. (C-19) can be now written as:

$$C_2(x,t) = C_2^0\int_0^t q(\tau)d\tau + \frac{M}{(1-R)A}\int_0^t q(\tau)*(\exp\{A(\tau - t)\} - 1)d\tau - \frac{M}{(1-R)A}\int_0^t f(\tau)*(\exp\{A(\tau - t)\} - 1)d\tau +$$
$$\frac{N}{(1-R)B}\int_0^t q(\tau)*(\exp\{B(\tau - t)\} - 1)d\tau - \frac{N}{(1-R)B}\int_0^t q(t-\tau)*u_{T_1}(\tau)(\exp\{B(T_1 - \tau)\} - 1)d\tau -$$
$$\frac{N}{(1-R)B}\int_0^t f'(\tau)*(\exp\{B(\tau - t)\} - 1)d\tau + \frac{N}{(1-R)B}\int_0^t f'(t-\tau)*u_{T_1}(\tau)(\exp\{B(T_1 - \tau)\} - 1)d\tau$$

$C_2(x,t) = A' + B'$ where

$$A' = C_2^0\int_0^t q(\tau)d\tau - \frac{M}{(k_1R - k_2)}\exp(-At)\int_0^t q(\tau)\exp(A\tau)d\tau + \frac{M}{(k_1R - k_2)}\int_0^t q(\tau)d\tau + \frac{M}{(k_1R - k_2)}$$
$$\exp(-At)\int_0^t f(\tau)\exp(A\tau)d\tau - \frac{M}{(k_1R - k_2)}\int_0^t f(\tau)d\tau - \frac{N}{(k_1 - k_2)}\exp(-Bt)\int_0^t q(\tau)\exp(B\tau)d\tau +$$
$$\frac{N}{(k_1 - k_2)}\int_0^t q(\tau)d\tau$$

(C-20)

$$B' = \frac{N}{(k_1 - k_2)}\exp(BT_1)\int_{T_1}^t q(t-\tau)\exp(-B\tau)d\tau - \frac{N}{(k_1 - k_2)}\int_{T_1}^t q(t-\tau)d\tau + \frac{N}{(k_1 - k_2)}$$
$$\exp(-Bt)\int_0^t f'(\tau)\exp(B\tau)d\tau - \frac{N}{(k_1 - k_2)}\int_0^t f'(\tau)d\tau - \frac{N}{(k_1 - k_2)}\exp(BT_1)\int_{T_1}^t f'(t-\tau)\exp(-B\tau)d\tau +$$
$$\frac{N}{(k_1 - k_2)}\int_{T_1}^t f'(t-\tau)d\tau$$

$t - \tau = \overline{T}$ **;** $-d\tau = d\overline{T}$ Then;

$$B' = \frac{N}{(k_1 - k_2)} \exp(B(T_1 - t)) \int_0^{t-T_1} q(\overline{T}) \exp(B\overline{T}) d\overline{T} - \frac{N}{(k_1 - k_2)} \int_0^{t-T_1} q(\overline{T}) d\overline{T} + \frac{N}{(k_1 - k_2)}$$
$$\exp(-Bt) \int_0^t f'(\tau) \exp(B\tau) d\tau - \frac{N}{(k_1 - k_2)} \int_0^t f'(\tau) d\tau - \frac{N}{(k_1 - k_2)} \exp(B(T_1 - t)) \int_0^{t-T_1} f'(\overline{T}) \exp(B\overline{T}) d\overline{T} +$$
$$\frac{N}{(k_1 - k_2)} \int_0^{t-T_1} f'(\overline{T}) d\overline{T}$$

(C-21)

$$A' = \left(C_2^0 + \frac{M}{(k_1 R - k_2)} + \frac{N}{(k_1 - k_2)} \right) Q(x,t) - \frac{M}{(k_1 R - k_2)} P(x,t) + \frac{M}{(k_1 R - k_2)} S(x,t) - \frac{M}{(k_1 R - k_2)} F(x,t)$$
$$- \frac{N}{(k_1 - k_2)} P_1(x,t)$$

and

$$B' = \frac{N}{(k_1 - k_2)} P_2(x,(t - T_1)) - \frac{N}{(k_1 - k_2)} S_3(x,(t - T_1)) + \frac{N}{(k_1 - k_2)} S_3(x,t) - \frac{N}{(k_1 - k_2)} F_3(x,t) +$$
$$\frac{N}{(k_1 - k_2)} F_3(x,(t - T_1)) - \frac{N}{(k_1 - k_2)} Q(x,(t - T_1))$$

where

$$Q(x,t) = \int_0^t q(\tau) d\tau \; ; P(x,t) = \exp(-At) \int_0^t q(\tau) \exp(A\tau) d\tau \; ; S(x,t) = \exp(-At) \int_0^t f(\tau) \exp(A\tau) d\tau$$

$$; F(x,t) = \int_0^t f(\tau) d\tau \; ; P_1(x,t) = \exp(-Bt) \int_0^t q(\tau) \exp(B\tau) d\tau$$

$$P_2\{x,(t - T_1)\} = \exp(B(T_1 - t)) \int_0^{t-T_1} q(\overline{T}) \exp(B\overline{T}) d\overline{T} \; ; \; Q\{x,(t - T_1)\} \int_0^{t-T_1} q(\overline{T}) d\overline{T} \; ;$$

$$S_3(x,t) = \exp(-Bt) \int_0^t f'(\tau) \exp(B\tau) d\tau \; ; F_3(x,t) = \int_0^t f'(\tau) d\tau \; ;$$

$$F_3\{x,(t - T_1)\} = \exp(B(T_1 - t)) \int_0^{t-T_1} f'(\overline{T}) \exp(B\overline{T}) d\overline{T} \; ; S_3\{x,(t - T_1)\} \int_0^{t-T_1} f'(\overline{T}) d\overline{T} \; .$$

In order to carry out the integral of Eq.(C-20) & (C-21), Eq. (C-8) (Abramowitz and Stegun, 1972) is used. Following is an example how one integral component in Eq. (C-21) is solved.

$$Q\{x,(t-T_1)\} = \int_0^{t-T_1} q(\overline{T})d\overline{T} = \exp\left(\frac{xv}{2D}\right)x\left(\frac{1}{4\pi D}\right)^{1/2}\int_0^{t-T_1}\exp\left[-\left(\frac{v^2}{4D}+k_2\right)\overline{T}-\frac{x^2}{4D\overline{T}}\right]\frac{d\overline{T}}{\overline{T}^{3/2}}$$

$$u = \overline{T}^{-1/2};\ du = -0.5T^{(-3/2)}d\overline{T};\ u^{-2} = \overline{T}$$

$$Q\{x,(t-T_1)\} = \exp\left(\frac{xv}{2D}\right)2x\left(\frac{1}{4\pi D}\right)^{1/2}\int_{(t-T_1)^{-1/2}}^{0}\exp\left[-\frac{x^2u^2}{4D}-\left(\frac{v^2}{4D}+k_2\right)\frac{1}{u^2}\right]du$$

Using Eq. (C-8);

$$a^2 = \frac{x^2}{4D}\ ;\ b^2 = \left(\frac{v^2}{4D}+k_2\right)$$

$$Q\{x,(t-T_1)\} = \exp\left(\frac{xv}{2D}\right)2x\left(\frac{1}{4\pi D}\right)^{1/2}\frac{\sqrt{(4D\pi)}}{4x}\left[\begin{array}{l}\exp\left(\frac{x}{2D}\sqrt{(v^2+4Dk_2)}\right)\\ erfc\left(\frac{xu}{2\sqrt{(D)}}+\frac{\sqrt{(v^2+4k_2D)}}{2\sqrt{D}u}\right)\\ +\exp\left(-\frac{x}{2D}\sqrt{(v^2+4Dk_2)}\right)\\ erfc\left(\frac{xu}{2\sqrt{D}}-\frac{\sqrt{(v^2+4k_2D)}}{2\sqrt{D}u}\right)\end{array}\right]$$

$$Q\{x,(t-T_1)\} = \frac{1}{2}\left[\begin{array}{l}\exp\left\{\frac{x}{2D}\left(v-\sqrt{(v^2+4Dk_2)}\right)\right\}erfc\left(\frac{x-(t-T_1)\sqrt{(v^2+4Dk_2)}}{\sqrt{4D(t-T_1)}}\right)+\\ \exp\left\{\frac{x}{2D}\left(v+\sqrt{(v^2+4Dk_2R)}\right)\right\}erfc\left(\frac{x+(t-T_1)\sqrt{(v^2+4Dk_2)}}{\sqrt{4D(t-T_1)}}\right)\end{array}\right]$$

Likewise, all the integrals of (C-20) & (C-21) can be carried out. Then;

$$\begin{array}{l}C_2(x,t) = C_2^0Q(x,t)+\frac{Rk_1C_1^0}{(k_1R-k_2)}\left[Q(x,t)-P(x,t)+S(x,t)-F(x,t)\right]\\ +\frac{(R-1)k_1'C_1^0}{(k_1-k_2)}\left[\begin{array}{l}Q(x,t)-Q(x,(t-T_1))+P_1(x,(t-T_1))-P_1(x,t)+\\ S_3(x,t)-S_3(x,(t-T_1))-F_3(x,t)+F_3(x,(t-T_1))\end{array}\right]\end{array} \qquad (5.28)$$

Where;

$$F(x,t)=\frac{1}{2}\left[\begin{array}{l}\exp\left\{\frac{x}{2D}\left(v-\sqrt{\left(v^2+4Dk_1R\right)}\right)\right\}erfc\left(\frac{x-t\sqrt{\left(v^2+4Dk_1R\right)}/R}{\sqrt{(4Dt/R)}}\right)+\\ \exp\left\{\frac{x}{2D}\left(v+\sqrt{\left(v^2+4Dk_1R\right)}\right)\right\}erfc\left(\frac{x+t\sqrt{\left(v^2+4Dk_1R\right)}/R}{\sqrt{(4Dt/R)}}\right)\end{array}\right] \quad (5.10)$$

$$Q(x,t)=\frac{1}{2}\left[\begin{array}{l}\exp\left\{\frac{x}{2D}\left(v-\sqrt{\left(v^2+4Dk_2\right)}\right)\right\}erfc\left(\frac{x-t\sqrt{\left(v^2+4Dk_2\right)}}{\sqrt{4Dt}}\right)+\\ \exp\left\{\frac{x}{2D}\left(v+\sqrt{\left(v^2+4Dk_2\right)}\right)\right\}erfc\left(\frac{x+t\sqrt{\left(v^2+4Dk_2\right)}}{\sqrt{4Dt}}\right)\end{array}\right] \quad (5.11)$$

$$P(x,t)=\frac{1}{2}\left[\begin{array}{l}\exp\{-At\}\exp\left\{\frac{x}{2D}\left(v-\sqrt{\left(v^2+4Dk_2-4DA\right)}\right)\right\}\\ erfc\left(\frac{x-t\sqrt{\left(v^2+4Dk_2-4DA\right)}}{\sqrt{(4Dt)}}\right)+\\ \exp\{-At\}\exp\left\{\frac{x}{2D}\left(v+\sqrt{\left(v^2+4Dk_2-4DA\right)}\right)\right\}\\ erfc\left(\frac{x+t\sqrt{\left(v^2+4Dk_2-4DA\right)}}{\sqrt{(4Dt)}}\right)\end{array}\right] \quad (5.12)$$

$$S(x,t)=\frac{1}{2}\left[\begin{array}{l}\exp\{-At\}\exp\left\{\frac{x}{2D}\left(v-\sqrt{\left(v^2+4Dk_1R-4DAR\right)}\right)\right\}\\ erfc\left(\frac{x-t\sqrt{\left(v^2+4Dk_1R-4DAR\right)}/R}{\sqrt{(4Dt/R)}}\right)+\\ \exp\{-At\}\exp\left\{\frac{x}{2D}\left(v+\sqrt{\left(v^2+4Dk_1R-4DAR\right)}\right)\right\}\\ erfc\left(\frac{x+t\sqrt{\left(v^2+4Dk_1R+4DAR\right)}/R}{\sqrt{(4Dt/R)}}\right)\end{array}\right] \quad (5.13)$$

$$P_1(x,t)=\frac{1}{2}\left[\begin{array}{l}\exp\{-Bt\}\exp\left\{\dfrac{x}{2D}\left(v-\sqrt{\left(v^2+4Dk_2-4DB\right)}\right)\right\}\\ erfc\left(\dfrac{x-t\sqrt{\left(v^2+4Dk_2-4DB\right)}}{\sqrt{(4Dt)}}\right)+\\ \exp\{-Bt\}\exp\left\{\dfrac{x}{2D}\left(v+\sqrt{\left(v^2+4Dk_2-4DB\right)}\right)\right\}\\ erfc\left(\dfrac{x+t\sqrt{\left(v^2+4Dk_2-4DB\right)}}{\sqrt{(4Dt)}}\right)\end{array}\right] \tag{5.29}$$

$$S_3(x,t)=\frac{1}{2}\left[\begin{array}{l}\exp\{-Bt\}\exp\left\{\dfrac{x}{2D}\left(v-\sqrt{\left(v^2+4Dk_1-4DBR\right)}\right)\right\}\\ erfc\left(\dfrac{x-t\sqrt{\left(v^2+4Dk_1-4DBR\right)}/R}{\sqrt{(4Dt/R)}}\right)+\\ \exp\{-Bt\}\exp\left\{\dfrac{x}{2D}\left(v+\sqrt{\left(v^2+4Dk_1-4DBR\right)}\right)\right\}\\ erfc\left(\dfrac{x+t\sqrt{\left(v^2+4Dk_1+4DBR\right)}/R}{\sqrt{(4Dt/R)}}\right)\end{array}\right] \tag{5.30}$$

$$F_3(x,t)=\frac{1}{2}\left[\begin{array}{l}\exp\left\{\dfrac{x}{2D}\left(v-\sqrt{\left(v^2+4Dk_1\right)}\right)\right\}erfc\left(\dfrac{x-t\sqrt{\left(v^2+4Dk_1\right)}/R}{\sqrt{(4D_1t/R)}}\right)+\\ \exp\left\{\dfrac{x}{2D}\left(v+\sqrt{\left(v^2+4Dk_1\right)}\right)\right\}erfc\left(\dfrac{x+t\sqrt{\left(v^2+4Dk_1\right)}/R}{\sqrt{(4Dt/R)}}\right)\end{array}\right] \tag{5.31}$$

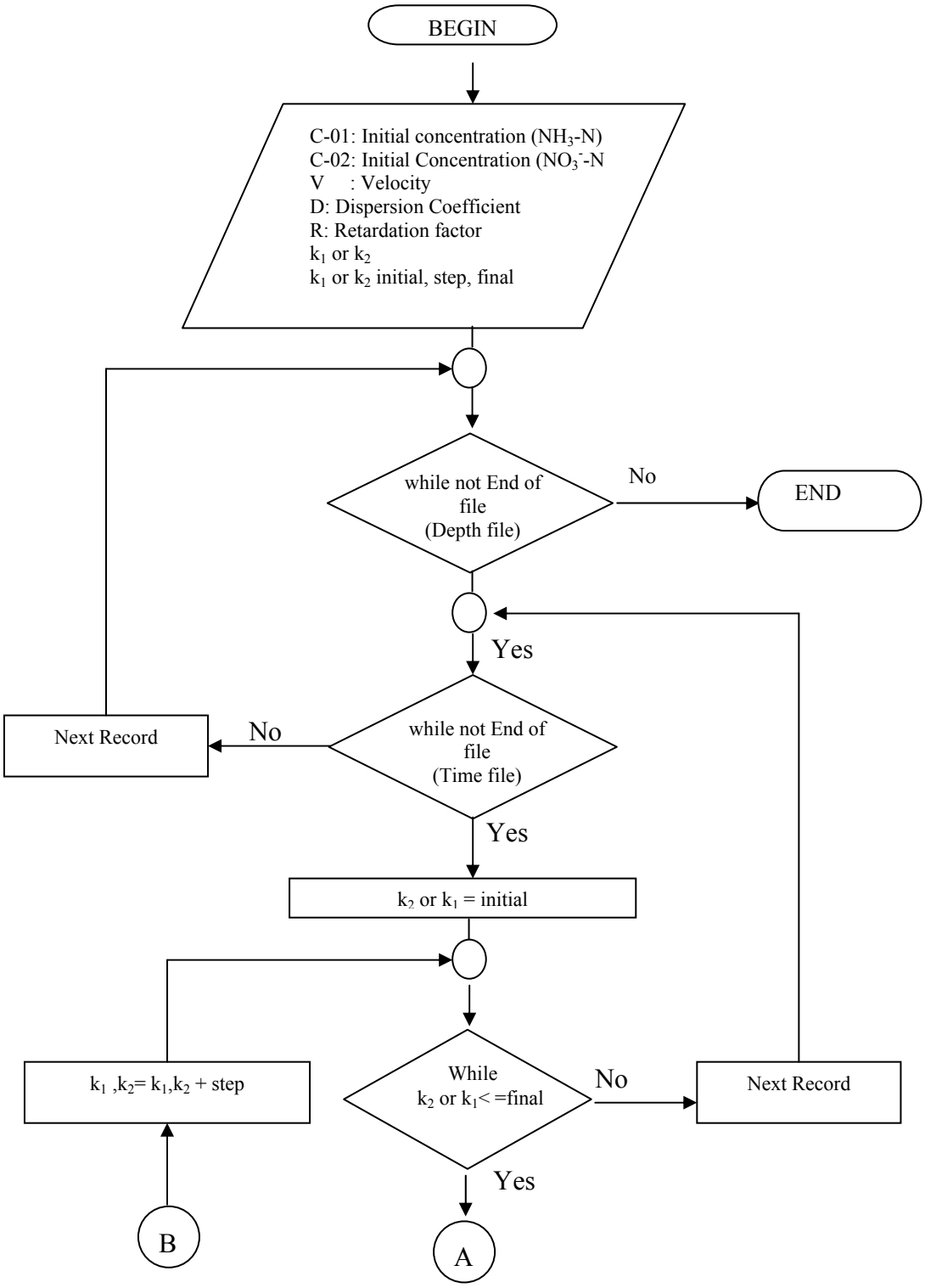
BEGIN
C-01: Initial concentration (NH_3-N)
C-02: Initial Concentration (NO_3^--N
V : Velocity
D: Dispersion Coefficient
R: Retardation factor
k_1 or k_2
k_1 or k_2 initial, step, final
while not End of file (Depth file)
No
END
Yes
Next Record
No
while not End of file (Time file)
Yes
k_2 or k_1 = initial
k_1 ,k_2= k_1,k_2 + step
While k_2 or k_1< =final
No
Next Record
Yes
B
A

PTO

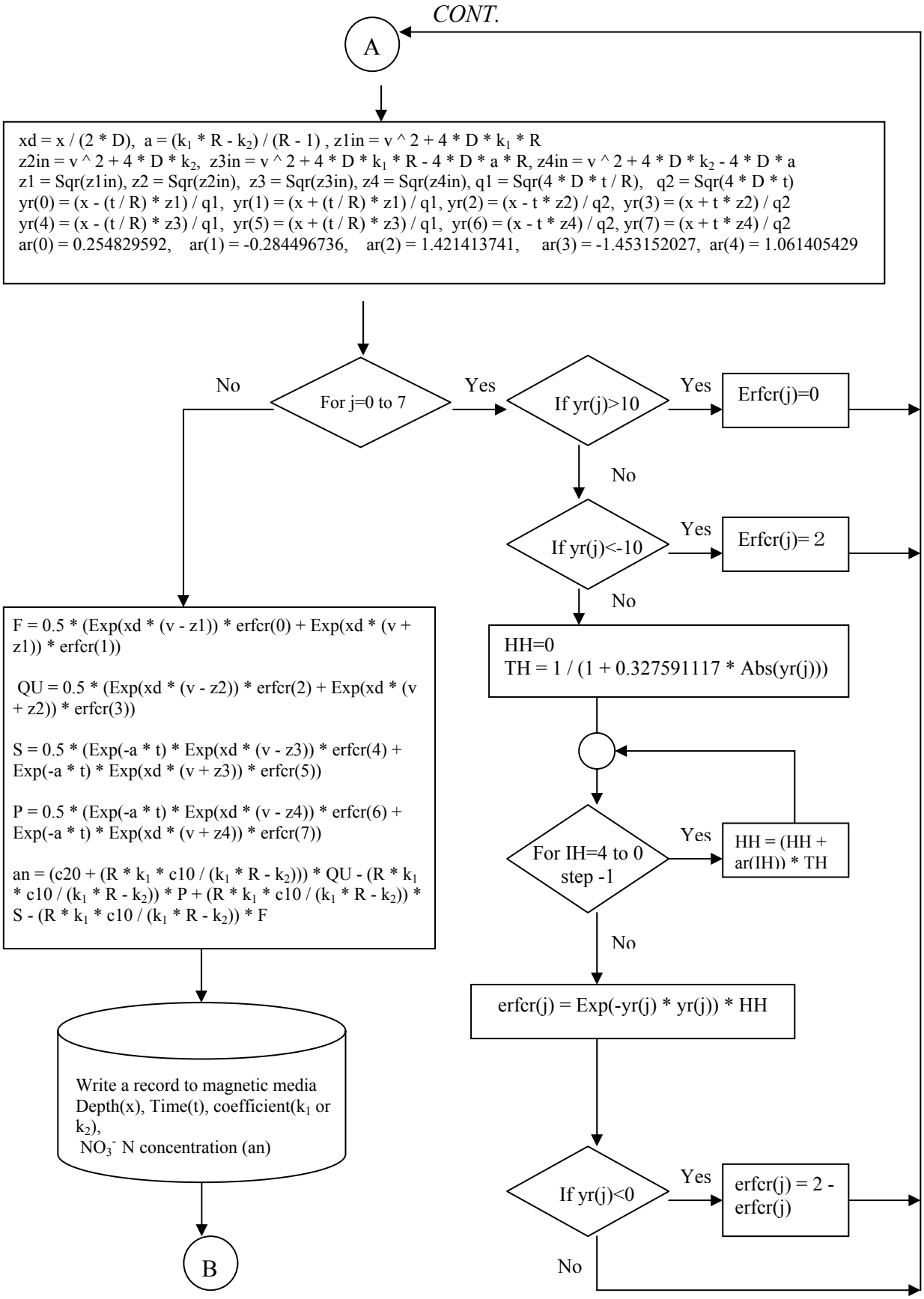

Fig. C-1 Flow chart of the computer program developed to compute NO_3^--N for a given data set of t and x, using a given range of k_1 or k_2 for CA of high porous soil.

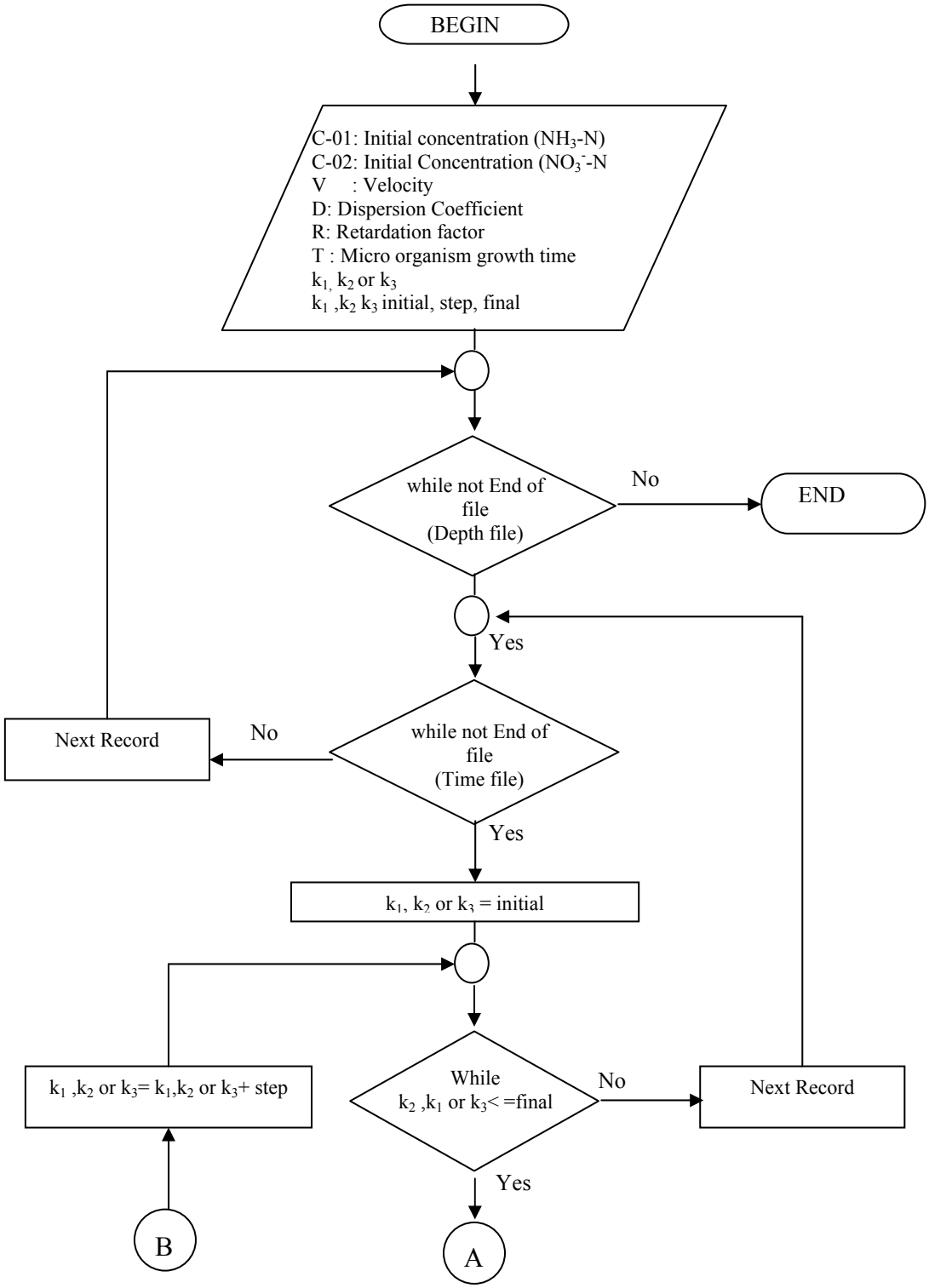
BEGIN
C-01: Initial concentration (NH_3-N)
C-02: Initial Concentration (NO_3^--N
V : Velocity
D: Dispersion Coefficient
R: Retardation factor
T : Micro organism growth time
k_1, k_2 or k_3
k_1 ,k_2 k_3 initial, step, final
while not End of file (Depth file)
No
END
Yes
Next Record
No
while not End of file (Time file)
Yes
k_1, k_2 or k_3 = initial
k_1 ,k_2 or k_3= k_1,k_2 or k_3+ step
While k_2 ,k_1 or k_3< =final
No
Next Record
Yes
B
A

PTO

CONT.

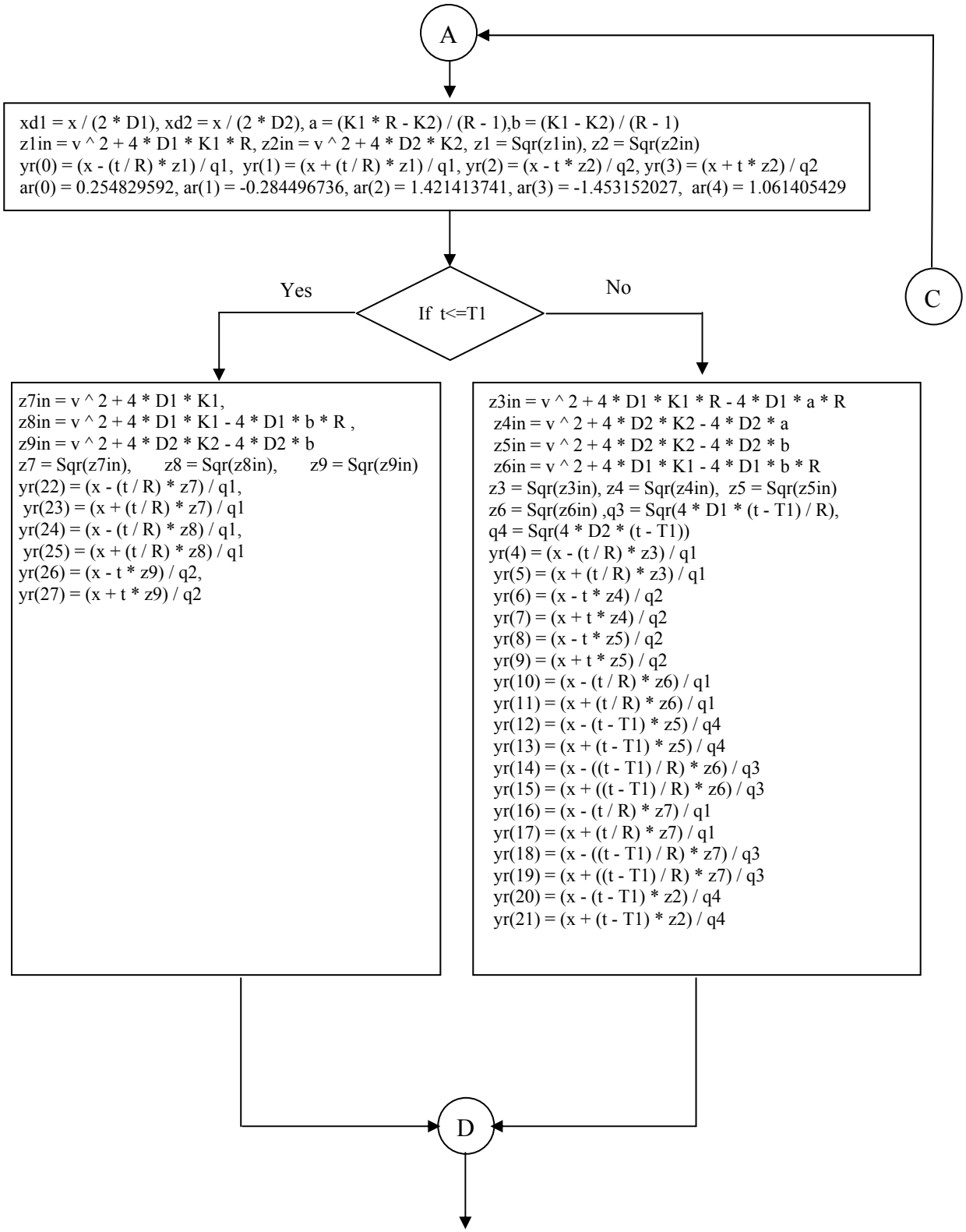
A
xd1 = x / (2 * D1), xd2 = x / (2 * D2), a = (K1 * R - K2) / (R - 1),b = (K1 - K2) / (R - 1)
z1in = v ^ 2 + 4 * D1 * K1 * R, z2in = v ^ 2 + 4 * D2 * K2, z1 = Sqr(z1in), z2 = Sqr(z2in)
yr(0) = (x - (t / R) * z1) / q1, yr(1) = (x + (t / R) * z1) / q1, yr(2) = (x - t * z2) / q2, yr(3) = (x + t * z2) / q2
ar(0) = 0.254829592, ar(1) = -0.284496736, ar(2) = 1.421413741, ar(3) = -1.453152027, ar(4) = 1.061405429
Yes
If t<=T1
No
C
z7in = v ^ 2 + 4 * D1 * K1,
z8in = v ^ 2 + 4 * D1 * K1 - 4 * D1 * b * R ,
z9in = v ^ 2 + 4 * D2 * K2 - 4 * D2 * b
z7 = Sqr(z7in), z8 = Sqr(z8in), z9 = Sqr(z9in)
yr(22) = (x - (t / R) * z7) / q1,
yr(23) = (x + (t / R) * z7) / q1
yr(24) = (x - (t / R) * z8) / q1,
yr(25) = (x + (t / R) * z8) / q1
yr(26) = (x - t * z9) / q2,
yr(27) = (x + t * z9) / q2
z3in = v ^ 2 + 4 * D1 * K1 * R - 4 * D1 * a * R
z4in = v ^ 2 + 4 * D2 * K2 - 4 * D2 * a
z5in = v ^ 2 + 4 * D2 * K2 - 4 * D2 * b
z6in = v ^ 2 + 4 * D1 * K1 - 4 * D1 * b * R
z3 = Sqr(z3in), z4 = Sqr(z4in), z5 = Sqr(z5in)
z6 = Sqr(z6in) ,q3 = Sqr(4 * D1 * (t - T1) / R),
q4 = Sqr(4 * D2 * (t - T1))
yr(4) = (x - (t / R) * z3) / q1
yr(5) = (x + (t / R) * z3) / q1
yr(6) = (x - t * z4) / q2
yr(7) = (x + t * z4) / q2
yr(8) = (x - t * z5) / q2
yr(9) = (x + t * z5) / q2
yr(10) = (x - (t / R) * z6) / q1
yr(11) = (x + (t / R) * z6) / q1
yr(12) = (x - (t - T1) * z5) / q4
yr(13) = (x + (t - T1) * z5) / q4
yr(14) = (x - ((t - T1) / R) * z6) / q3
yr(15) = (x + ((t - T1) / R) * z6) / q3
yr(16) = (x - (t / R) * z7) / q1
yr(17) = (x + (t / R) * z7) / q1
yr(18) = (x - ((t - T1) / R) * z7) / q3
yr(19) = (x + ((t - T1) / R) * z7) / q3
yr(20) = (x - (t - T1) * z2) / q4
yr(21) = (x + (t - T1) * z2) / q4
D

PTO

CONT.

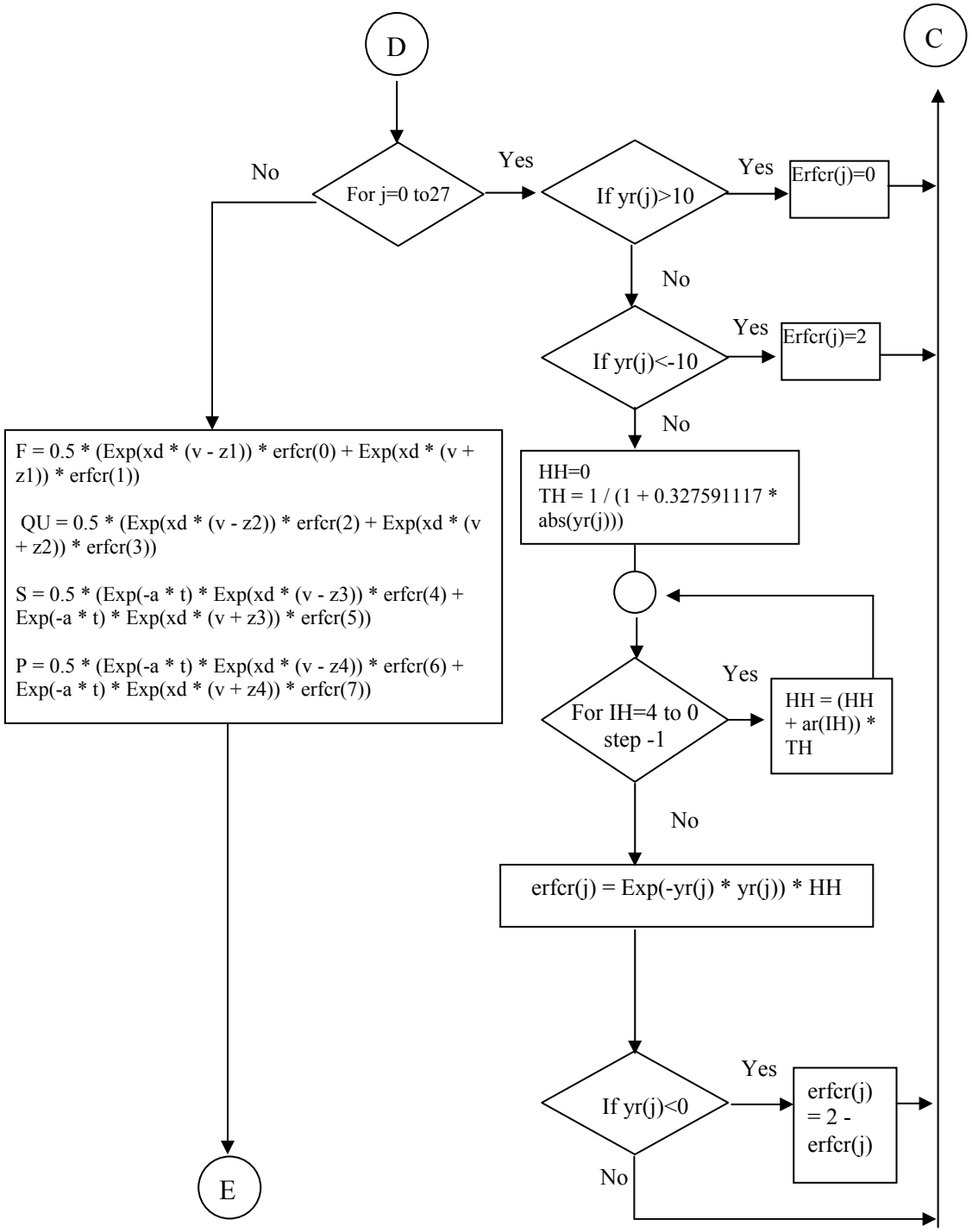
D
C
For j=0 to27
No
Yes
If yr(j)>10
Yes
Erfcr(j)=0
No
If yr(j)<-10
Yes
Erfcr(j)=2
No
F = 0.5 * (Exp(xd * (v - z1)) * erfcr(0) + Exp(xd * (v + z1)) * erfcr(1))
QU = 0.5 * (Exp(xd * (v - z2)) * erfcr(2) + Exp(xd * (v + z2)) * erfcr(3))
S = 0.5 * (Exp(-a * t) * Exp(xd * (v - z3)) * erfcr(4) + Exp(-a * t) * Exp(xd * (v + z3)) * erfcr(5))
P = 0.5 * (Exp(-a * t) * Exp(xd * (v - z4)) * erfcr(6) + Exp(-a * t) * Exp(xd * (v + z4)) * erfcr(7))
HH=0
TH = 1 / (1 + 0.327591117 * abs(yr(j)))
For IH=4 to 0 step -1
Yes
HH = (HH + ar(IH)) * TH
No
erfcr(j) = Exp(-yr(j) * yr(j)) * HH
If yr(j)<0
Yes
erfcr(j) = 2 - erfcr(j)
No
E

PTO

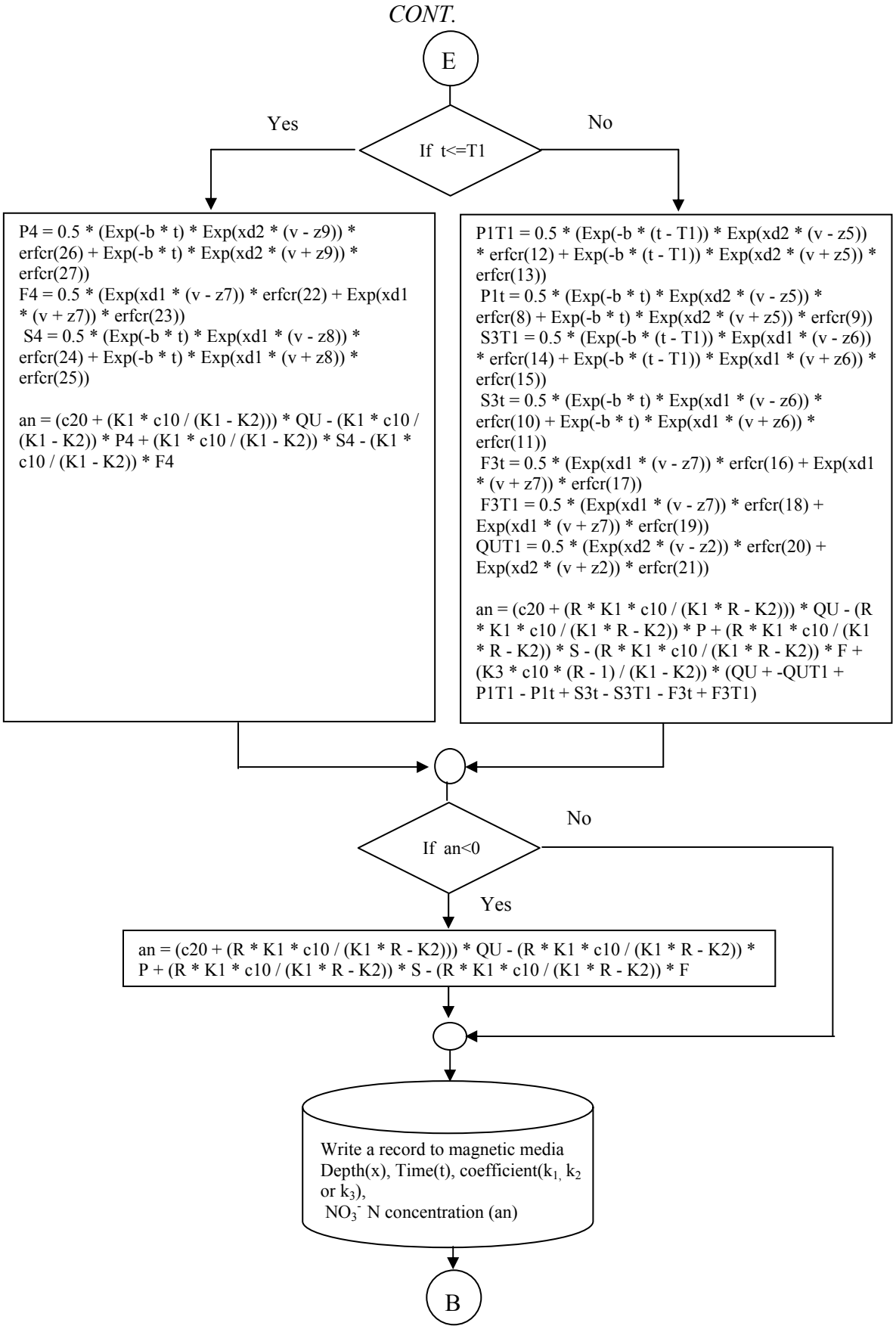

Fig. C-2 Flow chart of the computer program developed to compute NO_3^- -N for a given data set of t and x, using a given range of k_1 or k_2 for CA of low porous soil.

APPENDIX D

PHOTOS AND FIGURES ON LABORATORY SOIL COLUMN EXPERIMENTS

Sectional Front View

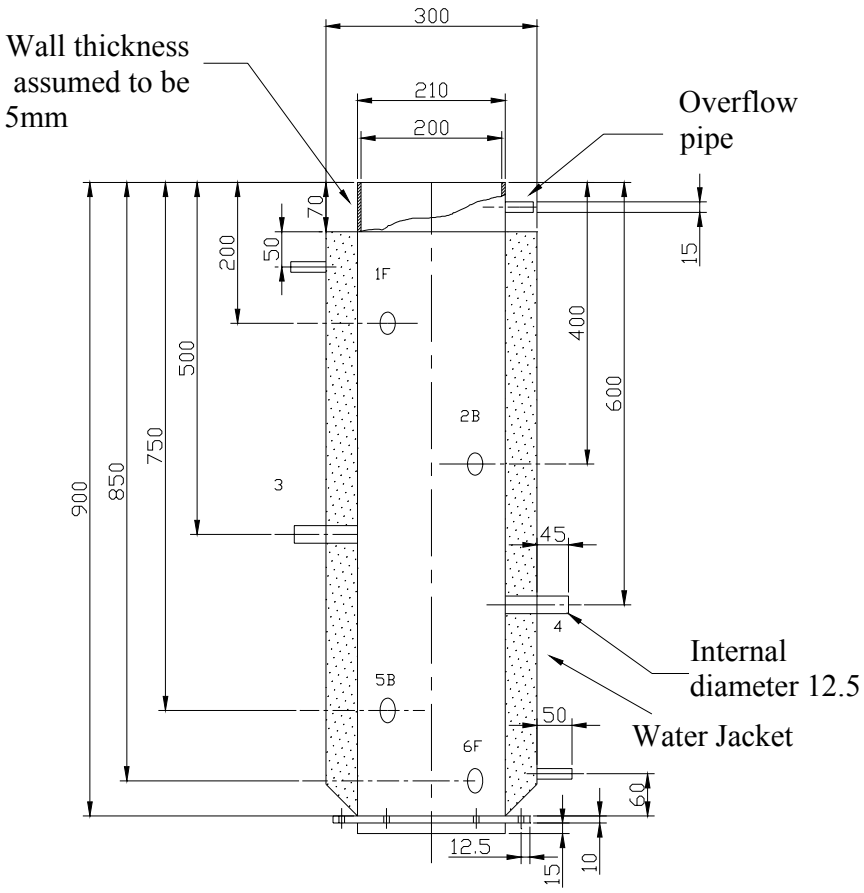

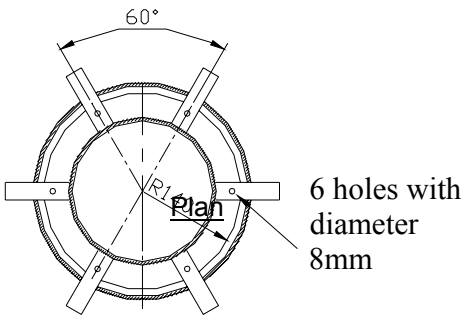

Plan

All dimensions are in millimeters

Fig. D-1 Engineering drawing of soil column without the funnel at the bottom.

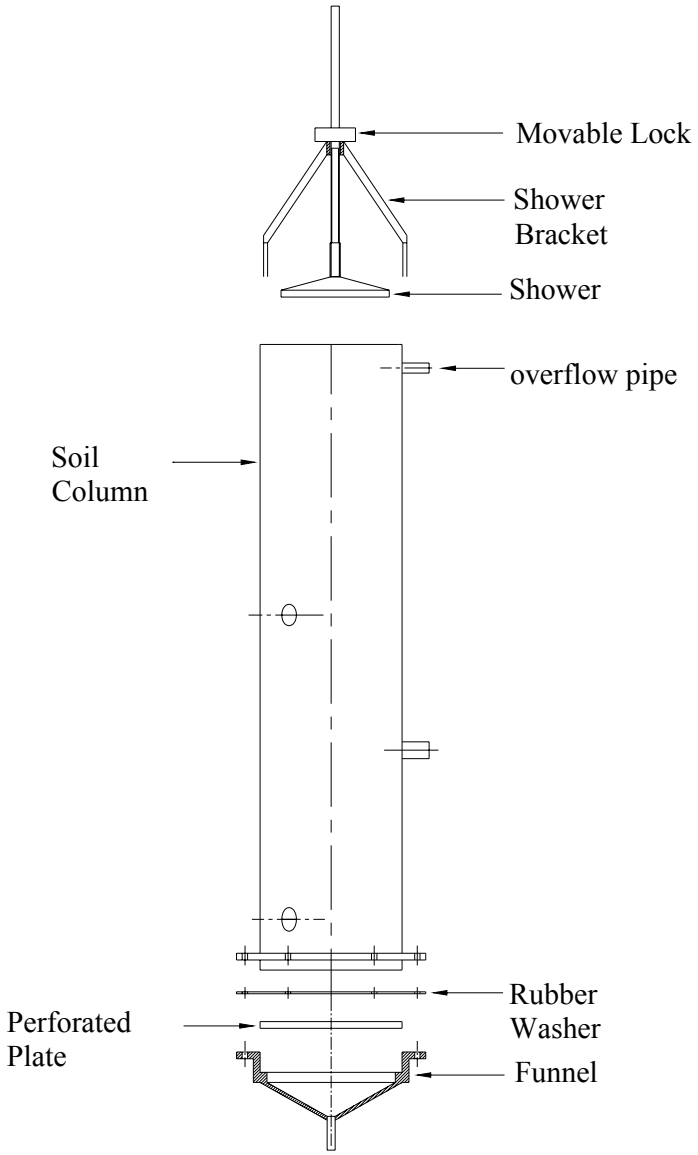

Fig. D-2 Engineering assembled drawing of soil column.

Fig. D-3 Four soil column experimental set ups.

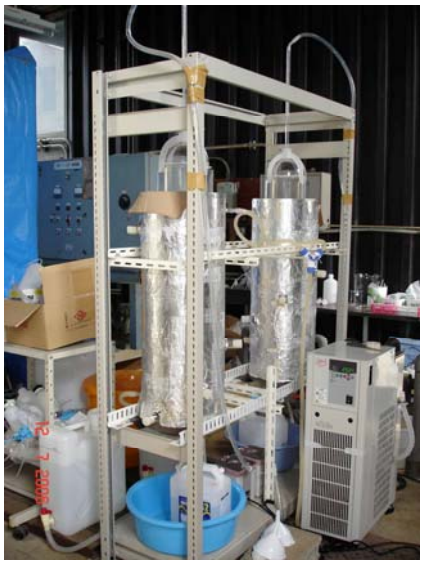

Fig. D-4 Two soil column experimental set ups during flushing out period.

Fig. D-5 Raw mudstone before loading in columns.

Fig. D-6 A field containing mudstone.

Fig. D-7 Raw limestone before loading in columns.

Fig. D-8 A field containing limestone.